

Georgia State University

ScholarWorks @ Georgia State University

Biology Dissertations

Department of Biology

7-31-2006

Functional Role of Dead-Box P68 RNA Helicase in Gene Expression

Chunru Lin

Follow this and additional works at: https://scholarworks.gsu.edu/biology_diss



Part of the [Biology Commons](#)

Recommended Citation

Lin, Chunru, "Functional Role of Dead-Box P68 RNA Helicase in Gene Expression." Dissertation, Georgia State University, 2006.

doi: <https://doi.org/10.57709/1063845>

This Dissertation is brought to you for free and open access by the Department of Biology at ScholarWorks @ Georgia State University. It has been accepted for inclusion in Biology Dissertations by an authorized administrator of ScholarWorks @ Georgia State University. For more information, please contact scholarworks@gsu.edu.

FUNCTIONAL ROLE OF DEAD-BOX p68 RNA HELICASE IN GENE EXPRESSION

by

CHUNRU LIN

Under the Direction of Zhi-ren Liu

ABSTRACT

How tumor cells migrate and metastasize from primary sites requires four major steps: invasion, intravasation, extravasation and proliferation from micrometastases to malignant tumor. The initiation of tumor cell invasion requires Epithelial-Mesenchymal Transition (EMT), by which tumor cells lose cell-cell interactions and gain the ability of migration. The gene expression profile during the EMT process has been extensively investigated to study the initiation of EMT. In our studies, we indicated that tyrosine phosphorylation of human p68 RNA helicase positively associated with the malignant status of tumor tissue or cells. Studying of this relationship revealed that p68 RNA helicase played a critical role in EMT progression by repression of E-cadherin as an epithelial marker and upregulation of Vimentin as a mesenchymal marker. Insight into the mechanism of how p68 RNA helicase represses E-cadherin expression indicated that p68 RNA helicase initiated EMT by transcriptional upregulation of Snail. Human p68 RNA helicase has been documented as an RNA-dependent ATPase. The protein is an essential factor in the pre-mRNA splicing procedure. Some examples show that p68 RNA helicase functions as a transcriptional coactivator in ATPase dependent or independent manner. Here we indicated that p68 RNA helicase unwound protein complexes to modulate protein-protein interactions by using protein-dependent ATPase

activity. The phosphorylated p68 RNA helicase displaced HDAC1 from the chromatin remodeling MBD3:Mi2/NuRD complex at the Snail promoter. Thus, our data demonstrated an example of protein-dependent ATPase which modulates protein-protein interactions within the chromatin remodeling machine.

INDEX WORDS: DEAD-box, p68, phosphorylation, EMT, Snail, HDAC1, NuRD, ATPase, transcriptional regulation, protein-protein interaction

FUNCTIONAL ROLE OF DEAD-BOX p68 RNA HELICASE IN GENE EXPRESSION

by

CHUNRU LIN

A Dissertation Submitted in Partial Fulfillment of Requirements for the Degree of

Doctor of Philosophy

in the College of Arts and Sciences

Georgia State University

2006

Copyright by
Chunru Lin
2006

FUNCTIONAL ROLE OF DEAD-BOX p68 RNA HELICASE IN GENE EXPRESSION

by

CHUNRU LIN

Major Professor:	Zhiren Liu
Committee:	Susanna F. Greer
	Jenny Y. Yang
	Chung-Dar Lu

Electronic Version Approved:

Office of Graduate Studies
College of Arts and Sciences
Georgia State University
August 2006

ACKNOWLEDGMENTS

The author would like to thank her supervisor Dr. Zhiren Liu for all his input, his scientific support and for providing her the opportunity to study such fascinating projects. His critical and encouraging advices from setting up experimental controls to suggestions on my writing skills are greatly appreciated.

The author would like to thank her dissertation committee member Dr. Jenny J. Yang for her thoughtful support and especially for providing me the guidance both on the works in the lab and future goals. The author would like to thank Dr. Susanna Greer, for her very effective instruction on the cell migration and transcriptional regulation and markedly, for her writing recommendation letters. The author also thanks Dr. Chung-Dar Lu for his dedication and outstanding advices. Special thanks go to Dr. Delon Barfuss, for his long-lasting support and helpful recommendation.

The author would also like to especially acknowledge Dr. Liuqing Yang for his endless technical assistance and selfless strengthening both for my projects and career opportunities. Great appreciation goes to author's parents for their noble support and wise suggestions. Thanks also go to the members of Dr. Zhiren Liu's lab for all the technical assistance and for making my graduate career enjoyable.

TABLE OF CONTENTS

LIST OF ABBREVIATION.....	xiii
LIST OF TABLES.....	xvi
LIST OF FIGURES.....	xvii
1. Chapter I: General Introduction.....	1
1.1 Regulation of Gene Transcription.....	1
1.2 The Pre-mRNA Splicing and the Spliceosome Assembly.....	3
1.3 DEAD-Box Protein Family.....	5
1.4 DEAD-Box Protein p68 RNA Helicase.....	8
1.4.1 p68 RNA helicase is an Essential Splicing Factor.....	10
1.4.2 p68 RNA Helicase in Transcriptional Regulation.....	11
1.4.3 The Cellular p68 Interacting Proteins.....	15
1.5 Kinase and Phosphatases.....	15
1.6 p68 RNA Helicase can be Phosphorylated at Ser/Thr/Tyr Residues.....	17
1.7 Signal to DEAD-Box Protein p68.....	18
1.8 Epithelial-Mesenchymal Transition (EMT).....	19
1.8.1 EMT is Critical for Tumor Metastasis.....	20
1.8.2 Downregulation of E-cadherin is a Hallmark of EMT.....	21
1.9 Mechanisms of E-cadherin Downregulation during EMT.....	23
1.10 Snail is a Strong Repressor of E-cadherin.....	24
1.11 Other Transcription Factors Involved in E-cadherin Repression.....	26
1.12 Signal to Snail.....	28

1.13	Regulation of Snail Expression.....	30
1.14	Chromatin Remodeling and Histone Deacetylation.....	32
1.14.1	The NuRD Complex.....	33
1.15	The ATPase Activity in Modulating RNA-RNA, RNA-protein Interactions.....	36
1.16	Tyrosine Phosphorylated p68 Promotes EMT.....	40
1.17	The Molecular Basis of p68-mediated EMT.....	41
1.18	Aims of Dissertation.....	43
2.	Chapter II: ATPase/Helicase Activities of p68 RNA Helicase Are Required for the Pre-mRNA Splicing but Not for Assembly of the Spliceosome	51
2.1	Abstract.....	51
2.2	Introduction.....	52
2.3	Results.....	55
2.3.1	p68 Mutants Lack ATPase and RNA Unwinding Activities.....	55
2.3.2	p68 Mutants that Lack ATPase and Helicase Activities do not Support the Pre-mRNA Splicing.....	57
2.3.3	p68 Mutants that Lack ATPase and RNA Unwinding Activities Interact with the U1:5'ss Duplex but do not Support the Dissociation of the U1 from the 5' Splice Site.....	58
2.3.4	The ATPase and RNA Unwinding Activities of p68 are not Required for the Assembly of the Spliceosome.....	60
2.3.5	p68 RNA helicase Affected the Pre-mRNA Splicing <i>In Vivo</i>	62
2.4	Discussion.....	64

3. Chapter III: PDGF/c-Abl Signaling Axis Induces the Tyrosine

Phosphorylation of DEAD-box p68 RNA Helicase.....	86
3.1 Abstract.....	86
3.2 Introduction.....	86
3.3 Results.....	91
3.3.1 The Tyrosine Phosphorylation Status of p68 Correlates with Tumor Malignancy.....	91
3.3.2 PDGF/c-Abl Signaling Pathway Induces the Tyrosine Phosphorylation of p68 in SW620 cells.....	92
3.3.3 PDGF Autocrine is one of the Mechanisms to Phosphorylate p68 in SW620 Cells.....	94
3.3.4 Y593 is the Tyrosine Phosphorylation Site of p68.....	96
3.3.5 Tyrosine Phosphorylated p68 Promotes Tumor Cell EMT.....	97
3.4 Discussion.....	99

4. Chapter IV: Phosphorylation of p68 RNA Helicase Activates Snail Transcription by Dissociating HDAC1 from the MBD3: Mi-2/NuRD

Complex at the Promoter	114
4.1 Abstract.....	114
4.2 Introduction.....	115
4.3 Result.....	118
4.3.1 The Phospho-p68 Represses E-cadherin Expression by Indirect Mechanisms.....	118

4.3.2 Snail Mediates the Effect of Phosphor-p68 on E-cadherin	
Suppression.....	121
4.3.3 p68 Associates with MBD3:Mi-2/NuRD Complex.....	125
4.3.4 MBD3 Mediates the Loading of p68 on the Snail Promoter.....	128
4.3.5 The Phospho-p68 Displaces HDAC1 from the Snail	
Promoter.....	129
4.3.6 The Phosphor-p68 has Protein-Dependent ATPase Activities.....	132
4.3.7 Displacement of HDAC1 from the Snail Promoter Requires the	
ATPase Activity of p68.....	134
4.4 Discussion.....	135
5. Chapter V: Examine the Potential Role of Phosphorylated p68 in Cancer	
Metastasis.....	161
5.1 Introduction.....	161
5.2 Results.....	164
5.2.1 The Tyrosine-to-glutamic Acid Substitution of p68 Functions	
Similarly to the Tyrosine Phosphorylated p68.....	164
5.2.2 Expression of Y593E Promotes Tumor Cell Migration.....	167
5.2.3 <i>In Vivo</i> Assessment of Tumor Growth and Potential Metastasis..	167
5.3 Discussion.....	169
6. Chapter VI: Conclusion.....	183
6.1 p68 RNA helicase is an Essential Splicing Factor.....	184
6.2 p68 Regulates Snail Transcription through protein-dependent ATPase	
activity.....	186

6.3 Implications in Cancer.....	190
7. Chapter II: Material and Methods.....	197
7.1 Material.....	197
7.1.1 Chemicals.....	197
7.1.2 Other material and kits.....	199
7.1.3 Laboratory equipments.....	200
7.1.4 Enzymes and recombinant proteins.....	200
7.1.5 Antibodies.....	201
7.1.6 Vectors and siRNA sequence.....	201
7.1.7 Bacteria Strains.....	201
7.1.8 The mammalian cell lines.....	202
7.1.9 Buffers.....	203
7.1.10 Computer software.....	203
7.2 Bacteria culture.....	204
7.2.1 Transformation.....	204
7.3 Deoxyribonucleic acid techniques.....	205
7.3.1 Preparation of plasmid DNA.....	205
7.3.2 Quantification of nucleic acid concentration.....	206
7.3.3 Agarose gel electrophoresis of nucleic acids.....	206
7.3.4 DNA extraction from agarose gel.....	207
7.3.5 Polymerase chain reaction (PCR).....	208
7.3.6 Restricted endonuclease digestion.....	209
7.3.7 Ligation.....	210

7.3.8 Dephosphorylation and insert DNA phosphorylation.....	210
7.3.9 Cloning of pET-30a-p68.....	211
7.3.10 Cloning of pHM6-p68.....	212
7.3.11 Cloning of Lenti6-p68 and generation of lentiviral Expression system.....	212
7.3.12 Site-directed mutagenesis.....	213
7.4 Protein techniques.....	214
7.4.1 Recombinant protein purification.....	214
7.4.2 Determination of protein concentration.....	217
7.4.3 Recombinant protein modification.....	217
7.4.3.1 Dephosphorylation.....	217
7.4.3.2 Phosphorylation by c-Abl kinase.....	219
7.4.4 Generation of anti-p68 antibody.....	219
7.4.5 Preparation of lysates.....	220
7.4.5.1 Whole cell lysates.....	220
7.4.5.2 Tissue lysates.....	220
7.4.5.3 Preparation of nuclear extraction.....	221
7.4.6 Western blotting.....	221
7.4.6.1 SDS-PAGE.....	221
7.4.6.2 Transfer to Nitrocellulose.....	222
7.4.6.3 Immunoblotting.....	223
7.4.7 Co-immunoprecipitation.....	224
7.4.8 Kinase assay.....	225

7.4.8.1 Peptide kinase assay.....	225
7.4.8.2 <i>In Vitro</i> kinase assay.....	225
7.4.8.3 Endogenous kinase assay.....	226
2.4.8.4 Immune complex kinase assay.....	224
7.4.9 Chromatin immunoprecipitation (CHIP).....	227
7.5 Ribonucleic acid techniques.....	229
7.5.1 <i>In vitro</i> transcription.....	229
7.5.2 Formation of double-stranded RNA.....	230
7.5.3 ATPase assay.....	231
7.5.4 RNA binding assay.....	232
7.5.5 RNA duplex dissociation assay.....	232
7.5.6 The Pre-mRNA splicing assay.....	233
7.5.7 Trioxsalen crosslinking assay	235
7.5.8 Methylene blue crosslinking assay	236
7.5.9 Spliceosome complex assay.....	237
7.5.10 RNA isolation.....	237
7.5.11 Reverse transcriptase PCR (RT-PCR).....	238
7.5.12 RNA immunoprecipitation.....	238
7.6 Cell culture.....	239
7.7 Transfection.....	239
7.7.1 Plasmid transfection.....	239
7.7.2 siRNA transfection.....	240
7.7.3 Protein delivery.....	241

7.8 Establish stable cell lines.....	242
7.9 Reporter gene assay.....	242
7.9.1 Dual reporter gene assay.....	242
7.9.2 Splicing reporter gene assay.....	243
7.10 HDAC activity assay.....	243
7.11 Immunostaining.....	244
7.12 Invasive assay.....	245
8. Reference.....	248
9. Appendix.....	278
9.1 Genome-wide Gene Expression Profiles Affected by Tyrosine Phosphorylated DEAD-box p68 RNA Helicase.....	279
9.1.1 Abstract.....	279
9.1.2 Introduction.....	279
9.1.3 Material and method.....	281
9.1.3.1 Total RNA isolation.....	281
9.1.3.2 Target labeling.....	281
9.1.3.3 Array hybridization and scanning.....	282
9.1.3.4 Data Analysis.....	282

LIST OF ABBREVIATION

aa	Amino acid
ADP	Adenosine diphosphate
AF	Autonomous activation function
AKAP95	cAMP-dependent protein kinase-anchoring protein 95
aPKC	Atypical protein kinase C
ATP	Adenosine triphosphate
BAF	BRG1-or hbrm-associated factors
BMP	Bone morphogenetic proteins
BSA	Bovine serum albumin
CBP	CREB binding protein
cDNA	Copy of complementary DNA
CREB	cAMP response element binding protein
CTP	Cytidine triphosphate
DD	Death domain
DEAD	Asp-Glu-Ala-Asp
DEPC	Diethyl pyrocarbonate
DMEM	Dulbecco`s modified eagles media
DNA	Deoxyribonucleic acid
DNase	Deoxyribonuclease
dNTP	Deoxynucleotide triphosphate
DMSO	Dimethylsulfoxide
ds	Double stranded
DTT	Dithiothreitol
ECM	Extracellular matrix
<i>E. coli</i>	<i>Escherichia coli</i>
EDTA	Ethylenediaminetetraacetic acid
EGTA	Ethylene glycol bis(2-aminoethyl ether)-N,N,N',N'-tetraacetic acid
EMT	Epithelial-mesenchymal transition
et al.	<i>et alter</i>
FCS	Fetal calf serum
GAPDH	Glyceraldehyde 3-phosphate dehydrogenase
GSK-3 β	Glycogen Synthase Kinase-3 beta

HAT	Histone acetyltransferase
HDAC	Histone deacetylase
HDMC	Histone demethylases
HEK293	Human embryonic kidney 293
HEL299	Human embryonic lung 299
HEPES	N-(2-hydroxyethyl)piperazine-N'-(2-ethanesulfonic acid)
HGF	Hepatocyte growth factor
HMEC	Human mammary epithelial cells
HMT	Histone methyltransferase
hr	hour(s)
IL-2	Interleukin-2
ILK	Integrin-linked kinase
IP	Immunoprecipitation
IPTG	Isopropylthiogalactoside
LB	Lauria-Bertani
LBD	Ligand-binding domain
LEF-1	Lymphoid enhancer binding factor 1
MAPK	Mitogen activated protein kinase
MBD2	Methyl-CpG-binding domain-containing protein 2
MBD3	Methyl-CpG-binding domain-containing protein 3
MDCK	Madin–Darby canine kidney
MEK	Mitogen-activated protein kinase kinase
min	minute(s)
MMP-3	Matrix metalloproteinase-3
mRNA	Messenger RNA
MTA1	Metastasis-associated protein 1
MTA2	Metastasis-associated protein 2
MTA3	Metastasis-associated protein 3
NF- κ B	Nuclear factor kappa B
N-CoR	Nuclear receptor corepressor
NES	Nucleus export sequence
NTP	Nucleoside triphosphate
NuRD	Nucleosomes remodeling and histone deacetylase
NURF	Nucleosome remodeling factor)
p68	p68 DEAD-box RNA helicase
PAGE	Polyacrylamid gel electrophoresis

PBS	Phosphate buffer saline
PDGF	Platelet-derived growth factor
PE	Parietal endoderm
pH	Potentia hydrogenii
PIPES	Piperazine-N,N'-bis(2-ethanesulfonic acid)
PTH(rP)	Parathyroid-hormone-related-protein
Rac1	Ras-related C3 botulinum toxin substrate 1
RNA	Ribonucleic acid
RNAi	RNA interference
RNase	Ribonuclease
ROS	Reactive oxygen species
rpm	rounds per minute
RPMI	Roswell Park Memorial Institute
RT	Reverse transcription
SDS	Sodium dodecyl sulfate
SIP	Smad-interacting protein
siRNA	small interfering RNA
Smad	Signaling mother against decapentaplegic
SMRT	Silencing mediator of retinoid acid and thyroid hormone receptor
SWI/SNF	Mating-type switch/sucrose nonfermenting
SRC	Steroid receptor coactivator
SV40	Simian virus 40
β -Trecp	Beta-Transducin repeat containing protein
TEMED	N,N,N',N'-tetramethylethylenediamine
TGF- β	Transforming growth factor beta
TNF- α	Tumor necrosis factor alpha
TRAIL	Tumor necrosis factor-related ligand
Tris	Tris(hydroxymethyl) aminomethane
U	unit(s)
UTP	Uridine 5'-triphosphate
VEGF	Vascular endothelial growth factor
Wnt1	Wingless-related MMTV integration site 1
WT	Wild type
ZEB-1/TCF8	Transcription factor 8
ZEB-2/SIP1	Smad-interacting protein 1

LIST OF TABLES

Table 1: <i>In vivo</i> incidence of tumor growth and liver metastasis.....	172
Table 2: Effect of expression of Y593E and wt-p68 in liver metastasis.....	173
Table 3: Transcription vectors used in this study.....	246
Table 4: The PT-PCR primers used in this study.....	247
Table 5. Identification of genes affected by p68 RNA helicase.....	289
Table 6. Identification of genes affected by phosphorylation of p68.....	290

LIST OF FIGURE

Figure I-1. The pre-mRNA splicing process.....	45
Figure I-2. The conserved motifs of DEAD-box proteins.....	47
Figure I-3. The conserved domain and motif sequence of p68 RNA helicase.....	49
Figure II-1. p68 mutants that lack ATPase and RNA unwinding activities.....	69
Figure II-2. p68 mutants that lack ATPase and helicase activities do not support pre-mRNA splicing.....	71
Figure II-3. p68 mutants that lack ATPase and RNA unwinding activities interact with the U1:5'ss duplex but do not support the dissociation of the U1 from the 5' splice site.....	73
Figure II-4. p68 mutants that lack ATPase and RNA unwinding activities interact with the U1:5'ss duplex during splicing.....	75
Figure II-5. The ATPase and RNA unwinding activities of p68 are not required for the assembly of the spliceosome.....	77
Figure II-6. p68 RNA helicase affects the pre-mRNA splicing <i>in vivo</i>	80
Figure II-7. p68 RNA helicase associates with pre-mRNA <i>in vivo</i>	83
Figure III-1. Tyrosine phosphorylation of p68 correlates to tumor malignancy.....	102
Figure III-2. PDGF/c-Abl signaling pathway induces tyrosine phosphorylation of p68 in SW620 cells.....	105
Figure III-3. PDGF autocrine loop induces phosphorylation of p68 in SW620 cells.....	107
Figure III-4. Y593 is the tyrosine phosphorylation site.....	109
Figure III-5. Tyrosine phosphorylation of p68 promotes EMT.....	111

Figure IV-1. The phosphor-p68 represses E-cadherin by indirect mechanism.....	139
Figure IV-2. Snail mediates the effect of phosphor-p68 on E-cadherin transcription.....	141
Figure IV-3. p68 associates with MBD3:Mi2/NuRD complex.....	146
Figure IV-4. MBD3 mediates the loading of p68 on Snail promoter.....	149
Figure IV-5. The phosphor-p68 displaces HDAC1 from the Snail promoter.....	151
Figure IV-6. The phosphor-p68 has a protein-dependent ATPase activity.....	155
Figure IV-7. Displacement of HDAC1 from Snail promoter requires ATPase activity of p68.....	159
Figure V-1. The tyrosine-to-glutamic acid substitution of p68 functions similar to the tyrosine phosphorylation.....	174
Figure V-2. Expression of Y593E promotes tumor cell migration.....	177
Figure V-3. <i>In vivo</i> tumor assessment of growth.....	179
Figure V-4. Generation of spontaneous colon tumor metastasis.	181
Figure VI-1. The hypothetical model of DEAD-box RNA helicase in the pre-mRNA splicing.....	193
Figure VI-2. The minimal model of protein-dependent ATPase activity of p68	195
Figure IX-1. The schematic illustration of targeting labeling and array hybridization.....	283
Figure IX-2. The expression of HA-tagged p68s in HEK 293 and SW620 cells.....	285
Figure IX-3. Reproducibility of the genes identified by the microarray technology.....	287

CHAPTER I

GENERAL INTRODUCTION

It is crucial for eukaryotic cells to respond to extracellular signals rapidly and precisely through regulation of protein expression, in order to survive in the living environment. Three major routines control the protein expression levels: genetic modulation of gene or DNA sequence, including homologous recombination and transposable element; epigenetic chromatin modification via methylation and acetylation and transcriptional regulation through recruitment of transcriptional activators or repressors. Post-translational modifications can alter protein stability and activity via ubiquitination, phosphorylation, methylation, acetylation, sulfation, prenylation and glycosylation etc. These modifications play decisive roles in cell signaling pathways in response to immense intracellular and extracellular signals. In this thesis, I will focus on protein phosphorylation in the signaling transduction pathway(s) and the mechanisms of gene transcriptional regulation.

1.1 Regulation of Gene Transcription

Purification of bacterial transcriptional repressors and activators helps to elucidate how transcriptional machinery is being regulated in the eukaryotic system (Jacob and Monod 1961; Englesberg, Irr et al. 1965). In eukaryotes, repressors control transcription of genes through interactions with particular DNA sequences upstream of transcriptional start point by preventing binding of RNA polymerase II. Positive regulation by activators

occurs via binding with the *cis*-element of transcription – the promoter (Ippen, Miller et al. 1968). Protein-protein interactions between the activators and the general transcriptional machinery facilitate the assembly of a stable and catalytically activated transcription-initiation complex (Chen, Ebright et al. 1994; Li, Moyle et al. 1994). Sequence-specific DNA-binding transcription factors are one of the most important elements ensuring that genes are transcribed in a highly regulated fashion (Tjian 1978; McKnight and Kingsbury 1982). More importantly, signaling pathways modulate gene expression patterns predominantly by controlling the activities of the transcription factors.

Epigenetic modification of chromatin acts as another important method to regulate gene transcription. Gene expression has been shown to be primarily repressed by DNA methylation (Holliday and Pugh 1975). DNA methylation is known to repress gene expression by recruiting histone deacetylase complex to methylated DNA to alter chromatin structure (Nan, Ng et al. 1998). Nucleosomes, the basic building block of chromatin, consist of DNA string enwrapped around a histone octamer. Acetylation of histone tails prevents the interaction of histone with transcription regulatory proteins (Hecht, Laroche et al. 1995). These interactions are also required for promoter-dependent specific gene transcription (Durrin, Mann et al. 1991) and for changing chromatin to a more open conformation (Tsukiyama, Becker et al. 1994). Multi-proteins chromatin remodeling complexes, termed SWI/SNF (mating-type switch/sucrose non-fermenting) (Cote, Quinn et al. 1994; Kwon, Imbalzano et al. 1994), NURF (nucleosome remodeling factor) (Tsukiyama, Daniel et al. 1995; Tsukiyama and Wu 1995) and NuRD

(Nucleosomes remodeling and histone deacetylase) (Tsukiyama, Daniel et al. 1995; Zhang, Ng et al. 1999) have been described to alter chromatin architecture and stimulate transcription factor binding to promoter in an adenosine triphosphate (ATP)-dependent manner. Furthermore, the two antagonistic enzymatic activities of histone acetyltransferases and deacetylases either activate or repress gene transcription, thus functioning as transcriptional regulators.

1.2 The Pre-mRNA Splicing and the Spliceosome Assembly

For most eukaryotic genes, the precise exclusion of pre-mRNA introns from mRNA precursor transcripts through the process of pre-mRNA splicing is an important step in gene expression. The splicing apparatus must identify and remove introns to ensure the correct protein production. Furthermore, certain genes must be alternatively spliced to generate appropriate protein isoforms in a strictly regulated manner (Collins and Guthrie 2000; Smith and Valcarcel 2000). The splicing reaction is accompanied by ATP hydrolysis. The spliceosome, a multi-protein complex contains five small nuclear ribonucleoprotein particles (snRNPs) (U1, U2, U4, U5 and U6) and a large number of non-snRNP proteins. By acting through complicated RNA-RNA, protein-protein and RNA-protein interactions, the spliceosome precisely excises each intron and ligates exons together in a correct order to form a mature mRNA (Sharp 1994; Jurica and Moore 2003).

Most introns have a consensus 5' splice site (5'ss) and a consensus branchpoint sequence followed by a 3' splicing site (3'ss). During the splicing process, the spliceosome is assembled on the pre-mRNA in a dynamic manner with several discrete

intermediates (**Figure I-1**) (Klein Gunnewiek, van de Putte et al. 1997). Firstly, recognition of the 5'ss by the U1 snRNP, along with the binding of the polypyrimidine tract and the branch point by U2 auxiliary factor (U2AF) and splicing factor1 (SF1) results in the formation of the commitment complex. Secondly, recruitment of the U2 snRNP to the commitment complex leads to the formation of complex A or the pre-spliceosome. At this point, a pre-formed U4/U6•U5 tri-snRNP joins the pre-spliceosome complex, leading to the formation of the spliceosome complex B (Hodges and Beggs 1994; Madhani and Guthrie 1994; Abovich and Rosbash 1997). Next, by remodeling RNA-protein and RNA-RNA interactions, catalytically competent complex C is formed. Finally, a two step chemical reaction is catalyzed by the spliceosome to remove the introns from the pre-mRNA and join the exons (Madhani and Guthrie 1994).

The splicing process is characterized by a series of changes of snRNA-pre-mRNA and snRNA-snRNA interactions. Previous base-pair interactions are later dissociated and new base-pairing interactions are formed via remodeling of secondary and tertiary structures of snRNP molecules (Hamm and Lamond 1998). Recognition of the 5'ss is an early event in the pre-mRNA splicing process. The 5'ss is recognized by 5 – 7 base pair interactions between the 5'ss and 5'-end of the U1 snRNA (Staley and Guthrie 1998). The U1:5'ss duplex is unwound to expose the same 5'ss sequence for pairing with the U6 snRNA prior to the first step chemical reaction of splicing (Liu, Wilkie et al. 1996; Singh 2002). However, before the U1:5'ss unwinding, the U4/U6•U5 tri-snRNP must be added to the pre-spliceosome. Presumably, addition of the tri-snRNP, unwinding of the U1:5'ss duplex and formation of the U6:5'ss duplex must be tightly coupled. Therefore, the

multiple steps of recognition of a splice site in the spliceosome involve the formation and the remodeling of a number of RNA-RNA and RNA-protein interactions (Staley and Guthrie 1998; Singh 2002; Jurica and Moore 2003).

1.3 DEAD-Box Protein Family

It is generally believed that the remodeling the complex RNA-RNA and RNA-protein interactions in the spliceosome is catalyzed by a family of DEAD/DExH (refer as DEAD: Asp-Glu-Ala-Asp) box putative RNA helicases (Schwer 2001; Will and Luhrmann 2001). This RNA helicase family, together with DNA helicase belongs to a helicase superfamily. According to the conserved amino acid motifs of the so-called “helicase motifs”, all putative helicases are grouped into four super families. The DEAD-box proteins are members of superfamily II (Hall and Matson 1999). The DEAD-box proteins have eight conserved motifs within the helicase core across the different species (**Figure I-2**). Mutational analyses and structural studies suggest that these conserved motifs are related to ATP hydrolysis, substrate binding or helicase activity. A new motif, Q motif, was identified referring to a glutamine residue rich motif (Tanner 2003; Tanner, Cordin et al. 2003). This Q motif is believed to bind and hydrolyze ATP.

The x-ray crystal structures of a few members of DEAD-box proteins have been solved, including eIF4A (Benz, Trachsel et al. 1999; Caruthers, Johnson et al. 2000), the DEAD-box protein of *Methanococcus jannaschii* (Story, Li et al. 2001), *Bacillus stearothermophilus* (Carmel and Matthews 2004) and *Drosophila* Vasa (Sengoku, Nureki et al. 2006). According to the biochemical data, the Q motif, motif I, motif II of domain I

and motif VI of domain II constitute part of the ATP-binding site, whereas motifs Ia, Ib, IV and V are involved in the process of RNA binding. To illustrate how a DEAD-box protein unwinds RNA duplex, biochemical analyses from *Drosophila* Vasa demonstrate that motifs Ia, Ib, VI and V form a cleft on the substrate binding site. There is a strict bend in the RNA substrate. This sharp bend of RNA facilitates the separation of the RNA duplex (Sengoku, Nureki et al. 2006).

DEAD-box proteins have been reported to be involved in most RNA-related metabolism, including transcription, translational initiation, pre-mRNA splicing, mRNA decay, mRNA export and rRNA biogenesis. Although DEAD-box proteins function in different cellular processes, they act through similar enzymatic activities to modulate RNA-RNA or RNA-protein interactions to rearrange or assemble complex machinery. *In vitro* studies demonstrate that many members of DEAD-box protein family have RNA-dependent ATPase activities and RNA unwinding activities. Despite the high similarity of DEAD-box proteins with DNA helicase, DEAD-box proteins are not processive and only unwind short RNA-RNA duplex locally.

A large body of evidence has shown that RNA helicase eIF4A is required for translation initiation (Rogers, Komar et al. 2002). Eukaryotic translation initiation factor (eIF4F) is a large protein complex recruiting the ribosome to mRNA. The DEAD-box protein eIF4A is proposed to form part of the cap-binding complex with the requirement for ATPase/helicase activity (Gingras, Raught et al. 1999). So far, two models are suggested to illustrate the role of eIF4A in translation initiation. One is that eIF4A prepares for small ribosomal subunit scanning along 5' eukaryotic mRNA by unwinding

or rearranging RNA-RNA duplex and tertiary structure of mRNA. The second model is that eIF4A removes the coating proteins from the mRNA through the energy-driven motor (Svitkin, Ovchinnikov et al. 1996; Rogers, Komar et al. 2002). Another DEAD-box protein Ded1 is demonstrated to be involved in eukaryotic translation initiation via a distinct mechanism (Chuang, Weaver et al. 1997; Noueiry, Chen et al. 2000).

It has been long known that ATP hydrolysis is required for the pre-mRNA splicing. Extensive RNA structure rearrangement is necessary during the pre-mRNA splicing process, which is achieved by the putative RNA helicases to modulate short RNA-RNA duplex formed between snRNA-snRNA and snRNA-pre-mRNA molecules. The RNA helicases unwind RNA-RNA base-pairing (Staley and Guthrie 1998) and rearrange RNA-protein interactions (Singh 2002) at the expense of the energy derived from ATP hydrolysis. To date, eight yeast splicing factors and six mammalian proteins that are homologous to the RNA helicase superfamily have been implicated in the pre-mRNA splicing process (Hamm and Lamond 1998; Luking, Stahl et al. 1998; Schwer 2001; Will and Luhrmann 2001). Many of these proteins exhibits RNA unwinding activities *in vitro* (Laggerbauer, Achsel et al. 1998; Raghunathan and Guthrie 1998; Wang, Wagner et al. 1998; Schwer and Meszaros 2000). These putative RNA helicases are involved in every step of the pre-mRNA splicing process, including unwinding of the U1:5'ss duplex and the U4/U6 RNA helixes, dissociation of the protein-RNA interactions at the branch point to promote U2-branch point interactions and dissociation of the spliced mRNA from the spliceosome.

1.4 DEAD-Box Protein p68 RNA Helicase

Human p68 RNA helicase is the gene product of DEAD-box polypeptide 5 (DDX5) located at chromosome 17q21. Translation product of this gene is 614 amino acids long and characterized by the conserved DEAD motif as the putative RNA helicase. Human p68 RNA helicase was first identified by anti-SV40 large T antigen monoclonal antibody DL3C4 (PAB204) because of the cross-reaction with DNA tumor virus oncogene SV40 large T antigen (Crawford, Leppard et al. 1982; Ford, Anton et al. 1988). Sequence analyses reveal similarities between p68 and eukaryotic initiation factor eIF-4A, suggesting that p68 may act as an ATP-dependent RNA helicase. Protein p68 shows a distinct nuclear distribution and is thought to be important for cells division and proliferation with the observation of its high expression in dividing cells (Ford, Anton et al. 1988). In 1989, p68 RNA helicase was purified from human HEK cells and the purified protein exhibited RNA-dependent ATPase activity and helicase activity *in vitro* (Hirling, Scheffner et al. 1989). Family members of DEAD-box proteins share conserved sequence, express ubiquitously in living cells and are considered to be involved in multiple RNA metabolism, including splicing, translation, RNA processing, RNA transport and rRNA biosynthesis/assembly (Iggo and Lane 1989; Chuang, Weaver et al. 1997; Pugh, Nicol et al. 1999).

The human p68 RNA helicase gene consists of 13 exons (Iggo and Lane 1989). Protein sequence contains 614 amino acids with a core region of 305 amino acids that consists of eight conserved sequence motifs (**Figure I-3**). The motifs I, III and VI have been reported to be functioning as the ATP binding and hydrolysis sites. Motif IV is

proposed to harbor the helicase activity. The motif V within helicase core is believed to be the RNA binding site (de la Cruz, Kressler et al. 1999). The functions of other motifs are still not very clear. p68 has a number of important sequence motifs located at the N- and C-terminus. An RGG (Arg-Gly-Gly) repeat and an IQ motif located within the C-terminus are suggested as the regulatory motifs by interacting with co-factors or harboring post-translational modification (Yang and Liu 2004; Yang, Yang et al. 2004; Yang, Lin et al. 2005; Yang, Lin et al. 2005).

The role of p68 RNA helicase in regulating cell growth and proliferation was first discerned by the observation that p68 RNA helicase was barely detectable in quiescent cells and its expression was induced by serum (Stevenson, Hamilton et al. 1998). Comparing the levels of p68 mRNA and protein in tissue samples suggests that p68 expression is developmentally regulated (Stevenson, Hamilton et al. 1998). Higher expression level of p68 is observed in developing brain and spinal cord of chick, frog and ascidians embryos, suggesting the important role of p68 in neural crest development (Seufert, Kos et al. 2000). An elevated p68 expression level was detected in tissue samples of colorectal adenoma patients in comparison to corresponding normal tissues. Furthermore, accumulated p68 protein is poly-ubiquitinated due to dysfunction of the proteasome-mediated degradation (Causevic, Hislop et al. 2001). The dysfunctional regulation of p68 expression may cause tumor development and growth (Dubey, Hendrickson et al. 1997; Causevic, Hislop et al. 2001).

Screening a cDNA library from nitric oxide (NO)-induced differential keratinocytes identified p68 RNA helicase, an important factor being upregulated upon

NO induction. Expression studies in wound-healing process revealed that despite the down-regulated expression level in wounded tissue, p68 RNA helicase is exclusively localized within the nucleus and enhances the serum-induced keratinocyte proliferation and vascular endothelial growth factor (VEGF) expression, which is very important during the wound-healing process (Kahlina, Goren et al. 2004). The studies suggest the fundamental role of p68 RNA helicase in cell proliferation, angiogenesis and wound-healing process through upregulation of VEGF. The molecular mechanism by which p68 regulates VEGF expression is not known.

Taken together, p68 RNA helicase plays a role in the whole spectrum of biological processes. Emerging evidences suggest a vital role of p68 in tumor growth and cell proliferation and differentiation programs.

1.4.1 p68 RNA Helicase is an Essential Splicing Factor

Protein p68 was speculated to be involved in the mRNA processing processes due to the unique nuclear localization. Nevertheless, solid evidence for the involvement of p68 RNA helicase in the pre-mRNA splicing was only documented recently. The experiments carried out in our laboratory demonstrated that p68 RNA helicase is an essential human splicing factor *in vitro* that plays a role in unwinding the transient U1:5' ss duplex (Liu, Sargueil et al. 1998; Liu 2002). Consistently, by large-scale proteomic analyses of human spliceosome, other research laboratories also suggested the existence of p68 RNA helicase in the human spliceosome (Rappsilber, Ryder et al. 2002; Zhou, Licklider et al. 2002; Guil, Gattoni et al. 2003).

During the pre-mRNA splicing process and the assembly of the spliceosome, a number of intramolecular RNA-RNA duplexes are formed and modulated by ATP-dependent helicases (Nilsen 2003). Dissociation of base pairs between 5'splicing site and U1 snRNP is critical for transformation from the pre-spliceosome to the spliceosome (Staley and Guthrie 1998). DEAD-box protein p68 RNA helicase was detected to crosslink with the U1 snRNA-5'ss duplex (Liu, Sargueil et al. 1998). Depletion of endogenous p68 RNA helicase from HeLa cell nuclear extract diminished the pre-mRNA splicing activity *in vitro* (Liu 2002). Moreover, although the deletion of p68 does not affect the loading of U1 snRNP to 5'ss, the dissociation of this duplex is impeded followed by the prohibition of the spliceosome assembly. These data established the essential role of p68 RNA helicase in the pre-mRNA splicing process *in vitro*.

Although the essential role of p68 RNA helicase in the pre-mRNA splicing process *in vitro* has been documented, the molecular basis by which p68 RNA helicase supports the pre-mRNA splicing *in vitro* remains unclear. Whether p68 RNA helicase also supports splicing process *in vivo* is unknown.

1.4.2 p68 RNA Helicase in Transcriptional Regulation

In addition to the essential role in the pre-mRNA splicing process (Liu 2002; Lin, Yang et al. 2005), p68 RNA helicase has been implicated in the transcription as transcriptional coactivator (Fujita, Kobayashi et al. 2003; Rossow and Janknecht 2003), or corepressor (Wilson, Bates et al. 2004).

The first example elucidating p68 as a transcriptional coactivator is the study of estrogen-receptor alpha (ER α) signaling pathway (Endoh, Maruyama et al. 1999; Kato 1999; Watanabe, Yanagisawa et al. 2001; Rossow and Janknecht 2003). ER belongs to a superfamily of ligand-inducible transcription factors with five or six conserved functional domains (termed A to F) (Mangelsdorf, Thummel et al. 1995). Both A/B (autonomous activation function/AF-1) and E/F (autonomous activation function/AF-2) regions contain transcription activation function upon ligand binding (Tora, White et al. 1989). The A/B and E/F regions have synergistic and transcriptional interference/squelching properties (Tasset, Tora et al. 1990). It is estimated that AF-1 function of the N-terminal (AB) domain of ER has a weak constitutive transcriptional activation function. AF-2 function of the ER ligand-binding domain (LBD) has a stronger estrogen-dependent transcriptional activation function (Kumar, Green et al. 1987; Tora, White et al. 1989). AF-1 and AF-2 synergize to present the overall level of estrogen activation. Putative cofactors mediate or activate AF-2 have recently been identified, including steroid receptor coactivator (TIF2/SRC-1) (Voegel, Heine et al. 1996; Anzick, Kononen et al. 1997), CREB binding protein (CBP)/p300 family (Chen, Lin et al. 1997), TIF1 (Le Douarin, Zechel et al. 1995), ARA70 (Yeh and Chang 1996) and others (Onate, Tsai et al. 1995; Xu and Li 2003).

p68 RNA helicase is isolated as coactivator of AF-1, but not AF-2, to enhance AF-1 transcription activity function in a cell-type specific manner. Interactions between p68 RNA helicase and A/B domain of ER α are essential for the activation of AF-1 with

dispensable helicase activity of p68 RNA helicase (Endoh, Maruyama et al. 1999; Watanabe, Yanagisawa et al. 2001; Fujita, Kobayashi et al. 2003). These studies also provide evidence for the interactions between p68 RNA helicase and CBP *in vitro* (Endoh, Maruyama et al. 1999). Studies from an independent group confirmed the association between p68 CBP/p300 and RNA polymerase II *in vivo* and *in vitro* (Rossow and Janknecht 2003). *In vitro* pull-down assays mapped the binding site of p68 with CBP/p300 at the N-terminus. Furthermore, p68 stimulated CBP transcription activity with p300 in a synergic manner (Rossow and Janknecht 2003). This interaction is confirmed by studies on *n*-butylbenzyl phthalate (BBP), an ER α agonist, which specifically induces ER binding with the coactivator complex. The estrogen receptor transcriptional activity is modulated by recruitment of coactivator complex or corepressor complex (N-CoR/SMAT) (Fujita, Kobayashi et al. 2003). Yeast two-hybrid screening demonstrated that the heterodimer p72/p68 associates with both AD2 domain of SRC-1/TIF2 and human ER A/B domain (Watanabe, Yanagisawa et al. 2001). Upon E₂ stimulation, p72/68 co-immunoprecipitates with SRC-1 and SRA, an RNA coactivator to form complex, which activates ER-targeted gene *pS2* expression. These findings suggest that DEAD-box protein RNA helicases, p72/p68, act as ER coactivators through binding with SRC-1 and other cofactors to form a multi-protein complex (Watanabe, Yanagisawa et al. 2001).

Studies of DNA damage-induced and p53-mediated apoptosis revealed that p68 RNA helicase is required for p53-responsive gene expression (Bates and Jones 2003).

p68 RNA helicase particularly associates with p53 and stimulates p53 induced gene expression with synergism. Examining the interactions between p68 and chromatin further evidences that p68 participates on the promoter of p53-responsive gene, p21 (Bates and Jones 2003). p68 RNA helicase also functions as transcription corepressor in a promoter-specific manner (Wilson, Bates et al. 2004). In addition, p68 associates with 5-MeC-DNA glycosylase, which removes the methyl group from hemimethylated DNA (Jost, Schwarz et al. 1999). It was suggested that RNA molecules are present in the 5-MeC-DNA glycosylase complex and guide the demethylation complex to the hemimethylated DNA sites (Jost, Schwarz et al. 1999). DEAD-box protein p68 resembles one of the components of the DNA demethylation complex. Furthermore, *Drosophila* homologue of the mammalian p68 RNA helicase is suggested to play a potential role in RNA export and gene suppression. P68 may be needed for rapid removal of transcripts from the transcription bulb and allows chromatin reset to quiescent state (Buszczak and Spradling 2006).

In summary, p68 RNA helicase functions as a transcriptional regulator. The protein may act at the gene promoter to modulate the multi-protein and nucleic acid complex of the promoter. Interestingly, whether p68 acts as transcription coactivator or corepressor is depended on the context of promoter and transcription complex. Although the role of p68 in transcriptional regulation is well-documented, the molecular basis by which p68 regulates gene transcription remains elusive.

1.4.3 The Cellular p68 Interacting Proteins

A number of interacting partners of p68 have been uncovered by previous studies. Calmodulin is reported to interact with p68 at the N-terminus and the interaction affects ATPase activity of p68 (Buelt, Glidden et al. 1994). p72, the highly related homolog of p68, is shown to tightly bind with p68 to form a heterodimer. The dimer is potentially involved in mRNA processing (Ogilvie, Wilson et al. 2003). p68/p72 interacts with histone deacetylase 1 (HDAC1) to repress gene expression through chromatin remodeling (Wilson, Bates et al. 2004). Extensive studies on TNF- α (Tumor necrosis factor α) /NF- κ B (Nuclear factor kappa B) signaling pathway demonstrate the interaction between MAP3K7 and p68. This interaction is a component of a complex consisting of over 80 previous unknown integrators (Bouwmeester, Bauch et al. 2004). In ER α signaling pathways, p68 interacts with CBP/p300 and RNA polymerase II to form a multi-protein complex (Endoh, Maruyama et al. 1999; Rossow and Janknecht 2003; Fujita, Jaye et al. 2004). The cyclic AMP (cAMP)-dependent protein kinase-anchoring protein AKAP95 is shown as the binding partner of p68 in nuclear matrix isolated from rat brain (Akileswaran, Taraska et al. 2001).

1.5 Kinase and Phosphatase

Phosphorylation by a particular kinase is the key event in the general cell signaling pathways. Modification of proteins by phosphor groups provides a fast and reversible method to turn on/off protein activity and function. ATP is the source of

phosphor group. Kinases and corresponding phosphatases regulate protein phosphorylation by attaching (phosphorylation) or removing phosphor group(s) (dephosphorylation). One example of the important role of phosphorylation is the multi-phosphorylation of the N-terminus of beta-catenin at multiple sites. Beta-catenin is a transcription coactivator promoting cell proliferation and growth. Phosphorylation of the N-terminal domain on serine and threonine residues induces beta-catenin ubiquitination and subsequent degradation. In contrast, unphosphorylated beta-catenin translocates to the nucleus and activates a number of targeted genes. Therefore, the level of beta-catenin within cytoplasm is tightly controlled by phosphorylation.

Serine, threonine and tyrosine are the common amino acid residues for protein phosphorylation. Antibodies specifically against phosphoserine, phosphothreonine and phosphotyrosine provide magnificent tools for studying phosphorylation. It is estimated that about 30% of total cellular proteins are potentially modified by phosphorylation. Proximately 2% of human genes encode about 500 different protein kinases. Protein kinases are known as major regulators for transmitting signals within cells. Because of the vital role of protein kinases, their activities are often tightly regulated by phosphorylation. Dysregulation of protein kinase activity that controls cell proliferation or death may lead to diseases. An example is BCR-Abl kinase, whose overactivation usually leads to uncontrolled cell growth and survival resulting in leukemia.

1.6 p68 RNA Helicase can be Phosphorylated at Ser/Thr/Tyr Residues

Early immunological studies and sequence comparisons discern a potential protein kinase C (PKC) phosphorylation site and a calmodulin binding site (termed IQ motif) at the C-terminus of p68 (Buel, Glidden et al. 1994). *In vitro* studies indicate p68 can be phosphorylated by PKC and binds to calmodulin in a Ca^{2+} -dependent manner. The consequences are the loss of the ATPase activity of p68 RNA helicase, suggesting a possibility that the function and activity of p68 may be regulated by phosphorylation and protein-protein interactions (Buel, Glidden et al. 1994). The possibility that p68 may be regulated by diverse signaling pathways is further supported by screening of substrates of Tlk1, a protein kinase down-regulated upon exposure to ionized radiation. Tlk1 phosphorylated p68 RNA helicase both *in vitro* and *in vivo*, suggesting p68 as the potential physiological substrate of Tlk1 (Kodym, Henockl et al. 2005).

Results from our lab revealed that the recombinant p68 protein expressed and purified from *E. coli* is phosphorylated on serine, threonine and tyrosine residues (Yang and Liu 2004). Tyrosine and threonine phosphorylations of p68 are also observed in HeLa nuclear extracts (Yang, Lin et al. 2005; Yang, Lin et al. 2005). Strikingly, p68 is tyrosine phosphorylated in six cancer cell lines derived from different tissue types, but not in cells derived from the corresponding normal tissues (Yang, Lin et al. 2005). Comparison of p68 phosphorylation in tumor tissue samples and corresponding normal tissue samples further support this pattern (Yang, 2006, in preparation). Moreover, the level of tyrosine phosphorylation of p68 correlates with tumor malignancy. p68 was tyrosyl phosphorylated at higher levels in more aggressive and invasive cancer cell lines.

These observations bring enormous interests in studying the biological role of tyrosine-phosphorylated p68 in tumor progression. The tyrosine phosphorylation of p68 RNA helicase seems to affect the ATPase and RNA unwinding activities of the protein (Yang, Lin et al. 2005). More importantly, tyrosine-phosphorylated p68 diminishes the activity of the protein in the pre-mRNA splicing process (unpublished data) (Yang, Lin et al. 2005). However, what signaling molecule(s) induce the tyrosyl phosphorylation of p68? What is the functional role of tyrosyl phosphorylated p68 in cancer cell lines and metastatic tissues? The research work in our lab investigating the tyrosine phosphorylation of p68 will be described in the following sections.

1.7 Signaling to DEAD-Box Protein p68

In an effort to identify the signaling pathways that stimulate the phosphorylation of p68, various growth factors and cytokines have been examined. TNF- α carries on dual effects on the phosphorylation of p68 in HeLa cells. p68 acquires threonine phosphorylation in a short time window upon TNF- α treatment. On the contrary, tyrosine residue(s) of p68 is dephosphorylated to undetectable level after 15 min treatment of TNF- α (Yang, Lin et al. 2005). Platelet-derived growth factor (PDGF) and Interleukin-2 (IL-2) treatments also affect the tyrosine phosphorylation of p68. Both of these signaling molecules induce significant tyrosine phosphorylation of p68 in a dose- and time-dependent manner (Yang, Lin et al. 2005). Tumor necrosis factor-related ligand (TRAIL), like TNF- α , stimulates dephosphorylation of p68 on tyrosine residue(s) and

phosphorylation on threonine residue(s). However, other anti-cancer drugs/apoptosis inducers, such as piceatannol, etoposide and taxol do not influence the tyrosyl phosphorylation of p68 (Yang, Lin et al. 2005). These results shed light on the close correlation between p68 phosphorylation and tumor development, which potentially provide a biological marker for cancer diagnosis and therapy. The phosphorylation status of p68 upon anti-cancer drugs treatment makes p68 RNA helicase a prospective prognostic marker.

p68 exclusively localizes in the nucleus (Ford, Anton et al. 1988; Iggo and Lane 1989). The candidate kinase(s) that phosphorylates p68 may be also located within the nucleus. Moreover, treatment of cancer cells with STI-571, a PDGF receptor and c-Abl tyrosine kinase specific inhibitor, inhibits the tyrosyl phosphorylation of p68, indicating that c-Abl is a possible candidate (Yang, Lin et al. 2005). The c-Abl kinase is a proto-oncogene non-receptor tyrosine kinase. The kinase localizes in the plasma membrane, the cytoplasm, as well as the cell nucleus (Zhu and Wang 2004). *In vitro* and *in vivo* studies identified c-Abl as the kinase that phosphorylates p68 upon PDGF stimulation (Yang, 2006, in preparation). Mass spectrum and mutation analyses indicated that Y593 residue is the phosphorylation site (Yang, 2006, in preparation).

1.8 Epithelial-Mesenchymal Transition (EMT)

Epithelial-mesenchymal transition (EMT) was first noted in epithelial tissues (Greenburg and Hay 1982). Scatter factor (identified as hepatocyte growth factor, HGF) was later been described as a stimulus that was able to convert Madin–Darby canine

kidney (MDCK) cells to fibroblast-like mesenchymal cells (Stoker and Perryman 1985). EMT is characterized by the loss of cell adhesion molecules and by the upregulation of mesenchymal markers, breakdown of epithelial contact and cell rearrangement or migration in extracellular matrix (Shook and Keller 2003). Epithelial cells may transiently lose their polarity and gain cell spreading in many developmental processes. These processes include mesoderm formation during gastrulation and immigration of neural-crest cells from neural tube (Duband, Monier et al. 1995; Sun, Baur et al. 2000). In mature organs, transcriptional loss of epithelial markers (i.e. E-cadherin) and induction of mesenchymal markers (i.e. Vimentin) in epithelial cells are necessary for the processes including tubulogenesis, tissue reorganization, wound healing and mammary gland branching (Viebahn 1995; Thiery 2002). Epithelial plasticity changes also occur in a variety of pathological processes. For instance, progression of benign tumors toward invasive, malignant carcinoma alters epithelial plasticity to migratory fibroblast phenotype (Hay 1995).

1.8.1 EMT is Critical for Tumor Metastasis

Tumor cells spread to distant organs, the process being called metastasis. Both genetic and epigenetic changes contribute to the metastatic ability of tumor cells. Recent gene expression analyses revealed that tumor subclones raised from the primary site probably already have progressed to invasive stage (Hynes 2003). Several sequential and obligated steps must be completed in order for tumor cells to migrate to distant organs (Fidler 2003). First, tumor cells have to disrupt cell-cell adhesion, break down basement

membrane and penetrate into neighborhood stroma, which allows them to dissociate from the primary site. EMT is critical for tumor cells to lose epithelial adhesions and gain the ability of migration. The second step is “intravasation”. During this process, tumor cells penetrate into the blood or the lymphatic vessels to allow them to be transported by circulation. Next, tumor cells circulate along with bloodstream until they reach the targeted organs. The tumor cells are stopped by microcirculation. Finally, after survival from the bloodstream, metastatic cells depart away from the bloodstream by a process termed “extravasation” and grow expediently from micro-metastasis to malignant tumor mass. For tumor cells to accomplish this deadly process, the first and the most important phenomenon is that tumor cells have to gain mobility and then invade into neighboring tissues (Vincent-Salomon and Thiery 2003; Guo and Giancotti 2004).

1.8.2 Downregulation of E-cadherin is a Hallmark of EMT

To break away from primary site, invasive tumor cells suppress expression of adhesion molecules to disrupt cell-cell interactions, degrade or remodel extracellular matrix and acquire migratory phenotype. Intensive studies indicate that the transition from non-metastatic adenoma (epithelial phenotype) to invasive carcinoma (mesenchymal phenotype) is driven by a distinct series of changes of adhesion proteins. These changes include loss of epithelial adhesion and catenin-dependent junction. The tumor cells also increase expression of proteins involved in cell migration and interactions with cell-extracellular matrix (ECM).

There are three types of cell junctions: tight junction, adherens junction and gap junction. E-cadherin plays a critical role in epithelial cell-cell adherens junction. The cytoplasmic domains of cadherin proteins interact with beta-catenin and other catenin molecules at different sites (Takeichi 1995; Tepass, Truong et al. 2000). Actin filaments bind with beta-catenin through alpha-catenin. Recent studies have shown that alpha-catenin may act as an actin kinetics regulator instead of a stable link between beta-catenin and actin (Drees, Pokutta et al. 2005; Yamada, Pokutta et al. 2005). Loss of epithelial polarity through downregulation of E-cadherin, mutations on *E-cadherin* gene or other mechanisms of preventing the adhesions junctions from formation are observed in malignant carcinoma cells. In human cancer patients, the loss of E-cadherin expression correlates with the advanced stage of tumor development and poor prognosis (Riethmacher, Brinkmann et al. 1995). In a transgenic mouse model, depletion of *E-cadherin* promotes the non-metastatic adenoma developing to invasive carcinoma (Christofori and Semb 1999). In this regard, *E-cadherin* gene is proposed as a tumor suppressor gene. During the transformation of invasiveness, the loss of *E-cadherin* appears to be critical for the development of migratory mesenchymal cells from non-invasive epithelial cells. *De novo* expression of *E-cadherin* promotes formation of adhesions junction between transformed mesenchymal cells. Disruption of the E-cadherins interactions by anti-E-cadherin antibody can interrupt adhesions junctions and promote mesenchymal phenotype (Imhof, Vollmers et al. 1983). Therefore, molecular analyses based in part on studying transgenic mouse model and cell phenotype reveal *E-cadherin* as the hallmark of EMT process and a potential tumor suppressor.

1.9 Mechanisms of E-cadherin Downregulation during EMT

Various mechanisms contribute to the disruption of adherens junction and cadherin-catenin complex of cancer cells. Loss-of-function mutant of *E-cadherin* is one of the factors for epithelial plasticity changes (Thiery 2002). In some tumor cells, a family of transcription factors, Snail/Slug, down-regulate *E-cadherin* gene transcription (Nieto 2002). Upon stimulation with growth factors, these stimulation signals from receptor tyrosine kinase (RTK) can disrupt adherens junction by repression of junction protein expression (Thiery 2002). Therefore, downregulation of E-cadherin in cancer progression is mediated through mechanisms including transcriptional suppression, chromatin silencing mediated by methylation or genetic mutation leading to absence or non-functional protein expression (Berx, Cleton-Jansen et al. 1995; Yoshiura, Kanai et al. 1995; Hennig, Lowrick et al. 1996).

E-cadherin expression is regulated by multiple mechanisms, including genetic, epigenetic and transcriptional modification. Although genetic changes in *E-cadherin* loci have been found infrequently, the loci of *E-cadherin* are intact in the majority of E-cadherin down-regulated carcinomas (Guilford, Hopkins et al. 1998). Chromatin modifications and transcription alteration emerge as the major mechanisms of E-cadherin repression (Yoshiura, Kanai et al. 1995). A decreased E-cadherin mRNA level correlates with reduced E-cadherin level, suggesting that suppression of E-cadherin protein is probably due to the decline in gene transcripts (Brabant, Hoang-Vu et al. 1993). Further insight into the promoter of the *E-cadherin* gene reveals the mechanism of transcriptional

regulation of the *E-cadherin* gene. The promoter of the *E-cadherin* gene has a short 81bp conserved region that is the main *cis*-regulatory element as revealed by depletion experiments. E-box 1 and E-box 2, within the conserved region uncovered by mutation analyses are involved in the suppression of the *E-cadherin* promoter activity in cancer cells (Girolidi, Bringuier et al. 1997). In addition, E-box 3 that is located within the first intron is identified to regulate the *E-cadherin* gene expression. The E-box elements have been proposed as the DNA targeting sequence of the basic helix-loop-helix (bHLH) family of transcription factors (Jan and Jan 1993; Weintraub 1993; Voronova and Lee 1994). Association of AP-2 with E1, E2 boxes and E3 box is sufficient and necessary for the *E-cadherin* promoter activity (Hennig, Lowrick et al. 1996). Recent studies have identified a number of transcription factors aiming at E-boxes to regulate the *E-cadherin* gene expression. Transcription factors including Snail/Slug, E12/E47, ZEB-1, ZEB-2 and Twist-1 will be discussed below.

1.10 Snail is a Strong Repressor of E-cadherin

Members of the Snail family are zinc-finger transcription factors that play the fundamental role in mesoderm formation in different species (Alberga, Boulay et al. 1991; Nieto, Sargent et al. 1994; Erives, Corbo et al. 1998; Carver, Jiang et al. 2001). The key role of Snail in triggering EMT has been illustrated by two experiments: Snail has been shown to convert epithelial cells to mesenchymal cells by repressing the *E-cadherin* gene expression directly (Batlle, Sancho et al. 2000; Cano, Perez-Moreno et al. 2000). In mouse embryo, downregulation of E-cadherin is essential for progression of mesodermal

cells at gastrulation stage (Burdal, Damsky et al. 1993). On the other hand, animals with knockout *Snail* retain E-cadherin expression, fail to undergo EMT and die at gastrulation stage (Carver, Jiang et al. 2001). Studies on tumor progression in carcinoma cells demonstrate the essential role of Snail in migration and invasion. Snail is present in fibroblast cells and some invasive E-cadherin-negative carcinoma cell lines. In several melanoma cell lines, Snail is upregulated when E-cadherin is down-regulated (Poser, Dominguez et al. 2001). Expression of Snail induces epithelial cells to acquire fibroblastic phenotype and invasive properties. More importantly, inhibition of Snail function restores *E-cadherin* expression in epithelial cancer cells in which *E-cadherin* is repressed (Batlle, Sancho et al. 2000; Cano, Perez-Moreno et al. 2000). Gene analyses indicate a list of candidate targets that are regulated directly or indirectly by Snail. Snail transfectants also suppress other epithelial markers, such as desmoplakin (Cano, Perez-Moreno et al. 2000) and upregulate mesenchymal markers, including Vimentin and Fibronectin (Cano, Perez-Moreno et al. 2000), suggesting the central role of Snail in promoting EMT process.

Although Snail is a strong repressor of the *E-cadherin* gene (Batlle, Sancho et al. 2000; Cano, Perez-Moreno et al. 2000; Poser, Dominguez et al. 2001) through direct interactions with three E-boxes located within the E-cadherin promoter (Batlle, Sancho et al. 2000), the molecular mechanism by which Snail represses the *E-cadherin* gene through E-box is not understood. It was reported that Snail modulates the *E-cadherin* gene expression through recruiting chromatin-modification activity, such as forming a

multi-protein complex with HDACs and corepressor mSin3A (Peinado, Ballestar et al. 2004).

Other members of the Snail family, such as Slug, also contribute to EMT process and E-cadherin downregulation. Slug binds to E-boxes of the *E-cadherin* promoter. The protein not only is expressed in E-cadherin-negative breast cancer cells (Hajra, Chen et al. 2002), but also promotes epithelial-mesenchymal transition in MDCK cells (Bolos, Peinado et al. 2003). More specifically, Slug binds to the E-box elements of the *E-cadherin* promoter, independent of Snail (Bolos, Peinado et al. 2003). The discrepant role of Snail and its family members may be due to tissue specificity or their involvement in distinct signaling pathways.

1.11 Other Transcription Factors Involved in E-cadherin Repression

Other transcriptional factors that have been implicated in repressing the *E-cadherin* promoter include E12/E47, ZEB-1 (EF-1), SIP-1 (ZEB-2) and Twist-1 (Grooteclaes and Frisch 2000; Comijn, Berx et al. 2001; Perez-Moreno, Locascio et al. 2001; Yang, Mani et al. 2004). E12/E47 is a basic helix-loop-helix transcription factor. The protein is isolated from one-hybrid screen as an *E-cadherin* repressor. Mouse E47 is not expressed in epithelial cells and highly expressed in invasive E-cadherin-negative cell lines. This is consistent with the observation that E47 is expressed during mesoderm formation. Stable or inducible E47 expression promotes fibroblastic and migratory phenotype through repression of E-cadherin expression by binding to E-boxes at the *E-cadherin* promoter (Perez-Moreno, Locascio et al. 2001; Bolos, Peinado et al. 2003).

ZEB-1 repressor is identified by Madeleine L Grooteclaes and co-workers (Grooteclaes and Frisch 2000). Adenovirus prototypical oncoproteins E1a protein induces expression of a set of epithelial genes, whose products interact with nuclear acetylases p300, CBP and corepressor protein CtBP. The CtBP-interacting protein δ EF1/ZEB-1 binds with the E-boxes of the *E-cadherin* promoter and the promoters of at least three other adhesion genes, suggesting the potential role of ZEB-1 in virus-induced cell junction downregulation (Grooteclaes and Frisch 2000).

Another transcription factor repressing the *E-cadherin* promoter is Smad-interacting protein (SIP1/ZEB-2), a zinc finger protein with specific DNA binding affinity. SIP1 downregulates the *E-cadherin* gene through interactions with conserved E-boxes of the minimal *E-cadherin* promoter. Interaction sites of SIP1 with E-boxes are partially overlapped with Snail binding sequence. Treatment of cells with TGF- β (Transforming growth factor β) induces SIP1 expression and subsequent E-cadherin silencing. SIP1 is also observed to abrogate E-cadherin-mediated cell adhesion and simultaneously promotes MDCK cells to transform into mesenchymal phenotype (Comijn, Berx et al. 2001).

Recently, another transcription factor Twist, is identified from DNA microarray analyses. Twist is essential for tumor metastasis and repression of the *E-cadherin* gene (Yang, Mani et al. 2004). Expression of Twist in both MDCK cells and human mammary epithelial cells (HMEC) promotes cell morphology change to fibroblast, migratory phenotype, which may contribute to tumor malignant transformation. Twist

directly or indirectly represses E-cadherin expression through E-boxes of the *E-cadherin* promoter (Yang, Mani et al. 2004). However, HMEC cells, which are exogenously expressed of mouse E-cadherin, retain spindle-like morphology and mesenchymal markers, suggesting that Twist modulates other targets in addition to *E-cadherin* to promote EMT.

1.12 Signaling to Snail

Snail is one of the major repressors of *E-cadherin* expression by targeting E-boxes during embryo development and carcinogenesis (Batlle, Sancho et al. 2000). Various cell signaling pathways that activate Snail gene subsequently initiate changes in epithelial plasticity and conversions from epithelial cells toward mesenchymal cells. TGF- β activates *Snail* gene transcription and subsequently triggers EMT through activation of Ras-Mitogen activated protein kinase (MAPK) pathway in both MDCK cells and in the bud formation of hair follicle morphogenesis (Peinado, Quintanilla et al. 2003; Jamora, Lee et al. 2005). Upon TGF- β 1 stimulation, MDCK cells express Snail, which repress the *E-cadherin* transcription and promotes fibroblastic phenotype. Unlike transcription factor signaling mother against decapentaplegic (Smad4), the induction of Snail is apparently dependent on mitogen-activated protein kinase kinase (MEK1/2) activity (Peinado, Quintanilla et al. 2003). The expression of Slug, a Snail family member is an important target of TGF- β 2 signaling during EMT in the developing chicken heart (Romano and Runyan 2000). The upregulation of Slug during

differentiation of dorsal cell types from neural plate cells is proposed to be induced by bone morphogenetic proteins (BMP), which is a member of TGF family (Liem, Tremml et al. 1995).

Given the observation that *E-cadherin* is suppressed upon activation of Wnt/ β -catenin signaling cascade (Garcia-Castro, Marcelle et al. 2002; Jamora, DasGupta et al. 2003; Suzuki, Watkins et al. 2004), it is speculated that Snail is regulated by Wnt signaling pathway. Although the mechanism of regulation of Snail by the Wnt is still not understood, Snail has a β -catenin-like canonical motif and can be phosphorylated by Glycogen Synthase Kinase-3 beta (GSK-3 β). The phosphorylation of Snail is subsequently ubiquitinated and degraded by the 21S proteasome. Wnt signaling inhibits Snail phosphorylation, resulting in stabilization of Snail. The consequence is promotion of EMT (Yook, Li et al. 2005). Whether Wnt signal-stabilized Snail/Slug regulates β -catenin signaling (Arias 2001) or augmented cytoplasmic β -catenin influences Snail expression and EMT remains to be a question.

Other factors that activate Snail/Slug gene expression includes parathyroid-hormone-related peptide, (PTH(rP)) (Veltmaat, Orelia et al. 2000), integrin-linked kinase (ILK) (Tan, Costello et al. 2001) and MMP-3 (stromelysin-1/matrix metalloproteinase-3) (Radisky, Levy et al. 2005). The *Snail* gene is an early target of PTH(rP), which is upregulated during differentiation of parietal endoderm (PE) of mice embryo. Expression of Snail is detected in the PE cells and is the first marker of EMT in mice embryonic development (Veltmaat, Orelia et al. 2000). In addition, the ILK pathway activates β -

catenin/Lymphoid enhancer binding factor 1 (LEF-1) mediated gene transcription and the *E-cadherin* gene downregulation. Interestingly, inhibition of ILK results in suppression of *Snail* gene transcription, which correlates with the stimulation of the E-cadherin expression. In contrast, overexpression of ILK leads to an increased Snail expression, which is β -catenin/LEF-independent (Tan, Costello et al. 2001). These data suggest a novel signaling pathway in regulation of *Snail* gene expression. Recently, MMP-3 is implicated in upregulation of Snail expression by inducing Rac1 and cellular reactive oxygen species (ROS). MMP-3 is previously observed to induce tumor formation, EMT and malignant cells transformation in mammary carcinoma (Lochter, Sternlicht et al. 1998; Vincent-Salomon and Thiery 2003). MMP-3 induces expression of alternative spliced form of Rac1 on mice mammary epithelial cells. Rac1 increases the cellular ROS level, which stimulates *Snail* gene expression and result in EMT and DNA damage (Radisky, Levy et al. 2005). These findings reveal a novel pathway for the effect of microenvironment on tumor cell EMT.

1.13 Regulation of Snail Expression

Snail is demonstrated to mediate EMT process both in embryonic development and tumor malignancy transformation. However, the molecular mechanism of regulation of the Snail expression remains elusive. Studies suggest that Snail may be regulated through chromatin remodeling, transcription regulation and post-translational modifications (Erives, Corbo et al. 1998; Dominguez, Montserrat-Sentis et al. 2003;

Fujita, Jaye et al. 2004; Zhou, Deng et al. 2004). A nucleus export sequence (NES) is identified that locates in the regulatory domain of Snail. Cytosolic distribution of Snail is dependent on the NES sequence (Dominguez, Montserrat-Sentis et al. 2003). Phosphorylation on a serine-rich sequence adjacent NES allows export of Snail from the nucleus to cytosol (Dominguez, Montserrat-Sentis et al. 2003). Another example of non-transcriptional mechanisms to regulate Snail is that because Snail is an unstable protein with a half-life of about 25 min (Zhou, Deng et al. 2004), Snail can be phosphorylated by GSK-3 β at two conserved motifs. Phosphorylation of Snail controls its stability by a dual mechanism. Phosphorylation on the first motif facilitates transduction repeat containing protein (β -Trecp)-mediated ubiquitination. Phosphorylation on the second motif regulates its subcellular localization (Zhou, Deng et al. 2004). Mutations that abolish these two phosphorylation sites stabilize Snail and lead to an exclusive nuclear localization. The consequence is promotion of EMT (Zhou, Deng et al. 2004).

Transcriptional regulation is the major mechanism to regulate the *Snail* gene expression. In the ascidian, *Ciana intestinalis*, Snail (ci-Sna) is expressed at 32-cell stage through a minimal 504bp B4.1 enhancer located at the *Snail* promoter. The homologue of Twist in the ascidian may be the major activator for the *Snail* gene expression (Erives, Corbo et al. 1998). In breast cancer, the product of human metastasis-associated protein 3 (*MTA3*) gene is identified as a component of Mi-2/NuRD transcription corepressor complex that associates with *Snail* promoter and selectively represses the *Snail* gene expression. Absence of MTA3 results in aberrant expression of Snail, leading to

epithelial cells transformation toward mesenchymal cells (Fujita, Jaye et al. 2004). The NuRD complex regulates gene expression through chromatin remodeling and histone deacetylation; however, the molecular mechanism by which the NuRD complex represses Snail transcription is not fully understood.

1.14 Chromatin Remodeling and Histone Deacetylation

Chromatin remodeling and histone deacetylation is emerging as one of the major mechanisms to regulate gene expression. The tails of histone proteins can be modified by different ways, particularly methylation and acetylation. Histone methylation is often accompanied by DNA methylation. DNA methylation is one of the major apparatus to silence gene transcription; however, the mechanism of methylation-mediated DNA silencing remains ambiguous (Holliday and Pugh 1975; Jones and Taylor 1980). The SWI/SNF complex, known as ATP-dependent chromatin remodeling complex (Wang, Cote et al. 1996; Wang, Xue et al. 1996), is able to stimulate the binding of DNA sequence-specific transcription factors, probably through directly interactions with DNA and changes on DNA topology (Cote, Quinn et al. 1994; Tsukiyama, Becker et al. 1994; Zhang, Ng et al. 1999; Dobosy and Selker 2001). The SWI/SNF complex is propositioned to cooperate with transcription activators to pinpoint the region targeted for nucleosome interruption. The complex subsequently disrupts the contact between DNA and histones to enhance accessibility for transcription factors (Tsukiyama and Wu 1995).

Two classes of multi-protein chromatin remodeling complex include histone acetyltransferases (HAT)/histone deacetylases (HDAC) and histone methyltransferases

(HMT)/histone demethylases (HDMC) are discovered to modify histone tails (Taunton, Hassig et al. 1996; Gray and Teh 2001; Neely and Workman 2002; Kurdistani and Grunstein 2003; Bannister and Kouzarides 2005; Martin and Zhang 2005). Intensive studies demonstrate the function of histone modifications in gene transcription regulation. HDAC1 or 2 is assisted by corepressors, such as silencing mediator of retinoid acid and thyroid hormone receptor (SMRT), nuclear receptor corepressor (N-CoR), Sin3 and other polypeptides to form large protein complexes that target to the promoter region (Alland, Muhle et al. 1997; Hassig, Fleischer et al. 1997; Heinzel, Lavinsky et al. 1997; Nagy, Kao et al. 1997). Therefore, histone modifications and chromatin remodeling complexes are important regulation apparatus of gene expression. Methylation and acetylation of histone proteins are pivotal epigenetic markers in transcriptional regulation.

1.14.1 The NuRD Complex

A series of studies demonstrate that the SWI/SNF chromatin remodeling complex and their mammalian homologue BRG1-or hbrm-associated factors (BAFs) disrupts nucleosomes and facilitates transcription factor accessibility via ATP-dependent chromatin remodeling activities. Searching for additional mammalian chromatin remodeling complex identified the NuRD complex, which has an ATP-dependent chromatin remodeling activity similar to the SWI/SNF complex. Furthermore, this complex also has histone deacetylase activity distinct from previously described SMAT/N-CoR/Sin3/HDAC1 complex. Antibody against the NuRD complex alleviated transcriptional repression (Xue, Wong et al. 1998). The deacetylase activity is stimulated

by ATP, suggesting that chromatin remodeling can contribute to transcriptional repression by facilitating transcription repressors gaining access to chromatin structure.

The NuRD complex is a multi-protein complex containing 8 components. The histone deacetylases HDAC1 and HDAC2 and the histone binding proteins, RbAp48 and RbAp46, form a core complex. The core complex is shared between Sin3-histone deacetylase complexes and the NuRD complex (Zhang, Ng et al. 1999). It is believed that the histone deacetylase activity of the core complex is tightly regulated by other polypeptide members, metastasis-associated protein 2 (MTA2) and the highly related polypeptides, MTA3. Mi-2 and methyl-CpG-binding domain-containing protein 3 (MBD3) are also subunits of the NuRD complex (Zhang, Ng et al. 1999; Fujita, Jaye et al. 2004). MTA2 is highly related to MTA1, whose expression level is elevated in metastatic breast cancer cell lines and tissues (Toh, Pencil et al. 1994; Toh, Oki et al. 1997). Although MTA2 does not affect the histone deacetylase activity, it promotes the assembly of the NuRD complex and is required for the formation of the functional complex (Yao and Yang 2003). Mi-2 is a member of the SWI/SNF helicase/ATPase family, which is proposed to remodel chromatin structure in an ATP-dependent manner (Wang and Zhang 2001). In addition, studies on *Drosophila* Mi-2 demonstrate that dMi-2 recognizes specific DNA sequence (Kehle, Beuchle et al. 1998), suggesting that Mi-2 potentially recruits the NuRD complex to specific genes (Zhang, Ng et al. 1999). Another important component of the NuRD complex is MBD3. Although MBD3 is unlikely to associate with methylated DNA (Saito and Ishikawa 2002), this protein is a splice variant of MBD2, which has been shown to bind to methylated DNA and possess demethylase

activity. Furthermore, MBD3 is demonstrated to link the NuRD complex with MBD2 (Zhang, Ng et al. 1999). It is likely that the DNA binding protein potentially directs the NuRD complex to interact with specific methylated DNA sequences. The novel member of the NuRD complex, MTA3 is proposed as estrogen-dependent component of this gene repressor complex. The *bona fide* function of MTA3 in the complex is unclear (Fujita, Jaye et al. 2004).

Given the functional role of individual components of the NuRD complex, it is likely that the chromatin remodeling and histone deacetylase activities of the NuRD are functionally related. The NuRD complex can be directed to sequence specific methylated DNA and provides gene silencing (Zhang, LeRoy et al. 1998). Thus, the repressed genes targeted by the NuRD are rather general. The cellular function of the NuRD complex is unclear. Based on the observation that MTA2 is vastly expressed in dividing cells, the NuRD complex is proposed to play a role in cell proliferation (Xue, Wong et al. 1998). Data collected from *Caenorhabditis elegans* suggest that the NuRD complex participates in vulval development (Solari and Ahringer 2000). Along with newly identified member of the NuRD complex, MTA3, the NuRD complex is proposed to be recruited to estrogen-dependent genes and suppresses the *Snail* gene expression, which contributes to breast tumor cell invasion and metastasis (Fujita, Jaye et al. 2004). The cellular functions of the NuRD complex are also linked to DNA methylation-mediated gene silencing (Wade, Geggion et al. 1999). However, the defined gene targets of the NuRD complex are beyond fully understood.

1.15 The ATPase Activity in Modulating RNA-RNA, RNA-Protein Interactions.

Most cellular processes, such as biosynthesis of nucleic acid require energy input. ATP is one of the most important energy currencies of the cell. ATPase is a type of enzyme that hydrolyze cellular ATP into adenosine diphosphate (ADP) and a free phosphor group. The energy released from this chemical reaction can be coupled to wide-range cellular processes. For instance, trans-membrane ATPases import metabolic nutrients and export wastes to maintain cell metabolism. Na, K-ATPase (sodium pump) that balances Na^+ and K^+ ions across the plasma membrane belongs to P-type ATPase. Another type of ATPase in eukaryote is F-type that pumps H^+ out of mitochondria using the energy of ATP decomposition.

Another large family of ATPase is helicase. DNA helicases and RNA helicases play important roles in DNA and RNA metabolism, including DNA replication, recombination, transcription, DNA repair, translation and pre-mRNA splicing. The common features of helicase are NTP-binding and hydrolysis, nucleic acid-binding and energy-dependent nucleic acid unwinding (Hall and Matson 1999). Structure-function analyses reveal that there are a set of highly conserved helicase motifs clustered together to form ATP hydrolyzing pocket and nucleic acid-binding site (Luking, Stahl et al. 1998). Using energy derived from ATP hydrolysis, these conserved motifs create an energy-driven motor to unwind nucleic acids duplex or to modulate nucleic acid-protein interactions during multiple cellular process. These motifs are probably shared by the ATPases participating in chromatin remodeling and provide essential energy to modulate protein-DNA interactions and chromatin structure (Hall and Matson 1999).

Although the chemical reaction of the pre-mRNA splicing catalyzed by the spliceosome does not require energy consumption (Moore and Sharp 1993), the ATPase activity is crucial for moderating the extensive RNA-RNA and RNA-protein interactions rearrangement during the pre-mRNA splicing. Several spliceosome-associated DEAD-box proteins exhibit single-stranded RNA-stimulated ATPase activity and are required for distinct steps of splicing (Hamm and Lamond 1998). The yeast proteins Prp16 and Prp22 have been described to disrupt RNA base pairs *in vitro* and induce RNA conformational change. The Prp22 is shown to be able to mediate the dissociation of splicing factor from mRNA substrate in an ATP-dependent reaction (Schwer and Gross 1998).

Because many RNA-RNA duplex in the spliceosome complex are short and may require proteins binding for stabilization, the substrate of some RNA helicases may be protein(s) that binds to RNA (Mount, Pettersson et al. 1983; Auble, Wang et al. 1997; Staley and Guthrie 1998). It is possible that the RNA-RNA unwinding during the splicing process is an indirect consequence of disruption of RNA-protein interactions. Members of DEAD-box proteins that have weak or non-detectable RNA-stimulated ATPase are plausible candidates as protein-stimulated ATPases (Staley and Guthrie 1998). Recent reports evidence that DEAD-box proteins rearrange RNA-protein interactions and catalyze protein displacement independent of RNA-RNA duplex (Chen, Stands et al. 2001; Jankowsky, Gross et al. 2001; Kistler and Guthrie 2001; Fairman, Maroney et al. 2004). Prp28p is demonstrated to counteract the effect of spliceosomal protein U1-C protein in stabilizing U1 snRNA-5' splice site duplex, thereby, promoting the dissociation of these

RNA-RNA base pairs (Chen, Stands et al. 2001). Vaccinia virus DEAD-box protein NPH-II displaces U1A from RNA in an ATP-dependent manner, supporting a model of coupling ATP hydrolysis to ribonucleoprotein assembly and reorganization (Jankowsky, Gross et al. 2001). Studies from two different model systems demonstrate that DEAD-box proteins work on single-stranded RNA and displace the complementary nucleic acid or protein in an ATP-dependent fashion (Fairman, Maroney et al. 2004). Therefore, the functions of DEAD-box proteins are not restricted to RNA-RNA duplex, but can act on wide range of substrates.

Chromatin remodeling mediated by yeast SWI/SNF, *Drosophila* NURF and their mammalian homologue complexes has been proposed as an important device to regulate DNA replication, DNA repair and gene transcription. Most of these complexes contain subunits that are closely related to the SWI2/SNF2 proteins, which belong to a family of NTP-binding proteins (Eisen, Sweder et al. 1995). Thus, the NTP-binding subunits are proposed to act as energy-driven motors to alter DNA-histone interactions and chromatin structure. Although SWI2/SNF2 and related proteins belong to the same family of DNA and RNA helicase, they are unlikely to unwind nucleic acid duplex. However, DNA-stimulated ATPase activity is required for their chromatin remodeling activities *in vivo* and *in vitro* (Cote, Quinn et al. 1994). Similar to superfamily II helicases, the SWI2/SNF2-like proteins harbor a set of seven conserved motifs, in which motif I, Ia, II and III are required for ATP binding and hydrolysis (Eisen, Sweder et al. 1995). The remodeling activity of the SWI/SNF complex can be directed to specific promoter sequence by interacting with a variety of gene-specific transcriptional activators.

Nevertheless, how the SWI/SNF complex utilizes energy derived from ATP hydrolyzation to alter chromatin conformation is still unknown. Motif V has been suggested to couple ATP hydrolysis to chromatin-remodeling activities in recent studies (Smith and Peterson 2005). Mi-2 is responsible for the chromatin remodeling activity processed by the NuRD complex (Zhang, LeRoy et al. 1998). Sequence analyses suggest that Mi-2 belongs to the SWI2/SNF2 helicase family and has potential ATPase-dependent nucleosomes remodeling activity (Seelig, Moosbrugger et al. 1995). Supporting this prediction, recombinant Mi-2 exhibits DNA-dependent ATPase activity. More importantly, recombinant Mi-2 disrupts the interactions of DNA and histone in an ATP-dependent fashion (Wang and Zhang 2001).

In general, ATPases participate in a number of cellular processes. The ATPase activities of this family of proteins are utilized to unwind or disrupt DNA/RNA duplex, RNA-protein and histone-DNA interactions. Given the highly conserved motif structure between the DNA/RNA helicase and the SWI2/SNF2 type ATPase, it is possible that one energy-driven motor is employed on different substrates. However, to select the specific substrate, on which the ATPase enzyme works, requires regulatory domains or additional adaptor proteins. Epigenetic modifications, such as phosphorylation, or ubiquitination will be remarkably important to regulate the activities of ATPases and ATPase containing complexes.

1.16 Tyrosine Phosphorylated p68 Promotes EMT

The human p68 is tyrosine phosphorylated exclusively in tumor tissue samples and the phosphorylation is undetectable in extracts of normal tissue samples (Yang, Lin et al. 2005). The exclusively tyrosine phosphorylation of p68 in tumor tissue and cell lines is intriguing. p68 RNA helicase is ubiquitously expressed (Heinlein 1998) and essential for maintaining normal cell growth (Ford, Anton et al. 1988). The protein is suggested to be required for tissue differentiation and maturation in fetus (Stevenson, Hamilton et al. 1998). In consistency, experiments in our laboratory demonstrated that p68 expresses at a higher level in embryonic cell lines HEK293 (human embryonic kidney 293) and HEL299 (human embryonic lung 299) (Yang, Lin et al. 2005). Therefore, it is speculated that tyrosyl phosphorylation of p68 is not associated with normal cell growth and maintenance. Tyrosyl phosphorylation of p68 affects the function of p68 RNA helicase in the pre-mRNA splicing process (Yang, Lin et al. 2005), suggesting that the biological function of p68 may be altered in cancer cells by tyrosyl phosphorylation.

Cellular signals that induce tyrosyl phosphorylation of p68 remain elusive. c-Abl tyrosine kinase is considered as aberrantly activated in leukemia and other cancer types (Konopka, Watanabe et al. 1984). Activated c-Abl is in part responsible for abnormal tyrosyl phosphorylation of p68 in cancer cells based on the evidence that c-Abl is one of the kinase to phosphorylate p68. PDGF stimulation activates the cellular c-Abl (Plattner, Kadlec et al. 1999). Thus, experimental data and those from other research laboratories suggest that PDGF maybe one of the signal molecules to induce tyrosyl phosphorylation

of p68. Further studies are necessary for an in depth understanding on regulation of p68 phosphorylation. In addition, p68 has been reported to be poly-ubiquitinated in colorectal tumors (Causevic, Hislop et al. 2001). Thus, it is possible that other types of post-translational modifications, such as methylation, acetylation and ubiquitination affect the biological roles of DEAD-box protein p68.

Although p68 RNA helicase is indicated to be essential for the pre-mRNA splicing both *in vitro* (Liu 2002) and *in vivo* (Lin, Yang et al. 2005), how phosphorylation influences the functional role of p68 is not understood. PDGF treatment of HT-29 cells, a human colorectal tumor cell line, in which p68 is not phosphorylated, induces changes on cell morphology from typical cobble-stone shape to fibroblast like phenotype. This observation sheds light on the possibility that phosphorylated p68 RNA helicase may play a role in epithelial-mesenchymal transition. Examinations on epithelial markers and mesenchymal markers expression in HT-29 cells before and after PDGF treatment confirm the PDGF-induced EMT. Strikingly, overexpression of unphosphorylatable mutant Y593F (Tyrosine → Phenylalanine) abolishes this transition, suggesting the essential role of phosphorylated p68 in EMT. Experiments from our laboratory also confirmed the fundamental position of c-Abl in promotion of EMT process. Treatment of STI-571, a c-Abl inhibitor, abolishes the PDGF-induced p68-mediated tumor cell EMT.

1.17 The Molecular Basis of p68-mediated EMT

Although p68 has been suggested acting as a transcriptional coactivator/corepressor (Endoh, Maruyama et al. 1999; Rossow and Janknecht 2003; Wilson, Bates

et al. 2004; Bates, Nicol et al. 2005), the detailed function of p68 in transcriptional regulation is not known. Due to tyrosyl phosphorylation of p68 in tumor cells, great efforts are made to identify interacting partners of phosphorylated p68 RNA helicase. Both co-immunoprecipitation and His-tag pull down assays demonstrated that β -catenin (a membrane-binding protein) bound p68 directly (Yang, 2006, in preparation). p68 RNA helicase was further demonstrated to be indispensable for β -catenin-dependent gene transcription and cell proliferation. These data lead to a conclusion that p68 promotes cell proliferation and tissue growth, which is consistent with previous studies (Ford, Anton et al. 1988). It is known that β -catenin disassociates from cadherin-dependent junction complex and subsequently translocates into nucleus during EMT (Thiery 2002). The experiments from our laboratory further showed that the tyrosyl phosphorylated p68 interacted with β -catenin in nucleus and the phosphorylated p68 promoted β -catenin translocation. There are two possible explanations for the observed phenomena: (1) the β -catenin nuclear localization is due to p68-mediated downregulation of cadherin proteins; (2) p68 promoted β -catenin nuclear translocation induces EMT and represses E-cadherin expression. Experiments by overexpression/knockdown E-cadherin indicated that decrease in E-cadherin did not significantly enhance β -catenin nuclear translocation. Interestingly, β -catenin was required for p68-mediated E-cadherin downregulation. Furthermore, nuclear β -catenin was obligatory for this E-cadherin repression. Taken together, a novel signaling axis by which phosphorylated p68 RNA helicase promoted β -catenin nuclear translocation was discovered. The nuclear β -catenin

was subsequently engaged in transcriptional programs that control EMT. Nevertheless, the molecular mechanism by which tyrosyl phosphorylated p68 promoting EMT is far away from fully understood.

1.18 Aims of Dissertation

The purpose of this dissertation is to study the molecular basis of cellular processes and transcriptional regulation by p68 and phosphorylation of p68.

I investigated the effects of mutations in conserved helicase core regions of p68 RNA helicase, which abolished the ATPase and helicase activities of p68 in the pre-mRNA splicing process. These p68 mutants abolished the pre-mRNA splicing *in vitro* and *in vivo*. p68 RNA helicase was demonstrated to unwind the U1 snRNA-5'ss RNA duplex and promote the spliceosome assembly. Furthermore, my studies showed that structure role of p68 RNA helicase in bridging the load of U4/U6•U5 tri-snRNP to the pre-spliceosome to form the spliceosome independent of ATPase activity. These findings highlighted the essential role of p68 in the pre-mRNA splicing.

I demonstrated the central role of p68 in downregulation of E-cadherin in colorectal tumor cells; explored the potential signal molecules that induce tyrosyl phosphorylation of p68 in aggressive tumor cell lines; pursued the target of p68 in transcription modulation; and identified a multi-protein complex associated with p68 to direct the downregulation of E-cadherin and initiation of EMT. Most importantly, I discovered an innovative mechanism to modulate protein-protein interactions in an energy-driven fashion. Phosphorylation of p68 RNA helicase at Y593 activated the

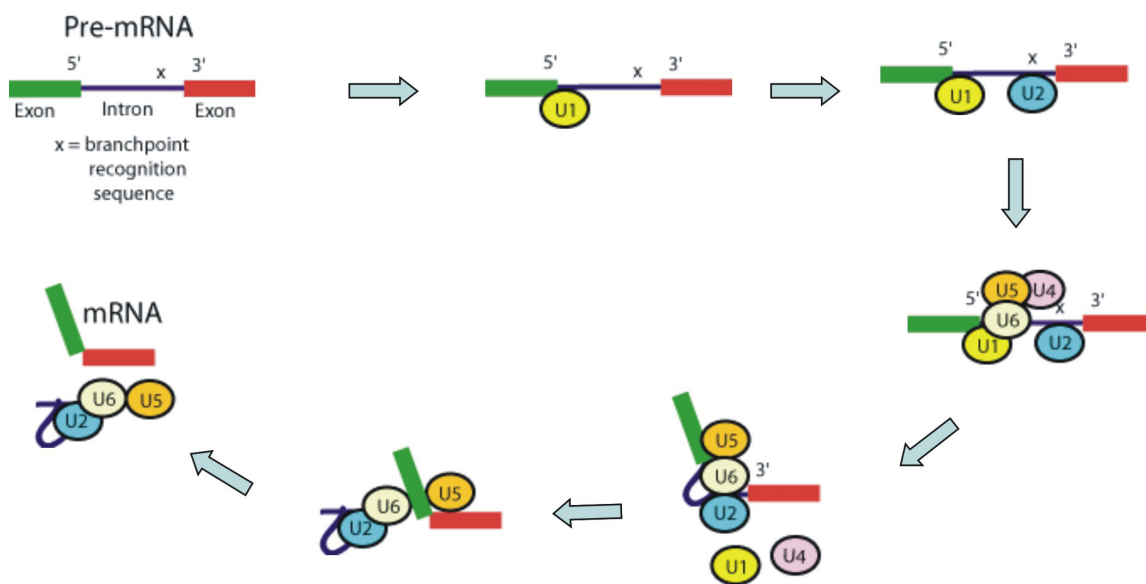
transcription of the *Snail* gene by displacing HDAC1 from the nuclear remodeling and deacetylation complex at the *Snail* promoter using its protein-dependent ATPase motor. Thus, my data demonstrated an example that a DEAD-box RNA helicases can function as a protein “unwindase” to modulate protein-protein interactions in a bio-macromolecular machinery.

The studies within this dissertation not only highlighted the essential and structure role of p68 RNA helicase in the pre-mRNA splicing process *in vitro* and *in vivo*, but also provided insight in the molecular basis of p68 as transcription coactivator, which has been long thought. Most importantly, I discovered the first example of RNA helicase modulating protein-protein interactions through an energy driven motor to direct transcriptional machinery. Discovery of this novel apparatus situated DEAD-box RNA helicase in the central position of multiple cellular processes and opened up new deliberation on every step of signaling transduction pathways.

Figure I-1 The pre-mRNA splicing process.

The dynamic model represents the pre-mRNA splicing process. The 5'ss is first recognized by the U1 snRNP. Recruitment of the U2 snRNP to the branch point leads to the formation of complex A, or the pre-spliceosome. At this point, a pre-formed U4/U6•U5 tri-snRNPs will join into the pre-spliceosome, leading to the formation of the spliceosome complex B. Next, by remodeling RNA-protein and RNA-RNA interactions, U1 and U4 snRNP are released from the spliceosome complex and catalytically competent complex C is formed. Finally, a two step chemical reaction is catalyzed by the spliceosome to remove the introns from the pre-mRNA and join the exons.

Figure I-1

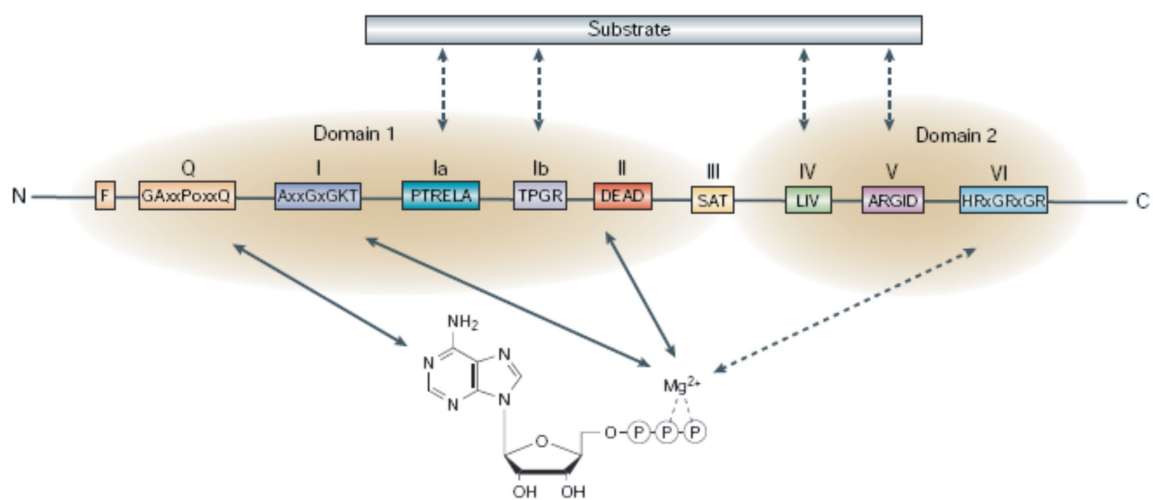


Klein Gunnewiek, JM et al., *Clin Exp Rheum* 1997;15:549-560

Figure I-2. The conserved domain structure of DEAD-box protein.

The DEAD-box proteins are highly conserved in eight conserved motifs within helicase core. These conserved motifs are related to ATP hydrolysis, substrate binding or helicase activity. Motif I, II of domain I and motif VI of domain II consist part of the ATP-binding site, whereas motifs Ia, Ib, IV, and V are in the process of RNA binding.

Figure I-2

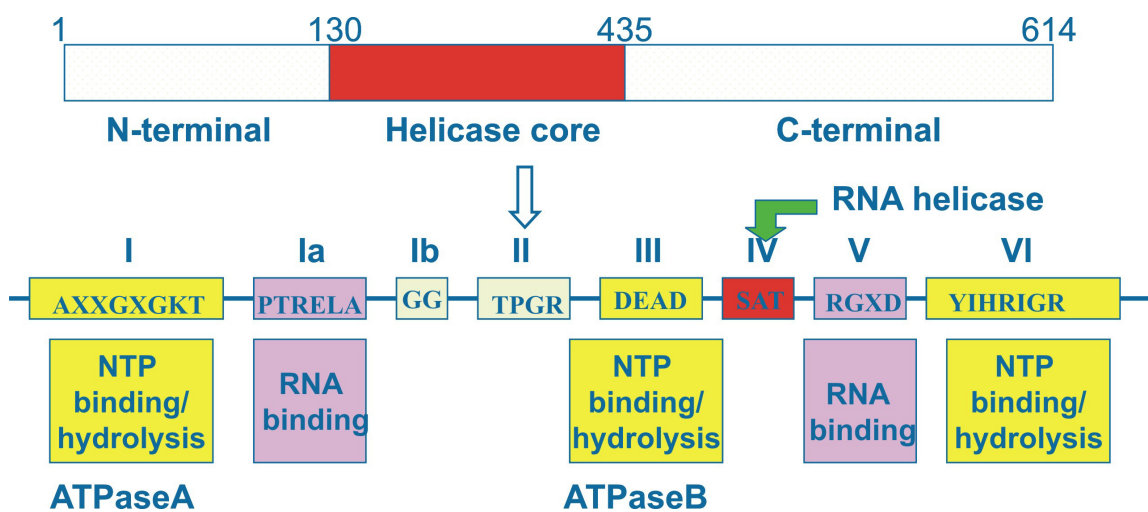


Sanda Rocak and Patrick Linder *Nature Review Mol. Cell Biol.*, 2004

Figure I-3. Schematic illustration of domain structure of p68 RNA helicase.

The lower panel represents the helicase-core region of DEAD-box proteins. Motifs AXXGXGKT, TPGR and DEAD comprise the nucleotide triphosphate (NTP)-binding and hydrolysis domains. SAT motif links NTP hydrolysis with unwinding activity. RGXD represents the substrate-binding motif. HRIGRXXR motif binds RNA.

Figure I-3



CHAPTER II

ATPASE/HELICASE ACTIVITIES OF p68 RNA HELICASE ARE REQUIRED FOR THE PRE-MRNA SPLICING BUT NOT FOR ASSEMBLY OF THE SPLICEOSOME

2.1 Abstract

We have previously demonstrated that p68 RNA helicase as an essential human splicing factor acts at the U1 snRNA and 5'splicing site duplex (5'ss) in the pre-mRNA splicing process. To further analyze the function of p68 in the spliceosome, we generated two p68 mutants (Motif III, RGLD → LGLD and Motif VI, HRIG → HLIGR). ATPase and RNA unwinding assays demonstrated that the mutations abolished the RNA-dependent ATPase activity and RNA unwinding activity. The function of p68 in the spliceosome was abolished by the mutations and the mutations also inhibited the dissociation of the U1 from the 5'ss, while the mutants still interacted with the U1:5'ss duplex. Interestingly, the non-active p68 mutants did not prevent the transition from the pre-spliceosome to the spliceosome. The data suggested that p68 RNA helicase might actively unwind the U1:5'ss duplex. The protein might also play a role in the U4/U6•U5 addition, which did not require the ATPase and RNA unwinding activities of p68. In addition, we presented evidence here to demonstrate the functional role of p68 RNA helicase in the pre-mRNA splicing process *in vivo*. Our experiments also showed that p68 interacted with unspliced but not spliced mRNA *in vivo*.

2.2 Introduction

Messenger RNA precursors (pre-mRNA) are spliced in a large RNA-protein complex, the spliceosome (Moore and Sharp 1993; Sharp 1994). The spliceosome assembly requires precise recognition each of the splice site, namely the 5' splice site (5'ss), branch point (BP) and 3' splice site (3'ss). Assembly of a functional spliceosome proceeds through an ordered addition of four small nuclear ribonucleoprotein particles (snRNPs) (U1, U2, U4/U6 and U5) as well as many non-snRNP proteins. This pathway leads to the formation of several intermediate spliceosome complexes. Recognition of the 5'ss by the U1 snRNP, along with binding of the polypyrimidine tract and the branch point by U2AF and SF1 results in the formation of the commitment complex. Recruitment of the U2 snRNP to the commitment complex leads to the formation of complex A, or the pre-spliceosome. At this point, the pre-formed U4/U6•U5 tri-snRNP will join into the pre-spliceosome, leading to the formation of the spliceosome (Hodges and Beggs 1994; Madhani and Guthrie 1994; Abovich and Rosbash 1997). After an extensive rearrangement, a two step chemical reaction is catalyzed by the spliceosome to remove the intron from the pre-mRNA.

The pre-mRNA splicing is remarkably accurate. The splicing accuracy is achieved by inspection of the individual splice site multiple times by multiple factors (Nasim, Chowdhury et al. 2002). Recognition of the 5' splice site is an early event in the pre-mRNA splicing process. The 5'ss is recognized by 5 – 7 base pair interactions between the 5'ss and 5'-end of the U1 snRNA (Staley and Guthrie 1998). Recent studies suggest that prior to the recognition of the 5'ss by the U1:5'ss RNA-RNA base pair

interactions the 5'ss is recognized by a protein factor, the U1 snRNP protein U1C. It is believed that binding of U1C to the 5'ss helps the base pair interactions between the U1 and the 5'ss (Will, Rumppler et al. 1996; Chen, Stands et al. 2001). The U1:5'ss duplex is unwound to expose the same 5'ss sequence for pairing with the U6 snRNA prior to the first step chemical reaction of splicing (Madhani and Guthrie 1994; Madhani and Guthrie 1994). However, before the U1:5'ss unwinding, the U4/U6•U5 tri-snRNP must be added to the pre-spliceosome. Presumably, addition of the tri-snRNP, unwinding the U1:5'ss duplex and the formation of the U6:5'ss duplex must be tightly coupled.

The multiple step procedure of recognition of a splice site in the spliceosome involves the formation and remodeling of a number of RNA-RNA and RNA-protein interactions (Staley and Guthrie 1998; Singh 2002; Jurica and Moore 2003). It is generally believed that remodeling the complex RNA-RNA and RNA-protein interactions in the spliceosome is catalyzed by a family of DEAD/DExH box putative RNA helicases (Schwer 2001; Will and Luhrmann 2001). The RNA helicases unwind RNA-RNA base pairing (Staley and Guthrie 1998) and RNA-protein interactions (Staley and Guthrie 1998; Singh 2002) at the expense of the energy derived from ATP hydrolysis. To date, eight yeast splicing factors and six mammalian proteins that are homologous to the superfamily of RNA helicases have been implicated in the pre-mRNA splicing (Hamm and Lamond 1998; Luking, Stahl et al. 1998; Schwer 2001; Will and Luhrmann 2001). Many of these proteins have demonstrated RNA unwinding activities *in vitro* (Laggerbauer, Achsel et al. 1998; Raghunathan and Guthrie 1998; Wang, Wagner et al. 1998; Schwer and Meszaros 2000). These putative RNA helicases are involved in

every step of the pre-mRNA splicing process, including unwinding the U1:5'ss duplex, unwinding the U4/U6 RNA helices, dissociation of the protein-RNA interactions at the branch point to promote the U2 – Branch point interactions and dissociation of the spliced mRNA from the spliceosome.

The nuclear p68 RNA helicase was first identified by cross-reaction with a monoclonal antibody PAb204 that was originally raised against SV40 large T-antigen two decades ago (Crawford, Leppard et al. 1982, Lane, 1980 #81). The protein is a prototypical member of the DEAD-box family of RNA helicases. As an early example of a cellular RNA helicase, the ATPase and the RNA unwinding activities of p68 RNA helicase were documented with the protein that was purified from human 293 cells (Iggo and Lane 1989, Ford, 1988 #66, Hirling, 1989 #73). It has been suggested that p68 RNA helicase might be involved in transcription regulation (Endoh, Maruyama et al. 1999; Watanabe, Yanagisawa et al. 2001; Fujita, Kobayashi et al. 2003; Rossow and Janknecht 2003) and DNA damage-repair pathways (Jost, Schwarz et al. 1999). Most recently, the experiments carried out in our laboratory demonstrated that p68 RNA helicase is an essential human splicing factor *in vitro* that plays a role in unwinding the transient U1:5' splice site duplex (Liu, Sargueil et al. 1998; Liu 2002). Consistently, by large-scale proteomic analyses of human spliceosome, other research laboratories also suggested the existence of p68 RNA helicase in the human spliceosome (Hartmuth, Urlaub et al. 2002; Honig, Auboeuf et al. 2002; Jurica, Licklider et al. 2002; Rappsilber, Ryder et al. 2002; Zhou, Licklider et al. 2002; Guil, Gattoni et al. 2003).

In this report, we used two p68 mutants that lack ATPase and RNA unwinding activities. The *in vitro* splicing assays show that the function of p68 in the spliceosome is abolished by the mutations. Our experiments also show that the mutations inhibit the dissociation of the U1 from the 5'ss, while the mutants still interact with the U1:5'ss duplex. Our results strongly suggest that p68 RNA helicase unwinds the transient U1:5'ss duplex during the spliceosome assembly process. Interestingly, the non-active p68 mutants do not prevent the transition from pre-spliceosome to the spliceosome. The mutants are also successfully assembled into both the pre-spliceosome and the spliceosome. Given our previous observation that depletion of p68 RNA helicase from HeLa nuclear extracts inhibited the pre-spliceosome to the spliceosome transition, our data indicated that p68 RNA helicase may play a role in the U4/U6•U5 addition, which does not require the ATPase and RNA unwinding activities of p68. Although previous data demonstrated the functional role of p68 in the *in vitro* pre-mRNA splicing process, whether p68 also plays a role in the pre-mRNA splicing process *in vivo* remains a question. We examined the pre-mRNA splicing efficiency in HeLa cells where p68 RNA helicase was knocked down by RNA interference (RNAi). Our data demonstrated that p68 RNA helicase plays a role in the pre-mRNA splicing *in vivo*.

2.3 Results

2.3.1 p68 Mutants Lack ATPase and RNA Unwinding Activities.

p68 RNA helicase is an essential human splicing factor in HeLa nuclear extracts (Liu 2002). The protein was detected interacting with the transient U1:5' splice site

duplex (Liu, Sargueil et al. 1998). It is thus suggested that p68 RNA helicase functions to unwind the RNA duplex during the spliceosome assembly process. If p68 actively unwinds the U1:5'ss duplex, we reasoned that ATPase and RNA unwinding activities must be essential for the function of the protein in the spliceosome. To test this conjecture, two p68 RNA helicase mutants were generated (**Figure II-1A**). The first mutant carried a mutation at the consensus sequence motif IV RGLD in the helicase-core region. The first R was changed to an L (ref to as LGLD). The second mutant carried a mutation at the conserved sequence motif VI HRIGRXXR. The second R was changed to an L (ref to as HLIGR). The wild type p68 and two mutants were expressed in bacteria *E. coli*. Three recombinant proteins were purified by a two column procedure (materials and methods) (**Figure II-1B**). ATP crosslinking, ATPase and RNA unwinding assays were carried out to characterize the expressed wild type and p68 mutants. Since the bacterially expressed recombinant p68 and mutants were phosphorylated at serine/threonine and tyrosine residues (Yang, Yang et al. 2004), the proteins were dephosphorylated by PP2A and PTP1B prior to the ATP crosslinking, ATPase and RNA unwinding analyses. Western blot with antibodies against specific phosphor-amino acids, phosphoserine, phosphothreonine and phosphotyrosine, showed that dephosphorylation of p68 was complete to an undetectable level (data not shown). ATP crosslinking with dephosphorylated p68 wild type and mutant showed that ATP binding was not affected by the mutations (**Figure II-1C**). ATPase assays demonstrated that these two mutations completely abolished the ATPase activity of p68 RNA helicase (**Figure II-1E**). RNA unwinding activity of wild type p68 and mutants was examined with a partial double-

stranded RNA (dsRNA) containing a short RNA duplex (~22 bp in length) and long 186 nt and 88 nt 3' overhangs on both sides (Huang and Liu 2002). The experiments indicated that the wild type p68 unwound the dsRNA. However, the two mutants were unable to unwind the dsRNA (**Figure II-1D**).

2.3.2 p68 Mutants that Lack ATPase and Helicase Activities do not Support the Pre-mRNA Splicing.

Next, we examined the effects of the mutations on the function of p68 in the pre-mRNA splicing process. We previously demonstrated that the bacterially expressed recombinant p68 RNA helicase was phosphorylated at serine/threonine and tyrosine residues (Yang, Yang et al. 2004). We observed that only the tyrosyl phosphorylation affected the function of p68 in the pre-mRNA splicing (Yang, In-press 2005). To obtain the recombinant p68 and mutants without tyrosine phosphorylations, the bacterially expressed recombinant proteins were dephosphorylated by PTP1B. Dephosphorylation of p68 was complete as indicated by western blot with a monoclonal antibody PY20 (data not shown). The dephosphorylated proteins were separated from the added protein phosphatase by Ni-NTA micro column. After elution and micro-dialysis, the dephosphorylated proteins were added to HeLa nuclear extracts in which p68 was immunodepleted. Splicing activity of the reconstituted HeLa nuclear extracts was examined with splicing substrate pPIP10A. It was evident that the splicing activity of the p68 depleted HeLa nuclear extracts was restored by addition of wild type recombinant p68 (**Figure II-2, lane 3**). On the other hand, the splicing activity was not recovered by

addition of the two p68 mutants to the HeLa extracts (**Figure II-2, lanes 4 & 5**). The results indicated that the mutations that abolished the ATPase and RNA unwinding activities of p68 also abolished the function of the protein in the pre-mRNA splicing process.

2.3.3 p68 Mutants that Lack ATPase and RNA Unwinding Activities Interact with the U1:5'ss Duplex but do not Support the Dissociation of the U1 from the 5' Splice Site.

In a previous report, we demonstrated that depletion of p68 RNA helicase from HeLa nuclear extracts inhibited the dissociation of the U1 from the 5'ss (Liu 2002). We reasoned that, if p68 RNA helicase is involved in unwinding the U1:5'ss duplex, the ATPase and RNA unwinding activities of the protein must be required for this action. To test this conjecture, we monitored the U1 – 5'ss RNA-RNA interactions in the p68 depleted HeLa nuclear extracts supplemented with p68 wild type or the two mutants. The trioxsalen crosslinking experiment similar to that described in our previous report was employed to analyze the U1 – 5'ss interactions (Liu 2002). The splicing substrate pPIP10A was used for our *in vitro* splicing. Crosslinks of the U1 snRNA to the pre-mRNA occurred in the intact HeLa nuclear extracts at 15 minutes time point (**Figure II-3A, lane 3**). The crosslinking signal completely disappeared after 180 minutes splicing (**Figure II-3A, lane 2**). When the p68 depleted HeLa nuclear extracts were supplemented with wild type recombinant p68 RNA helicase, the U1 – 5'ss crosslinks signal was very weak, even at the 5 minutes time point (**Figure II-3A, lane 11**) and almost completely

disappeared after 90 minutes (**Figure II-3A**, lane 14). In contrast, the pre-mRNA:U1 snRNA crosslinks remained almost constant in the same splicing time course in the HeLa nuclear extracts that were supplemented with the p68 mutants (**Figure II-3A**, lane 6 - 10 and 16 - 20). The data suggested that the dissociation of U1 from the 5'ss was inhibited by the mutations of p68 RNA helicase that abolished the ATPase and RNA unwinding activities of the protein.

p68 RNA helicase was first detected interacting with the transient U1:5'ss duplex by a methylene blue mediated RNA-protein crosslinking method (Liu, Wilkie et al. 1996; Liu 2002). The recombinant protein was also crosslinked to this short RNA duplex during the spliceosome assembly process (Liu 2002). We questioned whether these two p68 mutants that did not support splicing would interact with the U1:5'ss duplex during the spliceosome assembly. To this end, we employed the same MB crosslinking method to examine the interactions of the p68 mutants with the U1:5'ss duplex. Since the strongest p68 crosslinking signals were obtained with the splicing substrate GC+DX (a derivative from α -tropomyosin), the splicing substrate GC+DX was used in our experiments. Similar to our previous observations, a crosslinking band that co-migrated at about 65 kDa was detected in the p68 depleted HeLa nuclear extracts supplemented with p68 wild type or mutants (**Figure II-4A**). The crosslinks to the wt p68 reached maximum at about 10 minutes and decreased thereafter (**Figure II-4A**, left panel). However, the crosslinks to two mutants did not decrease over a 180 minutes time course (**Figure II-4A**, middle and right panels). Since the crosslinking band was precipitated by Ni-NTA column, this

indicated that recombinant p68 crosslinked to the U1:5'ss duplex (data not shown). The identity of this crosslinking band was further verified by immunoprecipitation of this crosslinking band with an antibody against 6xhis-tag (data not shown). To exclude the possibility that the different MB crosslinks was due the different amount of recombinant p68s (wt/mutant) added to the extracts, we immunoblotted the same MB crosslinking SDS-PAGE using anti-p68 antibody. The results showed that roughly the same amount of p68 (wt/mutant) was added to the crosslinking extracts (**Figure II-4B**).

2.3.4 The ATPase and RNA Unwinding Activities of p68 are not Required for the Assembly of the Spliceosome.

In the spliceosome assembly pathway, unwinding the U1:5'ss duplex must be tightly coupled with the addition of the U4/U6•U5 tri-snRNP. In our previous report, we demonstrated that depletion of p68 RNA helicase from HeLa nuclear extracts blocked the transition from the pre-spliceosome to the spliceosome (Liu 2002). In this study, we endeavored to examine the effects of p68 mutations on the spliceosome assembly. We employed native-gel electrophoresis to analyze the spliceosome complex formation in the p68 depleted HeLa nuclear extracts supplemented with recombinant p68 wt/mutant. The spliceosome complexes were assembled on the splicing substrate pPIP10A. It was evident that the spliceosome complexes A and B/C were assembled normally in intact HeLa nuclear extracts (**Figure II-5A**, lane 1). Consistent with our previous report, the formation of B/C complex was inhibited by p68 depletion (**Figure II-5A**, lane 2). Addition of wt p68 to the p68 depleted extracts restored the spliceosome complexes

assembly (**Figure II-5A**, lane 3). Interestingly, assembly of A and B/C complexes was not affected in the presence of p68 mutants that lacked ATPase and RNA unwinding activities (**Figure II-5A**, lane 4 & 5). To further elucidate the effects of mutation of p68 on the spliceosome assembly, we probed the assembly of the recombinant p68 wt/mutant in the spliceosome complexes by immunoblot. Since the recombinant proteins carried a His-tag, a commercially available monoclonal antibody against 6xhis was used in the immunoblot experiments. Our experiments showed that the recombinant wild type p68 and mutants were assembled into the A and B/C complexes (**Figure II-5B**, lanes 2, 3, 4).

To further analyze the effects of the mutations of p68 on the spliceosome complexes assembly, we monitored the complexes assembly in p68 depleted HeLa nuclear extracts. The p68, wt or mutants, was added to the p68 depleted extracts. The spliceosome complexes were assembled on the PIP10A in a time course and analyzed by native PAGE. It was evident that the assembly of the A and B complexes was not significantly affected in the presence p68, wt or mutant, in the time course of 30 minutes (**Figure II-5C**) with a slightly faster kinetics in the presence of p68 wild-type compared to that in the presence of mutant (data not shown, **Figure II-5C**). However, it was clear that there were significant decreases in the E/H and A, B/C complexes in the presence of wild-type p68 compared to that in the presence of mutant at 120 minutes time point (**Figure II-5C**). A decrease in E/H complex but not A, B/C complexes was observed in the presence of mutant (**Figure II-5C**). The data again indicated that the mutations of p68 did not affect the assembly of the spliceosome but affected the subsequent steps of the pre-mRNA splicing process.

2.3.5 P68 RNA helicase affected the pre-mRNA splicing *in vivo*.

p68 was shown to be an essential splicing factor in HeLa nuclear extracts. To analyze the functional role of p68 RNA helicase in the pre-mRNA splicing process *in vivo*, we employed RNA interference (RNAi) technique to knock down the endogenous p68 in HT-29 cells, a colon cancer cell line. Immunoblot demonstrated that the cellular level of p68 was reduced by over 90% by the RNAi knock down (**Figure II-6A**). The pre-mRNA splicing activity in p68 knock down cells was examined. We used a construct developed by Nasim, Md.T. and colleagues (Nasim, Chowdhury et al. 2002). This construct used a double reporter system to assay the changes in the ratio of spliced and total mRNA in the mammalian cells. It was evident that the ratio of spliced/total mRNA was dramatically reduced in p68 knock down cells (**Figure II-6B**). Exogenous expression of p68 wild-type in the p68 knock down HT-29 cells completely recovered the splicing (**Figure II-6B**). However, expression of HLIGR or LGLD mutant did not result in any splicing activity recovery (**Figure II-6B**).

The effects of p68 RNA helicase on the pre-mRNA splicing process in cells were further examined by probing the spliced or unspliced mRNA of endogenous Actin- β and GAPDH genes in HT-29 cells where the p68 RNA helicase was knocked down and p68 wt/mutant was expressed. The spliced or unspliced mRNA was probed by RT-PCR using primer targeting exon 4 and intron 4 or exon 4 and exon 5 of both genes. To eliminate the effects other than the pre-mRNA splicing, we used intronless histone H2A gene as a

control to normalize the RT-PCR products under different conditions. It was clear that knock down p68 RNA helicase led to accumulation of large amounts of unspliced mRNA of both Actin- β and GAPDH genes (**Figure II-6, C & D**). Under over-exposure conditions, a very faint band corresponding to spliced mRNA could be visualized in the p68 knock down cells (Data not shown). There was a larger accumulation of unspliced mRNA in HT-29 cells in which the non-active p68 mutant LGLD or HLIGR was expressed in p68 knock down cells (**Figure II-6, C & D**). However, the accumulation of unspliced mRNA disappeared in the p68 knock down cells in which the p68 wild-type was expressed. In fact, expression of wild-type p68 in the p68 knock down cells promoted the pre-mRNA splicing to some degree (**Figure II-6, C & D**). The result was consistent with the observations of the above double reporter assay.

Furthermore, we analyzed the effects of p68 RNA helicase on the pre-mRNA splicing process by RNA immunoprecipitation (RNA-IP) (Gilbert, Kristjuhan et al. 2004). The HA-p68, wild-type or HLIGR mutant, was expressed in HT-29 cells. The RNAs were precipitated by HA-antibody. It was clear that significant amounts of unspliced mRNA (both Actin- β and GAPDH) co-precipitated with the non-active p68 mutant HLIGR, while no detectable unspliced mRNA precipitated with wild-type HA-p68 in both the Actin- β and GAPDH cases (**Figure II-7C**). On the other hand, the p68, wt or HLIGR, did not interact with spliced mRNA as demonstrated by RT-PCR of RNA-IP using primers cross exon 4 and exon 5 of both genes (**Figure II-7C**). The results

provided the *in vivo* evidence that p68 RNA helicase interacted with pre-mRNA in both Actin- β and GAPDH cases.

Interestingly, we repeatedly observed the co-precipitation of p68 wild-type and mutant with histone mRNA in the RNA-IP experiments (**Figure II-7D**). There was no significant difference in the precipitation of histone mRNA by HA-p68, wild-type or mutant. To determine whether the co-precipitation of p68 with histone mRNA was histone mRNA specific, we carried out the RNA-IP experiments with another intronless gene CEBP with pair of RT-PCR primers (described in Table 2 in Material and Method). The same experimental procedure was employed. It was clear that the CEBP mRNA was also precipitated with p68 RNA helicase, wt and HLIGR mutant (**Figure II-7E**).

2.4 Discussion

p68 RNA helicase was shown to be an essential splicing factor *in vitro* that acted at the U1:5'ss duplex (Liu 2002). In this report, we further demonstrated the functional role of p68 RNA helicase *in vivo*. We showed that the ATPase activity were required for the function of the protein in the spliceosome. We showed here that the p68 mutants that lacked ATPase and RNA unwinding activities still interacted with the U1:5'ss duplex. Nevertheless, the U1:5'ss duplex was not unwound in the HeLa nuclear extracts supplemented with the p68 mutants. The requirement of the ATPase activity for the function of p68 in the spliceosome and for the dissociation of the U1:5'ss duplex strongly argued that p68 RNA helicase actively unwound the transient RNA duplex in the

spliceosome. P68 RNA helicase could directly unwind the U1:5'ss duplex RNA. Alternatively, p68 could also actively act on the protein factor(s) which stabilize the duplex. Given that p68 itself crosslinked to the RNA duplex and that the mutants also interacted with the RNA, it is most likely that the RNA helicase unwinds the RNA duplex. Interactions of p68 with the U1:5'ss duplex and assembly of p68 to the spliceosome complexes do not require ATPase/helicase activities, indicating that the ATPase/helicase activities of p68 is not required for the interactions of the helicase with the spliceosome machinery. We have generated specific p68 mutants that lack dsRNA or ssRNA binding properties (data not shown). It will be interesting to test whether or not these p68 mutants will be assembled to the spliceosome and interact with the U1:5'ss duplex.

During the spliceosome assembly process, the dissociation of the U1 from the 5' splice site is tightly coupled to the addition of the U4/U6•U5 tri-snRNP to the pre-spliceosome. In our experiments, assembly of the spliceosome B/C complex was not affected by the p68 mutations that abolished ATPase/helicase activities. Further, the U1:5'ss duplex was not unwound in the spliceosome containing p68 mutants. The experiments demonstrated an excellent example that the addition of the U4/U6•U5 tri-snRNP was uncoupled with the unwinding the U1:5'ss duplex in the spliceosome assembly process. Uncoupling of these two events by disrupting the biochemical activities of p68 certainly suggested a role of p68 in the communication between addition of the tri-snRNP to the pre-spliceosome and the U1:5'ss duplex unwinding. This is consistent with our previous observations that depletion of p68 inhibited the pre-

spliceosome to the spliceosome transition (Liu 2002). Taking together all of our experimental observations (Liu, Sargueil et al. 1998; Liu 2002), we propose a hypothetical model for the function of p68 RNA helicase in the pre-mRNA splicing process. p68 actively unwinds the U1:5'ss duplex by direct strand displacement of the RNA duplex or by destabilizing the protein factor(s) that stabilize the duplex. The protein also plays a role in the addition of the tri-snRNP to the pre-spliceosome. P68 may fulfill the role by interacting with both the 5'ss and the U4/U6•U5 tri-snRNP. The interactions may be direct or may act through other proteins (Kuhn, Li et al. 1999). The ATPase activity of p68 is not required for the interactions. This model is consistent with the observations of other laboratories that p68 RNA helicase is detected in the pre-spliceosome as well as the matured spliceosome (Neubauer, King et al. 1998; Hartmuth, Urlaub et al. 2002; Jurica, Licklider et al. 2002). The dual functions of p68 RNA helicase in the human spliceosome are reminiscent of the case of Prp22 in the yeast spliceosome. It was demonstrated that Prp22 plays two distinct roles. The protein plays an important role in second catalytic step of the pre-mRNA splicing. Prp22 is essential for releasing the matured mRNA from the spliceosome (Schwer and Gross 1998). Thus, it may be a general phenomenon that some DEAD/DExH box RNA helicases not only function in unwinding the target but also coordinate the events upstream and/or downstream.

The function(s) of p68 RNA helicase in the pre-mRNA splicing process remains to be an intriguing question. Our previous experiments demonstrated an essential role of the protein in the *in vitro* pre-mRNA splicing in HeLa nuclear extracts (Liu, Sargueil et al. 1998; Liu 2002). Consistently, other research laboratories have detected p68 RNA

helicase in the mammalian spliceosome that is assembled in HeLa nuclear extracts as a constitutive component (Neubauer, King et al. 1998; Hartmuth, Urlaub et al. 2002; Jurica, Licklider et al. 2002). On the other hand, Bach-Elias and colleagues observed that p68 helicase plays a role in regulating c-H-ras alternative splicing (Guil, Gattoni et al. 2003). All these experiments suggested a functional role of p68 in the pre-mRNA splicing process. However, these experiments also raised an important question. Is p68 a general human pre-mRNA splicing factor *in vivo* or does the protein only function in splicing a subset of pre-mRNA? We presented experimental results here to show that p68 RNA helicase functioned in splicing of two house-keeping genes, Actin- β and GAPDH, in HT-29 cells. In addition, the intron that was tested in the double reporter was derived from late transcripts of adenovirus. It would be expected that efficiency of splicing of these introns should reflect the efficiency of the general pre-mRNA splicing process in cells. Thus, we believe that p68 RNA helicase is a general splicing factor. In supporting our conclusion, we observed that the growth rate of p68 knock down cells was reduced by over three fold (data not shown). The growth of the cells in which the endogenous p68 was knocked down and the HLIGR/LGLD mutant was exogenously expressed was almost completely inhibited and the cells were eventually dead after several days (data not shown). It is also possible that, although p68 is an essential splicing factor, its function could be replaced by another RNA helicase in cells when p68 is absent. P72 could be a candidate for this redundant function. It is recently demonstrated that p68 and p72 exist as a heterodimer in cells (Ogilvie, Wilson et al. 2003). Furthermore, p72 was

shown to associate with the U1 snRNP (Lee 2002) and the protein plays a role in regulating the alternative 5'ss selection in xxx gene splicing (Honig, Auboeuf et al. 2002).

Co-precipitation of p68 RNA helicase (mutant) with pre-mRNA in the RNA-IP experiments demonstrated another evidence for the functional role of the protein in the pre-mRNA splicing process. The experiments also suggested the interactions of p68 with pre-mRNA *in vivo*, which is consistent with our previous observations with HeLa nuclear extracts (Liu, Sargueil et al. 1998), (Liu 2002). Co-precipitation of mRNAs of intronless genes, histone H2A and CEBP, with p68 RNA helicase, both wild-type and mutant, is an interesting observation. At the current stage, we do not know whether the precipitated RNAs are the mRNA precursor, matured mRNA, or both. It will be interesting to determine any differences in the RNAs precipitated by p68 wild-type or mutant. Unlike many mRNA precursors, the intronless histone or CEBP mRNA precursors are not spliced. Therefore, one potential explanation for the observation is that p68 RNA helicase is associated with all mRNA precursors. P68 participates the pre-mRNA splicing. After the splicing, the protein is removed from mRNA with the disassociation of components of the spliceosome. Without the splicing, p68 may 'stay' with the transcripts. However, this explanation opens several interesting questions. (1) How p68 is deposited at all mRNA precursors? (2) Whether p68 plays a potential role in the processing of the intronless mRNA precursors. How does p68 eventually dissociate from the intronless mRNAs before the mRNA exporting?

Figure II-1. p68 mutants lack ATPase and RNA unwinding activities.

(A) Schematically illustration of the sequence motifs in the helicase core of DEAD-box RNA helicase and the p68 LGLD and HLIGR mutants.

(B) Coomassie staining of SDS-PAGE of recombinant p68 wt (lane 1), LGLD mutant (lane 2), or HLIGR mutant (lane 3) that were expressed and purified from bacterial *E. coli*.

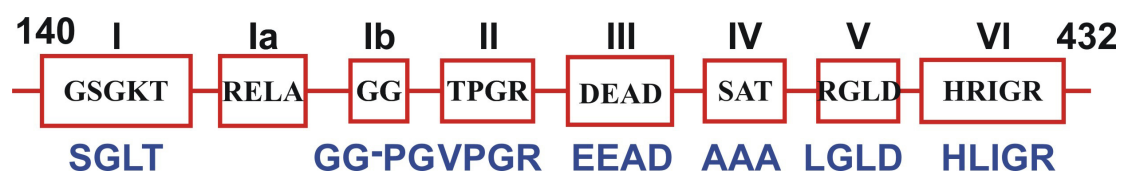
(C) Crosslinks of p68 wt (lane 1), LGLD mutant (lane 2), or HLIGR mutant (lane 3) to [γ - 32 P]-ATP are analyzed by SDS-PAGE followed by autoradiography.

(D) RNA unwinding by p68 wt (lane 3), LGLD mutant (lane 4), or HLIGR mutant (lane 5) is analyzed by SDS-PAGE followed by autoradiography. Lane 1 is duplex RNA denatured by heating to 95°C. Lane 2 is the duplex RNA.

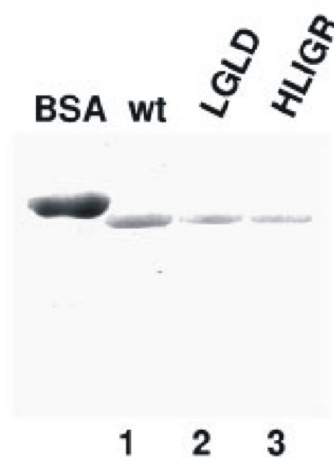
(E) ATPase activities of p68 wt/mutant (indicated) are measured by colorimetric assay. The ATPase activity (y-axis) is expressed as μ M Pi/mg of p68 or mutants.

Figure II-1

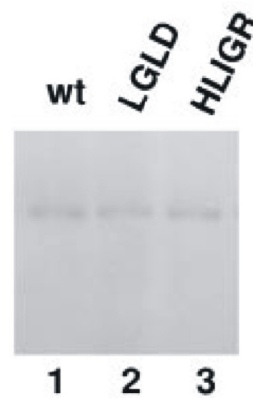
A



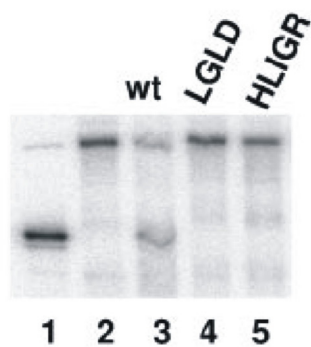
B



C



D



E

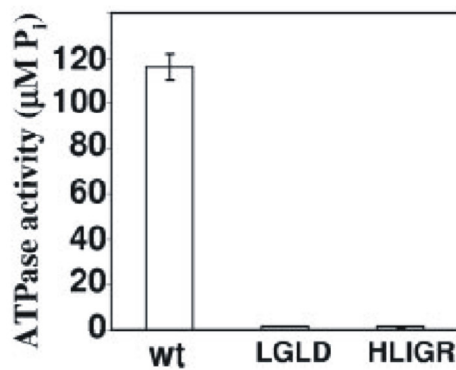


Figure II-2. p68 mutants that lack ATPase and helicase activities do not support the pre-mRNA splicing.

Splicing of transcript pIP10A in HeLa nuclear extracts in which the endogenous p68 is mock depleted (lane 2) or depleted by antibody against p68 (lane 3 & 4). The dephosphorylated recombinant p68 (Dp), protein buffer (lane 2), wild type (lane 3), mutant HLGR (lane 4), or mutant LGLD (lane 4), is added to the p68 depleted extracts. Lane 1 is the pre-mRNA (pPIP10A) without splicing.

Figure II-2

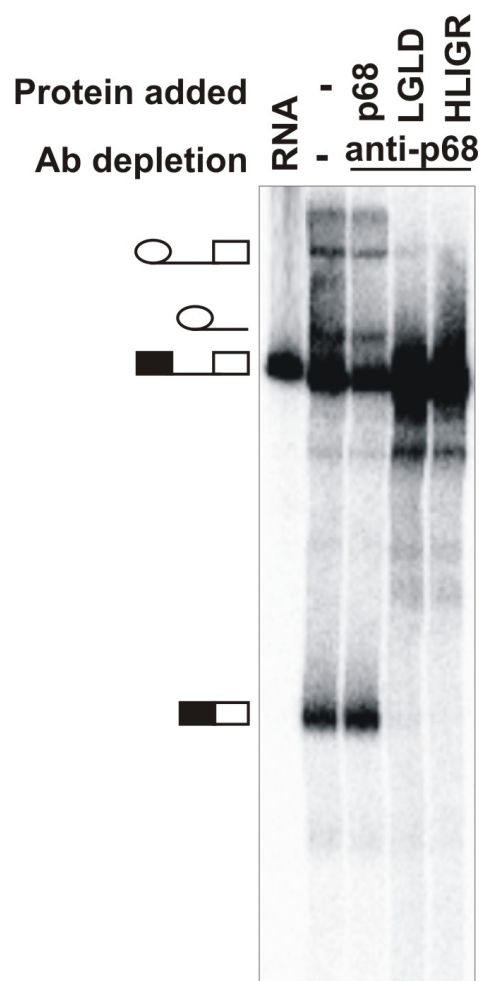


Figure II-3. p68 mutants that lack ATPase and RNA unwinding activities interact with the U1:5'ss duplex but do not support the dissociation of the U1 from the 5' splice site.

Trioxsalen crosslinking of the U1 snRNA to pre-mRNA in HeLa nuclear extracts. The U1:pre-mRNA crosslinking band is indicated in figure. The crosslinking reactions are carried out in the intact extracts (lane 2 – 5), p68 depleted extracts (lane 6 – 20) and in the p68 depleted extracts P68 wild-type (lane 11 – 15), mutant HLIGR (lane 6 -10), or mutant LGLD (lane 16 – 20) is added. The splicing are carried out for the indicated times before the trioxsalen is added to the splicing reactions. Lane 4 is crosslinked RNAs that are further treated with RNase H in the presence of DNA oligonucleotide α U1 that is complementary to U1 64-75 (α U1₆₄₋₇₅). Lane 5 is the crosslinked RNAs that are further treated with RNase H in the presence of random sequence DNA oligonucleotide Act1.

Figure II-3

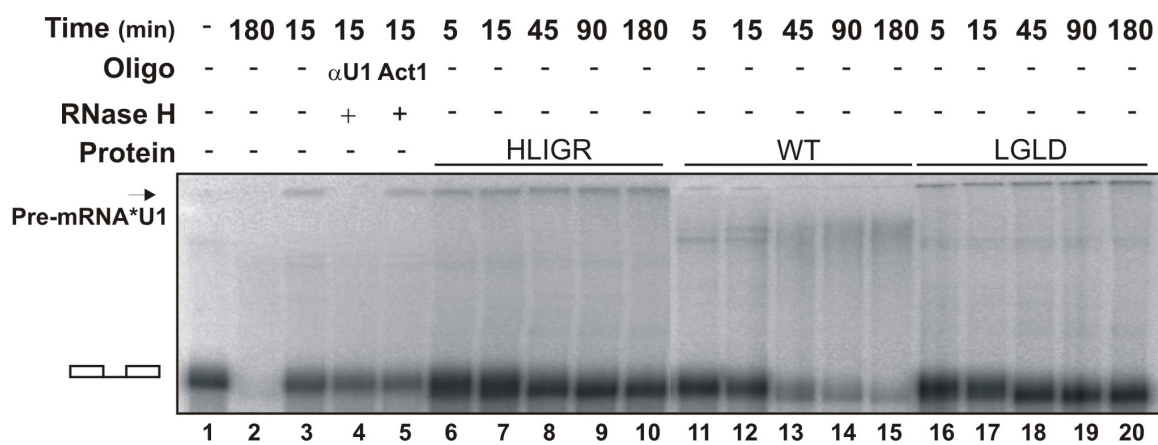


Figure II-4. p68 mutants that lack ATPase and RNA unwinding activities interact with the U1:5'ss duplex during splicing.

(A) MB crosslinking of His-p68, wild-type (left panel), mutant LGLD (middle panel), or mutant HLIGR (right panel), to the radio-labeled transcript pGC+DX in endogenous p68 depleted HeLa nuclear extracts. The splicing are carried out for the indicated times before the methylene blue is added to the splicing reactions. The lane marked p68 is the MB crosslinking carried out in intact HeLa nuclear extracts without addition of recombinant p68.

(B) The amount of p68 in the each crosslinking reactions are determined by immunoblot of the same MB crosslink SDS-PAGE with anti-His antibody.

Figure II-4

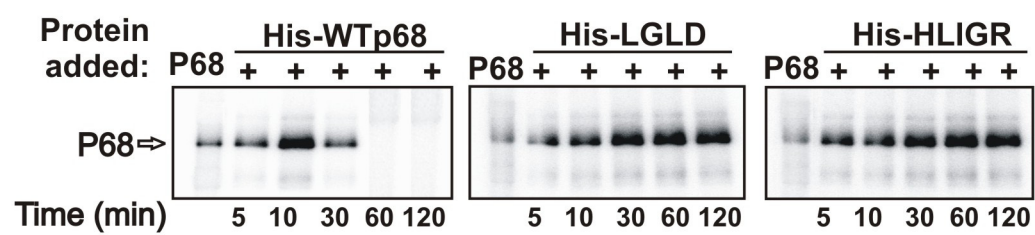
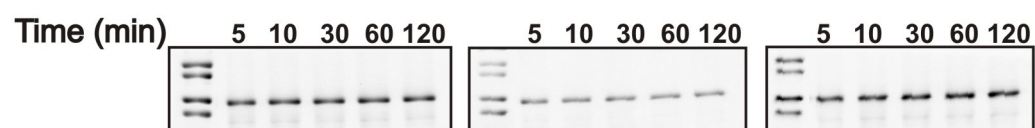
A**B**

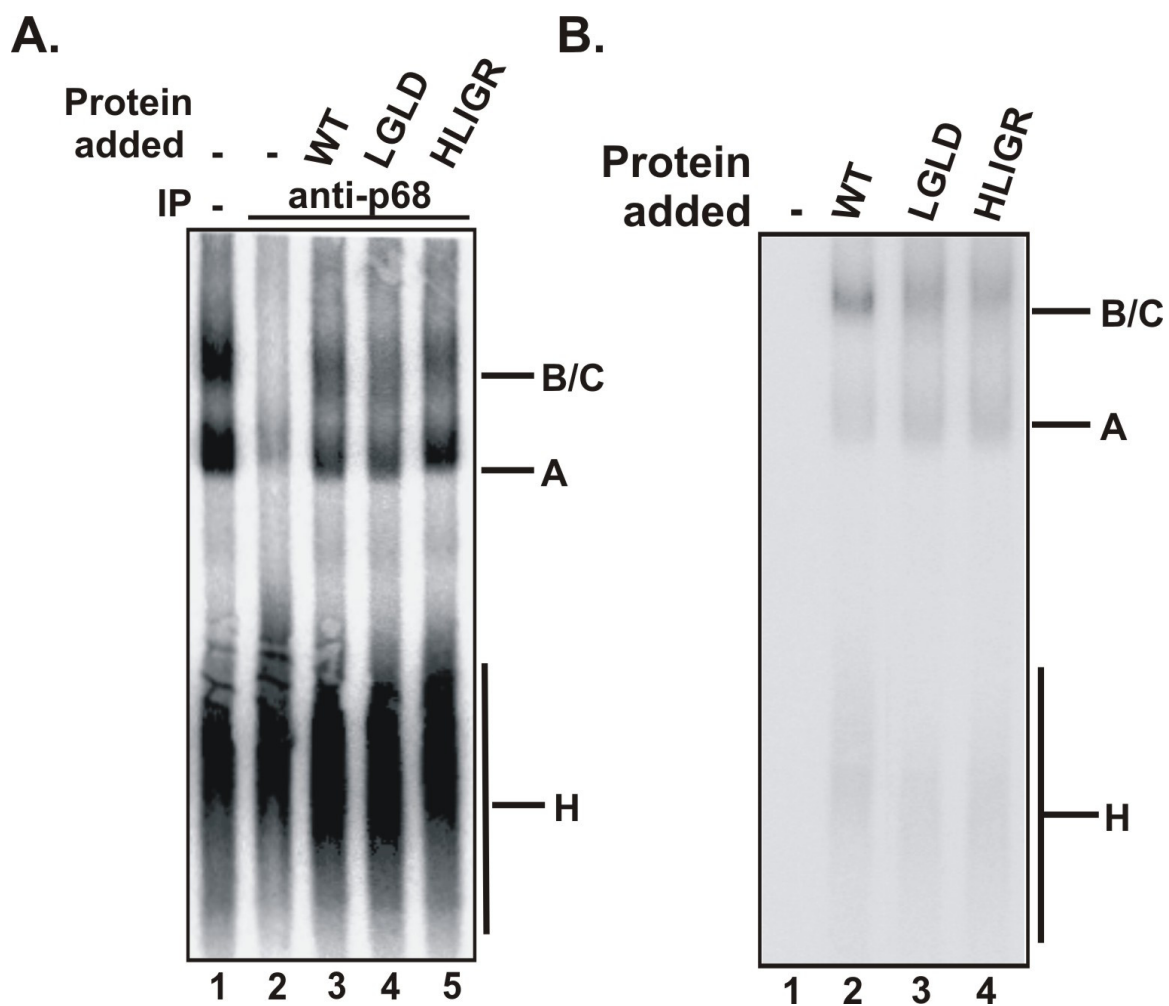
Figure II-5. The ATPase and RNA unwinding activities of p68 are not required for the assembly of the spliceosome.

(A) Electrophoretic separation of the spliceosome complexes. Splicing reactions were carried out with splicing substrate pPIP10A in the extracts: untreated (lane 1), p68 was depleted with antibody against p68 (lane 2), p68 was depleted and recombinant wt p68 was added (lane 3), p68 was depleted and recombinant LGLD mutant was added (lane 4) and p68 was depleted and recombinant HLIGR mutant was added (lane 5). All of the splicing reactions were incubated at 30°C for 30 min.

(B) Assembly of wt p68 (lane 2), the LGLD mutant (lane 3), or the HLIGR mutant (lane 4) into the spliceosome complexes in p68 depleted extracts was detected by immunoblotting of recombinant p68 using antibody against His6 tag. The recombinant p68s are dephosphorylated before adding to the splicing reactions. Lane 1 is the complexes assembled in the extracts without addition of recombinant p68.

(C) The spliceosome complex assembly in p68-depleted HeLa nuclear extracts to which wt p68 was added (lanes 2 to 4 and 11 and 12), mutant LGLD was added (lanes 5 to 7 and 13 and 14), or mutant HLIGR was added (lanes 8 to 10 and 15 and 16). The splicing reactions were carried out for the time indicated.

Figure II-5



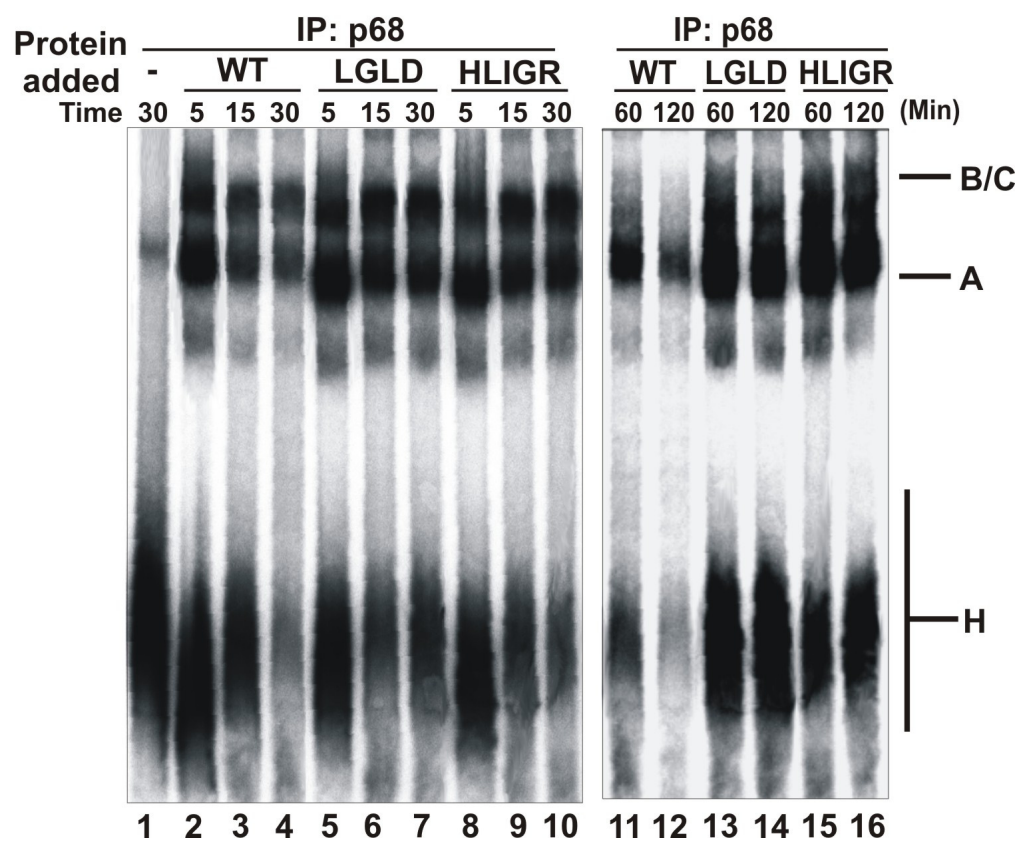
C.

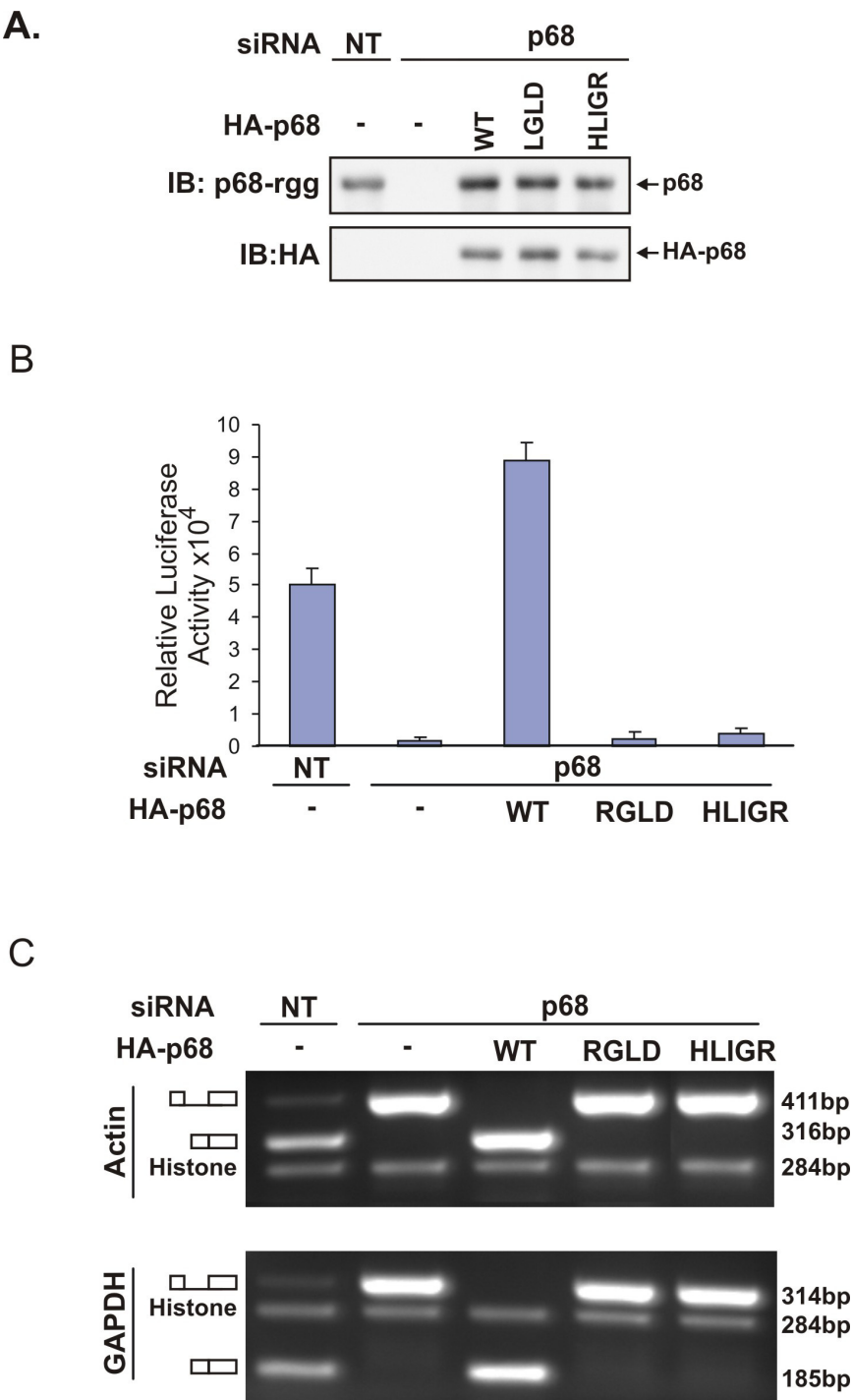
Figure II-6. p68 RNA helicase affected the pre-mRNA splicing *in vivo*.

(A) Knock down of p68 by RNA interference and exogenous expression of HA-p68 wt/mutant in HT-29 cells are analyzed by immunoblot using anti-p68 antibody (upper panel) or anti-HA antibody (bottom panel). NT means the cells were treated with non-specific siRNA duplex (control).

(B) Double reporter assays for the ratio of spliced/total pre-mRNA in HT-29 cells in which p68 is knocked down and p68 wt or mutant (indicated) is expressed. The spliced/total pre-mRNA ratio is expressed as the luciferase activity divided by \square -Gal activity (Nasim, Chowdhury et al. 2002).

(C) & (D) RT-PCR probe the spliced/unspliced mRNA of Actin- \square and GAPDH genes in HT-29 cells in which p68 is knocked down and p68 wt or mutant (indicated) is expressed. A pair of primers spans exon 4 and exon 5 **(C)** or exon 4 and intron 4 **(D)** are used in the RT-PCR reactions. In **(D)**, the bottom two panels were the quantization of the results in the upper panel by densitometer scanning. The band intensity of each RT-PCR product is normalized to the intensity of histone mRNA RT-PCR band.

Figure II-6



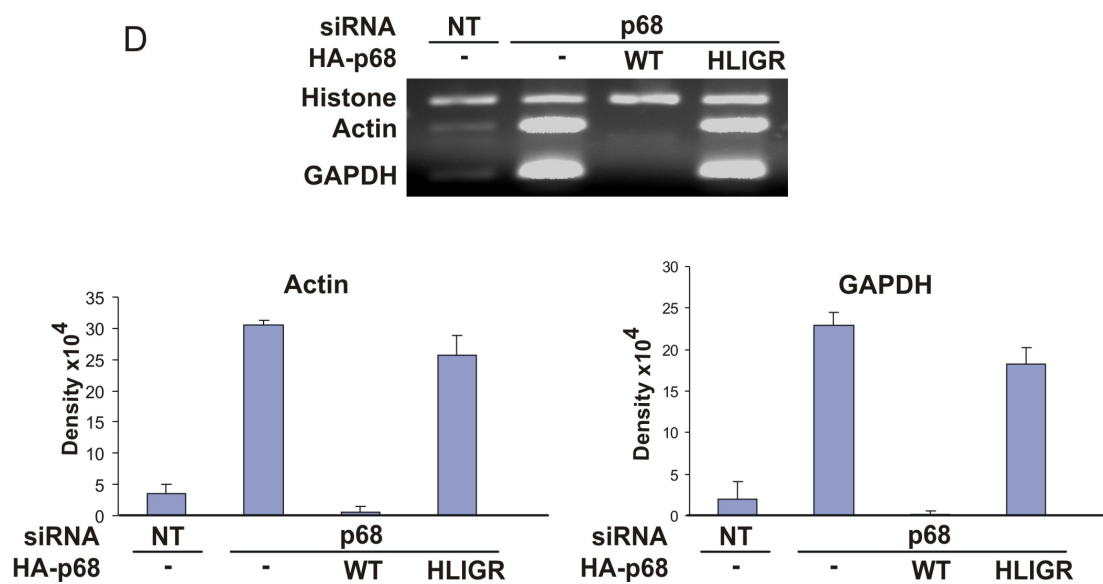


Figure II-7. p68 RNA helicase associates with pre-mRNA *in vivo*.

(A) RNA-IP of spliced/unspliced β -actin and GAPDH mRNA in HT-29 cells in which wt or mutant HA-p68 (indicated) is expressed. RNAs were precipitated by anti-HA antibody. Expression of HA-p68 wt/mutant was detected by immunoblotting with anti-HA antibody.

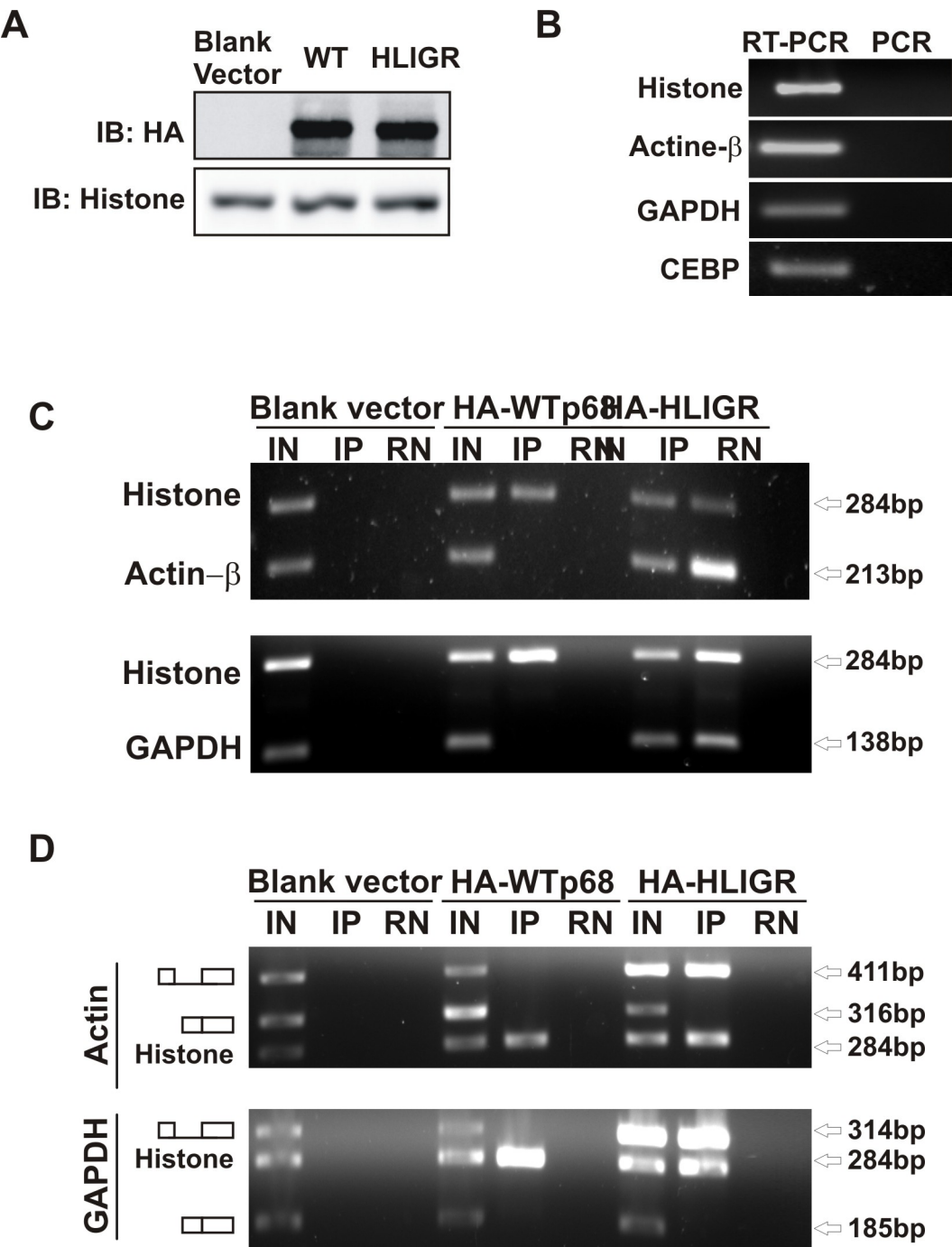
(B) The immunoprecipitated RNAs were detected by RT-PCR or PCR using the same primers as in panel C or D.

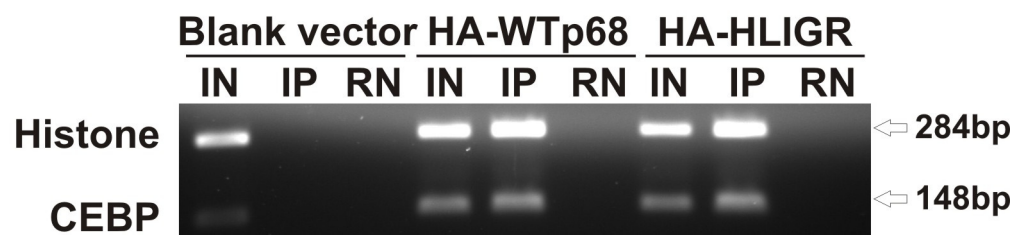
(C) The immunoprecipitated RNAs were detected by RT-PCR using a pair of primers crossing exon 4 and intron 4 of β -actin (upper panel) or GAPDH (bottom panel) genes.

(D) The immunoprecipitated RNAs were detected by RT-PCR using primers crossing both exon 4 and intron 4 or exon 4 and exon 5 (indicated) of β -actin (upper panel) or GAPDH (bottom panel) genes.

(E) The immunoprecipitated RNAs were detected by RT-PCR using a pair of primers annealed to histone 2B or CEBP (Table 1) genes. IN indicates input, where the RT-PCRs were performed with total RNA extracts without IP. IP indicates that the RT-PCRs were performed with the RNAs that were c-precipitated with anti-HA antibody. RN indicates the immunoprecipitated mixtures were treated with RNase before performing RT-PCRs.

Figure II-7



E

CHAPTER III

PDGF/c-ABL SIGNALING AXIS INDUCES TYROSINE PHOSPHORYLATION OF DEAD-BOX p68 RNA HELICASE

3.1 Abstract

Experiments from our laboratory have previously demonstrated that DEAD-box p68 RNA helicase can be Ser/Thr/Tyr phosphorylated in HeLa cells. Screening of patient tissue samples and cultured cell lines indicated that tyrosine phosphorylation of p68 correlated with tumor progression. The experiments of this dissertation demonstrated that PDGF autocrine induced the tyrosine phosphorylation of p68 in SW620 cells. Tyrosine kinase c-Abl was required for the tyrosine phosphorylation of p68. Furthermore, the tyrosine phosphorylated p68 was required for tumor cell epithelial-mesenchymal transitions. The phosphorylated p68 repressed the expression of E-cadherin and upregulated the expression of Vimentin. The tyrosine phosphorylated p68 also promoted cell invasion.

3.2 Introduction

Human p68 RNA helicase is the gene product of DEAD (Asp-Glu-Ala-Asp) box polypeptide 5 (DDX5). The translation product of this gene is 614 amino acids long and is characterized by the conserved DEAD motif as a putative RNA helicase. Human p68 RNA helicase was first detected by the monoclonal antibody DL3C4 (anti-SV40 large T antigen) (PAB204) due to cross-reaction (Crawford, Leppard et al. 1982; Ford, Anton et

al. 1988). Sequence analyses revealed the similarity between p68 with eukaryotic initiation factor eIF-4A, suggesting p68 may act as an ATP-dependent RNA helicase. Protein p68 shows a distinct nuclear distribution and is thought to be important for cell division and proliferation (Ford, Anton et al. 1988). Recombinant p68 RNA helicase was purified and exhibited RNA-dependent ATPase activity and helicase activity *in vitro* (Hirling, Scheffner et al. 1989). Family members of DEAD-box proteins share conserved sequences. They express ubiquitously in living cells and are considered to be involved in multiple RNA-related metabolism, including splicing, translation, RNA processing, RNA transport and rRNA biosynthesis (Iggo and Lane 1989).

In spite of its essential role in the pre-mRNA splicing process (Liu 2002; Lin, Yang et al. 2005), p68 RNA helicase has been shown to engage in diverse signaling pathways as a transcriptional coactivator or corepressor. The protein plays important roles in various cellular processes including cell proliferation, wound healing, apoptosis and tumor development (Stevenson, Hamilton et al. 1998; Causevic, Hislop et al. 2001; Guil, Gattoni et al. 2003; Rossow and Janknecht 2003; Kahlina, Goren et al. 2004; Wilson, Bates et al. 2004; Bates, Nicol et al. 2005; Kodym, Henockl et al. 2005). In human colon cancer tissue, accumulated p68 protein is poly-ubiquitinated. This accretion is apparently due to the dysfunction of proteasome-mediated degradation (Causevic, Hislop et al. 2001).

PDGF regulates wide-ranging cellular processes. There are four different isoforms in the PDGF family (Fredriksson, Li et al. 2004). These polypeptide isoforms assemble into five different dimers, PDGF AA, AB, BB, CC and DD. The ligands bind two

receptor tyrosine kinases, PDGF receptor α (PDGFR α) and β (PDGFR β). Unlike PDGF AA that exclusively binds to PDGFR α , PDGF BB interacts with both PDGFR α and β . The conventional PDGF ligands, AA and BB and their tyrosine kinase receptors are implicated in multiple processes associated with tumors, including autocrine-stimulated tumor cell growth, tumor angiogenesis, regulation and recruitment of stroma cells. The PDGF autocrine loop occurs in certain malignant tumors characterized by abnormal secretion of PDGF or mutational activation of PDGF receptors (Guha, Dashner et al. 1995; Lokker, Sullivan et al. 2002). The PDGF autocrine loop likely occurs in most solid tumors. Both PDGFs and the receptors play important roles in tumor progression.

The gene product of proto-oncogene c-Abl is a non-receptor tyrosine kinase. c-Abl localizes at the cytoplasmic membrane, the cytosol and the nucleus. c-Abl has a catalytic domain, polyproline rich regions, and SH2 and SH3 domains that are involved in protein-protein interactions. The C-terminal domain of c-Abl has nuclear localization signals (NLS) and nuclear export signals (Van Etten, Jackson et al. 1994; Wen, Jackson et al. 1996). Notably, the BCR-ABL plays significant roles in the development of human leukemia, including acute lymphocytic (ALL), chronic myelocytic (CML) and chronic neutrophilic (CNL) leukemia (Melo 1996). The nucleus pool of c-Abl is generally believed to be activated by DNA-damage or cell cycle signaling (Kipreos and Wang 1990; Kipreos and Wang 1992; Yuan, Huang et al. 1996; Shafman, Khanna et al. 1997; Yuan, Huang et al. 1997). The non-receptor tyrosine kinase Src is suggested to be active

upon PDGF treatment in fibroblasts and subsequently phosphorylates and activates c-Abl kinase (Plattner, Kadlec et al. 1999).

Epithelial-mesenchymal transition (EMT) was first noticed in epithelial tissues (Greenburg and Hay 1982). EMT was characterized by the loss of cell adhesion and upregulation of mesenchymal markers, breakdown of epithelial contact and cell rearrangement or migration in the extracellular matrix (Shook and Keller 2003). Epithelial cells may transiently lose their polarity and gain the ability to spread in many developmental processes. These processes include mesoderm formation during gastrulation and immigration of neural-crest cells from the neural tube (Duband, Monier et al. 1995; Sun, Baur et al. 2000). In mature organs, processes such as tubulogenesis, tissue reorganization, wound healing and mammary gland branching may cause the transcriptional loss of epithelial markers (i.e. E-cadherin) and the induction of mesenchymal markers (i.e. Vimentin) in epithelial cells (Viebahn 1995; Thiery 2002). Epithelial plasticity changes also occur in a variety of pathological processes. For instance, progression of benign tumors toward invasive and malignant carcinomas alters epithelial plasticity to migratory fibroblast phenotype (Hay 1995).

Intensive studies indicate that the transition from non-metastatic adenoma (epithelial phenotype) to invasive carcinoma (mesenchymal phenotype) is driven by a distinct series of changes in adhesion proteins. These changes include the loss of epithelial adhesion and catenin-dependent junctions, as well as expression of mesenchymal genes and expansion of proteins involved in cell migration and cell-ECM interactions. Loss of epithelial polarity by downregulation of E-cadherin, mutations in

the *E-cadherin* gene or other mechanisms that prevent the adhesions junction formation are observed in malignant carcinoma cells. In human cancer patients, the loss of E-cadherin expression correlates with advanced stages of tumor development and poor prognosis (Riethmacher, Brinkmann et al. 1995). In this regard, the *E-cadherin* gene is proposed as a tumor suppressor gene. Molecular analyses have identified the repression of the *E-cadherin* gene as the major mechanism of EMT.

Previous studies demonstrate that p68 is a potential substrate for protein kinase C (PKC) (Buelt, Glidden et al. 1994) and Tlk1 (Kodym, Henockl et al. 2005). Tyrosine and threonine phosphorylation of p68 has been observed in HeLa cell nuclear extracts in our lab (Yang, Lin et al. 2005; Yang, Lin et al. 2005). Strikingly, p68 has been shown to be tyrosine phosphorylated in six cancer cell lines derived from different tissues, but not in cells derived from the corresponding normal tissues (Yang, Lin et al. 2005). Comparison of p68 phosphorylation in cell lysates obtained from tumor cell lines and corresponding normal cell lines confirms the same observation. Moreover, tyrosine phosphorylation levels of p68 apparently correlate with tumor cell malignancy. These discoveries generate enormous interest in studying signaling pathways that induce the phosphorylation of p68. Our studies demonstrate that the PDGF autocrine loop induced the tyrosine phosphorylation of p68 in SW620 cells. Tyrosine kinase c-Abl acted as the kinase to phosphorylate p68 at the Y593 site. The PDGF-induced tyrosine phosphorylation of p68 is required for tumor cell EMT and invasion. These studies suggest the important role of the PDGF autocrine loop for tyrosine phosphorylation of p68 and, subsequently promoting tumor cell malignancy.

3.3 Results

3.3.1 The Tyrosine Phosphorylation Status of p68 Correlates with Tumor Malignancy.

Studies in our lab have previously characterized the role of tyrosine-phosphorylated p68 in β -catenin nuclear translocation and epithelial-mesenchymal transition (Yang, 2006, in preparation). To gain a comprehensive understanding of the role that p68 may play in tumorigenesis, patient tissue samples obtained from Southern Division, Cooperative Human Tissue Network (Birmingham, AL) were screened by immunoprecipitation using anti-p68 polyclonal antibody (PAbp68). The precipitated p68 was examined by immunoblotting using antibodies against p68 (p68-rgg) or phosphotyrosine residue (P-Tyr-100). The experiments were also carried out with corresponding normal tissue samples. p68 precipitated from tissue samples of adenocarcinoma (non-metastatic tissue) or carcinoma (metastatic tissue) of three different organ types (colon, ovary and lung) exhibited a unique pattern of tyrosine phosphorylation. The p68 phosphorylation closely correlated with tumor progression (**Figure III-1A** upper panel & lower panel). An elevated tyrosine phosphorylation level was observed in tumor tissue samples compared to that in corresponding normal tissue samples collected from same patients (**Figure III-1A** upper panel & lower panel). Furthermore, even higher tyrosine phosphorylation levels were detected in metastatic tissue samples, indicating that p68 may play potential roles in tumor metastasis.

The tyrosine phosphorylation status of p68 was also examined in three cell line pairs. H460 and H146 are derived from lung carcinoma. SW480 and SW620 are derived from colon carcinoma of the same patient. WM115 and SW266 are derived from melanoma. Among them, H460, SW480 and WM115 are derived from primary sites, where H146, SW620 and WM266 are derived from metastatic sites. p68 was immunoprecipitated from the cell extracts. The precipitated p68s were examined by immunoblotting using p68-rgg and P-Tyr-100. It is clear that a higher tyrosyl phosphorylation level of p68 was observed in lysates made from metastatic cell lines (**Figure III-1B**). In contrast, p68 immunoprecipitated from extract made from non-metastatic cell lines showed a lower or undetectable tyrosine phosphorylation level.

p68 was phosphorylated at higher levels on tyrosine residues in metastatic tissue samples and cell lines. To understand the functional role of p68 in tumor invasion and metastasis, we decided to probe the cellular signaling pathways that induce p68 phosphorylation. A cell line pair, SW480/SW620 derived from primary site (SW480) and metastatic lymph node (SW620) of colon tumor from same patient was chosen as the study system. As indicated in figure III-1, p68 displayed significant tyrosine phosphorylation level in SW620 cells, while this phosphorylation is undetectable in SW480 cells.

3.3.2 PDGF/c-Abl Signaling Pathway Induces the Tyrosine Phosphorylation of p68 in SW620 cells.

In the effort to address the question of which cell signal pathway induces tyrosine phosphorylation of p68 in metastatic cell lines, we examined the phosphorylation status of four different cell lines. Endogenous p68 was immunoprecipitated from extract made from four human colorectal cell lines (HT-29, HCT-116, SW480 and SW620). The precipitated p68s were examined by immunoblotting using antibodies against either p68 or phosphotyrosine residues. Comparison of tyrosine phosphorylation levels of p68 in these four cell lines confirmed that p68 was phosphorylated in the metastatic SW620 cells, but not in other three non-metastatic cell lines (**Figure III-2A**).

Previous studies in our lab demonstrated that PDGF molecules could stimulate tyrosine phosphorylation of p68 in human colorectal tumor cell line, HT-29. A PDGF/c-Abl/p68 signaling axis promotes cell proliferation and migration (Yang, 2006, in preparation). In this signaling axis, upon ligand PDGF binding the PDGF receptor, the receptors activate downstream c-Abl tyrosine kinase, which subsequently phosphorylates p68 at tyrosine residue Y593. To test whether the same signaling pathway also acts in SW620 cells, tyrosine phosphorylation of p68 was examined in SW620 cells. We employed the RNA interference (RNAi) strategy to transiently knock down the PDGF receptor and c-Abl kinase. Tyrosine phosphorylation of p68 was examined by the same experimental strategy. Upon treatment of SW620 cells with small interfering RNA (siRNA) that targets PDGF receptor β (PDGFR β) or c-Abl (Smartpool™, Dharmacon),

the tyrosine phosphorylation of p68 was abolished and the expression level of p68 was unaffected (**Figure III-2B** first and second panel from top). Upon RNAi knockdown of either PDGFR β or c-Abl, immunoblotting against PDGF receptor β or c-Abl from cell lysate indicated that the protein expression of PDGFR β and c-Abl were diminished upon siRNA treatment (**Figure III-2B** third and fourth panel from top). As a negative control, a non-targeting siRNA pool purchased from Dharmacon was used. The tyrosine phosphorylation of p68 was not affected by the treatment of SW620 cells with non-targeting siRNA. These results suggested that the signaling pathway of PDGF and subsequent activation of c-Abl kinase were required for the tyrosine phosphorylation of p68 in SW620 cells. The data is consistent with previous observations in HT-29 cells, which suggest that p68 is the downstream target of c-Abl (Yang, 2006, in preparation).

3.3.3 PDGF Autocrine is one of the Mechanisms to Phosphorylate p68 in SW620 Cells.

In some tumor cases, the PDGF autocrine loop pivotally drives tumorigenesis and metastasis, especially in astrocytomas and gliomas (Hermanson, Funa et al. 1992; Guha, Dashner et al. 1995; Lokker, Sullivan et al. 2002). We have demonstrated that in SW620 cells, PDGF stimulation is required for p68 tyrosine phosphorylation. In SW620 cells, the PDGF signaling pathway may be constitutively activated in order to maintain the invasive and aggressive behavior of SW620 cells. It is possible that the PDGF autocrine loop may acts in SW620 cells and controls the tyrosine phosphorylation of p68. To probe

whether the PDGF autocrine loop plays a role in tyrosine phosphorylation of p68 in SW620 cells, antibodies targeting either PDGF AA or PDGF BB were supplemented to cell culture media to neutralize the potential secreted PDGF molecules. Tyrosine phosphorylation of p68 was analyzed by the same strategy to test whether antibody neutralization could block the tyrosine phosphorylation of p68. Upon neutralization of PDGF BB, but not AA, the tyrosine phosphorylation of p68 was abolished in SW620 cells (**Figure III-3A**). The PDGF antibody treatments did not alter the expression level of p68. These findings argued that the PDGF autocrine loop presents in colorectal tumor cell line and the PDGF autocrine loop may be responsible for the induction of p68 tyrosine phosphorylation.

Unlike SW620 cells, SW480 cells are derived from the primary cancer site of the same patient. The cells are non-metastatic and non-invasive. We observed that p68 is phosphorylated to much lesser extent in SW480 cells (see figure III-2A). To test whether PDGF treatment is also able to induce p68 tyrosine phosphorylation in SW480 cells, the SW480 cells were treated with PDGF AA or BB. The p68 tyrosine phosphorylation was examined in the treated cells (**Figure III-3B**). It is evident that the PDGF AA, but not PDGF BB, induced tyrosine phosphorylation of p68 in SW480 cells. Although the PDGF signaling pathway is necessary to induce tyrosine phosphorylation of p68 both in SW620 and SW480 cells, different members of PDGF are required in different cell lines. This may be due to the expression of different isoforms of PDGF receptors in different cells. The observed potential PDGF autocrine loop in SW620 cells may be due to the upregulation of PDGF expression and secretion by unknown

mechanisms. Taken together, these data confirmed the important role of PDGF in induction of p68 phosphorylation and linked PDGF signaling pathway with colon cancer metastasis. It is proposed that the PDGF autocrine loop may be one of the mechanisms which promote colon tumor metastasis and anti-PDGF drugs may be applied to wider range of tumor therapy.

3.3.4 Y593 is the Tyrosine Phosphorylation Site of p68.

We next probed the phosphorylation site of p68 in SW620 cells. Experiments from our laboratory have suggested that Tyrosine 593 at the C-terminus of p68 was phosphorylated in HT-29 cells upon PDGF stimulation. To test whether p68 is phosphorylated at Y593 in SW620 cells, we generated Y593 → F mutant by site-directed mutagenesis. We utilized RNAi to knock down endogenous p68. Exogenous HA-tagged p68 (wild type p68 or Y593F mutant) were expressed in the p68-knockdown cells (refer as SW620^{-p68/+wt} or SW620^{-p68/+Y593F}). To avoid targeting of exogenous HA-p68s by RNAi, four nucleotides within the siRNA targeting sequence of p68 were mutated. The amino acid sequence of exogenously expressed HA-p68s was not changed (**Figure III-4A**). The SW620 cells were transfected with non-targeting siRNA or siRNA targeting p68. Subsequently, the HA-tagged p68s (wt or Y593F) were expressed. Immunoblotting of p68 using antibody against p68 indicated that endogenous expression of p68 was greatly reduced by p68 siRNA (**Figure III-4B** first panel). HA-tagged p68s were expressed as revealed by immunoblotting using antibody against HA epitope (**Figure III-4B** second panel). p68 phosphorylation was examined by immunoblotting of

HA-tag immunoprecipitates using P-Tyr-100. The results demonstrated that, unlike wild type HA-p68, the exogenously expressed Y593F protein was not tyrosine-phosphorylated (**Figure III-4B** third panel). These results suggested that Y593 was the phosphorylation site of p68 in SW620 cells. The results were in agreement with other experiments in our laboratory.

3.3.5 Tyrosine Phosphorylation of p68 Promotes Tumor cell EMT.

We investigated the biological role of tyrosyl phosphorylated p68. The experiments from our laboratory previously demonstrated that phosphorylation of p68 at Y593 mediated PDGF induced epithelial-mesenchymal transition in HT-29 cells. We questioned whether phosphor-p68 also mediates the EMT and the invasive behavior of SW620 cells.

During the EMT process, a number of epithelial markers are down-regulated and certain mesenchymal markers are upregulated. We tested the role of phosphor-p68 in regulating the expression of epithelial markers and mesenchymal markers. E-cadherin and Vimentin were probed as examples. The E-cadherin expression was probed in SW620 cells in which the endogenous p68 was knocked down and the HA-p68s (wild-type or Y593F) were exogenously expressed. Immunoblotting of p68 and HA from cell lysates revealed that p68 was knocked down by RNAi and the exogenous HA-p68s were expressed (**Figure III-5A** first and second panel from top). Immunoblotting using P-Tyr-100 of the HA-tagged immunoprecipitates confirmed the exogenously expressed HA-p68 wt was phosphorylated and HA-Y593F mutant was not phosphorylated (**Figure III-5A**

third panel from top). E-cadherin was expressed in a very low level in SW620 cells reflecting the fact that the SW620 cell line is a metastatic cancer cell line. The E-cadherin level was not dramatically affected by p68-knockdown (**Figure III-5A** fourth panel from top). However, expression of E-cadherin was further repressed in SW620^{-p68/+wt} cells. In contrast, the expression of E-cadherin was significantly increased in SW620^{-p68/+Y593F} cells (**Figure III-5A** fourth panel from top). The cellular level of Vimentin, a mesenchymal marker, was not significantly affected by p68 knock down (**Figure III-5A** fifth panel from top). However, expression of Vimentin was upregulated in SW620^{-p68/+wt} cells, while expression of Vimentin was almost completely inhibited in SW620^{-p68/+Y593F} cells (**Figure III-5A** fifth panel from top).

Upon the same treatment as described above, SW620^{-p68/+wt} cells and SW620^{-p68/+Y593F} cells cultured on microslides were fixed and stained by primary antibodies against E-cadherin or Vimentin. Immunostaining of E-cadherin and Vimentin in SW620^{-p68/+wt} or SW620^{-p68/+Y593F} cells confirmed the results of the immunoblotting (**Figure III-5B**). These findings suggested that tyrosine phosphorylation of p68 at Y593 residue is required for the repression of epithelial markers and the upregulation of mesenchymal markers. Furthermore, mutation of phosphorylation site Y593 not only abolished the tyrosine phosphorylation of p68, but also prevented the EMT by relieving E-cadherin repression and repressing expression of Vimentin.

Another important property of mesenchymal cells compared to epithelial cells is their mobility. To further test whether phosphorylated p68 promotes epithelial cell changes toward mesenchymal cells, we examined cell invasion of SW620 cells. HA-

tagged p68s, (wt or Y593F mutant) were stably expressed in SW620 cells using a lentivirus gene expression system. The cells with or without exogenous expression of p68 were examined for cell invasion. The treated cells were pre-labeled with fluorescence and seeded into the upper chamber of 24-well plates with the bottom sealed by extracellular matrix gel. After incubation, the bottom chambers were scanned by a micro plate reader to detect the migrated cells by fluorescence. Without HA-p68 wt expression, SW620 cells showed a moderate level of invasiveness, whereas expression of wild type p68 dramatically increased cell invasiveness (**Figure III-5C**). In contrast, expression of Y593F mutant significantly reduced the cell invasion, indicating the tumor cell mobility and invasiveness were affected by tyrosine phosphorylation of p68 (**Figure III-5C**). On the other hand, the cell invasion of SW480 cells in which p68 wt or mutant were expressed was also monitored under PDGF treatment. HA-tagged p68s, wild type or Y593F mutant were stably expressed in SW480 cells using the same lentivirus gene expression system. The stable cell lines with or without PDGF treatment were examined for cell invasion. Exogenous expression of HA-p68 wt greatly increased PDGF-stimulated cell invasiveness. However, expression of Y593F mutant inhibited the PDGF-stimulated SW480 cell invasion and migration (**Figure III-5D**). Interestingly, overexpression of p68 wild type alone did not affect cell mobility. Thus, PDGF-induced phosphorylated-p68 is required to promote cell invasion.

3.4 Discussion

In this chapter, we observed that p68 acquired tyrosine phosphorylation at the Y593 residue in metastatic cancer cells. The PDGF autocrine loop induced the tyrosine phosphorylation of p68. Tyrosine kinase c-Abl phosphorylated p68 upon PDGF stimulation. The phosphorylated p68 repressed the expression of E-cadherin and upregulated the expression of Vimentin. The phosphorylated p68 also promoted cell invasion. These mechanisms illustrate the promising role of phosphorylated p68 in tumor cell migration and metastasis.

Treatment of SW480 cells with PDGF AA stimulates tyrosine phosphorylation of p68. It is likely that PDGF receptors alpha are expressed in SW480 cells. However, in SW620 cells, PDGFR β is required for the phosphorylation of p68. One possibility to explain this observation is that different isoforms of PDGF receptor are expressed in different cell lines. The upregulation of specific PDGF BB molecule in SW620 cells is possibly due to transcription dysregulation, or genetic mutation on PDGF promoter. It will be interesting to investigate the molecular devices that control the expression of PDGF, which will strengthen the understanding of the role of PDGF in tumor formation and metastasis.

Tyrosine 593 that located at the C-terminus of p68 and the flanking sequence contains the consensus sequence of tyrosine kinase c-Abl (YXXP) (Wu, Afar et al. 2002). Studies in our lab indicated that c-Abl phosphorylates p68 at Y593. The cytoplasmic membrane and cytosolic pool of c-Abl is activated upon PDGF and other growth factor

stimulation. The nuclear pool of c-Abl is activated by DNA-damage (Kipreos and Wang 1990; Kipreos and Wang 1992; Yuan, Huang et al. 1996; Shafman, Khanna et al. 1997; Yuan, Huang et al. 1997). On the other hand, p68 is localized to the cell nucleus. It is surprising that c-Abl mediates the effect of PDGF and induces the tyrosine phosphorylation of p68. c-Abl has been shown to shuttle between the cytoplasm and the nucleus (Lewis, Baskaran et al. 1996; Taagepera, McDonald et al. 1998). Therefore, it is possible that, upon PDGF stimulation, the activated cytoplasmic c-Abl translocates to the nucleus and phosphorylates p68. Alternatively, nuclear p68 may translocate to the cytoplasm, where p68 is phosphorylated. After phosphorylation, p68 translocates back to the nucleus.

Tumor metastasis is a remarkably complicated process, manipulated by many mechanisms. Although it is very difficult to observe the bona fide EMT process during tumor metastasis, EMT is proposed to play a central role in tumor progression. The tyrosine phosphorylation of p68 promotes tumor cell EMT and invasion. Therefore, we speculate that phosphorylated p68 promotes tumor metastasis *in vivo*. Mutation of the tyrosine phosphorylation site of p68 is thought to abrogate orthopedic tumor development and progression.

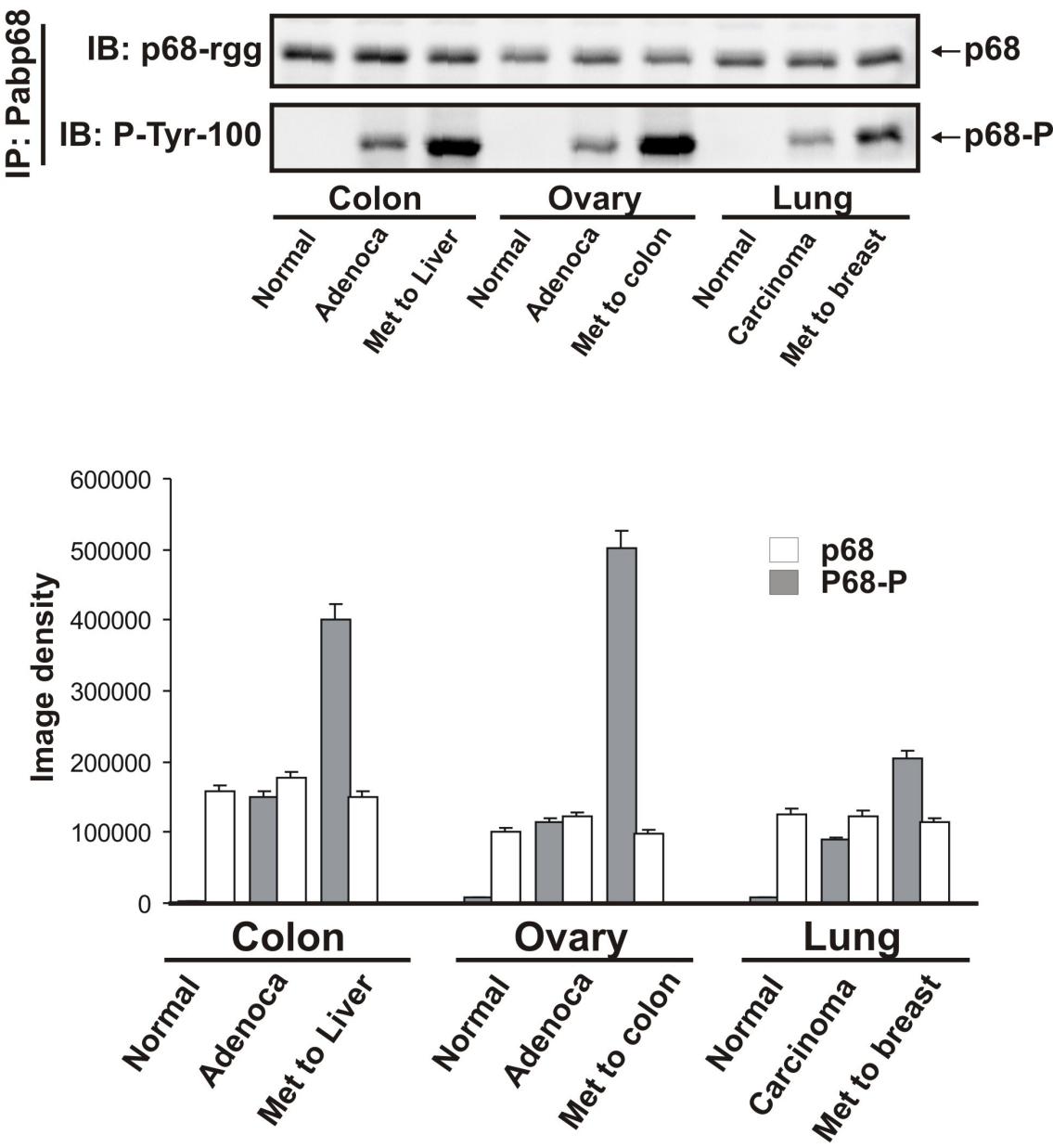
Figure III-1. Tyrosine phosphorylation of p68 correlates with tumor malignancy.

(A) Tyrosine phosphorylation of p68 RNA helicase in nine tissue samples. Patient tissue samples were obtained from Southern Division, Cooperative Human Tissue Network (Birmingham, AL). The tissue samples were collected from three organs, colon, ovary and lung; each organ group contains samples from normal tissue (normal), adenocarcinoma (adenoca) and metastases. Upper panel, the p68 protein was immunoprecipitated (IP) from tissue lysates with antibody against p68 and followed by immunoblotting (IB) with appropriate antibody (indicated). The immunoblotting using antibody p68-rgg was the loading control. Lower panel is the quantitatively scanning of immunoblotting signal using UVP BioImaging and analysis System (Upland). The scanning densities of blots are shown as indicated.

(B) Examination of p68 tyrosine phosphorylation in three cell line pairs established from primary tumor site (P) or metastatic site (M). Immunoprecipitates of p68 was detected by immunoblotting using appropriate antibodies as indicated. The immunoblotting using p68-rgg antibody was the loading control.

Figure III-1

A



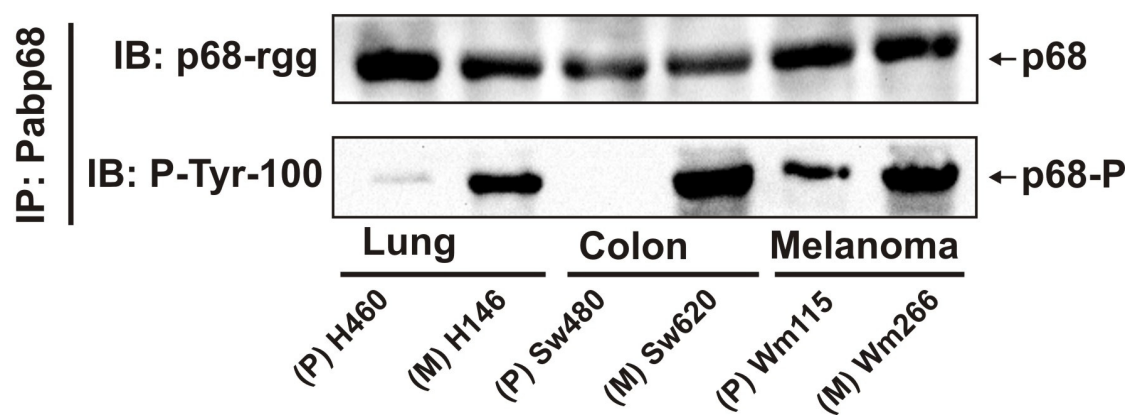
B

Figure III-2. PDGF/c-Abl signaling pathway induces tyrosine phosphorylation of p68 in SW620 cells.

(A) p68 RNA helicase is tyrosyl phosphorylated in four cell lines established from human colorectal tumors. Tyrosine phosphorylations of p68s in these cells were analyzed by immunoblotting of anti-p68 immunoprecipitates using antibody p-Tyr-100 (second panel from top). The immunoblotting using p68-rgg antibody was the loading control.

(B) PDGF/c-Abl signaling pathways induce tyrosine phosphorylation of p68 in SW620 cells. SW620 cells were treated with siRNA targeting PDGF receptor β or c-Abl kinases. Immunoprecipitates of p68 were examined by immunoblotting using P-Tyr-100. Protein levels of PDGFR β and c-Abl from cell lysates were examined by immunoblotting using appropriate antibodies as indicated. The immunoblotting using p68-rgg antibody was the loading control.

Figure III-2

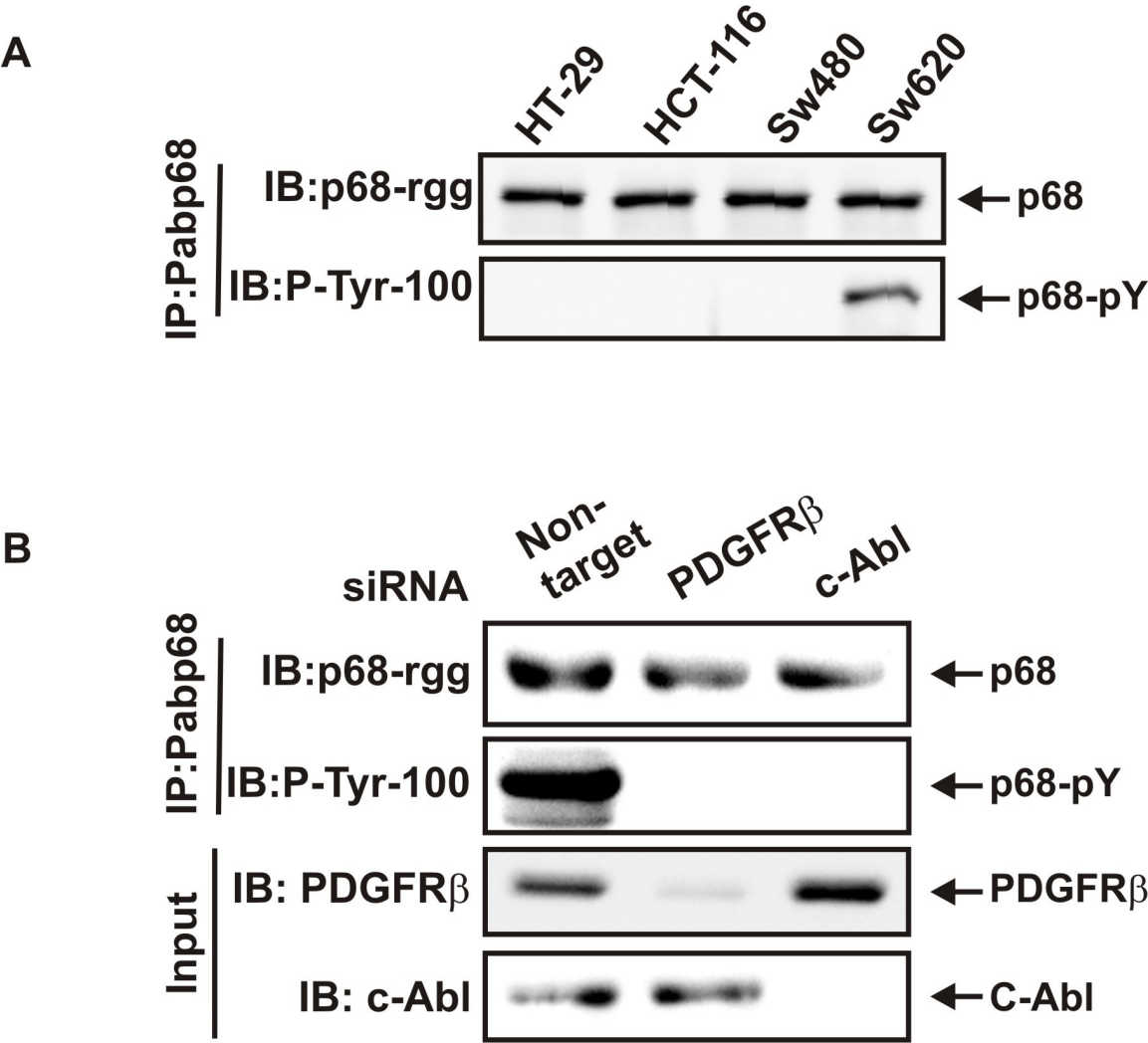


Figure III-3 PDGF autocrine loop induces phosphorylation of p68 in SW620 cells.

(A) PDGF autocrine loop in SW620 cells. Anti-PDGF AA or BB antibodies (1 μ g/ml) were added to SW620 cell culture media. The cells were incubated for overnight. p68s were immunoprecipitated from cell lysates and the immunoprecipitates were examined by immunoblotting using antibody P-Tyr-100. The immunoblotting using p68-rgg antibody is loading control.

(B) PDGF induces p68 tyrosine phosphorylation in SW480 cells. SW480 cells were treated with PDGF AA or BB (20 ng/ml) for overnight. The tyrosine phosphorylation levels of p68 were detected by immunoblotting of anti-p68 immunoprecipitates as indicated. Immunoblotting using p68-rgg antibody was loading control.

Figure III-3

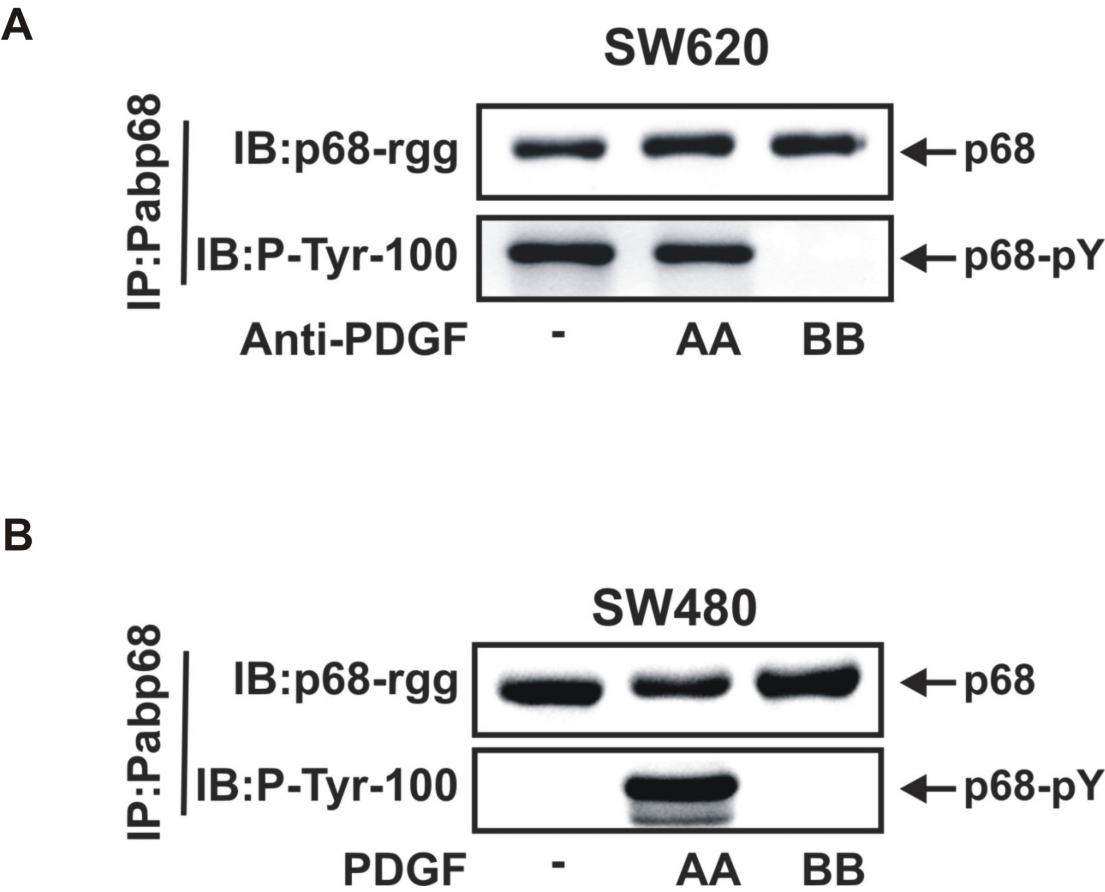


Figure III-4 Y593 is the tyrosine phosphorylation site of p68.

(A) RNAi resistant p68 expression vectors. Small interference RNA sequence targets open reading frame of p68 as shown. Exogenous HA-tagged p68 expression vector coding WT or Y593F mutant are mutated at four nucleotides to avoid RNAi-mediated degradation.

(B) Y593 is the tyrosine phosphorylation site of p68 in SW620 cells. SW620 cells were treated with siRNA to knockdown endogenous p68. The exogenous HA-tagged p68s (wt or Y593F) were expressed in the p68-knockdown cells. Immunoprecipitated p68 were detected by immunoblotting using antibodies against HA or P-Tyr-100. Immunoblotting using p68-rgg antibody indicates the knockdown efficiency by RNAi (First panel).

Figure III-4

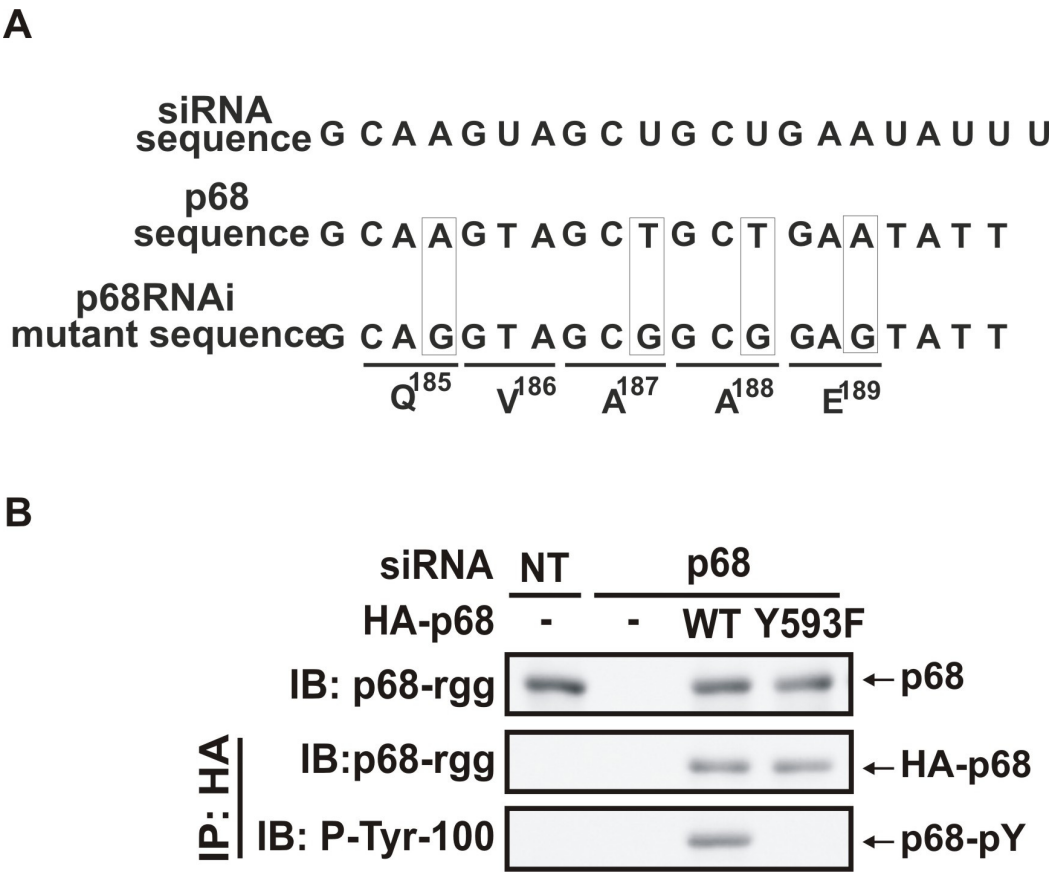


Figure III-5. Tyrosine phosphorylation of p68 promotes EMT.

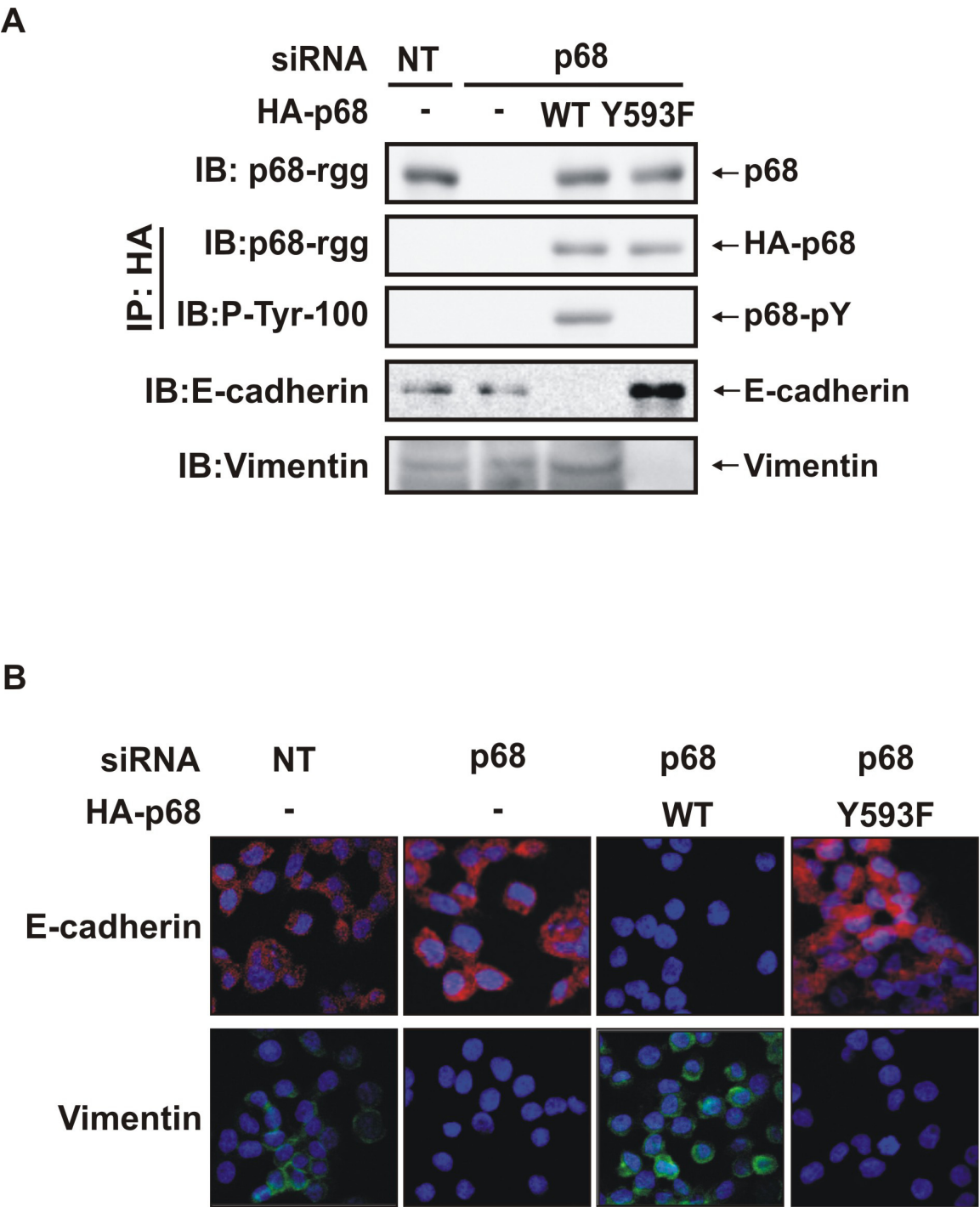
(A) Phosphor-p68 down-regulates epithelial marker and upregulates mesenchymal marker. HA-p68s (wt or Y593F) were expressed in p68-knockdown cells. Immunoblotting using antibodies against E-cadherin or Vimentin in cell lysates were shown as indicated. HA Immunoprecipitates were examined by immunoblotting using antibody against HA or P-Tyr-100 as indicated. Immunoblotting using p68-rgg antibody was expression control.

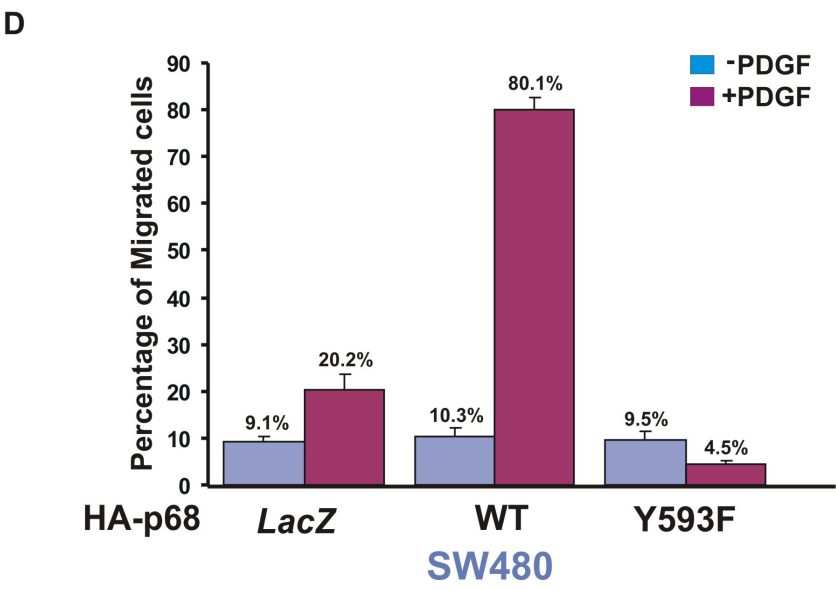
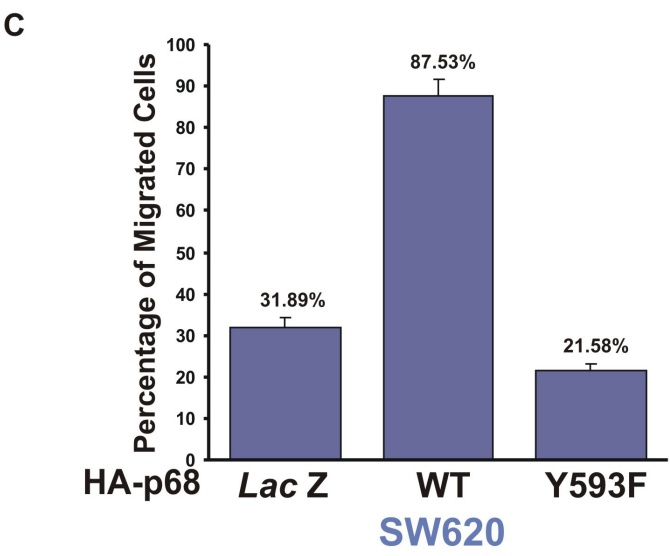
(B) SW620 cells were cultured on chambered microslides (BD Biosciences) and transfected with siRNA to knockdown endogenous p68. HA-p68s (wt or Y593F) were expressed in p68-knockdown cells. The treated SW620 cells were fixed with 3.7% formaldehyde. After permeabilization and blocking, cells were stained by proper primary and secondary antibodies and viewed using Zeiss LSM510 Confocal Microscope.

(C) SW620 cells that stably expressed HA-tagged p68s (wt or Y593F mutant) were analyzed by invasive assay (BD Bioscience, Ja Jolla). Relative invasive activity is presented as percentage of total cell numbers pass through collagen matrix. The results were the average of three independent experiments.

(D) SW480 cells that stably express LacZ (control) and HA-p68s (wt or Y593F) were treated/untreated with PDGF (20 ng/ml) for overnight before performing invasive assay (BD Bioscience, Ja Jolla). Relative invasive activity is presented as percentage of total cell numbers pass through collagen matrix. The result presents three independent experiments.

Figure III-5





CHAPTER IV

PHOSPHORYLATION OF p68 RNA HELICASE ACTIVATES SNAIL TRANSCRIPTION BY DISSOCIATING HDAC1 FROM THE MBD3:MI-2/NURD COMPLEX AT THE PROMOTER

4.1 Abstract

The initiation of tumor cell invasion requires Epithelial-Mesenchymal Transition (EMT), by which tumor cells lose cell-cell interactions and gain the ability of migration. The gene expression profile during the EMT process has been extensively investigated to study the initiation of EMT. In our studies, we indicated that tyrosine phosphorylation of human p68 RNA helicase positively associated with the malignant status of tumor tissue or cells. Studying of this relationship revealed that p68 RNA helicase played a critical role in EMT progression by repression of E-cadherin as an epithelial marker and upregulation of Vimentin as a mesenchymal marker. Insight into the mechanism of how p68 RNA helicase represses E-cadherin expression indicated that p68 RNA helicase initiated EMT by transcriptional upregulation of Snail. Human p68 RNA helicase has been documented as an RNA-dependent ATPase. The protein is an essential factor in the pre-mRNA splicing procedure. Some examples show that p68 RNA helicase functions as a transcriptional coactivator in ATPase dependent or independent manner. Here we indicated that p68 RNA helicase unwound protein complexes to modulate protein-protein interactions by using protein-dependent ATPase activity. The phosphorylated p68 RNA helicase displaced HDAC1 from the chromatin remodeling MBD3:Mi2/NuRD complex

at the Snail promoter. Thus, our data demonstrated an example of protein-dependent ATPase which modulates protein-protein interactions within the chromatin remodeling machine.

4.2 Introduction

Tumor cells spread out to distance organs of human body through metastasis. For tumor cells to perform this deadly behavior, invasive cells suppress adhesion protein expression to escape from cell-cell interactions, degrade or remodel extracellular matrix which blocks tumor cells destination and acquire migratory phenotype. Intensive studies indicated that the transition from non-metastatic adenoma to invasive carcinoma is driven by a distinct series of changes of adhesion proteins. These changes include loss of epithelial adhesion and catenin-dependent junction, as well as expression of mesenchymal gene and expansion of migratory, invasive phenotype. This process is generally termed as Epithelial-mesenchymal transition (EMT). EMT is characterized by the loss of cell adhesions and upregulation of mesenchymal markers, breakdown of epithelial contact and cell rearrangement or migration in extracellular matrix (Shook and Keller 2003). Epithelial cells may transiently lose their polarized phenotype and achieve cell spreading in many developmental and pathological processes (Duband, Monier et al. 1995; Hay 1995; Viebahn 1995; Sun, Baur et al. 2000; Thiery 2002). Various mechanisms contribute to the disruption of adhesions junction and cadherin-catenin complex of cancer cells. For some tumors, a family of transcription factors, Snail/Slug, down-regulate the *E-cadherin* gene transcription (Nieto 2002).

Members of Snail family are indicated to be involved into EMT and epithelial cells transformation toward mesenchymal cells (Alberga, Boulay et al. 1991; Burdsal, Damsky et al. 1993; Nieto, Sargent et al. 1994). Expression of Snail induces epithelial cell acquire fibroblastic phenotype and invasiveness properties. Inhibition of Snail function restores E-cadherin expression in epithelial cancer cell line in which E-cadherin has been lost (Batlle, Sancho et al. 2000; Cano, Perez-Moreno et al. 2000). Furthermore, Snail is indicated to bind three E-boxes located on the E-cadherin promoter and represses transcription of the *E-cadherin* gene directly (Batlle, Sancho et al. 2000). Therefore, Snail may be considered as malignancy marker and plays a central role of EMT.

Multiple signal molecules have been investigated to trigger Snail mediated EMT both in embryonic development and tumor malignancy transformation; however, the mechanism that regulate Snail remains uncertain. Several research groups have indicated that Snail can be regulated probably through chromatin remodeling/transcription and post-translational modification pathways (Erives, Corbo et al. 1998; Dominguez, Montserrat-Sentis et al. 2003; Fujita, Jaye et al. 2004; Zhou, Deng et al. 2004). Transcriptional regulation is one of the major mechanisms to regulate Snail expression, which has been studied in both embryonic development and tumor transformation. ER has been long thought as a critical marker of prognosis and therapy in breast cancer (Masood 1992). Product of human *MTA3* gene is identified as a component of Mi2/NuRD transcription corepressor in epithelial breast cancer. MTA3 and MBD3, a known component of the NuRD complex associates with the *Snail* promoter upstream of transcription start site and selectively repress the *Snail* gene expression.

Absence of MTA3 results in aberrant expression of Snail, leading to epithelial cells transformation toward mesenchymal cells (Fujita, Jaye et al. 2004). The elusive mechanism by which the NuRD complex represses Snail transcription is intriguing and remains discussion.

Human p68 RNA helicase is the gene product of DEAD (Asp-Glu-Ala-Asp) box polypeptide 5 (DDX5). Translation product of this gene is 614 amino acids long and characterized by the conserved DEAD motif as a putative RNA helicase. Human p68 RNA helicase was first detected by anti-SV40 large T monoclonal antibody DL3C4 (PAB204) due to the specifically cross-reaction (Crawford, Leppard et al. 1982; Ford, Anton et al. 1988). Protein p68 shows a distinct nuclear distribution and is thought to be important for cell division and proliferation (Ford, Anton et al. 1988). Recombinant p68 RNA helicase was purified and exhibited RNA-dependent ATPase activity and helicase activity *in vitro* (Hirling, Scheffner et al. 1989). Family members of DEAD-box proteins share conserved sequence, express ubiquitously in living cells and being considered to be involved in multiple RNA metabolism, including splicing, translation, RNA processing, RNA transport and rRNA biosynthesis/assembly (Iggo and Lane 1989). p68 RNA helicase has been indicated to engage in diverse signaling pathways as transcriptional coactivator or corepressor and play important role in various cellular processes including cell proliferation, wound healing, apoptosis and tumor development (Stevenson, Hamilton et al. 1998; Causevic, Hislop et al. 2001; Guil, Gattoni et al. 2003; Rossow and Janknecht 2003; Kahlina, Goren et al. 2004; Wilson, Bates et al. 2004; Bates, Nicol et al. 2005; Kodym, Henockl et al. 2005). In human colon cancer tissue, accumulated p68

protein is poly-ubiquitinated and this accretion is apparently due to the unktion of proteasome-mediated degradation (Causevic, Hislop et al. 2001).

In our studies, we indicated that tyrosine phosphorylation level of human p68 RNA helicase is positively associated to malignant status of tumor tissue or cells. Previous studies revealed that p68 RNA helicase plays a critical role in EMT progression by repression the expression of E-cadherin and upregulation Vimentin. Insight into the mechanism of how p68 RNA helicase represses E-cadherin expression indicated that p68 RNA helicase initiated EMT by transcriptional upregulation of Snail, a regulator of EMT. Human p68 RNA helicase has been documented as a RNA-dependent ATPase, which is an essential factor in the pre-mRNA splicing process. Some examples showed that p68 RNA helicase functions as a transcriptional coactivator in ATPase dependent or independent manner. Here we indicated that p68 RNA helicase unwinds protein complex to modulate protein-protein interactions by using protein-dependent ATPase activity. The phosphorylated p68 RNA helicase disassociated HDAC1 from chromatin remodeling complex MBD3:Mi2/NuRD complex at the *Snail* promoter. Thus, our data demonstrated an example of protein-dependent ATPase which modulates protein-protein interactions in chromatin remodeling machine.

4.3 Results

4.3.1 The Phosphor-p68 Repressed E-cadherin Expression by Indirect Mechanisms.

Our experiments demonstrated that tyrosine phosphorylation of p68 at Y593 suppresses E-cadherin expression. Several mechanisms control the repression of E-

cadherin during EMT process, such as gene mutation and transcription repression (Yoshiura, Kanai et al. 1995; Guilford, Hopkins et al. 1998; Poser, Dominguez et al. 2001; Peinado, Ballestar et al. 2004). Suppression of E-cadherin on transcriptional regulation is a main mechanism for regulation of cell adhesions protein expression during EMT (Berx, Cleton-Jansen et al. 1995; Christofori and Semb 1999). To understand the role of the phosphorylated p68 in EMT, we tested the transcription activity of E-cadherin promoter in SW620 cells using a luciferase reporter, fused to the E-cadherin promoter containing three E-boxes (Hajra, Ji et al. 1999). We utilized RNAi to knockdown endogenous p68. Exogenous HA-tagged p68s (wt or mutant Y593F) was expressed in p68-knockdown cells. E-cadherin reporter and Renilla reporter vectors were cotransfected. After incubation, the cells were harvested for dual reporter assay. The luciferase activities of Renilla were used as internal control. E-cadherin transcription activity was not significantly affected by p68-knockdown but was substantially down-regulated in SW620 cells in which wild type p68 was exogenously expressed (**Figure IV-1A**). Interestingly, the E-cadherin transcription was significantly upregulated in SW620^{p68/+Y593F} cells, suggesting that tyrosine phosphorylation of p68 is required for suppression of the *E-cadherin* gene expression. These data supported the assumption that downregulation of E-cadherin in p68 phosphorylated cells may due to inhibition of the *E-cadherin* gene transcription.

We asked whether the phosphor-p68 regulated the E-cadherin transcription directly or the regulatory effects are mediated through other cellular factors. We reasoned that if p68 regulates E-cadherin transcription directly, p68 might participate into

transcriptional complex assembled at the *E-cadherin* promoter. Therefore, we examined whether the phosphor-p68 interacted with the *E-cadherin* promoter by chromatin immunoprecipitation (ChIP) experiments. In the ChIP experiments, proteins that interact with DNA will be crosslinked by formaldehyde. After DNA fragmentation, a target protein will be immunoprecipitated. DNA fragments that co-immunoprecipitated with the target protein will be analyzed by a PCR reaction with a pair of primers targeted to specific DNA element(s). The ChIP experiments will argue whether the target protein directly participate the protein complex that assembled on a specific DNA element(s), such as a transcriptional promoter.

The -108 to +49 region of E-cadherin promoter has been intensively studied. The region harbors three E-box elements that are bound by regulatory transcription factors. The ChIP experiment was designed to targeting this region of E-cadherin promoter. The SW620^{-p68/+wt} or SW620^{-p68/+Y593F} cells were fixed by formaldehyde. DNA and DNA bound proteins were crosslinked. After sonication to break down chromatin to small fragments (~500 bp), HA-tagged proteins were immunoprecipitated by antibody against HA epitope. The immunoprecipitates were extensively washed and de-crosslinked. After clearance and concentration, co-immunoprecipitated DNA fragment were detected by PCR reaction using primers targeting -108 to +49 region of E-cadherin promoter. It was clear from the ChIP experiment that neither p68 wild-type nor the Y593F mutant interacted with the *E-cadherin* promoter (**Figure IV-1B**). A small fraction of chromatin as input (without immunoprecipitation) was used as positive control. We concluded that

the phosphor-p68 might regulate the E-cadherin expression through other regulatory molecules.

4.3.2 Snail Mediates the Effect of Phosphor-p68 on E-cadherin Suppression.

Snail/Slug and SIP1 are the master regulators that regulate E-cadherin transcription (Comijn, Berx et al. 2001; Poser, Dominguez et al. 2001; Bolos, Peinado et al. 2003). Snail is also suggested to promote EMT during tumor metastasis (Batlle, Sancho et al. 2000; Cano, Perez-Moreno et al. 2000). It is possible that Snail or other transcription factors mediate the effect of phosphor-p68 in controlling E-cadherin transcription during EMT process. Thus, we examined the effects of the p68 phosphorylation on the expression of Snail. HA-p68s (wt or Y593F) were expressed in p68-knockdown SW620 cells. Immunoblotting using antibody against Snail from cell lysate showed that cellular levels of Snail were increased in the SW620^{-p68/+wt} cells and decreased in the SW620^{-p68/+Y593F} cells (**Figure IV-2A** fourth panel from top). The Snail upregulation correlated with the p68 phosphorylation at Y593 (**Figure IV-2A** third and fourth panel from top). Interestingly, knockdown of endogenous p68 reduced Snail protein expression to undetectable level, suggesting a direct role of p68 in controlling Snail expression.

The cellular level of Snail can be regulated through transcriptional regulation or post-translational modification. To determine whether the regulation of cellular level of Snail was due to transcriptional regulation, we carried out luciferase reporter assays in SW620^{-p68/+wt} or SW620^{-p68/+Y593F} cells, using a luciferase reporter fused with Snail

promoter (Fujita, Jaye et al. 2004). Snail reporter and Renilla reporter vectors were expressed in SW620^{-p68/+wt} or SW620^{-p68/+Y593F} cells. After incubation, the cells were harvested for dual reporter gene assay. The luciferase activities of Renilla were used as internal control. The transcription activity of the reporter in untreated cells was defined as 100. Consistent with immunoblotting data, knockdown of endogenous p68 inhibited the Snail gene transcription (**Figure IV-2B**). It was evident that the transcription activity of Snail promoter was activated in SW620^{-p68/+wt} cells, while the transcriptional activity of the Snail promoter was repressed in SW620^{-p68/+Y593F} cells (**Figure IV-2B**). These results indicated that phosphorylation of p68 at Y593 regulated the transcriptional activity of the Snail gene.

We then tested whether the phosphor-p68 regulated the Snail transcription directly or indirectly by performing the same ChIP experiments with the Snail promoter. Previous studies demonstrated that Snail gene transcription is regulated through binding of transcription factor at a region from -700 to -300 of the *Snail* promoter. ChIP experiments were carried out to examine the association of p68 with the *Snail* promoter. The ChIP experiments were performed by precipitation of exogenously expressed HA-p68s (wt or Y593F mutant) in SW620 cells, in which endogenous p68 were knocked down. The DNA fragments precipitated with HA-tagged p68s were examined by PCR with primers targeting to the region from -700 to -500. Both p68 wild-type and Y593F mutant precipitated with the Snail promoter (**Figure IV-2C**), indicating that p68 was directly involved in the transcriptional regulation of the *Snail* gene. Surprisingly, both phosphorylated p68 (wt) and unphosphorylatable p68 (Y593F) interacted with the

promoter region of the *Snail* gene by ChIP experiment. This observation was not agreed with our previous immunoblotting and reporter gene experiments that demonstrated that phosphorylation of p68 regulated the *Snail* gene transcription. One explanation is that tyrosine phosphorylation of p68 modulates the interactions of p68 with other potential cofactors or transcriptional machinery. Thus, it is highly likely that phosphorylated p68 cooperate with unidentified transcriptional regulatory complex to regulate the transcription of *Snail* gene.

We reasoned: if the phosphor-p68 repressed E-cadherin through regulation of transcription of Snail, the Snail expression must be required for the effects of the Y593 phosphorylation on the E-cadherin repression. To test this conjecture, we examined the effects of the p68 phosphorylation on the cellular levels of E-cadherin in SW620 cells in which Snail was knocked down by RNAi. SW620 cells were first transfected with siRNA targeting Snail and subsequently transfected with HA-p68s, (wt or mutant). Immunoblotting of Snail using antibodies against Snail indicated that Snail expression was efficiently knocked down (**Figure IV-2D** first panel from top). The expression of E-cadherin and Vimentin were examined by immunoblotting using antibodies against E-cadherin and Vimentin. Firstly, E-cadherin was repressed and Vimentin was upregulated by expression of p68 wild-type in SW620 cells without knocking down Snail. By expression of Y593F mutant, E-cadherin was up regulated and Vimentin was suppressed (**Figure IV-2D** second and third panel from top). However, knockdown of Snail abolished the effects of exogenous expression of p68s on cellular levels of E-cadherin and Vimentin (**Figure IV-2D** second and third panel from top). The results supported

the conclusion that the phosphorylated p68 represses E-cadherin through regulation of Snail transcription. Knockdown of the Snail gene does not affect expression level or tyrosine phosphorylation level of p68 in SW620 cells (**Figure IV-2D** fourth and fifth panel from top). These findings supported the perception that Snail is downstream target of the phosphorylated p68.

To further confirm the essential role of Snail in EMT process promoted by phosphorylated p68, the invasive capability of SW620 cells that stably expressed HA-p68s (wt, Y593F mutant) was examined. The Snail gene was knocked down in the cell expressing HA-p68s. The cells were labeled by fluorescence and seeded into upper chamber of invasion assay plates. Fluorescence signals were detected by micro plate reader after incubation for appropriate time. Consistently, overexpression of p68 in SW620 cells induced very high cell invasion activity, whereas knockdown of Snail abolished the effect of phosphor-p68 in promoting cell invasion (**Figure IV-2E**). Moreover, in SW620 cells, in which HA-Y593F were expressed, Snail knockdown did not affect the cells invasive capability.

Our experiments suggested that phosphor-p68 played a role in repression of E-cadherin expression through the regulation of transcription factor Snail. The phosphorylated p68 directly participated into the protein complex assembled at the promoter of *Snail*. The phosphorylated p68 may regulate Snail transcription probably through modulating interactions of p68 with other transcriptional regulatory factors. It is possible that other transcription factors, such as TWIST or Slug, may contribute to the phosphor-p68-mediated EMT and cell migration. However, knockdown of Snail

abolished the cell phenotype transformation and invasion capability. Furthermore, knockdown of Snail exhibited similar effect compared with expression of Y593F mutant on cellular markers expression and cell mobility, ruling out the possibilities of diverse signaling pathways. Thus, it is highly likely that Snail specifically mediates the PDGF-induced, phosphor-p68-mediated tumor cell EMT and invasion.

4.3.3 p68 Associates with MBD3: Mi-2/NuRD Complex.

The preceding experiments suggested the role of the phosphor-p68 in repression of E-cadherin through the regulation of transcription of the *Snail* gene. To further understand the molecular mechanism by which the phosphor-p68 regulated transcription of the *Snail* gene, we attempted to probe the protein or protein complex that interacted with the phosphor-p68 at the Snail promoter. Recently, Fujita and co-workers demonstrated that MTA3 targeted the nuclear remodeling and deacetylation complex Mi-2/NuRD to the Snail promoter and directly regulated the Snail gene transcription (Fujita, Jaye et al. 2004). Thus, we asked whether the phosphor-p68 interacted with the MBD3: Mi-2/NuRD complex in SW620 cells. To this end, we carried out co-immunoprecipitation with the nuclear extracts made from SW620 cells using an antibody against p68. As a comparison, the co-immunoprecipitation experiments were also performed with nuclear extracts made from SW480, a cell line derived from the tissue of the same patient from whom SW620 was derived. SW480, however, was derived from tissue of non-metastatic adenocarcinoma. The tyrosine phosphorylation of p68 was almost undetectable in SW480 cells (see Figure III-2A). The immunoprecipitates of p68

from cell lysates made from SW480 and SW620 were examined by immunoblotting using antibodies as indicated. It was clear that the antibody of p68 precipitated MBD3, Mi-2 and HDAC1 in the extracts made from SW480 cells (**Figure IV-3A** second to fourth panel, left part). The antibody also precipitated MBD3 and Mi-2 in the extracts made from SW620 cells. Interestingly, the p68 antibody did not precipitate HDAC1 in the nuclear extracts made from SW620 cell (**Figure IV-3A** fourth panel, right part). It was clearly that the interactions observed by co-immunoprecipitation experiment were not due to non-specific binding, because immunoprecipitation without anti-p68 polyclonal antibody (IgG) did not detect these interactions. Immunoblotting using p68-rgg suggested that similar amount of p68 were participated in this experiment. A portion of cell lysates were examined by immunoblotting to detect the endogenous expression of MBD3, Mi-2 and HDAC1. Given that MBD2, Mi-2 and HDAC1 are core components of the NuRD complex, this experiment suggested that p68 might associate with this complex.

To confirm the co-immunoprecipitation results, we performed additional set of co-immunoprecipitation experiments using antibodies against MBD3, Mi-2 and HDAC1. The immunoprecipitates of MBD3, Mi-2 and HDAC1 were examined by immunoblotting using p68-rgg. The co-precipitation of p68 with MBD3, Mi-2 and HDAC1 in the extracts made from SW480 cells was clearly evident. P68 also co-precipitated with MBD3 and Mi-2 in the co-immunoprecipitation experiments with the extracts made from SW620 cells (**Figure IV-3B** upper panel). Nevertheless, p68 did not precipitate with HDAC1 in the extracts made from SW620 cells using antibody against HDAC1 (**Figure IV-3B**

upper panel). The immunoprecipitates of p68 were also inspected by immunoblotting using P-Tyr-100. It is evident that p68 is tyrosine phosphorylated in SW620 cells. The experiments suggested that unphosphorylated p68, but not tyrosyl-phosphorylated p68 associated with HDAC1. The protein-protein interaction studies indicated that p68 associated with MBD3: Mi-2/NuRD complex in both SW480 and SW620 cells except that the interactions between HDAC1 and other components of the NuRD complex are regulated by the tyrosine phosphorylation of p68.

We further tested the role of the phosphorylation of p68 at Y593 in the association of p68 with the MBD3: Mi-2/NuRD complex. p68 was knocked down in SW620 cells by RNAi and the HA-p68s (wt or Y593F mutant) were exogenously expressed. We then carried out co-immunoprecipitation with the nuclear extracts made from the cells using anti-HA antibody. Immunoblotting of the immunoprecipitates using antibodies against MBD3 and Mi-2 demonstrated that MBD3 and Mi-2 co-immunoprecipitated with the HA-p68s (wt and Y593F mutant) (**Figure IV-3C** third and fourth panel, right part). However, this experiment suggested that HDAC1 only interacted with the Y593F mutant but not with the wild type p68 (**Figure IV-3C** second panel, right part). Immunoblotting of cell lysate verified the expression of HA-p68s, endogenous MBD3, Mi-2 and HDAC1 (**Figure IV-3C** first to fourth panel, left part). The results indicated that p68 associated with the MBD3: Mi-2/NuRD complex. However, only the unphosphorylated p68 facilitated the MBD3/Mi-2-HDAC1 complex formation. HDAC1 was not able to associate with MBD3: Mi-2/NuRD in the presence of the phosphor-p68.

4.3.4 MBD3 Mediates the Loading of p68 on the Snail Promoter

We next asked whether the interactions between p68 and MBD3: Mi-2/NuRD is required for the association of p68 and/or MBD3: Mi-2/NuRD with the *Snail* promoter. We performed the chromatin immunoprecipitation experiments in SW620 cells in which either p68 or MBD3 was knocked down by RNAi. Immunoblotting demonstrated an efficient knock down of MBD (over 90%) and p68 (**Figure IV-4A** first panel and see figure III-5A). We then exogenously expressed HA-p68s (wt or Y593F mutant) in MBD3 knockdown cells. The knockdown of MBD3 did not affect cellular house-keeping gene, Actin-beta expression (**Figure IV-4A** second and third panel from top). The chromatin fragments immunoprecipitated with HA or MBD3 were examined by PCR using primers targeting -700 to -500 region of the *Snail* promoter. Anti-HA antibody did precipitate the *Snail* promoter in control knockdown cells (**Figure IV-4B** second lane). However, knockdown of MBD3 blocked the association of HA-tagged p68s with Snail promoter in the presence of wild type p68 or Y593F mutant (**Figure IV-4B**). On the contrary, antibody against MBD3 did precipitate the *Snail* promoter in the p68-knockdown cells (**Figure IV-4C** third lane). Expression of HA-p68s (wt or Y593F mutant) also did not affect the MBD3-Snail promoter precipitation (**Figure IV-4C** fourth and fifth lanes). The data suggested that association of p68 with the MBD3: Mi-2/NuRD is not required for the association of MBD3: Mi-2/NuRD complex with the *Snail* promoter. In contrast, MBD3 was required for association of p68 with Mi-3/NuRD complex at the *Snail* promoter. p68 has been demonstrated to act as a transcriptional coactivator or corepressor in different gene promoters (Endoh, Maruyama et al. 1999; Rossow and Janknecht 2003;

Kahlina, Goren et al. 2004; Bates, Nicol et al. 2005). It is speculated that p68 may associate with various transcription regulatory machineries to regulate the expression of targeted genes.

4.3.5 The phosphor-p68 displaces HDAC1 from the Snail promoter.

There were two possible explanations for the observation that HDAC1 did not co-precipitate with p68 in SW620 cells. (1) The unphosphorylated p68 recruited HDAC1 to the MBD3: Mi-2/NuRD complex. The phosphor-p68 could not function as a recruiter. (2) The phosphor-p68 ‘unwound’ HDAC1 from the complex. The unphosphorylated p68 could not function as a protein ‘unwindase’. To determine the mechanism, we first probed association of HDAC1 with the *Snail* promoter in SW620^{-p68}, SW620^{-p68/+wt} and SW620^{-p68/+Y593F} cells by chromatin immunoprecipitation experiments. Immunoprecipitates using antibody against HDAC1 were examined by PCR reaction to detect the promoter of Snail. Chromatins extracted from SW480 and SW620 cells transfected with non-targeting siRNA were also immunoprecipitated using anti-HDAC1 antibody. It was clear that knockdown of p68 dramatically enhanced the association HDAC1 with the Snail promoter (**Figure IV-5A** fourth lane). However, expression of HA-p68 wt in the p68-knockdown cells diminished the association of HDAC1 with the *Snail* promoter. The HDAC1 associated with the *Snail* promoter in the cells expressing Y593F mutant (**Figure IV-5A** the fifth and sixth lanes). In non-treated SW620 cells, HDAC1 associated with Snail promoter in a very low level. In the case that p68 was knocked down, the interactions of HDAC1 with Snail promoter were greatly enhanced,

suggesting that more HDAC1 were loaded to the *Snail* promoter. The results ruled out the possibility that p68 might recruit HDAC1 to *Snail* promoter. It is more likely that phosphorylated p68 displaces HDAC1 from *Snail* promoter by unknown mechanisms. When p68 was knocked down or mutated at phosphorylation site, HDAC1 was not displaced from *Snail* promoter. Histone deacetylases remove acetyl group modification from histone tails of nucleosomes, which is believed to condense chromatin architecture and prevent the access of transcription factor (Kimura, Matsubara et al. 2005; Verdone, Caserta et al. 2005). Therefore, the ChIP experiments suggested that the phosphor-p68 displaced HDAC1 from the *Snail* promoter and subsequently upregulated the *Snail* expression.

We questioned whether the p68 phosphorylation affected the HDAC1 activity at the *Snail* promoter. To this end, the HA-p68s (wt or Y593F mutant) were stably expressed in SW620 cells using the commercially available lentiviral gene expression system. The expression levels of HA-p68s (wt or mutant) was revealed by the immunoblotting using anti-HA antibody (**Figure IV-5B**). The exogenously expressed p68s were immunoprecipitated from the nuclear extracts by anti-HA antibody. The deacetylase activity of the immunoprecipitates was analyzed by HDAC Activity Colorimetric Assay kit (BioVision). Briefly, the immunoprecipitates with or without a general histone deacetylase inhibitor, trichostatin A (TSA), were incubated with artificial substrates. After incubation, the products were labeled with dye and analyzed by micro plate reader. It was evident that overexpression of wt HA-p68 suppressed the deacetylase activities by 2 folds (**Figure IV-5C**). In contrast, overexpression of Y593F mutant led to

the increase of deacetylase activities by over 4 fold (**Figure IV-5C**). The enhancement of deacetylase activity was verified by the treatment of TSA. Since p68 does not have known deacetylase activity, the detected changes in deacetylase activity were due to deacetylase that co-immunoprecipitated with p68.

To further investigate whether the p68 phosphorylation affected the HDAC activity at the *Snail* promoter, we measured the *Snail* promoter activity in the presence and absence of HDAC inhibitor TSA in SW620 cells, in which HA-p68s (wt or mutant) was overexpressed. The SW620 cells that stably express HA-p68s (wt or Y593F mutant) were transfected by *Snail* reporter and Renilla reporter. Before harvesting, the cells were treated with TSA (100 ng/ml) overnight. The cells were harvest in the next day and performed dual reporter gene assay. The data indicated that the phosphor-p68 indeed enhanced the *Snail* gene transcription (**Figure IV-5D**). Overexpression of unphosphorylatable Y593F mutant suppressed the expression of *Snail*. This suppression effect could be relieved by treatment of cells with TSA (**Figure IV-5D**). On the other hand, TSA treatment did not affect the *Snail* transcription in the presence of phosphor-p68. This observation was consistent with our findings that HDAC1 did not presented at *Snail* promoter in the presence of the phosphorylated p68. We previous ruled out the possibility that unphosphorylated p68 recruits HDAC1 to the NuRD complex and the *Snail* promoter. Thus, it is highly likely that phosphor-p68 displaced HDAC1 from the complex and consequently relieved the *Snail* gene from suppression. This may explain the invasive behavior of SW620 cells. In contrast, in certain cell lines that p68 are not

tyrosine phosphorylated, such as SW480 cells, it is speculated that unphosphorylated p68 associates HDAC1 and inhibits Snail transcription.

4.3.6 The Phosphor-p68 has Protein-dependent ATPase Activities.

Since p68 is a DEAD-box RNA helicase, to test whether the function of displacement of HDAC1 from the Snail promoter by the phosphor-p68 was due to a DNA/RNA dependent ATPase or unwindase activity, we carried out co-immunoprecipitation with nuclear extracts that were treated with DNase I and RNase. Cell lysates extracted made from SW480 or SW620 were incubated with DNase I (40 U/50 μ l lysate) or RNase mix (3 U/50 μ l lysate). p68 were immunoprecipitated from treated cell lysates by polyclonal antibody of p68. The immunoprecipitates were examined by immunoblotting of antibodies against p68, HDAC1 and MBD3. It was evident that p68 co-immunoprecipitated with MBD3 and HDAC1 in DNase/RNase treated extracts made from SW480 cells (**Figure IV-6A** second and third panel). However, p68 did not co-immunoprecipitate with HDAC1 in DNase/RNase treated extracts made from SW620 cells (**Figure IV-6B** second and third panel). p68 were precipitated at similar amount by the antibody in each samples as indicated by immunoblotting of anti-p68 antibody (**Figure IV-6 A & B** first panel). Immunoblotting of Actin β verified that the DNase/RNase treatment did not cause protein degradation. The experiments suggested that the HDAC1 displacement was not DNA/RNA dependent.

It was intriguing that the phosphor-p68 was able to displace HDAC1 from the MBD3: Mi-2/NuRD complex in a DNA/RNA independent manner. We also observed that the phosphor-p68 was able to 'unwind' Axin from cytoplasmic β -catenin (Yang et al, in preparation). We speculated that phosphorylation of p68 at Y593 might change the enzymatic activities of the protein. To test this conjecture, we generated a p68 mutant that carried a mutation at the DEAD motif (Ref to as EEAD), which located at the highly conserved motif II within helicases core (Rocak and Linder 2004). This mutation has been shown to abolish the ATPase activity of p68 (Huang and Liu 2002; Lin, Yang et al. 2005). We expressed and purified recombinant His-p68s (wt, Y593F or EEAD mutant) in *E. coli*. The His-tagged p68s were dephosphorylated by PP2A and PTP to remove the potential phosphor group attached to p68s. The dephosphorylated proteins were purified and concentrated and further re-phosphorylated by the recombinant c-Abl kinase (Yang, Lin et al. 2005). After clearance, the ATPase activity of the phosphor-p68 (wt or mutant) was examined. The recombinant p68s, phosphorylated or non-phosphorylated were incubated with 4 mM ATP and different potential substrates (dsDNA, ssDNA, dsRNA, ssRNA, BSA or β -catenin). Consistent with our previous observation, the ATPase activity of p68 was RNA-dependent (Huang and Liu 2002; Lin, Yang et al. 2005; Yang, Lin et al. 2005). There was a sharp decrease in dsRNA dependent ATPase activity upon Y593 phosphorylation. Double strand DNA (dsDNA) stimulated minor ATPase activity of the protein and single-stranded DNA (ssDNA) did not stimulate ATP hydrolysis (**Figure IV-6C**). Interestingly, a strong ATPase activity of the phosphor-p68 was

detected in the presence of β -catenin, a protein interacting with the phosphor-p68 (Yang et. al, in preparation) (**Figure IV-6C**). Similarly, a strong ATPase activity of the phosphor-p68 was detected in the presence of recombinant MBD3. This ATPase activity was not detected with unphosphorylated p68 or with the Y593F mutant (**Figure IV-6D**). This protein-dependent ATPase activity was also undetectable in the presence of BSA, a non-specific protein that does not interact with p68. Furthermore, *in vitro* phosphorylated His-EEAD mutant abolished the ATPase activity including the protein-dependent ATPase activity, confirming that phosphor-p68 did hydrolyze ATP in the presence of β -catenin or MBD3 (**Figure IV-6D**). Hence, we concluded that the phosphor-p68 gained a protein-dependent ATPase activity upon the Y593 phosphorylation.

4.3.7 Displacement of HDAC1 from Snail Promoter Requires ATPase Activity of p68.

To further test the active displacement of HDAC1 from the MBD3: Mi-2/NuRD complex at the Snail promoter complex, the HA-P68s, wt, Y593F or EEAD were expressed in p68-knockdown cells. The expression of HA-p68s were revealed by immunoblotting using anti-HA antibody (**Figure IV-7A**). We then examined the association of HDAC1 with the *Snail* promoter in p68-knockdown SW620 cells in which The HA-P68s, wt, Y593F or EEAD mutant were expressed by chromatin immunoprecipitation assays using the antibody against HDAC1. It was clear that the mutation that abolished the ATPase activity also abolished the displacement of HDAC1

from the MBD3: Mi-2/NuRD complex at the *Snail* promoter (**Figure IV-7B**), indicating that the ATPase activity of p68 was required for the displacement of HDAC1 from the MBD3: Mi-2/NuRD complex at the *Snail* promoter. The observation provided additional evidence that the protein-dependent ATPase activity of the phosphor-p68 displaces HDAC1 from the MBD3: Mi-2/NuRD complex. Thus, our data demonstrated that tyrosine phosphorylation of DEAD-box protein p68 regulated *Snail* transcription via remodeling the interactions of components of a multi-protein complex.

4.4 discussions

In this chapter, an important role of p68 in tumor cell EMT was investigated. We observed that p68 acquired tyrosine phosphorylation at Y593 in metastatic cancer cells. Tyrosine kinase c-Abl phosphorylated p68 upon PDGF stimulation. The phosphorylated p68 repressed E-cadherin through upregulation of the *Snail* gene expression. The phosphorylated p68 activates transcription of the *Snail* gene by displacing HDAC1 from the nuclear remodeling and deacetylation complex MBD3: Mi-2/NuRD using its protein-dependent ATPase activity. p68 RNA helicase has been implicated in transcriptional regulation of a number of genes. However, it is not known how a DEAD-box RNA helicase functions in transcriptional regulation. Our studies may provide a good model to explain the functional role of p68 or other DEAD-box RNA helicases in the transcriptional process.

Active dissociation of HDACs from the NuRD complex at the *Snail* promoter by the phosphor-p68 is unique. Histone deacetylases are enzymes that modify chromatin

structure and subsequently regulate gene expression. HDACs are usually recruited to a particular regulatory site with their associated multi-protein complexes, such as the NuRD or the Sin3 complex (Knoepfler and Eisenman 1999; Narlikar, Fan et al. 2002). While most studies concentrated on the mechanism by which the HDAC activity and its associated complex is recruited to a specific gene promoter (Forsberg and Bresnick 2001; Kurdistan and Grunstein 2003), our studies demonstrated an example that HDACs can also be displaced from their associated complex by a DEAD-box helicase. Given that tyrosine phosphorylations of p68 were closely associated with cancer development (Yang, Lin et al. 2005), it is tempting to speculate that displacement of HDACs by the phosphor-p68 is a dysregulated route for tumor progression through activation of specific genes. The functional role of the unphosphorylated p68 in the NuRD complex remains to be elucidated. Our data demonstrated that the unphosphorylated p68 did not function as a recruiter nor as an “unwindase” at the Snail promoter. One possibility is that the unphosphorylated p68 may function similarly as the phosphor-p68 (as a protein-dependent “unwindase”) at different promoters. Whether p68 is a constitutive member of the NuRD complex is another question. p68 was not identified in the originally isolated the NuRD complex (Xue, Wong et al. 1998; Zhang, Ng et al. 1999; Bowen, Fujita et al. 2004). Our data showed that the association of p68 with the NuRD complex was DNA/RNA independent. This seems to argue that association of p68 with the NuRD complex is not determined by DNA contents and p68 is a part of protein components of the NuRD complex.

The protein-dependent ATPase activity of the phosphor-p68 is intriguing. The DEAD/DExH box of RNA helicases were originally defined as a family of enzymes that unwound double-stranded RNA (dsRNA) using the energy derived from NTP (ATP in most cases) hydrolysis (Tanner and Linder 2001). Lately, it has been suggested that the RNA-dependent ATPase can also be used to dissociate RNA-protein interactions (Jankowsky, Gross et al. 2001; Fairman, Maroney et al. 2004). Our observations further expand the view for the functions of DEAD/DExH box of RNA helicases as a modulator for protein-protein interactions independent of RNA/DNA. The detailed mechanism by which the phosphor-p68 hydrolyzes ATP in binding to its substrate protein is not clear. A well known example of protein-dependent ATPase motor is SecA, the preprotein translocase (Schekman 1994). Although the motor actions of the phosphor-p68 apparently differ from that of SecA, the mechanism by which protein substrates stimulate ATP hydrolysis may resemble each other. One question is whether the same set of sequence motifs that are used in RNA-dependent ATP hydrolysis are required for the protein-dependent activity. One would speculate that sequence motifs that are involved in RNA binding in coupling to ATP hydrolysis may not be necessary for the protein-dependent ATPase activity. Another interesting question is whether the Y593 phosphorylation of p68 is required for the protein-dependent 'unwinding' activity. It is possible that p68 RNA helicase may gain a 'protein-dependent ATPase' activity after the tyrosine phosphorylation. Alternatively, appropriate substrate may also stimulate the protein-dependent ATPase activity of unphosphorylated p68. In this regard, it will be interesting to identify the substrate protein.

Taken together, these findings provide the first example that DEAD-box proteins modulate protein-protein interactions in an ATP-dependent fashion. The novel function of p68 fine-tunes the mechanism by which p68 regulates gene transcriptional regulation as a coactivator or corepressor. It might be general that DEAD-box proteins or ATPases control transcriptional regulatory machinery by altering the protein-protein interactions within multi-protein complex. In addition, it is potentially possible that the protein-protein interactions which contribute to most cellular processes are dynamically manipulated by wide-ranging ATPases. Therefore, our findings extend the understanding of the functional role of DEAD-box proteins in gene transcriptional regulation.

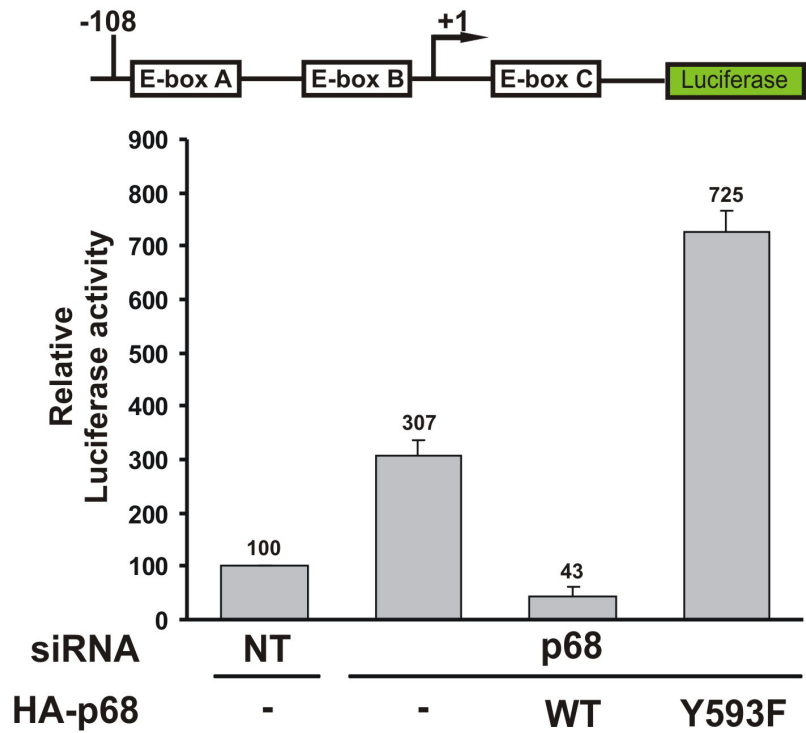
Figure IV-1. The phosphor-p68 represses E-cadherin by indirect mechanism.

(A) p68 represses E-cadherin through transcription regulation. Luciferase reporter gene construct of E-cadherin promoter fused with luciferase was co-transfected along with 0.01 μ g of pRL null into p68-knockdown SW620 cells expressing HA-p68s, wt or mutant (indicated). The luciferase activity was expressed as relative luciferase activity (numbers on top of bars) by compared to the luciferase activity of SW620 cells without p68-knockdown (NT) (define as 100) and without HA-p68s expression. The values plotted were the average \pm S.E. of triplicate samples from typical experiments.

(B) Protein p68 does not load on the promoter of E-cadherin. Chromatin immunoprecipitation (ChIP) of the E-cadherin promoter by anti-HA antibody in SW620 cells with/without (NT/p68) p68-knockdown. The HA-p68s (WT or Y593F mutant) were exogenously expressed in p68-knockdown cells. The primers positions for PCRs were indicated. ChIP by mouse IgG and antibody against TFIIB were used as positive and negative controls. Inputs were PCR products from DNA extracts without anti-HA immunoprecipitation.

Figure IV-1

A



B

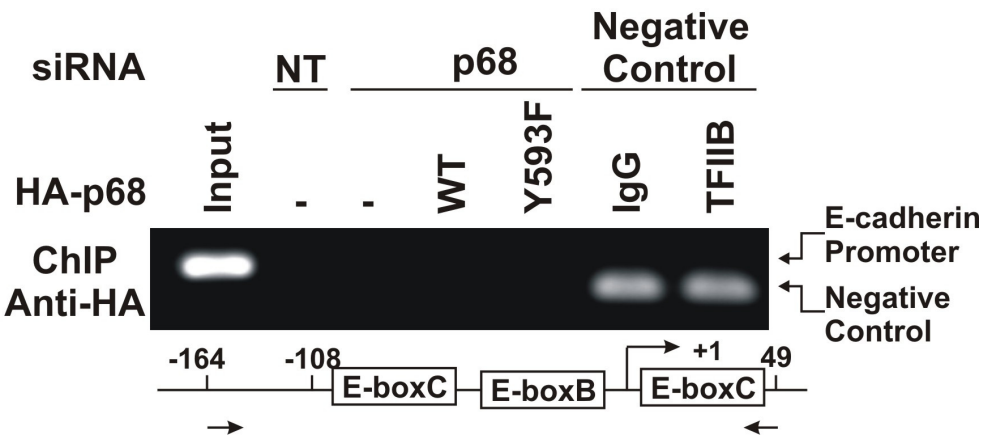


Figure IV-2. Snail mediates the effect of phosphor-p68 on E-cadherin transcription.

(A) Phosphorylation of p68 correlates with Snail expression. Immunoblotting analyzes the cellular levels of Snail (the fourth panel from top) and exogenously expressed HA-p68s plus endogenous p68 (the first panel). Tyrosine phosphorylation of HA-p68s was analyzed by immunoblotting of anti-HA immunoprecipitates via antibody P-Tyr-100 (third panel from top). SW620 cells were treated with p68 siRNA (p68) or non-specific siRNA (NT). Immunoblotting of histone 2A (H2A) was a loading control.

(B) Luciferase reporter of Snail promoter was cotransfected into p68-knockdown SW620 cells along with HA-p68s, wt or mutant (indicated). The luciferase activity was expressed as relative luciferase activity (numbers on top of bars) by compared to the luciferase activity of SW620 cells without p68-knockdown (NT) and without HA-p68s expression (define as 100). The values plotted were the average \pm S.E. of triplicate samples from typical experiments.

(C) Chromatin immunoprecipitation (ChIP) of the Snail promoter by anti-HA antibody in SW620 cells with/without (NT/p68) p68-knockdown. The HA-p68s (wt or Y593F mutant) were exogenously expressed. The primers positions for PCRs were indicated. Inputs were PCR products from DNA extracts without ChIP.

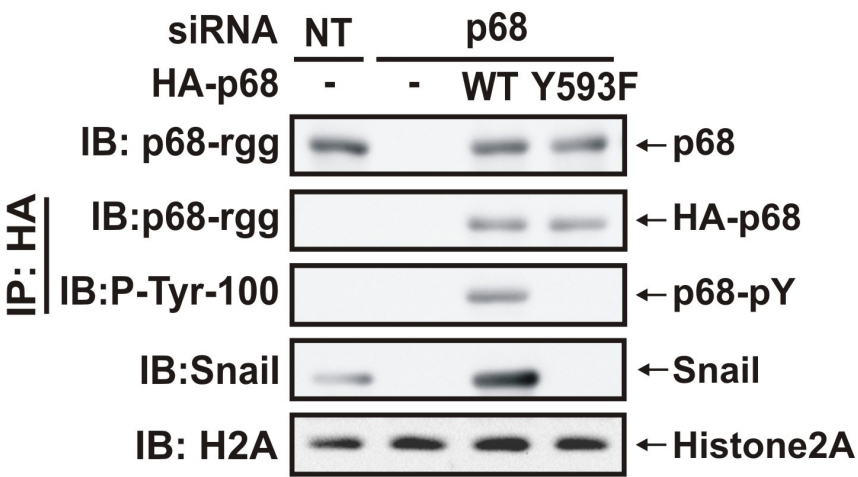
(D) Cellular levels of E-cadherin (second panel from top) and Vimentin (third panel from top) were detected by immunoblotting of cellular extracts made from SW620 cells with/without (Snail/NT) Snail siRNA knockdown and exogenous expression of HA-p68s (wt or Y593F mutant). Tyrosine phosphorylation of HA-p68s was analyzed by

immunoblotting of anti-HA immunoprecipitates using antibody P-Tyr-100 (fifth panel from top).

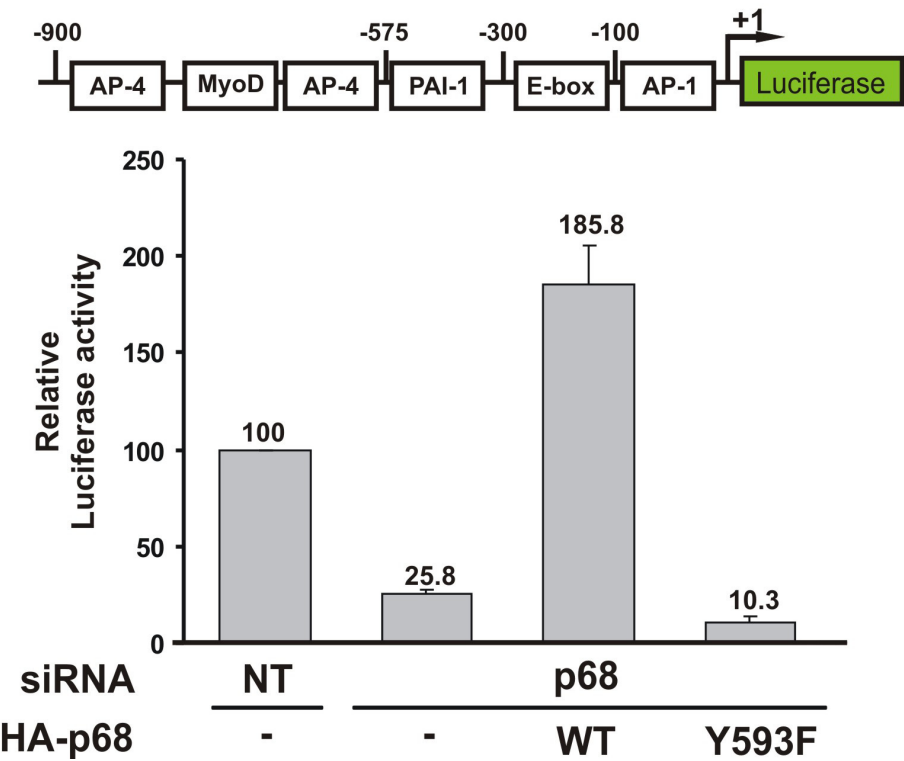
(E) Cell invasive assays were performed for SW620 stable cells with or without Snail siRNA knockdown (NT/Snail). SW620 stable cells were derived from SW620 parental cells with stable overexpression of p68s, WT, Y593F or YIH. 72 hours post siRNA transfection, 2×10^5 SW620 stable cells were labeled by fluorescence, seeded into upper-chamber of 24-cell plates and performed cell invasion assay (BD Bioscience). 2×10^5 cells migrating into lower-chamber were defined as 100%. The values plotted were the average \pm S.E. of triplicate samples from typical experiments.

Figure IV-2

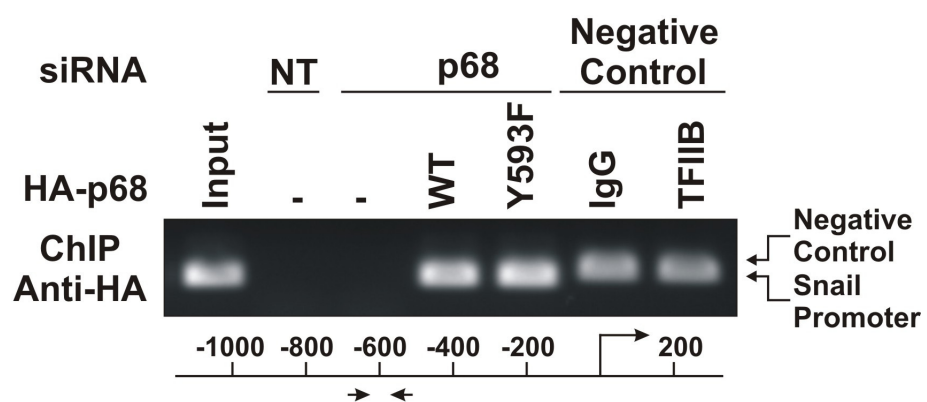
A



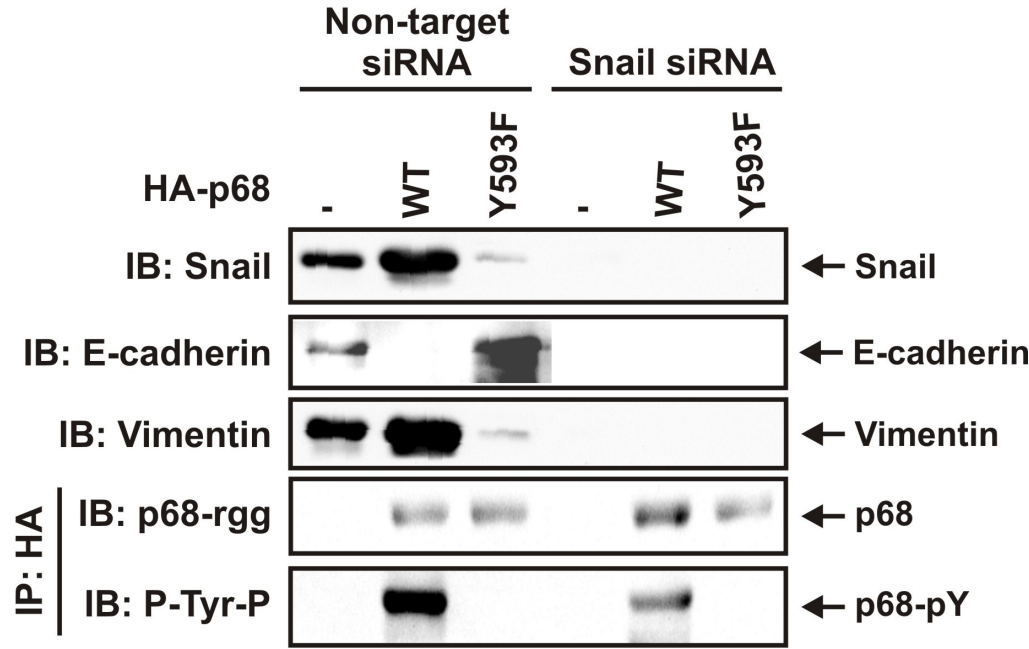
B



C



A



B

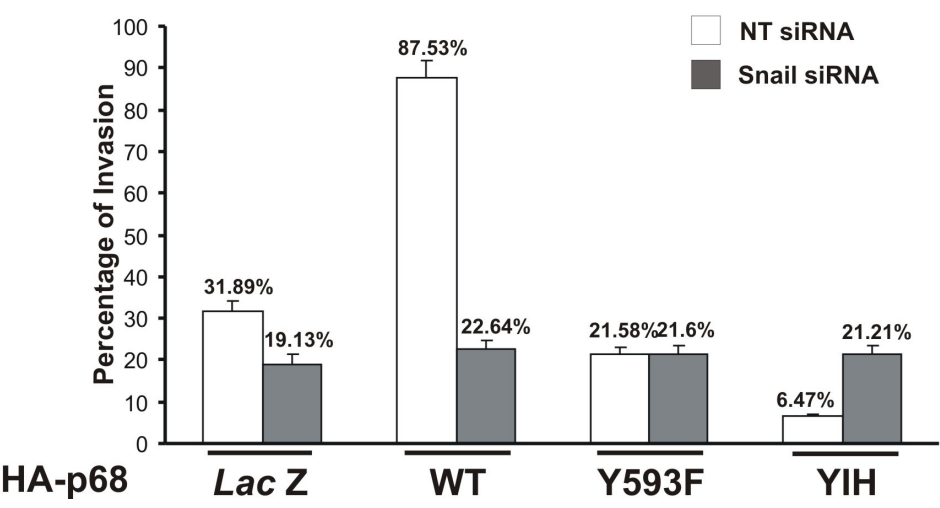


Figure IV-3. p68 associates with MBD3:Mi2/NuRD complex.

(A) Co-immunoprecipitates of MBD3, Mi-2 and HDAC1 with p68 in SW480 and SW620 cells were detected by immunoblotting of p68 co-immunoprecipitates using appropriate antibodies (indicated). p68 was precipitated by polyclonal antibody PAbp68. Rabbit IgG was used as a negative control antibody. Inputs were the immunoblottings of extracts without immunoprecipitation.

(B) Co-immunoprecipitation of p68 with MBD3, Mi-2 and HDAC1 in SW620 (620) and SW480 (480) cells were detected by immunoblottings of co-immunoprecipitates of antibodies (anti-MBD3, anti-Mi-2, anti-HDAC1) using monoclonal antibody p68-rgg. Mouse IgG was used as control IP antibody. The inputs were the immunoblottings of extracts without immunoprecipitation. The tyrosine phosphorylation of p68 was detected by immunoblotting of PAbp68 immunoprecipitated p68 using antibody P-Tyr-100.

(C) Co-immunoprecipitation s of MBD3, Mi-2 and HDAC1 with exogenously expressed HA-p68s (wt or Y593F mutant) in SW620 cells were detected by immunoblottings of anti-HA co-immunoprecipitates (IP:HA) using appropriate antibodies (indicated). SW620 cells were treated with p68 siRNA (P68) or non-specific siRNA (NT). Inputs were the immunoblottings of extracts without immunoprecipitation.

Figure IV-3

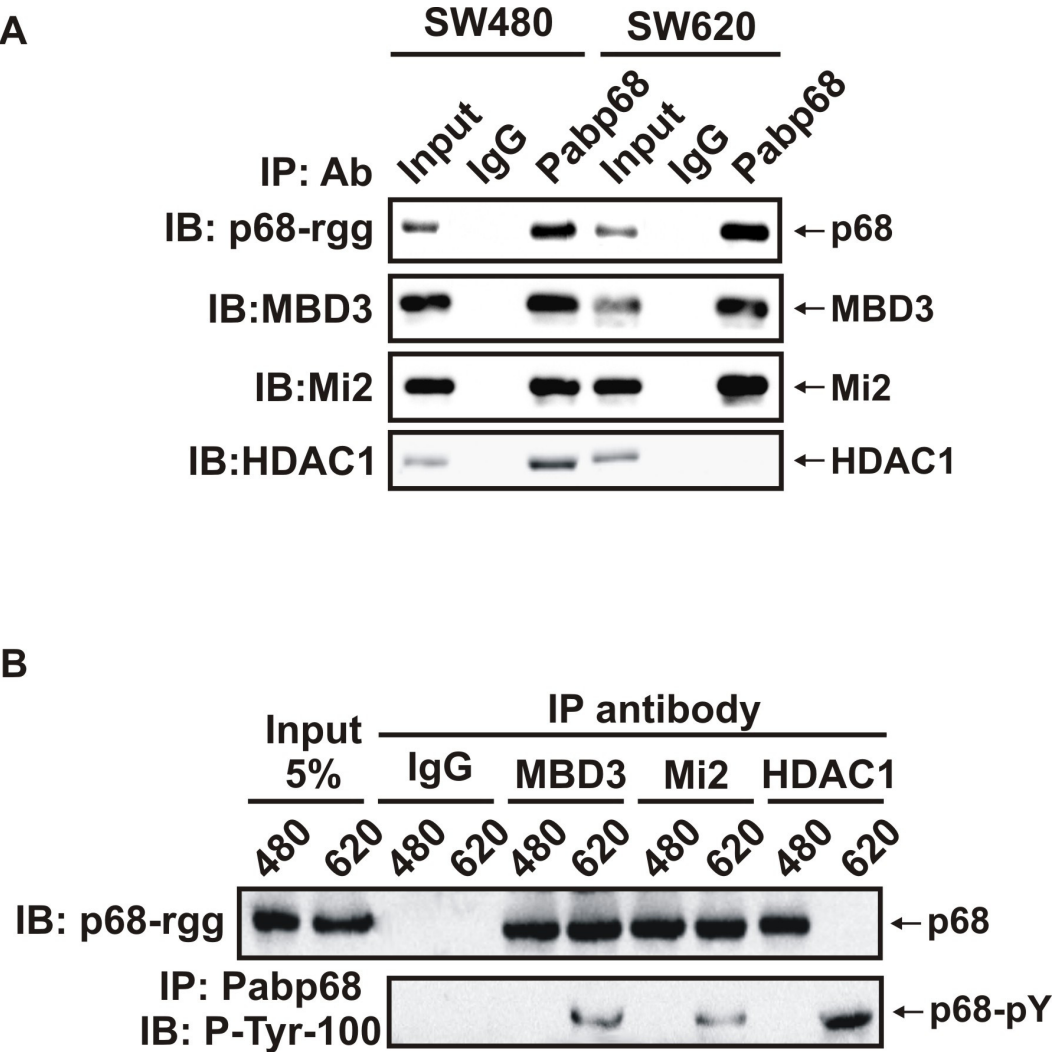


Figure IV-4. MBD3 mediated the loading of p68 on the Snail promoter.

(A) Cellular levels of MBD3 and exogenously expressed HA-p68s (wt or Y593F mutant) were analyzed via immunoblotting using appropriate antibodies (indicated). The immunoblottings were performed with cellular extracts made from SW620 cells that were treated with MBD3 siRNA (MBD3) or non-targeting siRNA (NT). Immunoblotting of Actin was a loading control.

(B) ChIP of Snail promoter by using anti-HA antibody in SW620 cells with/without (MBD3/NT) MBD3 siRNA knockdown. HA-p68s (wt or mutant) was exogenously expressed in MBD3 knockdown cells or control siRNA treated cells. The primers positions for PCRs were indicated. ChIP by mouse IgG and antibody against TFIIB were used as positive and negative controls. Inputs were PCR products from DNA extracts without anti-p68 immunoprecipitation.

(C) ChIP of Snail promoter by anti-MBD3 antibody in SW620 cells with/without (p68/NT) p68-knockdown. HA-p68s (WT or Y593F mutant) was exogenously expressed in p68-knockdown cells. The primers positions for PCRs were indicated. ChIP by mouse IgG and antibody against TFIIB were used as positive and negative controls. Inputs were PCR products from DNA extracts without anti-p68 immunoprecipitation.

Figure IV-4

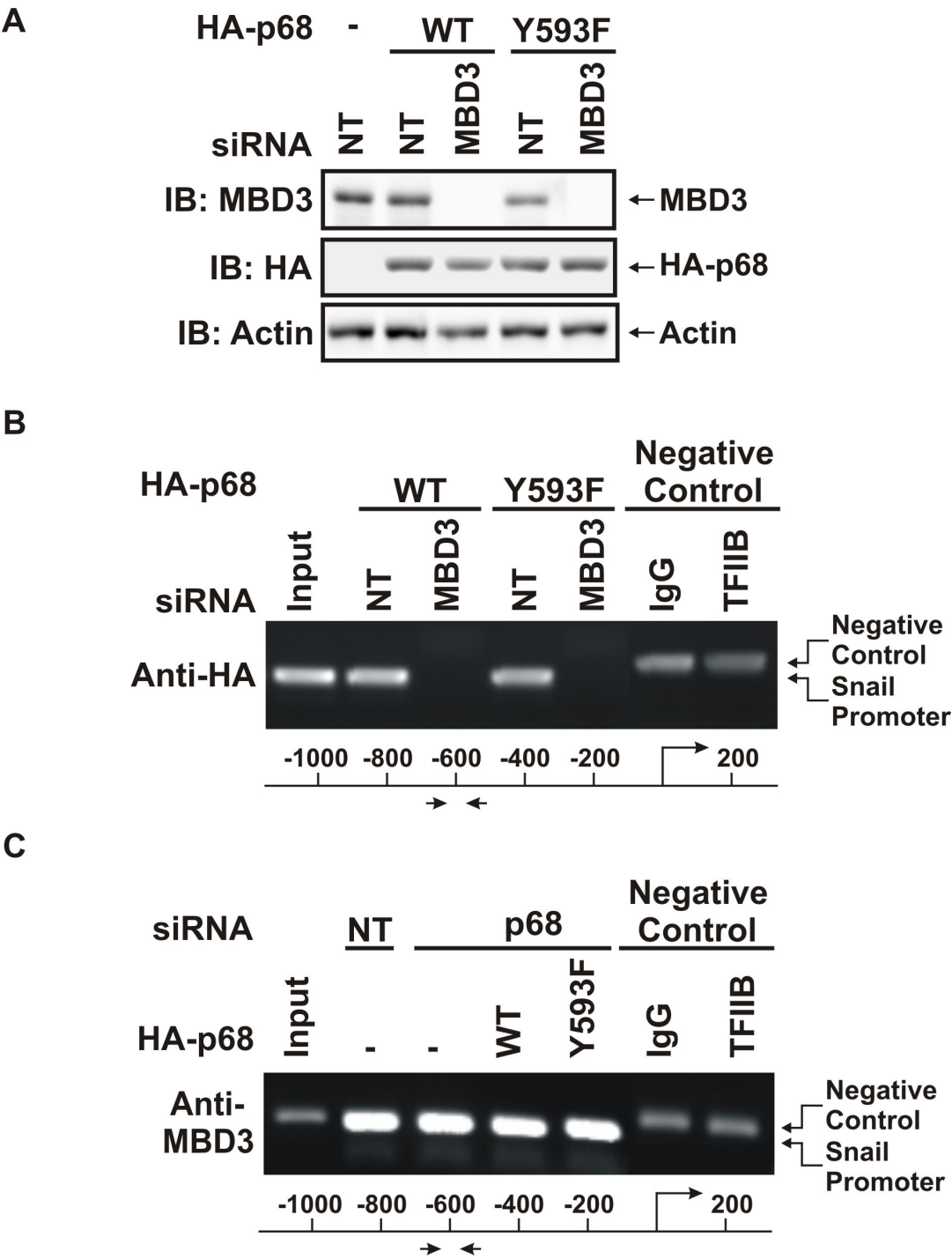


Figure IV-5. The phosphor-p68 displaces HDAC1 from the Snail promoter.

(A) ChIP of the Snail promoter by anti-HDAC1 antibody in SW620 cells. SW620 cells were treated with p68 siRNA (p68) or non-targeting siRNA (NT). HA-p68s (wt or Y593F mutant) was exogenously expressed. ChIP in SW480 cells was a control. ChIP by mouse IgG and antibody against TFIIB were used as controls. The primers positions for PCRs were indicated.

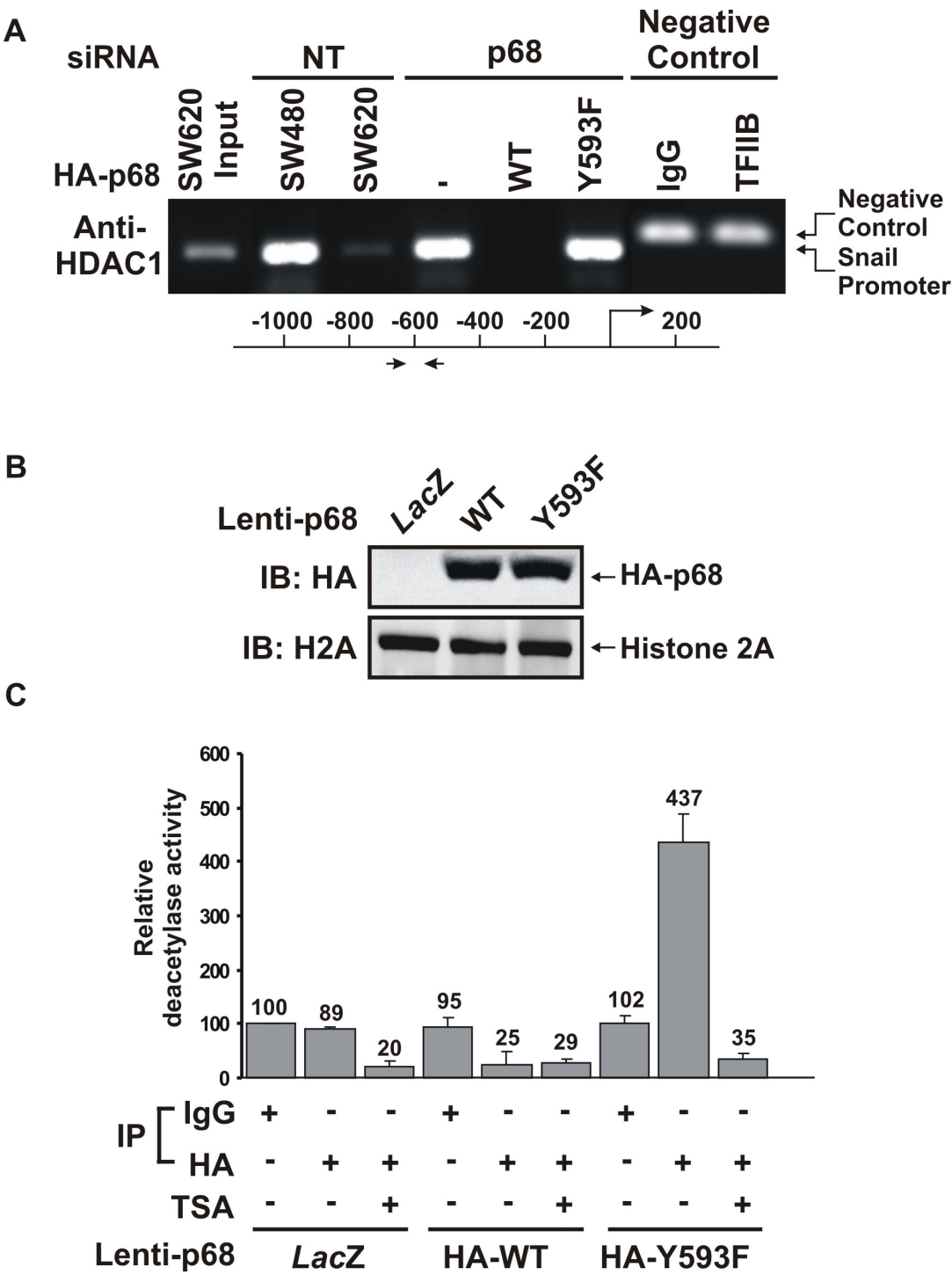
(B) Cellular levels of exogenous expressed HA-p68s (wt or Y593F mutant) were analyzed by immunoblotting using appropriate antibodies (indicated). The immunoblottings were performed with cellular extracts made from SW620 cells that were stably expressed HA-p68s using Lentiviral gene expression system. Immunoblotting of Histone 2A was a loading control.

(C) Deacetylase activities of co-immunoprecipitates by mouse IgG (IgG) and anti-HA antibody (HA) from cellular extracts made from SW620 cells were analyzed. HA-p68s (wt or Y593F mutant) were stably expressed using Lentiviral gene expression system. The immunoprecipitates were treated/untreated with 100 ng/ml of TSA. The deacetylase activity was expressed as relative deacetylase activity by define the activity of co-immunoprecipitation by mouse IgG without TSA treatment without HA-p68 expression as 100.

(D) Luciferase reporter of Snail promoter was transfected into SW620 cells in which HA-p68, wt or mutant (indicated) was stably expressed. Twenty four hours post transfection, cells were treated/untreated (filled bars/open bars) with TSA (100 ng/ml) overnight. Luciferase activities were then analyzed. The luciferase activity was expressed as relative

luciferase activity (numbers on top of bars) by compared to the luciferase activity of SW620 cells without HA-p68s expression and TSA treatment (define as 100).

Figure IV-5



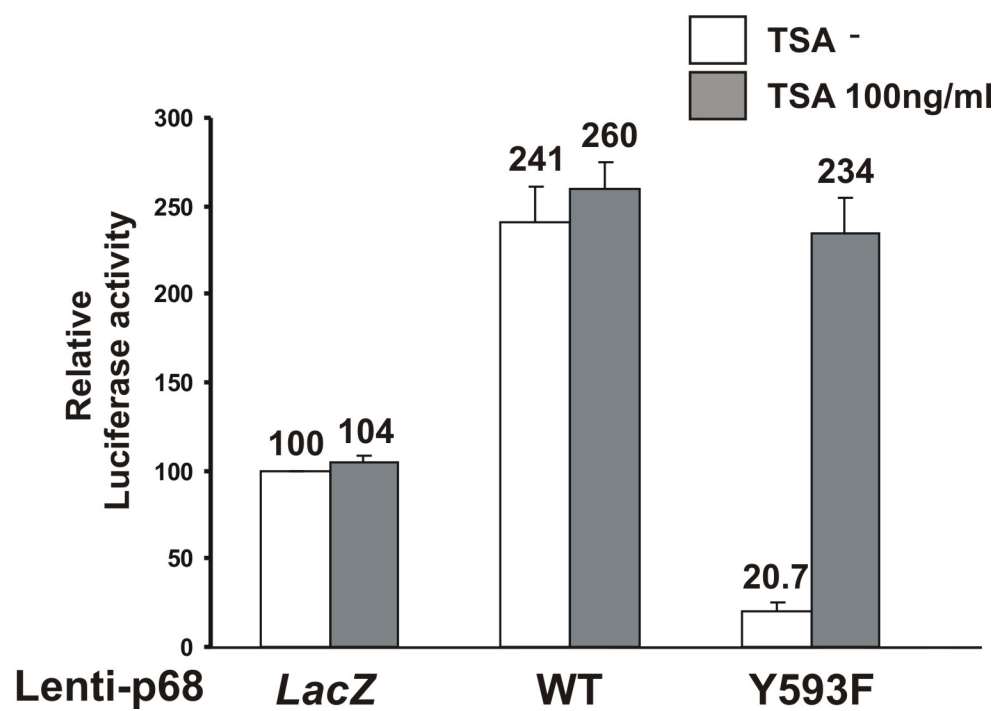
D

Figure IV-6. The phosphor-p68 has a protein-dependent ATPase activity.

(A) DNase and RNase treatment in SW480 cells. Anti-HA immunoprecipitates were treated with DNase (50 U/500 μ l lysate) or RNase (3 U/500 μ l lysate) and incubated at 37°C for 30 min. The treated immunoprecipitates were examined by immunoblotting using proper antibodies as indicated. Rabbit IgG was used as a negative control antibody. Inputs were the immunoblottings of extracts without immunoprecipitation.

(B) DNase and RNase treatment in SW620 cells. Anti-HA immunoprecipitates were treated with DNase or RNase as described above. The treated immunoprecipitates were examined by immunoblotting using proper antibodies as indicated. Rabbit IgG was used as a negative control antibody. Inputs were the immunoblottings of extracts without immunoprecipitation.

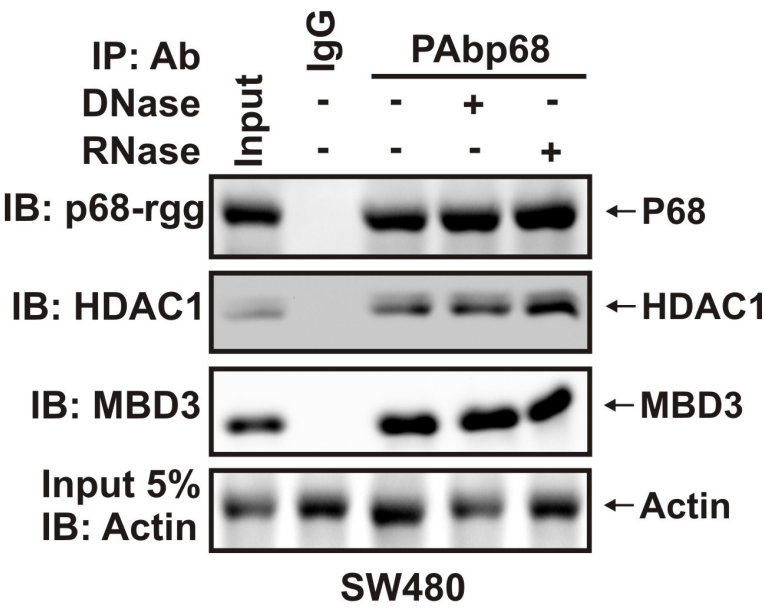
(C) ATPase activities of recombinant phosphorylated/unphosphorylated His-p68s (wt or mutants) in the presence different substrates. The recombinant his-p68s (wt or mutant) were phosphorylated by recombinant c-Abl by *in vitro* kinase assay. After separate His-p68s from c-Abl kinase, the recombinant proteins or BSA were incubated with different substrates (indicated) in the presence of 4mM ATP. Reaction products were mixed with Malachite green solution and read under OD 630. ATPase activity was expressed as μ M of hydrolyzed inorganic phosphate in the ATPase assay reactions.

(D) ATPase activities of recombinant phosphorylated/unphosphorylated His-p68s (WT, Y593F or EEAD mutants) in the presence MBD3. The recombinant his-p68s (wt or mutants) were phosphorylated by recombinant c-Abl by *in vitro* kinase assay. After

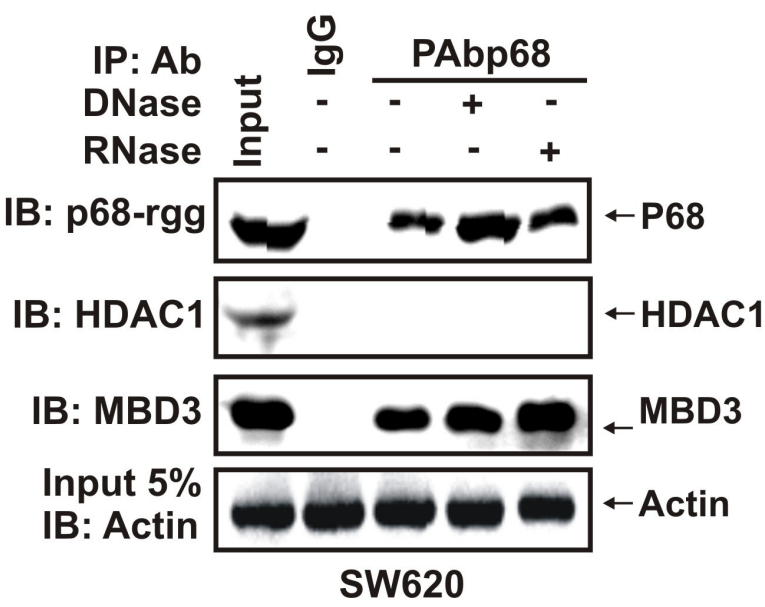
separate His-p68s from c-Abl kinase, the recombinant proteins or BSA were incubated with different substrates (BSA, β -catenin or MBD3 recombinant protein) in the presence of 4mM ATP. Reaction products were mixed with Malachite green solution and read under OD 630. ATPase activity was expressed as μ M of hydrolyzed inorganic phosphate in the ATPase assay reactions.

Figure IV-6

A



B



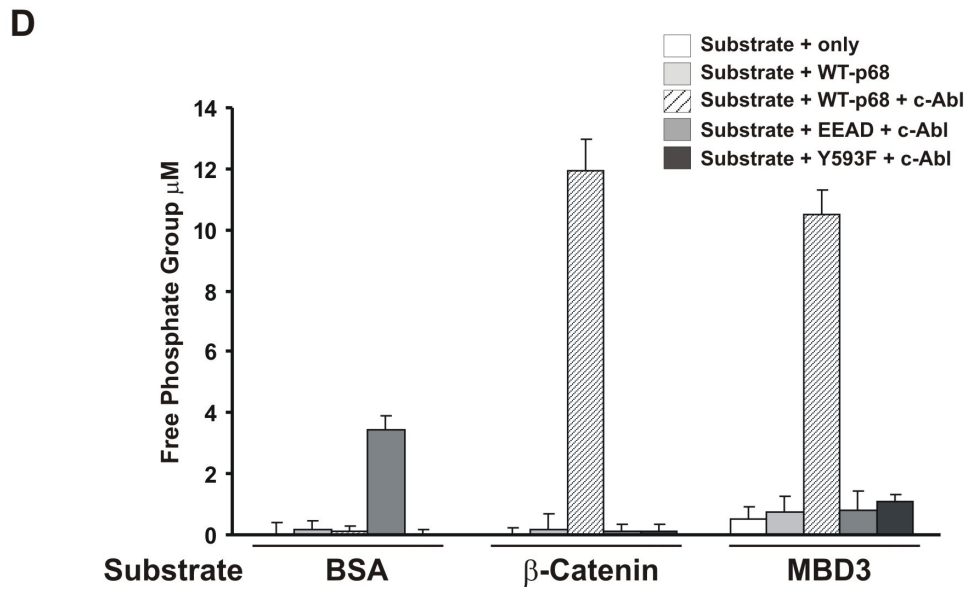
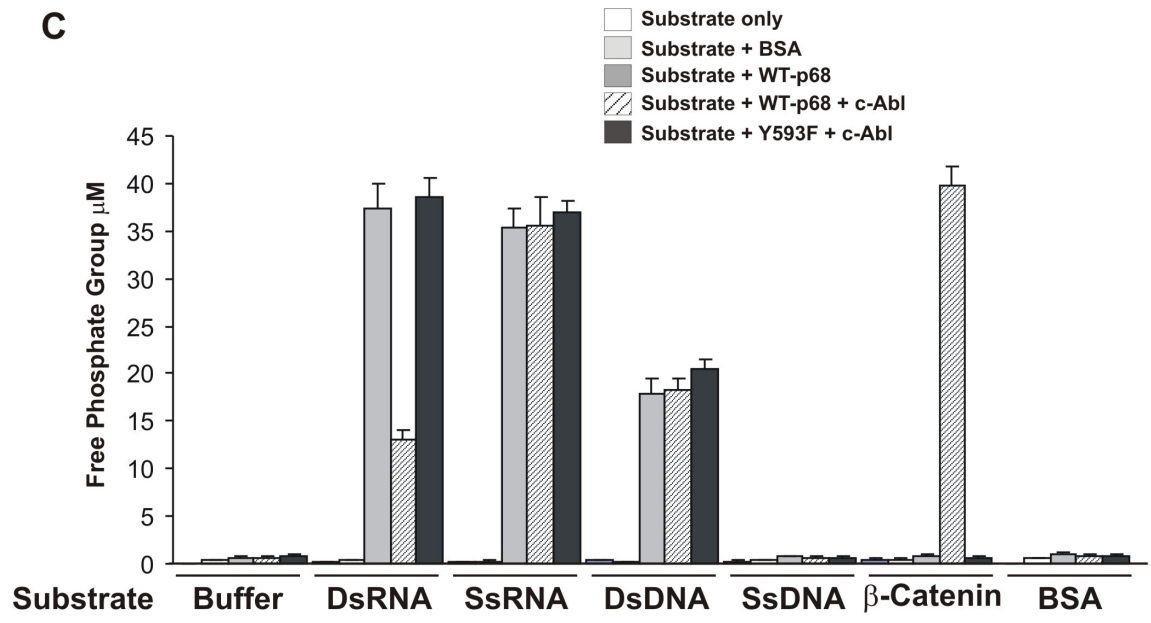
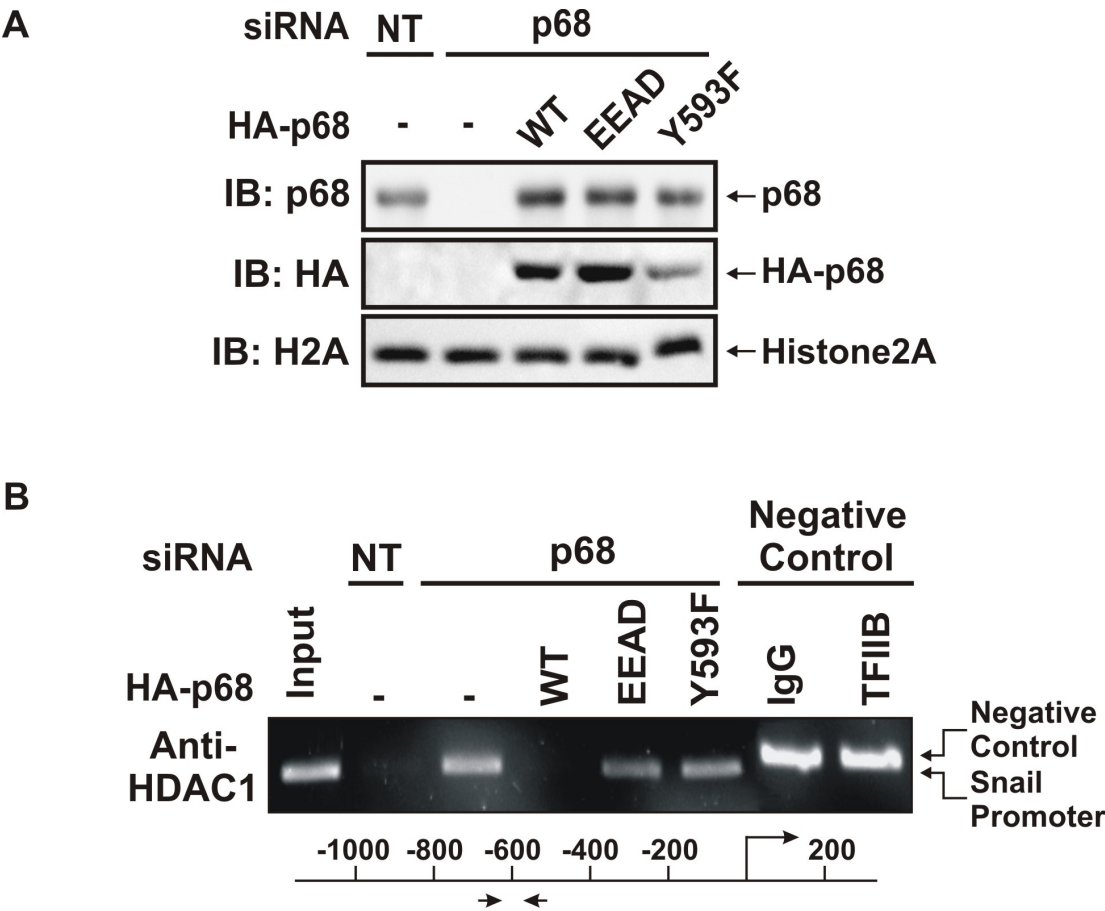


Figure IV-7. Displacement of HDAC1 from Snail promoter requires ATPase activity of p68.

(A) Cellular levels of exogenously expressed HA-p68s (WT, Y593F or EEAD mutant) were analyzed by immunoblotting using appropriate antibodies (indicated). Immunoblotting of Histone 2A was loading control.

(B) ChIP of Snail promoter by anti-HDAC1 antibody in SW620 cells. The SW620 cells were treated with p68 siRNA (p68) or non-targeting siRNA (NT). HA-p68s (wt or EEAD, Y593F mutant) was exogenously expressed. Inputs were PCR products from SW620 DNA extracts without ChIP. ChIP by mouse IgG and antibody against TFIIB were used as controls. The primers positions for PCRs were indicated.

Figure IV-7



CHAPTER V

EXAMINE THE POTENTIAL ROLE OF PHOSPHORYLATED p68 IN CANCER METASTASIS

5.1 Introduction

Cancer metastasis is characterized by tumor cells spread from a primary site and formation of new tumors in distance organs. It is believed that the actions of multiple genes are required for the conversion of metastatic tumor through multistep processes. Key signaling pathways and regulators allow certain tumor cells pass through basement membrane barrier, survive in blood circulation and proliferate at distant organs (Chambers, Groom et al. 2002). Since the cancer metastases are responsible for the most cancer deaths, it is vital to study the molecular basis of cancer metastasis and develop novel approach for cancer therapy.

Some types of cancer show an organ-specific metastasis pattern, such as breast cancer often metastasize to bone, lung and brains; prostate cancer usually metastasize to bone; and colorectal cancer frequently spread to liver. Two theories have been proposed to illustrate the organ-specific tumor metastasis. One is “seed and soil” theory, suggesting that organs preferentially support the specific tumor grow. Another proposal claims that the circulatory connections between primary tumor and secondary sites are responsive to the tumor metastasis pattern (Weiss 1992). Experimental data from laboratory mice support both of these theories.

To study the mechanism of cancer metastasis, the ultimate approach is to use animal model to identify the genes and examine the roles of key molecules. In experimentally modeled assays, tumor cells will be injected into the modeled animals, orthotopically or directly into the blood circulation. These assays are spontaneous or experimental metastasis models respectively. The experimental metastasis model only can be used to study the later phases of metastasis by which tumor cells have penetrated into blood stream. By the end of both types of assays, visible secondary site metastases are formed. Coupe of mice model with genome-wide gene profile technology allows the identification and characterization of genes and signaling molecules that contribute to cancer metastasis. On the other hand, the animal models can be used to study particular gene products or specific signaling pathways in cancer metastasis.

A number of spontaneous mice tumor models have been established. For mammary tumor, a set of subpopulation of murine tumor cell lines (67NR, 168FARN, 4TO7 and 4T1) were isolated from a single mammary tumor. While these cell lines grow neoplasm spontaneously in mammary fatpad with no difference, these cell lines differ from the ability of metastasis. 67NR cells grow in primary site, but no tumor cells are detectable in blood, neighboring lymph nodes and lung. For cell line 168FARN, the tumor cells spread out from primary site to lymph node. However, the cells are rarely isolated from blood and lung. 4TO7 cell lines can be cultured from lung tissue, suggesting that this cell line is able to invade to lung. Nevertheless, no visible metastatic node can be observed in lung, indicating that this cell line fails to colonize in distant organ. Cells of 4T1 complete all steps of metastasis and spontaneously metastasize to

brain, lung, bone and liver (Aslakson and Miller 1992). The properties of these cell lines reveal the progression of cancer metastasis. Comparison of gene expression profiles of these four cell lines will dissect the processes of cancer metastasis and identify genes associated with their invasion ability.

To study colorectal tumor metastasis, metastatic colorectal tumor cells can be injected into the cecal wall of BALB/c mice. Spontaneously metastasizing tumor colonies are formed in liver (Bresalier, Hujanen et al. 1987). Using this model, gene products supporting or repressing tumor metastasis can be examined. Human colorectal tumor cell line SW480 and SW620 are isolated from the same patient. SW480 is derived from the primary site, while SW620 is derived from metastatic lymph node (Leibovitz, Stinson et al. 1976). Injection of SW620 cells into the cecal wall of BALB/c mice leads to metastasis of liver. On the contrary, injection of SW480 cells does not reproduce the invasion (Witty, McDonnell et al. 1994). This model can be used to study the mechanisms of colon tumor metastasis. This model may also be useful to develop strategies for colon cancer therapy.

Prostate cancer is another leading cause of cancer death. Orthotopic inoculation of androgen-independent and androgen-sensitive human prostate cancer cells into male nude mice induces tumor growth. However, the tumor cells often spread to lung and lymph nodes (Sato, Gleave et al. 1997; An, Wang et al. 1998). Injection of one of sublines of human prostate tumor cell line LNCaP induces the osseous metastasis with an incidence of 11%-50% (Thalmann, Anezinis et al. 1994). Androgen-independent PC-3 human prostate tumor cell line expressing green fluorescent protein (GFP) is

orthotopically inoculated in the prostate (Yang, Jiang et al. 1999). The subsequent micrometastasis and metastasis are visualized through out the skeleton and nerve system by fluorescence. The metastasis colonies were also observed in lung, liver, kidney and other systemic organs.

The tyrosine phosphorylation of DEAD-box p68 RNA helicase closely correlates with tumor malignancy and metastasis. Studies from our laboratory indicated that the tyrosyl phosphorylated p68 promotes tumor cell EMT and invasion *in vitro*. It is likely that the tyrosine phosphorylated p68 supports tumor metastasize *in vivo*. In this chapter, an orthotopical human colorectal tumor nude mice model is tested. The preliminary data investigating the potential role of phosphorylated p68 in tumor metastasis and further direction are also included.

5.2 Results

5.2.1 The Tyrosine-to-glutamic acid Substitution of p68 Functions Similar to the Tyrosine Phosphorylated p68.

The phosphorylation at Y593 has been suggested to promote tumor cell EMT *in vitro*. The phosphorylation of p68 regulates gene transcription through recruitment of β -catenin nuclear localization and displacement of HDAC1 from NuRD complex. We reasoned that if the phosphorylation of p68 at Y593 positively modulate tumor cell EMT, the introduction of negatively charged amino acid residues, such as aspartic acid or glutamic acid in the same position may enhance tumor cells invasion and migration. The

substitution of tyrosine with glutamic acid has been successfully used to study the roles of amino acid residues in mediating protein-protein interactions (Lock, Frigault et al. 2003) or cellular function (Zhang, Izaguirre et al. 2004). To test this conjecture, we introduced glutamic acid to tyrosine 593 to generate Y593E mutant. To test the expression of exogenous proteins, the HA-tagged p68s (wt or Y593E) were expressed in HT-29 cells. The cell lysates were examined by immunoblotting using antibodies against HA epitope (**Figure V-1 A**). To generate the cells stably expressing Y593E mutant, SW480 cells were transfected with Y593E mutant with Lentiviral gene expression system. The transfected cells were selected using Blasticidin S (6 μ g/ml) for two weeks. The colonies were isolated and amplified under the same selection condition. Three colonies were examined (#4, 21 and 41), comparing with parental cells SW480 and SW620. Immunoblotting using anti-HA antibody indicated the expression of HA-tagged Y593E in these colonies (**Figure V-1 B** first panel). The cell lysates were examined by immunoblotting using antibodies against E-cadherin and Snail as indicated. SW620 cells express lower level of E-cadherin and higher level of Snail compared to cell lysates made from SW480 cells (**Figure V-1 B** second and third panel). Immunoblotting of Actin is loading control. It evidenced that Y593E-41 derived from SW480 cells upregulated Snail expression and repressed E-cadherin expression. The morphology of Y593E-41 also altered from parental cells under microscope. The SW480 cells exhibited an epithelial appearance and tended to form multicellular aggregates. The SW480 cells stably expressing Y593E cells exhibited a round, elongated-fibroblast-like and dispersed

morphology (**Figure V-1 C**). The molecular and morphological changes suggested that substitution of tyrosine with glutamic acid transformed SW480 cells to mesenchymal-like cells. These phenomena consist with the observation that tyrosine phosphorylated p68 promotes tumor cell EMT.

Solid evidence suggested that tyrosine phosphorylated p68 associates with β -catenin which is important for growth factor induced cell proliferation and EMT. The phosphorylated p68 also displaces HDAC1 from the NuRD complex at the promoter of Snail. Thus, one would reason that if the negative charge of Y593E reproduces the function of phosphorylated p68, the Y593E mutant should be able to interact with β -catenin and exhibit HDAC1/MBD3-dependent ATPase activity. Cell lysate made from SW480 cells stably expressing Y593E mutant (refer as SW480-Y593E), or SW620 cells stably expressed p68-wt (refer as SW620-WT) were immunoprecipitated using antibody against β -catenin. The β -catenin immunoprecipitates were detected by immunoblotting using antibodies against p68 (**Figure V-1 D**). The result clearly evidenced that in SW480 cells, the interaction of β -catenin with p68 is barely detectable. In contrast, expression of Y593E mutant enhanced this interaction, suggesting that the negative charge of glutamic acid promotes the interaction of p68 with β -catenin (**Figure V-1 D**, second panel). Expression of wild type p68 in SW620 cells further increased the bound β -catenin with p68. Moreover, the association level of p68 with β -catenin correlated with the expression level of E-cadherin (**Figure V-1 D**, third panel). Taken together, these findings

suggested that the expression of Y593E has similar role compared with tyrosine phosphorylation of p68.

5.2.2 Expression of Y593E Promotes Tumor Cell Migration.

Previous studies from our laboratory suggested the tyrosine phosphorylation of p68 supports cell invasion. It is possible that the expression of Y593E mutant in SW480 cells may promote cell migration similarly. To test this hypothesis, SW480 cells and SW480-Y593E were examined by cell culture wound assay. The two sublines of cells were cultured in a monolayer at 6-well plates till proximately 80% confluence. Wounds were created by pipette tips. After rinsed by PBS thoroughly to remove any free-floating cells, the cells were incubated with serum-free medium at 37°C for indicated time points. Photomicrographs were obtained at 0, 4, 8, 16 and 24 hours after standard scrape wounding. The parental SW480 cells almost showed no migration. In contrast, the SW480-Y593E migrated significantly toward the scrapes (**Figure V-2**). These data suggested that expression of Y593E promotes cell migration. Comprehensive experiments including invasion assay and MMP activity assay will validate the role of p68 in regulating cell migration and invasion.

5.2.3 *In vivo* Assessment of Tumor Growth and Potential Metastasis.

Based on our cell culture data, we speculated that expression of p68-Y593E would affect tumor metastasis *in vivo*. To develop an appropriate animal model of metastasis, the tumorigenesis of SW480 and SW620 cells were tested. SW480 or SW620

cells (1×10^7) were injected subcutaneously into the flanks of CD-1 nude mice ($n = 3$ for each group). The flank xenografts were monitored for SW480 and SW620 cells (**Figure V-3 A and B**). In the mice injected with SW620 cells, measurable tumor appeared within one week and grown to an average volume of 860 mm^3 by 4 weeks after injection. In the mice injected with SW480 cells, the tumor grew in similar pattern with an average volume of 400 mm^3 by 4 weeks after injection (**Figure V-3C**). These data suggested that both SW480 and SW620 cells are able to develop tumors subcutaneously in nude mice. Histochemistry and Immunostaining of antibodies against human gene products will validate the homo sapiens-derived tumor.

In order to determine the impact of phosphorylated p68 in tumor metastasis, a spontaneous human colorectal tumor mice model is intended to be generated. We injected SW620 and SW480 cells (1×10^7) into the cecal wall of nude mice ($n = 5$). 8 weeks after injection, the xenograft growth and the potential metastasis were examined. The mice were euthanized and subjected to autopsy. The SW620 cells has 60% incidence for primary tumor grow with 0% liver metastasis. SW480 cells has 20% incidence of primary tumor grow and 0% liver metastasis (**Table 3**). For a typical SW620 injection, tumor growth is visible on the injection side (**Figure V-4A**). A tumor mass grew inside of the muscular layer (**Figure V-4B**). Large tumor loci on the surface of cecum and one tumor locus on the surface of liver were observed (**Figure V-4 B-D**). The tumor cells were injected into the cecal wall of nude mice, however, the major tumor mass grew on the inside of muscular layer. It is possible that the injected cells invade though the basement membrane of the cecal wall and spread to the muscular layer. The tumor

growth on the surface of the cecum suggested the success of orthotopical tumor growth. The liver metastatic of SW620 cells requires validation of histochemistry.

We suspected that the low incidence of liver metastasis for aggressive cell line SW620 cells may due to the relative short incubation after injection. SW480, SW480-Y593E, SW620 and SW620-WT sublines (1×10^7) were injected into the cecal wall of nude mice ($n = 5$). 12 weeks after injection, the xenograft growth and the potential metastasis were examined (**Table 4**). The SW480 cells has 0% incidence for primary tumor grow with 0% liver metastasis. The SW480-Y593E cells has 20% incidence of primary tumor grow and 0% liver metastasis. The incidence of SW620 cells grew at primary site was 60% with no liver metastasis. Expression of wild type p68 in SW620 cells had 40% tumor growth with 0% liver metastasis. These data suggested that expression of Y593E slightly increased the tumor growth *in situ*. However, the potential metastasis ability of SW480 cells was not obviously enhanced by expression of Y593E.

5.3 Discussion

In this chapter, we aimed to investigate the potential role of phosphorylated p68 in tumor metastasis. Stably expression of Y593E mutant in SW480 cells correlated with the upregulation of Snail and downregulation of E-cadherin. The interaction of p68-Y593E and β -catenin is likely to be enhanced. Furthermore, expression of Y593E mutant of p68 greatly promoted cell migration. In the animal model experiments, the SW620 cells grew orthotopically in a relative low incidence with no liver metastasis observe. Expression of

Y593E in SW480 cells slightly enhanced the incidence of tumor growth. However, no liver metastasis observed in our animal model experiments. These data suggested that the negative charge of glutamic acid probably mechanically and functionally similar to the tyrosyl phosphorylation of p68 *in vitro*. More research works are needed to generate the spontaneously metastasis model *in vivo*.

For the purpose to study the role of phosphorylated p68 in tumor metastasis, expression of unphosphorylatable mutant of p68 (Y593F) to inhibit the metastasis tendency of metastatic cell line SW620 will provide solid evidence. A great effort has been made to generate the sublines of SW620 cells in which Y593F of p68 is stably expressed. However, stable expression of Y593F in SW620 cells probably greatly suppresses the cell proliferation. Alternatively, the tyrosine-to-glutamic acid substitution provides a possibility to imitate the function of tyrosyl phosphorylation of p68. Biochemical and molecular studies suggested that the negative charges provided by phosphor-group of p68 may play an important role in promoting tumor invasion and metastasis. The stable expression of unphosphorylatable mutant of p68, Y593F in metastatic cell lines will certainly validate the role of phosphorylated p68 in tumor invasion.

The spontaneously colorectal tumor model injecting SW620 cells into the cecal wall of nude mice has been used successfully to study the mechanism of tumor metastasis (Morikawa, Walker et al. 1988; Bresalier, Byrd et al. 1998; Minard, Herynk et al. 2005). Our previous studies are based on the human colorectal tumor cell lines (HT-29, SW480, and SW620). Molecular studies have demonstrated that in SW620 cells, phosphorylated

p68 promote tumor EMT and invasion. It will be appropriate to study the role of p68 in tumor metastasis by the spontaneous colon tumor metastasis model. The low incidence of SW620 cells grows orthotopically and liver metastasis is unexpected. It was suggested that injection of SW480 and SW620 cells orthotopically, the incidence of tumor growth is 14/15 and 9/13 respectively. Although the SW480 cells have not been observed to metastasize to liver, the SW620 cells have a 50% incidence of liver metastasis (6/13) (Witty, McDonnell et al. 1994). One of the reason would be the vitality of cells was affected due to the long-standing detachment (5 – 7 hours) during operation. Improvement of cell storage using operation may retain cell vitality and increase the incidence of tumor growth and liver metastasis. On the other hand, experimental tumor metastasis modeling using tail vein injection or in spleen injection may be useful to examine the role of phosphorylated p68 in tumor metastasis.

Table 1. *In vivo* incidence of tumor growth and liver metastasis.

Group	No. of mice with cecum tumor growth (%)	No. of mice with liver metastasis (%)
SW620	3/5 (60%)	0/5 (0%)
SW480	1/5 (20%)	0/5 (0%)

Table 2. Effect of expression of Y593E and wt-p68 in liver metastasis.

Group	No. of mice with cecum tumor growth (%)	No. of mice with liver metastasis (%)
SW480	0/5 (0%)	0/5 (0%)
SW480-Y593E	1/5 (20%)	0/5 (0%)
SW620	3/5 (60%)	1/5 (20%)
SW620-wt-p68	2/5 (40%)	1/5 (20%)

Figure V-1 The tyrosine-to-glutamic acid substitution of p68 functions similar to the tyrosine phosphorylation.

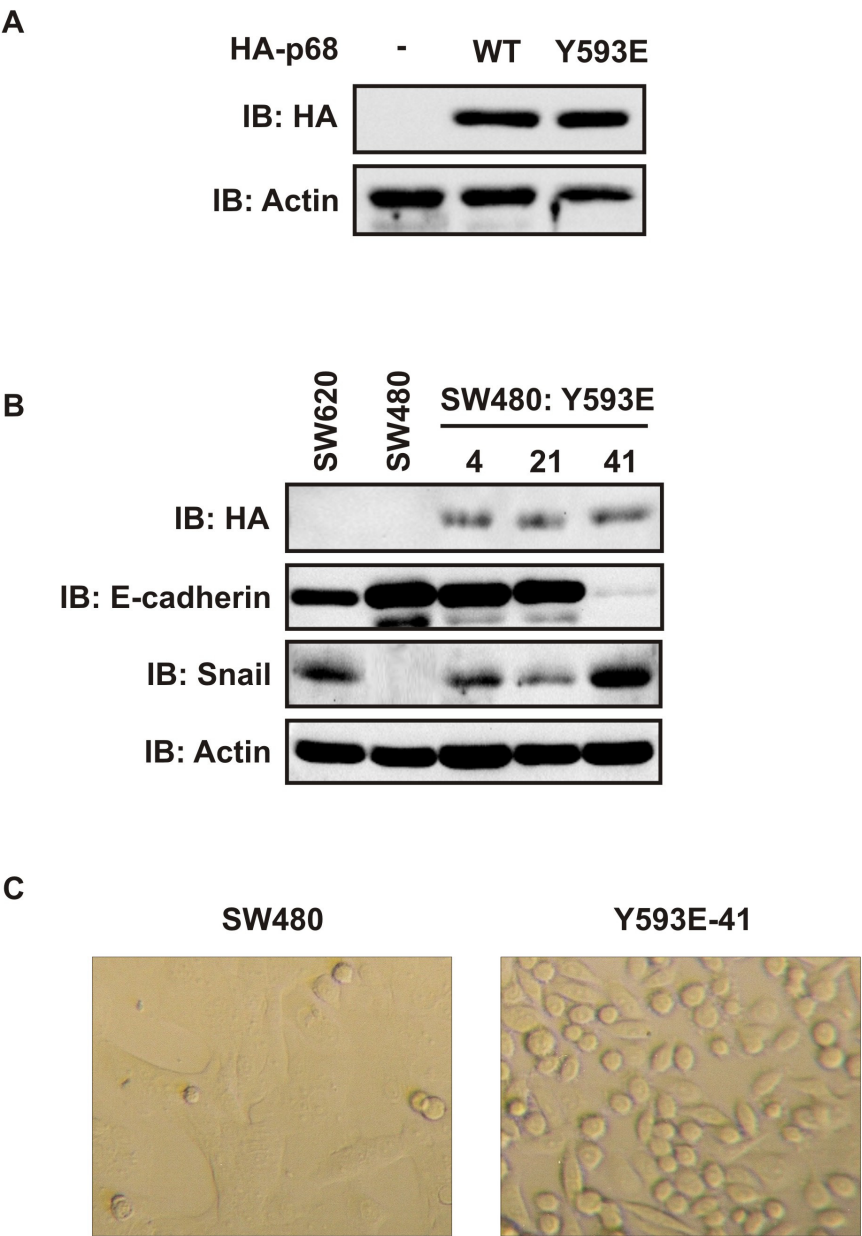
(A) The HT-29 cells were expressed HA-tagged p68s (wt or Y593E). the expression of exogenous proteins were examined by immunoblotting using antibody against HA epitope. The immunoblotting of actin is loading control.

(B) The cell lysates made from colonized SW480 cells stably expressing Y593E of p68 and cell lysates made from SW620 and SW480 cells were examined by immunoblotting using antibodies against HA, E-cadherin, Snail and Actin as indicated.

(C) Representative phase-contrast images of monolayer cultures of SW480 and SW480 stably expressing Y593E.

(D) The cell lysates made from SW480, SW480-Y593E, SW620 and SW620-wt sublines were immunoprecipitated using antibody against β -catenin. The β -catenin immunoprecipitates were examined by immunoblotting using antibodies against p68-rgg. Immunoblotting using antibodies against E-cadherin and Actin were indicated.

Figure V-1



D

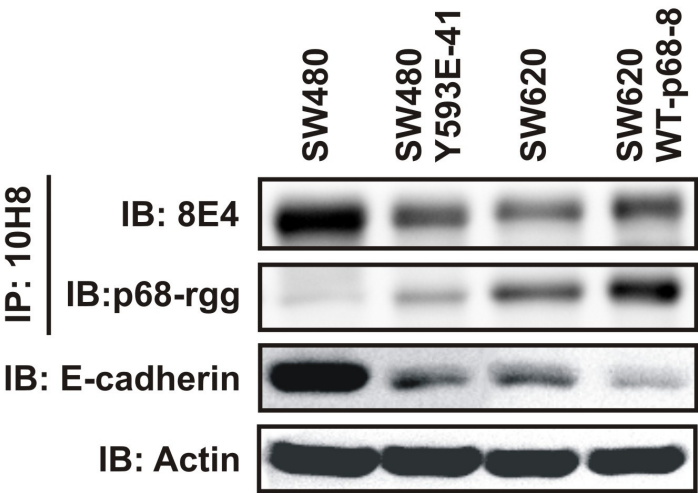


Figure V-2 Expression of Y593E promotes tumor cell migration.

SW480 cells and SW480-Y593E were examined by cell culture wound assay. The two sublines of cells were cultured in a monolayer at 6-well plates till proximately 80% confluence. Wounds were created by pipette tips. After rinsed by PBS thoroughly to remove any free-floating cells, the cells were incubated with serum-free medium at 37°C for indicated time points. Photomicrographs were obtained at 0, 4, 8, 16 and 24 hours after standard scrape wounding. Representative photomicrographs of cell migration were obtained.

Figure V-2

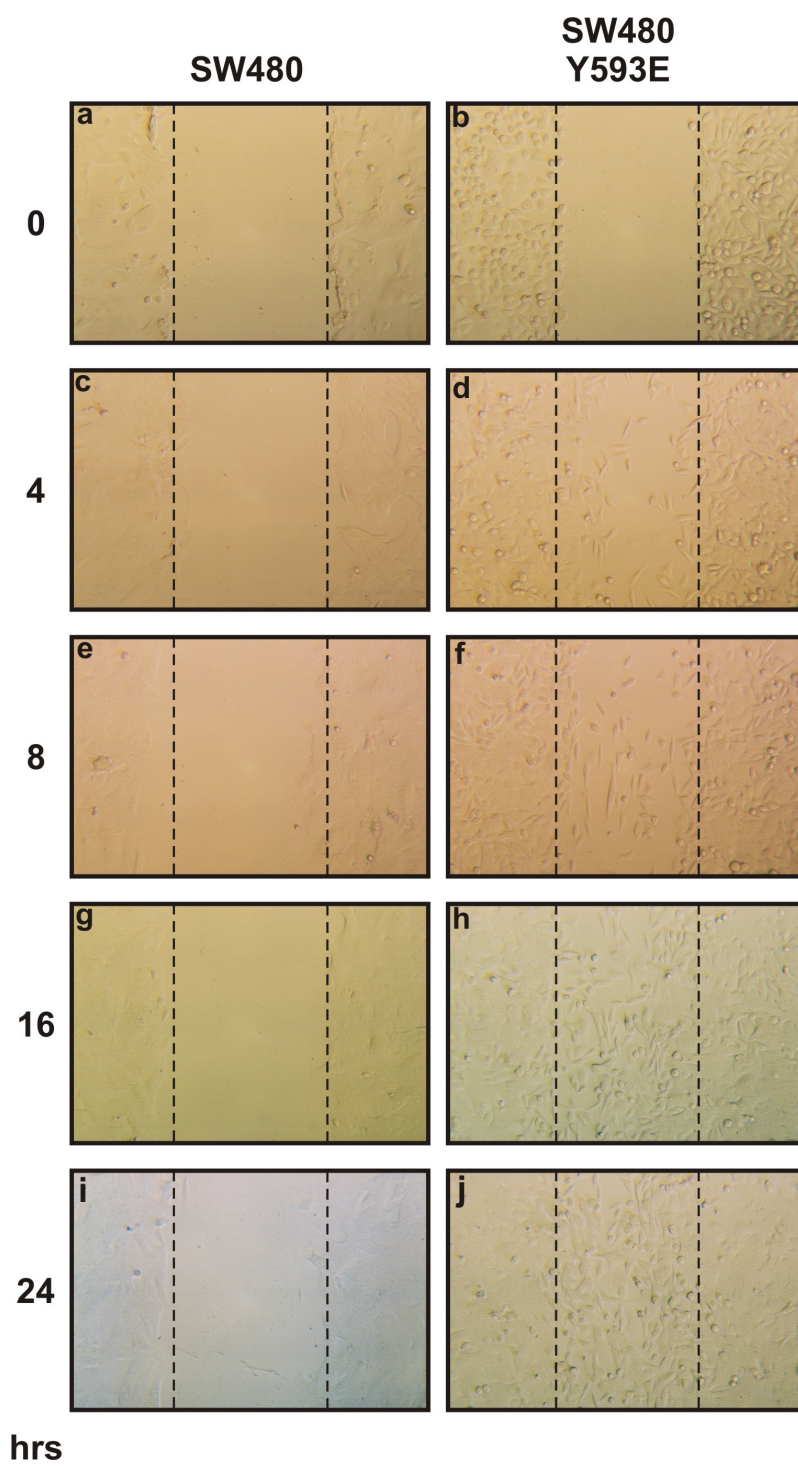


Figure V-3. *In vivo* tumor assessment of growth.

(A) and (B) SW480 (A) or SW620 (B) cells (1×10^7) were injected subcutaneously into the flanks of CD-1 nude mice ($n = 3$ for each group). The flank xgenographs were examined 4 weeks after injection.

(C) SW480 or SW620 cells (1×10^7) were injected subcutaneously into the flanks of CD-1 nude mice. The volumes of flank xgenographs were monitored after injection for each group. Each bar represents average of 3 mice.

Figure V-3

SW480



SW620

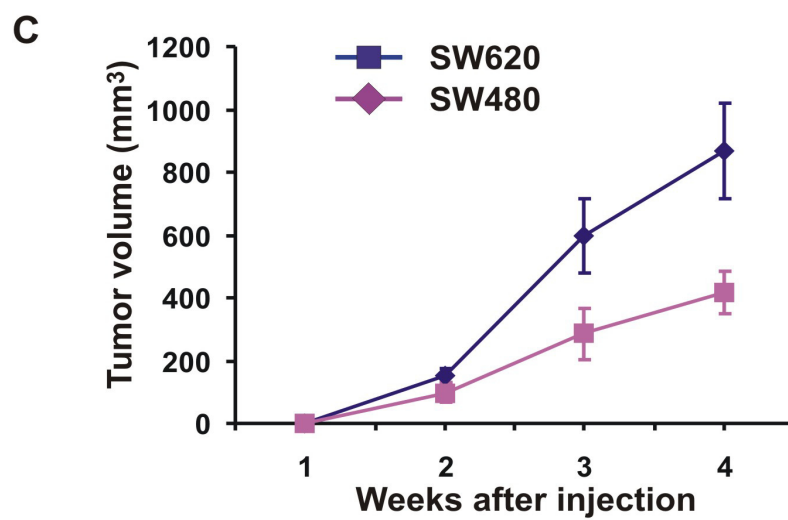
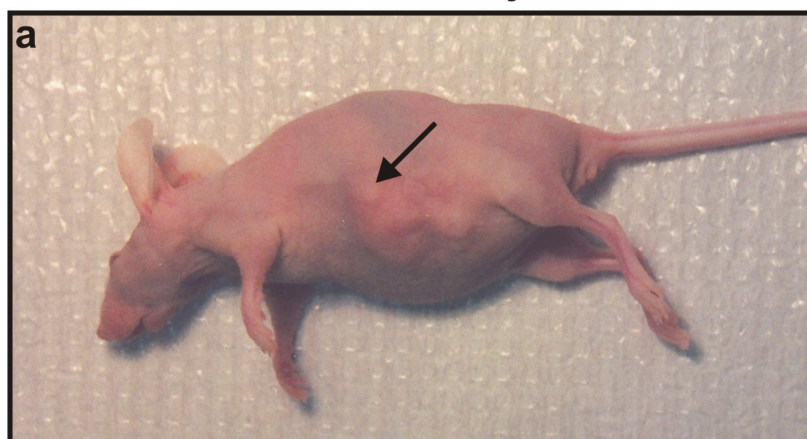
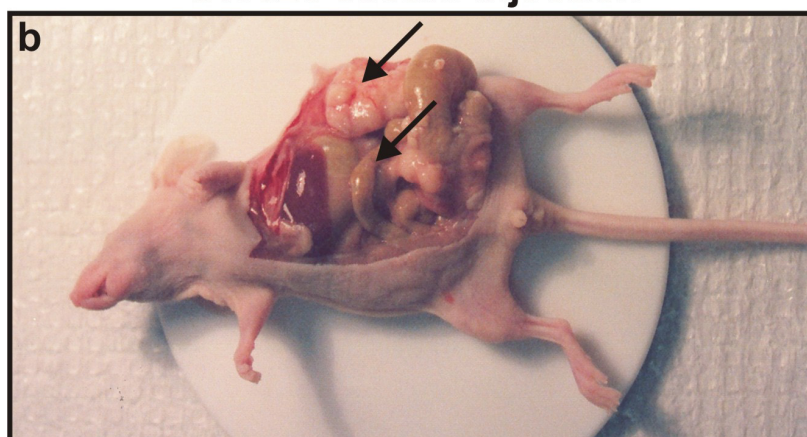
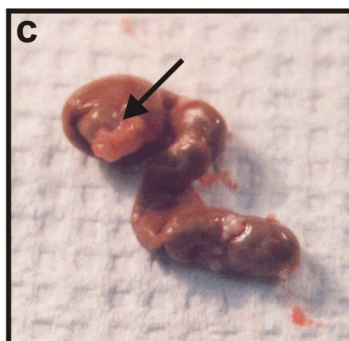
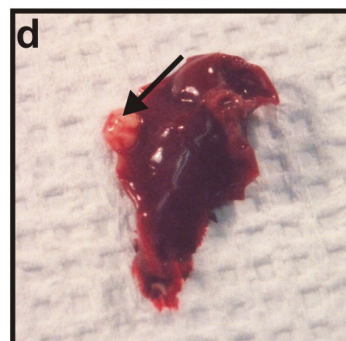


Figure V-4. Generation of spontaneous colon tumor metastasis.

(A) to (D) The SW620 cells (1×10^7) were injected into the cecal wall of CD-1 nude mice. 12 weeks after injection, the mice were euthanized and subjected to autopsy.

Figure V-4**SW620 cecum injection****SW620 cecum injection****Cecum****Liver**

CHAPTER VI

CONCLUSION

In the first part of this dissertation, we demonstrated that p68 acted as an RNA helicase to recognize and dissociate the U1 snRNA-5' splice site duplex using energy derived from ATP hydrolysis during the early stage of splicing process (Liu 2002); (Lin, Yang et al. 2005). We showed that the ATPase and helicase activities of p68 were indispensable for the pre-mRNA splicing. Furthermore, p68 also plays a role in the spliceosome assembly without requirement of the ATPase activity. Most importantly, *in vivo* experiments elucidated that p68 acted as a general splicing factor. Consistent with our *in vitro* data, p68 interacts with the unspliced, but not spliced form of mRNA precursor *in vivo*.

An important role of p68 in tumor cell EMT was illustrated in this dissertation. We observed that p68 acquired tyrosine phosphorylation at Y593 residue in metastatic cancer cells. Tyrosine kinase c-Abl phosphorylated p68 upon PDGF stimulation. The phosphorylated p68 repressed *E-cadherin* gene expression through up-regulation of the *Snail* gene. The phosphorylated p68 activated transcription of the *Snail* gene by displacing HDAC1 from the nuclear remodeling and deacetylation complex MBD3: Mi-2/NuRD complex using its protein-dependent ATPase activity. P68 RNA helicase has been implicated in transcriptional regulation of a number of genes. However, it is not known how a DEAD-box RNA helicase functions in transcriptional regulation. Our

studies may provide a good model to explain the functional role of p68 or other DEAD-box RNA helicases in the transcriptional process.

Taken together, this dissertation study provides insight into the essential roles of p68 RNA helicase in the pre-mRNA splicing process *in vitro* and *in vivo*. This dissertation also investigated the molecular basis of phosphorylated p68 as transcriptional coactivator. Furthermore, this dissertation demonstrated the first example of RNA helicases modulating protein-protein interactions through an energy driven motor to direct transcription regulation.

6.1 p68 is an essential splicing factor

Combining the data from the previous studies of our laboratory and from this dissertation (Liu, Sargueil et al. 1998; Liu 2002), a hypothetical model for the function of p68 RNA helicase in the pre-mRNA splicing process is proposed (**Figure VI-1**). P68 actively unwinds the U1:5'ss duplex by direct displacement of the RNA duplex or by destabilizing the protein factor(s) that stabilize the duplex. The protein also plays a role in the addition of the tri-snRNP to the pre-spliceosome. P68 may fulfill the role by interacting with both the 5'ss and the U4/U6•U5 tri-snRNP. The interactions may act directly or through other proteins (Kuhn, Li et al. 1999). The ATPase activity of p68 is not required for these interactions. This model is consistent with the observations of other laboratories that p68 RNA helicase is detected in the pre-spliceosome as well as the matured spliceosome (Neubauer, King et al. 1998; Hartmuth, Urlaub et al. 2002; Jurica, Licklider et al. 2002). The dual functions of p68 RNA helicase in the human spliceosome

are reminiscent of the case of Prp22 in the yeast spliceosome. It was demonstrated that Prp22 plays two distinct roles. The protein plays an important role in the second catalytic step of the pre-mRNA splicing. Prp22 is also essential for releasing the matured mRNA from the spliceosome (Schwer and Gross 1998). Thus, it may be a general phenomenon that some DEAD/DExH box RNA helicases not only function in unwinding the target, but also coordinate the events upstream and/or downstream.

Co-precipitation of p68 with intronless mRNA is intriguing. The function of p68 in intronless mRNA processing is unclear. The dual role of p68 in spliced and unspliced mRNA is reminiscent another DEAD-box protein Sub2p. The yeast DEAD-box protein RNA helicase Sub2p is an ortholog of splicing factor UAP56. Sub2p is required for the pre-mRNA splicing process and the spliceosome assembly (Libri, Graziani et al. 2001; Zhang and Green 2001). Sub2p has also been implicated in mRNA surveillance (Jensen, Boulay et al. 2001; Strasser and Hurt 2001). Sub2p associates with active genes during transcription elongation and facilitates the recruitment of the export receptor to the messenger ribonucleoprotein (mRNP) complex (Zenklusen, Vinciguerra et al. 2002). Therefore, transcription and mRNA exportation are probably functionally linked. P68 may be an important protein factor that is involved in general pre-mRNA processing. One would reason that p68 participates the pre-mRNA splicing. After the splicing, the protein is removed from mRNA with the disassociation of components of the spliceosome. Without the splicing, p68 may 'stay' with the transcripts. The association of p68 with unspliced mRNA may be part of the exosome-dependent surveillance mechanism targeting improperly assembled mRNPs for degradation.

6.2 p68 regulates Snail transcription through protein-dependent ATPase activity.

Histone acetylation and chromatin remodeling are targets of phosphor-p68 in regulating Snail expression. Experiments from our laboratory proposed a minimal model to illustrate the functional role of p68 in gene transcription regulation (**Figure VI-2**). P68 associates with one of the mammalian histone deacetylases (HDAC1) in the contents of the chromatin remodeling the NuRD complex. Tyrosine phosphorylated p68 modulates the interactions of HDAC1 with the NuRD complex at the *Snail* promoter. HDAC1 associates with the NuRD complex at the *Snail* promoter and represses *Snail* expression in the presence of unphosphorylated p68. The interaction is functional as unphosphorylated p68-associated HDAC1 exhibits histone deacetylase activity *in vitro*. The phosphorylated p68 dissociates HDAC1 from the NuRD complex at the *Snail* promoter in an ATP-dependent fashion. Consequently, the *Snail* gene is activated.

P68 has been reported to be involved in multiple signaling pathways and acts as transcriptional coactivator (Endoh, Maruyama et al. 1999; Rossow and Janknecht 2003) or corepressor (Wilson, Bates et al. 2004; Bates, Nicol et al. 2005). However, how a DEAD-box protein facilitates or represses gene transcription is unknown. Four mechanisms have been proposed. One possibility is that p68 acts as an adaptor protein for recruitment of transcriptional factors. For ER responsive genes, the ATPase activity of p68 is not required for E₂-induced gene expression (Endoh, Maruyama et al. 1999). It is possible that p68 facilitates the assembly of the transcription coactivator complex containing p68, CBP/p300 and RNA polymerase II (Rossow and Janknecht 2003).

Secondly, ATPase-dependent chromatin remodeling factors, such as SWI2/SNF2 are structurally related to DEAD-box RNA helicase. DEAD-box RNA helicase DP97 has been reported to repress gene expression through a similar mechanism of repressor protein N-CoR and SMAT (Rajendran, Nye et al. 2003). It is possible that DEAD-box p68 alters chromatin structure via the ATPase motor. Subsequently, DEAD-box p68 activates or represses gene expression. Another possibility is that p68 regulates gene transcription through the recruitment of HDAC1. P68 interacts with HDAC1 and targets to sequence-specific promoters. The recruitment of HDAC1 to the promoter represses the gene transcription (Wilson, Bates et al. 2004). Finally, our studies provide a mechanism by which p68 regulates gene expression by modulating the interactions of components of transcriptional regulatory complex. P68 actively displaces HDAC1 from the promoter and consequently activates gene transcription. Therefore, the actions of p68 in regulating gene expression are probably dependent on the context of promoter and transcriptional regulatory complex.

It is probable that more genes are regulated by p68 and the p68-associated the NuRD complex. The promoter specificity is probably mediated by other components of the complex. For example, MBD3 has been suggested to direct the NuRD complex to methylated chromatin sites. Although p68 does not associate with DNA, which rules out the possibility that p68 recognizes promoter sequences; it is possible that p68 or phosphorylated p68 associates with the protein factor(s) that directly or indirectly recognize specific promoter sequences. By recognizing promoter sequences, p68 might guide the transcriptional complex to the particular gene promoter regions.

DEAD-box RNA helicases are involved in most RNA metabolism. The functional relationship between phosphorylated/unphosphorylated p68 is an interesting issue. One speculation is that unphosphorylated p68 serves as the “default” function of p68 to maintain normal cellular processes for cell growth and life span, including the pre-mRNA splicing. However, tyrosine phosphorylation of p68 alters the function of p68. The consequence is that the phosphorylated p68 promotes abnormal cell growth and EMT. The phosphorylation of p68 may change the substrate binding of p68. Therefore, the phosphor-p68 targets different sets of genes due to the altered substrate recognition. It is also possible that the phosphorylation changes the enzymatic activity of p68. As demonstrated in this dissertation study, phosphorylated p68 becomes a protein “unwindase” to displace HDAC1 from the NuRD complex at the *Snail* promoter.

Whether p68 is a constitutive member of the NuRD complex is unknown. p68 was not identified in the originally isolated the NuRD complex. One possibility is that the association of p68 with the NuRD complex is tissue or cell specific. Alternatively, p68 may only associate with a sub-family of the complex. We have shown that the phosphorylated p68 displaces HDAC1 from the NuRD complex using the unique protein-dependent ATPase activity. The functional role of the unphosphorylated p68 in the NuRD complex remains elusive. It is possible that unphosphorylated p68 plays a structural role in facilitating the assembly of the NuRD complex.

The notion of protein-dependent ATPase activity of p68 RNA helicase is intriguing. The DEAD-box RNA helicases were originally defined as a family of enzymes that unwind dsRNA using the energy derived from ATP (in most cases)

hydrolysis (Tanner, 2001). Lately, it has been suggested that the RNA-dependent ATPase can also be used to dissociate RNA-protein interactions (Jankowsky, 2001; Fairman, 2004). Although, the detailed mechanism by which the phosphorylated p68 RNA helicase hydrolyzes ATP in binding to protein substrate is not clear, certain proteins such as β -catenin and MBD3 dramatically stimulated ATPase activity of Y593 phosphorylated p68 RNA helicase but not the unphosphorylated protein. These results further expand the view for the function of DEAD-box RNA helicase as a modulator for protein-protein interactions independent of RNA/DNA. One question is: how the ATPase activity of p68 RNA helicase is activated in the NuRD complex. The answer to this question leads to an important speculation that tyrosine phosphorylation at Y593 may trigger a conformational change in C-terminal domain of p68 RNA helicase. This conformational change allows substrates binding switches from RNAs to proteins. Consistent with this, tyrosine phosphorylation of p68 RNA helicase inhibited RNA substrate stimulated ATPase activity of the protein.

It will be important to verify the protein-dependent ATPase activity in another protein-protein context. Defining the target protein or multi-protein complexes for p68 remains a decisive point for further understanding the function of phosphorylated p68. Another crucial question is whether this protein-dependent ATPase activity is a general phenomenon for most DEAD-box proteins. Two DEAD-box proteins have been suggested to modulate RNA-protein interactions without unwinding double stranded RNA duplex. The DEAD-box proteins containing protein-binding domains, such as SH2 and SH3 domains will be possible candidates to have protein-dependent ATPase activity.

An additional concern is the kinetics of the protein-dependent ATPase activity. The half-life of tyrosine phosphorylated p68 is more than six hours. Cofactors that regulate the protein-dependent ATPase activity and facilitate p68 substrate binding need to be identified. How DEAD-box protein p68 are inactivated or directed to targets in a timely fashion is also a challenging question.

6.3 Implications in cancer.

Tumor metastasis is a remarkably complicated process that is controlled by a number of mechanisms. Although, it is very difficult to observe the bona fide EMT process during tumor metastasis, strong evidences support that EMT is an essential step during epithelial derived tumor metastasis. Our data demonstrated that PDGF autocrine loop and c-Abl is required for tyrosine phosphorylation of p68. The phosphorylated p68 subsequently promotes EMT in SW620 cells. The PDGF-induced phosphorylated p68 also promoted tumor cells migration and invasion, which is critical for tumor metastasis. Our observations are supported by studies of other groups. The expression of p68 is critical for the wound healing process (Kahlina, Goren et al. 2004). P68 is suggested to participate in the partial EMT and tissue remodeling processes. Molecular studies indicate that p68 directly associates with Smad3 upon TGF- β stimulation (Warner, Bhattacharjee et al. 2004), suggesting the potential role of p68 in EMT (Oft, Heider et al. 1998). Therefore, we suspect that phosphorylated p68 is a new molecular factor that promotes tumor metastasis. The best system to ultimately test our speculation is to

examine the metastasis of xenograft models of human cancer cell lines. Mutations that abolish the tyrosine phosphorylation site of p68 should abrogate tumor development and progression.

For tumor metastasis to occur, signaling pathways promoting cell survival and proliferation are also critical (Barcellos-Hoff 2001; Hynes 2003). Tumor cells must be able to survive in blood circulation without anchorage and under surveillance of immune cells until they are arrested by a second organ. In secondary sites, it is critical for tumor cells to be able to proliferate from micro-metastasis to metastatic tumor. From our data, phosphorylated p68 is demonstrated to promote cell proliferation and anti-ligand-induced apoptosis (Yang, 2006, in preparation). Therefore, it is likely that phosphorylated p68 causes tumor metastasis through multiple mechanisms of promoting tumor cell EMT, cell proliferation and anti-apoptosis.

Our data indicated that tyrosine phosphorylation of p68 closely correlates to tumor development and progression. These findings suggested that p68 may be used as a potential tumor marker for monitoring tumorigenesis and metastasis. An ideal tumor marker can be used for tumor screening, diagnosis and prognosis. Although, it is unlikely that a tumor marker will be applicable to every type of malignant tumor, our data demonstrated that the tyrosine phosphorylation of p68 exhibits strong correlations with tumor malignancies of different organs, including colon, liver, ovary and lung. More importantly, dephosphorylation at tyrosine residues respond to treatment of certain anti-tumor drugs. Thus, it is possible that monitoring the level of tyrosine phosphorylation of

p68 can be a cancer marker for several types of tumor. Additional tests are required for the application of the tyrosine phosphorylation of p68 as a cancer marker.

Experiments in our laboratory demonstrated that the PDGF autocrine loop induced tyrosine phosphorylation of p68 in metastatic cell lines, suggesting the significant role of PDGF in tumor invasion and metastasis. The function of PDGF regulates a wide-range of cellular processes such as tumor angiogenesis. The PDGF autocrine loop likely occurs in most solid tumors. Our observation gave another example that PDGF may promote tumor malignancy and invasion. Designed drugs targeting PDGF receptors, such as Gleevec may be applied to solid tumors for cancer treatment. Indeed, Gleevec has been used for the treatment of breast cancer (Thiery and Sleeman 2006). To inhibit the function of tyrosine phosphorylation of p68, small peptide chains containing Y593 phosphorylation sites can be designed to compete with endogenous phosphorylated p68. This strategy may lead to blocking Snail transcription and subsequent EMT genes. Such therapeutic strategies might prevent tumor invasion and metastasis *in vivo*.

Figure VI-1 The hypothetical model of DEAD-box RNA helicase in the pre-mRNA splicing.

DEAD-box p68 RNA helicase recognizes and actively unwinds the U1 snRNP-5' splice site duplex in an ATP-dependent manner. p68 RNA helicase also bridges the addition of U4/U6•U5 tri-snRNP and subsequently promotes the assembly of the spliceosome. The ATPase activity of p68 RNA helicase is not required for these interactions.

Figure VI-1

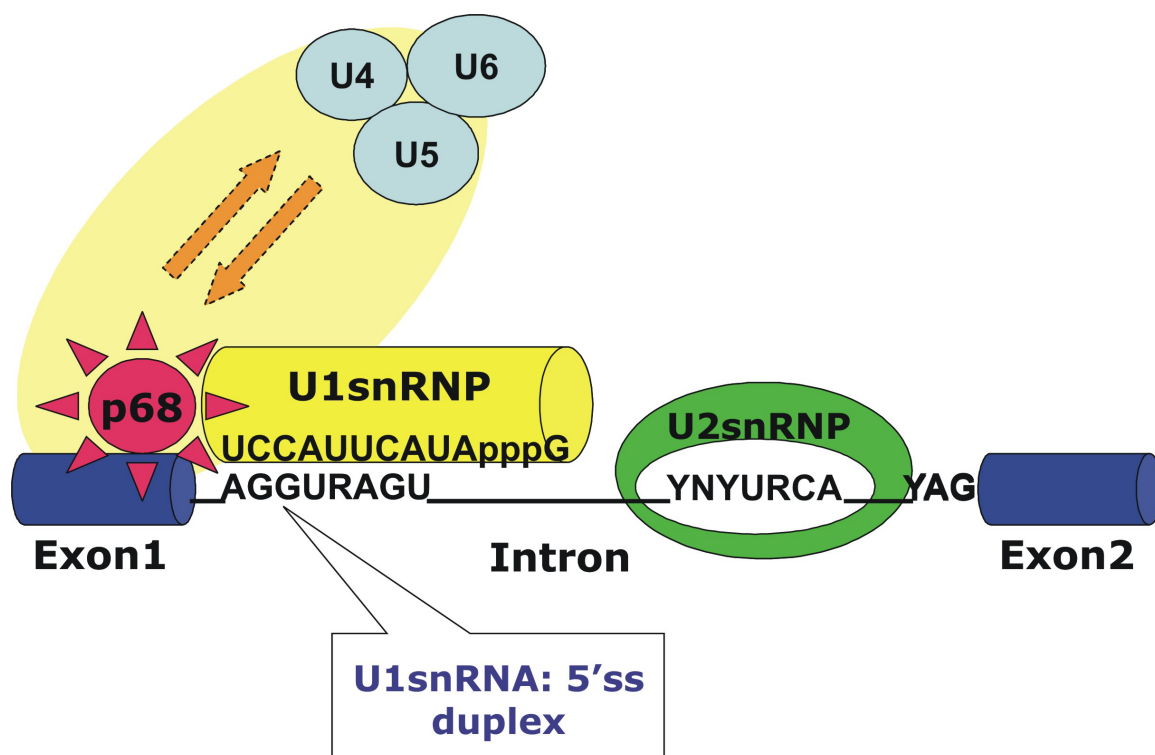
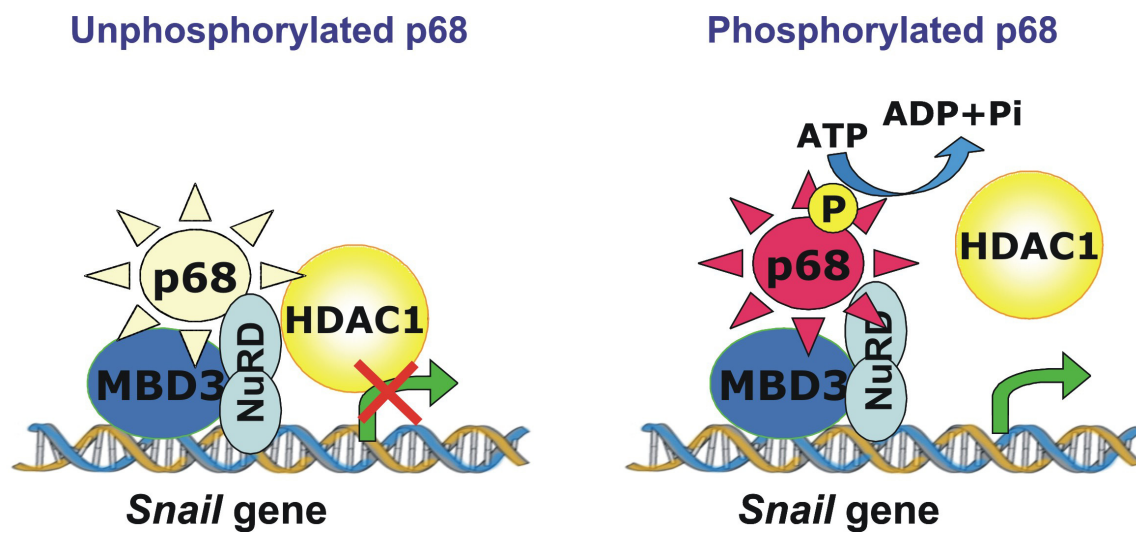


Figure VI-2. The minimal model of protein-dependent ATPase activity of p68.

P68 associates with one of the mammalian histone deacetylases (HDAC1) in the contents of chromatin remodeling the NuRD complex. Tyrosine phosphorylated p68 modulates the interactions of HDAC1 with the NuRD complex at the Snail promoter. HDAC1 associates with the NuRD complex at the Snail promoter and represses Snail expression in the presence of unphosphorylated p68. The interaction is functional as unphosphorylated p68-associated HDAC1 exhibits histone deacetylase activity *in vitro*. The phosphorylated p68 dissociates HDAC1 from the NuRD complex at the Snail promoter in an ATP-dependent fashion. Consequently, the Snail gene is activated.

Figure VI-2



CHAPTER VII

MATERIAL AND METHODS

7.1 Material

7.1.1 Chemicals

[α - ³² P]ATP	Amersham Biosciences Corp, Piscataway
[γ - ³² P]ATP	Amersham Biosciences Corp, Piscataway
Alcohol	VWR international, West Chester
Acetone	VWR international, West Chester
Acetic Acid	VWR International, West Chester
Acrylamide	Fisher BioReagent, Fairlawn
Adenosine triphosphate solution	Fermentas, Hanover
Agar	Sigma Aldrich, St. Louis
Agarose	National diagnostics, Atlanta
Ammonium Persulfate	Sigma Aldrich, St. Louis
Ampicillin	Sigma Aldrich, St. Louis
Ascorbic Acid	Sigma Aldrich, St. Louis
Bacto Yeast Extract	BD Bioscience, Spark
Bacto Tryptone	BD Bioscience, Spark
β -Mercaptoethanol	Sigma Aldrich, St. Louis
Bromophenol Blue	EMD, San Diego
Cell culture media	Cellgro, Herndon
Coomassie blue	Sigma Aldrich, St. Louis
DL-Dithiothreitol	Sigma Aldrich, St. Louis
Dissolve methyl sulfoxide	EMD, San Diego
Ethidium Bromide	Sigma Aldrich, St. Louis
Ethylenedinitrilo-tetraacetic acid	Sigma Aldrich, St. Louis
Formaldehyde	Calbiochem, San Diego
Formalin	VWR International, West Chester
Glycerin	VWR International, West Chester
Glycine	VWR International, West Chester

HEPES	Sigma Aldrich, St. Louis
Hydrochloric acid	VWR International, West Chester
Igepal	Sigma Aldrich, St. Louis
Imidazole	Sigma Aldrich, St. Louis
Isopropyl- β -D-thiogalactopyranosid	Sigma Aldrich, St. Louis
Kanamycin	Sigma Aldrich, St. Louis
Malachite Green Oxalate salt	Sigma Aldrich, St. Louis
Magnesium Chloride	Fisher Biotech, Fairlawn
Methanol	VWR International, West Chester
Ni-NTA agarose	Qiagen, Hilden
N,N-Methylene Bis-Arylamide	Fisher Biotech, Fairlawn
Penicillin-Streptomycin solution	Cellgro, Herndon
Perchloric Acid	Sigma Aldrich, St. Louis
Phenol/Chloroform	Promega, Madison
Phenylmethylsulfonyl-Fluoride	Fluka, Sigma Aldrich, St. Louis
2-[4-(2-sulfoethyl)piperazine-1-yl]ethanesulfonic acid	Sigma Aldrich, St. Louis
Ponceau solution	Sigma Aldrich, St. Louis
Phenol/Chloroform	Promega, Madison
Polyvinyl Alcohol	VWR International, West Chester
Polyvinylpyrrolidone	Sigma Aldrich, St. Louis
2-Propanol	VWR International, West Chester
Protein G agarose	Upstate, Charlottesville
Protein inhibitor cocktail	Sigma Aldrich, St. Louis
n-Propyl Alcohol	Sigma Aldrich, St. Louis
sephadexG-50	Sigma Aldrich, St. Louis
Sodium Acetate solution	Promega, Madison
Sodium Chloride	Fisher Biotech, Fairlawn
Sodium Bicarbonate	Sigma Aldrich, St. Louis
Sodium Dodecyl Sulfate	Fisher Biotech, Fairlawn
Sodium Fluoride	Sigma Aldrich, St. Louis
Sodium Hydroxide	Fisher Biotech, Fairlawn
Sodium Orthovanadate	Sigma Aldrich, St. Louis

Sodium Pyruvate solution	Cellgro, Herndon
D-sorbitol	Sigma Aldrich, St. Louis
N,N,N,N -TetramethylEthylenediamine	Fluka, Sigma Aldrich, St. Louis
trichostatin A	Sigma Aldrich, St. Louis
Tris base	Fisher Biotech, Fairlawn
Triton X-100	Sigma Aldrich, St. Louis
Trioxsalen	Sigma Aldrich, St. Louis
Trypan Blue	Sigma Aldrich, St. Louis
0.25% Trypsin-EDTA	Cellgro, Herndon
Tween-20	Sigma Aldrich, St. Louis
Urea	Fisher Biotech, Fairlawn

7.1.2 Other Material and Kits

Bio-Rad Protein Assay	Bio-Rad Laboratories, Hercules
Biocoat Tumor Invasion System	BD Bioscience, Rockville
Chariot Protein Delivery Kit	Active Motif Carlsbad
Dual-Luciferase Reporter Assay	Promega, Madison
Dual-light® System	Applied Biosystem, Foster city
Nuclear Extraction Kit	Active Motif Carlsbad
HDAC Activity Colorimetric Assay Kit	BioVision, Mountain view
Mammalian Cell Transfection Kit	Cell & Molecular Technologies, Phillipsburg
RNeasy® Mini Kit	Qiagen, Valencia
QIAprep Spin Miniprep Kit	Qiagen, Valencia
QIAquick Gel Extraction Kit	Qiagen, Valencia
QuikChange® II Site-Directed Mutagenesis Kit	Stratagene, La Jolla
Titan One Tube RT-PCR System	Roche Applied Science, Indianapolis
TOPO Cloning Kit	Invitrogen, Carlsbad
Wizard® plus DNA purification System	Promega, Madison
Virapower® Lentiviral Expression System	Invitrogen, Carlsbad

7.1.3 Laboratory Equipments

Allegra™ 6R Centrifuge	Beckman Coulter, Fullerton
BioChemi System	UVP BioImaging and analysis System, Upland
C25 Incubator shaker	New Brunswick Scientific, Edison
Purifier Class II Biosafety Cabinet	Labconco, Kansas City
Sirius Luminometer	Berthold Detection System, Oak Ridge
Unicorn™ 4.11 HPLC	Amersham Bioscience, Piscataway
UV-1700 Spectrophotometer	Shimadzu Corporation, Columbia
Victor ³ V 1420 Multilabel Counter	Perkin Elmer, Wellesley
Zeiss LSN 510 META	Zeiss, Jena

7.1.4 Enzymes and Recombinant Proteins

Alkaline phosphatase, Shrimp	Promega, Madison
DNAase	Promega, Madison
GSK-aPKC active/inactive	Dr. Jorge Moscat, Madrid, Spain
HDAC1	Panomics, Redwood
His/Myc mPLK/IRAK	Dr. Maureen Harrington
IRAK kinase	Tularik, San Francisco
MBD3	BioClone, San Diego
2.5S NGF	Bioproducts for Science, Indianapolis
<i>Pfu</i> -DNA polymerase	Stratagene
Protein Kinase C-iota	Calbiochem, San Diego
Proteinase K	Sigma Aldrich, St. Louis
PDGF-BB	Pepre Tech, Rocky Hill
RNase A and T1	Fermantas, Hanover
Restriction enzymes	Fermantas, Hanover
RNA polymerase T7 and Sp6	Promega, Madison
T4 Polynucleotide Kinase	Promega, Madison
T4-DNA ligase	Fermantas, Hanover

7.1.5 Antibodies

Anti Actin- β antibody (mouse monoclonal)	Santa Cruz Biotechnology, Santa Cruz
Anti-E-cadherin (mouse, monoclonal)	BD Bioscience, Rockville
Anti-HA antibody (mouse monoclonal)	Roche Applied Science, Indianapolis
Anti-HA antibody (rabbit polyclonal)	Upstate, Charlottesville
Anti-His antibody (rabbit polyclonal)	Santa Cruz Biotechnology, Santa Cruz
Anti-Histone 2A (rabbit polyclonal)	Cell Signaling Technology, Beverly
Anti-HDAC1 antibody (rabbit polyclonal)	Cell Signaling Technology, Beverly
Anti-HDAC1 antibody (mouse monoclonal)	Santa Cruz Biotechnology, Santa Cruz
Anti-IRAK antibody (mouse monoclonal)	BD Transduction Laboratories, San Diego
Anti-IRAK antibody (rabbit polyclonal)	Santa Cruz Biotechnology, Santa Cruz
Anti Mi-2 antibody (goat polyclonal)	Santa Cruz Biotechnology, Santa Cruz
Anti-MBD3 antibody (rabbit polyclonal)	ABGENT, San Diego
Anti-MBD3 antibody (mouse monoclonal)	Imgenex Corporation, San Diego
Anti-MyD88 antibody (mouse monoclonal)	Santa Cruz Biotechnology, Santa Cruz
Anti-Myc antibody (rabbit polyclonal)	Santa Cruz Biotechnology, Santa Cruz
Anti-p68 RNA helicase(C-termini) antibody (rabbit polyclonal)	Invitrogen, Carlsbad
Anti-P68-rgg (C-termini) antibody (mouse monoclonal)	Auburn University Hybridoma Facility
Anti-SNAI 1 antibody (Goat polyclonal)	Santa Cruz Biotechnology, Santa Cruz
Anti-p75 antibody (rabbit, polyclonal)	Promega, Madison
Anti-P-Tyr-100 antibody (mouse monoclonal)	Cell Signaling Technology, Beverly
Anti-PKC-iota antibody (mouse monoclonal)	BD Laboratories, San Diego
Anti-TRAF6 antibody (rabbit polyclonal)	Santa Cruz Biotechnology, Santa Cruz
Anti-Vimentin antibody (mouse monoclonal)	BD Laboratories, San Diego

7.1.6 Vectors and siRNA Sequence

pBluescript® II Phagemid Vectors	Stratagene, La Jolla
pHM6 mammalian expression vector	Roche Applied Science, Indianapolis

pLenti6/V5-D-TOPO	Invitrogen, Carlsbad
pLenti6/V5-DEST	Invitrogen, Carlsbad
Snail-pGL2	Fujita, et al. (2003)
Human c-Abl	Smart Pool, Dharmacon, Lafayette
Human DDX5 NM_004396	GCAAGUAGCUGCUGAAUAUUU, Dharmacon, Lafayette
Human MBD3 NM_003926	Smart Pool, Dharmacon, Lafayette
Human PDGFRB, NM_002609	GAAAGGAGACGUCAAAUAUUU, Dharmacon, Lafayette

7.1.7 Bacteria Stains

BL21-CodonPlus®(DE3)-RIL	Stratagene, La Jolla
JM109	Promega, Madison
One shot Stbl3	Invitrogen, Carlsbad
XL1-Blue supercompetent cells	Stratagene, La Jolla

7.1.8 The Mammalian Cell Lines

Cell line	ATCC No.	Medium	Source
HeLa	CRL-2.2	F-12K	Cervix
HEK 293	CRL-1573	DMEM	Kidney
HT-29	HTB-38	Mccoy's 5A	Colon
HCT-116	CRL-247	Mccoy's 5A	Colon
SW480	CCL-228	L-15	Colon
SW620	CCL-227	L-15	Colon
WM115	CRL-1675	MEM	Melanoma
WM266	CRL-1676	MEM	Melanoma
H460	HTB-177	RPMI 1640	LUNG
H146	HTB-173	RPMI 1640	LUNG
686LN	N/A	F12K/DMEM 50/50	H & N
M4c1	N/A	F12K/DMEM 50/50	H & N
M4d4	N/A	F12K/DMEM 50/50	H & N

M4e	N/A	F12K/DMEM 50/50	H & N
HCT-116	CRL-247	Mccoy's 5A	Colon
4T1	CRL-2539	RPMI 1640	Breast
PC12	CRL-1721	DMEM	Adrenal gland

7.1.9 Buffers

Coomassie Blue Stain Buffer	0.025% Coomassie Blue, 50% Methanol, 10% Acetic Acid
Destain Buffer	7% Acetic Acid, 5% Methanol
PBS-buffer 10X	1.5M NaCl, 30mM KCl, 15mM KH ₂ PO ₄ , 60mM Na ₂ HPO ₄
RIPA buffer, 10X	Upstate, Charlottesville
SDS Running Buffer	25 mM Tris, 200 mM Glycine, 0.1% SDS
TBE-buffer 10X	900mM Tris-HCl, 440 mM Boric Acid, 20mM EDTA
TBS-buffer 10X	200 mM Tris-HCl (pH 7.5), 1.37 M NaCl,
TE Buffer	10 mM Tris-HCl (pH 8.0), 1 mM EDTA
Transfer Buffer	25 mM Tris, 200 mM Glycine, 20% Methanol

7.1.10 Computer Software

DNA/protein homology search	BLAST search (National Center of Biotechnology)
Gel Imaging	LabWorks™ Image Acquisition and Analysis Software, UVP BioImaging Systems
Graphic Processing	Corel Draw 12.0
Micro plate Reader	Wallac 1420 Software Version 3.00
Presentations	PowerPoint 2003
Protein Purification	Unicorn 4.11, Amersham Bioscience

Statistical Analysis

Excel 2003

Text Processing

Microsoft Word 2000

7.2 Bacteria Culture

All *E. coli* strains BL-21 (Stratagene), JM109 (Promega), One shot Stl3 (Invitrogen) and XL1-blue (Stratagene) were used for amplification of plasmid DNA or expression of recombinant protein. Bacteria were grown in liquid LB (Lauria-Bertani) medium (1% bacto-tryptone w/v, 0.5% bacto-yeast-extract w/v and 1% NaCl w/v). For selection, the media contained ampicillin (50 µg/ml), kanamycin (50 µg/ml) or Blasticidine (50 µg/ml). Agar-plates were generated with LB-ampicillin, - kanamycin or - blasticidine medium supplemented with agar (15 g/L). For long-term preservation of transformed bacteria (2.2.2), cells were mixed with sterile glycerol [30% (v/v)] and stored at -80°C.

7.2.1 Transformation

100 µl of a competent bacteria suspension (2.1.7) were thawed on ice and 10 µl of the ligation reaction (2.3.7) was added. The bacteria/DNA mixture was remained on ice for additional 30 min followed by incubation at 42°C for 45 sec. The bacteria were chilled on ice again for 2 min, before 300 µl of LB-medium were added. For initial expression of the plasmid encoded ampicillin resistance, bacteria were incubated for 45 min at 37°C on a circular shaker. Subsequently, 100 µl of this transformation solution

were plated on ampicillin containing agar plates. The plates were incubated overnight at 37°C.

7.3 Deoxyribonucleic Acid Techniques

7.3.1 Preparation of plasmid DNA

Plasmids have been routinely isolated from bacterial cultures using a modified protocol originally described by Birnboim and Doly (Birnboim and Doly 1979). Small quality of DNA plasmids were purified by using QIAprep® Spin Miniprep Kit as described by Manufacture. High amounts of pure plasmid DNA (up to 100 µg) were prepared using the Wizard® plus DNA purification System. Generally, 2ml of medium containing appropriate antibiotic(s) were inoculated with a single bacterial colony from a selective agar plate and incubated overnight (16 to 18 hours) by vigorous shaking at 37°C. 1.5ml of the cell suspension was centrifuged for 1 min at 10,000rpm and the medium was removed by aspiration. The bacterial pellets were suspended by 250µl of suspension buffer supplemented with RNase A. Bacterial were lysed under alkaline condition and the lysates is subsequently neutralized and adjusted to high-salt binding conditions. After lysates clearing, the sample was applied to silica column. Endonuclease was efficiently removed by a brief wash step, to ensure that plasmid DNA was not degraded. Salts were also being removed by another wash step. High-quality plasmid DNA was then eluted from the QIAprep column with 50µl of elution buffer or water.

For high amount of plasmid DNA, 100ml of antibiotic(s)-selected LB medium was inoculated with 100 μ l of small culture and incubated overnight (16 to 18 hours) by vigorous shaking at 37°C. Bacteria culture was centrifuged 6,000rpm for 10 min at 4°C and purified by Wizard® plus DNA purification System using similar principle.

7.3.2 Quantification of Nucleic Acid Concentration

Concentrations of nucleic acids were determined photometrically using a wavelength of 260 nm (UV-1700 Spectrophotometer, Shimadzu Corporation, Columbia). An optical density (OD) of 1 corresponds to approximately 50 μ g/ml double-stranded DNA or 40 μ g/ml for single stranded DNA and RNA ((Sambrook and Gething 1989)). The ratio between the readings at 260 nm and 280 nm (OD₂₆₀/OD₂₈₀) provides an estimation of the purity of the nucleic acid preparation. Highly pure DNA or RNA is characterized by ratios between 1.8 and 2.0.

7.3.3 Agarose Gel Electrophoresis of Nucleic Acids

Nucleic acids were separated by electrophoresis, which using agarose gel to separate and sometimes purify nucleic acid that differs in size. Unlike proteins, nucleic acids have a consistent negative charge imparted by their phosphate backbone and migrate toward the anode. For separation of DNA molecules from 0.5 to 2 kbp usually 1% agarose gels (w/v) were used. Smaller DNA fragments (100-500 bp) were separated in high density gels (1.5-2% agarose gels) (Sambrook and Gething 1989). Agarose

(National Diagnostics) was dissolved in 1x TBE gel electrophoresis buffer. Ethidium bromide was added to a final concentration of 500 ng/ml. Ethidium bromide intercalates between DNA base pairs and enables an ultraviolet fluorescence illumination of nucleic acids. The DNA/RNA probes were diluted with loading buffer (6X loading dye, MBI Fermentas) and transferred into the appropriate gel wells. Electrophoresis was performed in 1x TBE buffer with a voltage of 5-10 V/cm gel. DNA fragment sizes were estimated using molecular weight markers (MBI Fermentas).

7.3.4 DNA Extraction from Agarose Gel

QIAquick Gel Extraction Kit (Qiagen) was used for extraction and purification of DNA from agarose gel according to instruction of manufacture. This system use uniquely designed silica membrane which is able to isolate DNA from both aqueous solutions and agarose gels without binding with unwanted primers and impurities. Buffer QG in the QIAquick Gel Extraction Kit solubilizes the agarose gel slice and provides the appropriate conditions for binding of DNA to the silica membrane. Buffer QG also contains a pH indicator, allowing easy determination of the optimal pH for DNA binding. The followed washing step by ethanol-containing buffer removes salts, agarose and dyes. Contrary to adsorption, elution is most efficient under basic conditions and low salt concentrations. DNA is eluted with 50 or 30 μ l of the provided Buffer EB (10 mM Tris-HCl, pH 8.5), or water.

7.3.5 Polymerase Chain Reaction (PCR)

PCR can characterize, analyze and synthesize any specific piece of DNA by exploiting the remarkable natural function of enzymes known as polymerases. For all PCR reaction, PfuUltra™ High-Fidelity DNA Polymerase (Stratagene) was used. There are three basic steps in PCR. First, the target genetic material must be denatured—that is, the strands of its helix must be unwound and separated by heating to 90-96°C. The second step is hybridization or annealing, in which the primers bind to their complementary bases on the now single-stranded DNA. The third is DNA synthesis by a polymerase. Starting from the primer, the polymerase can read a template strand and match it with complementary nucleotides. The result is two new helices in place of the first, each composed of one of the original strands plus its newly assembled complementary strand (Mullis and Faloona 1987). The components containing in PCR reaction mixture is list below.

Polymerase Chain Reaction:	10X Pfu Buffer	5 µl
	10mM dNTP	1 µl
	DNA template	1 µl (100 ng)
	Primer 5'	1 µl (100 ng)
	Primer 3'	1 µl (100 ng)
	Pfu	1 µl
	Total Volume	50 µl
	H ₂ O	Add to 50 µl

The reaction was performed in a thermocycler (Mastercycler Gradient, Eppendorf) with 28-32 cycles of following steps: 30 sec 94°C, 30 sec 55°C and 2 min 72°C. The amplification was completed with the final step of 10 min incubation at 72°C.

PCR products were either storage at 4°C or directly analyzed and purified by gel extraction (2.3.4).

7.3.6 Restricted Endonuclease Digestion

Restriction endonucleases, due to their high specificity and ease of use, are important tools in studies of DNA primary structure, recombinant DNA technology and other fields of molecular genetics and molecular biology. A restriction enzyme which recognizes specific DNA sequences and is able to cleave the foreign invading DNA upon entering the bacterial cell and a modification enzyme (methylase) responsible for protecting host DNA against the action of its own restriction endonuclease (Arber and Dussoix 1962). Most restricted endonucleases are type II enzymes, which recognize asymmetric base sequences and cleave DNA at a specified position up to 20 base pairs outside of the recognition site. The standard digestion reaction is list below. After 2 hours of incubation, digestion products were either analyzed by gel electrophoresis (2.3.3) or purified by gel extraction (2.3.4). For ligation purpose, scaled up reactions were incubated overnight with digestion of up to 10 µg of DNA. All reactions were incubated in 37°C.

DNA restriction digestion:	10X buffer	1 µl
	DNA	5 µl
	Restricted endonuclease	0.5 µl
	Total Volume	10 µl
	H ₂ O	Add to 10 µl

7.3.7 Ligation

Joining linear DNA fragments between the 5'-phosphate and the 3'-OH of DNA fragments together with covalent bonds is called ligation. The enzyme used to ligate DNA fragments is T4 DNA ligase, which originates from the T4 bacteriophage. This enzyme will ligate DNA fragments having overhanging, cohesive ends that are annealed together. In order to avoid self circularization and/or formation of tandem oligomers of insert and linearized vector, ligation reaction mixture should contain >1-3 fold molar excess of foreign DNA to vector DNA. Restricted and purified DNA plasmids and PCR products were directly ligated by ligation reaction. The ligation reaction will be incubated at 4°C for overnight, followed by transformation (2.1.1) or storage at 4°C.

Ligation:	5X Ligation Buffer	1 µl
	Vector	1 µl (~500 ng)
	PCR product	3 µl (~300 ng)
	H2O	Add to 10 µl
	Total Volume	10 µl

7.3.8 Dephosphorylation and insert DNA phosphorylation

In the instance of single restricted enzyme cloning, alkaline phosphatases are used to prevent recircularization and religation of linearized cloning vehicle DNA by removing phosphate groups from both 5'-termini. Shrimp Alkaline Phosphatase (SAP) catalyzes the dephosphorylation of 5' phosphates from DNA. Unlike Calf Intestinal Alkaline Phosphatase, SAP is completely and irreversibly inactivated by heating at 65°C for 15 minutes. To this end, the restricted DNA was incubated with SAP for 30 min at

37°C. Afterwards, reaction products were heated at 65°C for 15 min to deactivate the phosphatase.

Dephosphorylation:	10X Buffer	1 μ l
	Restricted Vector	2 μ l (~1 μ g)
	SAP	1 μ l
	H ₂ O	Add to 10 μ l
	Total Volume	10 μ l

Phosphorylation of insert DNA may be required for ligation with a dephosphorylated vector. T4 Polynucleotide Kinase (T4 PNK) catalyzes the transfer of the γ -phosphate from ATP to the 5'-terminus of polynucleotides or to mononucleotides bearing a 3' phosphate group. T4 PNK is widely used to end-label short oligonucleotide probes. The following reaction was used for non-radioactive phosphorylation of insert DNA. Dephosphorylated and phosphorylated products were cleared up by phenol/chloroform extraction and ethanol precipitation. Resuspended DNAs were performed ligation, described in (2.3.7).

Phosphorylation:	10X Buffer	1 μ l
	PCR product	5 μ l (~1 μ g)
	T4 PNK	1 μ l
	H ₂ O	Add to 10 μ l
	Total Volume	10 μ l

7.3.9 Cloning of pET-30a-p68

The open reading frame (ORF) of human p68 RNA helicase was amplified according to the GenBankTM sequence (GenBankTM accession number [AF015812](#)), by using a pair of primers, 5'GCGGATCCTCGAGTGACCGAGACCGC3' as 5' primer and

5'ATTGGGAATATCCTGTTG3' as 3' primer from a cDNA library (Stratagene). The PCR products were cloned into pBluescript SK (+) vector. The obtained DNA clones were examined by auto-DNA sequencing and the sequences of resultant DNA completely match the DNA sequences of p68 RNA helicase retrieved from GenBankTM. The ORF of p68 RNA helicase was subcloned into an expression vector pET-30a by BamHI/HindIII sites with 6xHis tag on the N-terminus.

7.3.10 Cloning of pHM6-p68

To express p68 RNA helicase in the mammalian cell lines, p68 ORF were subcloned into the mammalian expression vector pHM6 (Roche) by HindIII site, starting without start codon and ending with downstream stop codon TAA. Subcloned p68 has HA tag at the N-terminus of protein sequence. To verify the correct sequence, cloned plasmid was amplified and sent to auto-sequence.

7.3.11 Cloning of Lenti6-p68 and Generation of Lentiviral Expression System

The lentiviruses, including HIV-1, are unique in their ability to infect non-dividing cells. They can accommodate long sequences, the products of which will be stably expressed due to integration into the cell chromosome. Use of the ViraPowerTM Lentiviral Expression System Efficiently delivers the gene of interest to the mammalian cells in culture or *in vivo* (Dull *et al.*, 1998). This system also provides stable, long-term expression of a target gene.

To generate Lentiviral expression construct with p68 gene, the ORF of p68 with HA tag in the 5'-terminus and additional 3' stop codon TAA was subcloned into an entry vector V5/TOPO via TOPO technique. The HA-tagged p68 gene was transferred to Lenti6/DEST gateway vector via homologous recombination. The expression plasmid that contains p68 gene and elements that allow packaging of the construct into virion was transfected into 293FT cells together with packaging plasmids (pLP1, pLP2 and pLP/VSVG). Harvest and titer-determined virus stocks were stored at -80°C.

7.3.12 Site-directed Mutagenesis

In vitro site-directed mutagenesis is an invaluable technique for characterizing the dynamic, complex relationships between protein structure and function, for studying gene expression elements and for carrying out vector modification. Stratagene's QuikChange® II site-directed mutagenesis kit was used to make point mutations, replace amino acids and delete or insert single or multiple adjacent amino acids. The general procedure utilizes a double strand DNA plasmid with an insert of interest and two synthesized oligonucleotide primers both containing the desired mutations. The oligonucleotide primers, each complementary to opposite strand of DNA vector were extended by *PfuUltra*™ high-fidelity (HF) DNA polymerase. Extension of the oligonucleotide primers generated a mutated plasmid containing staggered nicks. Following temperature cycling, the product was treated with *Dpn* I. The *Dpn* I endonuclease (target sequence: 5'-Gm6ATC-3') is specific for methylated and hemimethylated DNA used to digest the parental DNA template and to select for

mutation-containing synthesized DNA. (DNA isolated from almost all *E. coli* strains is dam methylated and therefore susceptible to *DpnI* digestion.) The nicked vector DNA containing the desired mutations is then transformed into XL1-Blue supercompetent cells for nick repair. To verify the correct mutations, manipulated DNA plasmids were auto-sequenced.

7.4 Protein Techniques

7.4.1 Recombinant Protein Purification

The expression and purification of recombinant proteins facilitates production and detailed characterization of virtually any protein. Purification procedures construct fusion proteins in which specific affinity tags are added to the protein sequence of interest; the use of these affinity tags simplifies the purification of the recombinant fusion proteins by employing affinity chromatography methods. Nickel-nitrilotriacetic acid (Ni-NTA) metal-affinity chromatography matrices for biomolecules which have been tagged with 6 consecutive histidine (6xHis) residues were used to purify all recombinant proteins. The 6xHis affinity tag facilitates binding to Ni-NTA beads. In most cases, the 6xHis tag does not interfere with structure or function of recombinant protein.

In *E. coli* strains, pET-30a vector confers kanamycin resistance and constitutively expresses the *lac* repressor protein encoded by the *lac I* gene. Expression of recombinant proteins encoded by pET-30a vectors is rapidly induced by the addition of isopropyl- β -D-thiogalactoside (IPTG) which binds to the *lac* repressor protein and inactivates it. Once the *lac* repressor is inactivated, the host cell's RNA polymerase can transcribe the

sequences downstream from the promoter. The transcript product will be further translated to recombinant protein.

ORF of human p68 RNA helicase was subcloned in pET-30a⁺ vector (Novagen) by *Bam*HI/*Hind*III sites with 6xHis tag on the N-terminus (2.3.9). Single amino acid were mutated as DEAD → EEAD, RGLD → LGLD, HRIGR → HLIGR and Y593 → F as described in 2.3.12. Expression vectors verified by sequence were transformed in BL21-CodonPlus® (DE3)-RIL competent cells. Five individual colonies were cultured in small volume of LB media (2 ml) with 50 µM kanamycin for shaking at 37°C overnight. On the second day, 100 µl of bacteria culture were transferred to 2ml fresh media for further incubation of 1.5hr. 1mM final concentration of IPTG was added to culture media for induction for 4hrs at 37°C. 20 µl of bacteria culture before and after IPTG induction were collected and lyzed by protein loading dye. After remove debris by brief centrifuge, clear lysates were analyzed by SDS-PAGE gel followed by coomassie blue staining (2.4.6.1).

Colony with best induction ratio was selected for large amount of protein purification. 200 µl of same small bacteria culture was inoculated into 100 ml LB media for vicious shaking at 37°C overnight. The second day, 100 ml bacteria culture was transferred to 1 liter pre-warmed media with proper antibiotics. Until an absorbance of 0.8 at 600nm was obtained, 1 mM IPTG was added to culture for another 4hrs incubation. Bacteria were centrifuged 10,000rpm at 4°C for 10min. After washing with PBS, cell pellets were either stored at -80°C or continue performed protein purification.

Wet cell pellets were weighted suspended by lysis buffer (10 ml/1 g wet weight). Cell suspensions were supplemented with lysozyme (Novagen) to final concentration of 1mg/ml for incubation 30 min at 4°C. Brief sonication 6 x 20 s with 30 s pause at 200-300 W was used to break down DNA. The solution should be translucent after lysis. Clear the lysates by centrifuge at 10,000 x *g* at 4°C for 20–30 min.

All recombinant proteins were purified under naïve conditions by using imidazole. The imidazole ring is part of the structure of histidine in the 6xHis tag bind to the nickel ions immobilized by the NTA groups on the matrix. Endogenous proteins with histidine residues that interact with the Ni-NTA groups can be washed out of the matrix with stringent conditions achieved by adding imidazole at a 10–50 mM concentration. If the imidazole concentration is increased to 100–250 mM, the 6xHis-tagged proteins will also dissociate because they can no longer compete for binding sites on the Ni-NTA resin.

To binding tagged protein into Ni-NTA agarose column, Ni-NTA agarose was first packaged into disposable column and equilibrate by lysis buffer. Cleared cell lysates were applied to pre-equilibrated column and allow lysates pass through column by gravity. Columns were subsequently washed by wash buffer 4 ml for three times. For elution, 500 µl of elution buffer was applied to each column and collect the elute in five tubes and analyzed by SDS-PAGE (2.4.6.1).

Lysis buffer:	50 mM Tris-HCl (pH 7.5)
	300 mM NaCl
	10 mM imidazole

Wash buffer:	50 mM Tris-HCl (pH 7.5) 300 mM NaCl 20 mM imidazole
Elution buffer:	50 mM Tris-HCl (pH 7.5) 300 mM NaCl 250 mM imidazole

7.4.2 Determination of protein concentration

The amount of protein in cellular and tissue lysates was determined using Bio-Rad Protein Assay (Bio-Rad). 1 μ l of the samples diluted in 799 μ l of distilled water were combined with 200 μ l Bio-Rad 5x dye solution. Different BSA concentrations (2.0-10.0 μ g/ml) were used to generate a standard curve. After 5 min of incubation, the optical density was measured at a wavelength of 595 nm using a spectrophotometer (Shimadzu). The absorption values were calculated according standard curve.

7.4.3 Recombinant Protein Modification

7.4.3.1 Dephosphorylation

Bacterially expressed human p68 RNA helicase recombinant protein was discovered as phosphorylated on both serine/threonine and tyrosine residues (Yang and Liu 2004). To study the potential role of p68 phosphorylation in the mammalian cells, recombinant protein with phosphate group need to be removed. Protein phosphatases are enzymes that remove phosphate groups that have been attached to amino acid residues of proteins by protein kinases. There are two major groups of protein phosphatases,

serine/threonine specific protein phosphatases and tyrosine specific protein phosphatases, which remove phosphate group from relative amino acids.

Recombinant p68 was dephosphorylated by both Protein Phosphatase 2A (PP2A, serine/threonine specific protein phosphatase) and Protein Tyrosine Phosphatase 1B (PTP1B, tyrosine specific protein phosphatase). About 5 μ g recombinant protein was incubated with 4 U of phosphatase in the manufacture suggested condition buffer at 37°C for 90 min. The dephosphorylated protein was separated from the added protein phosphatases by Ni-NTA beads spin column (Active Motif). After extensive washes, the dephosphorylated protein was eluted with Elution Buffer. The protein was then micro-dialyzed against the Dialysis Buffer with 100 mM of imidazole (Pierce). After dialysis, dephosphorylated protein was concentrated by VIVAspin 500 (VIVAScience) for experiment or *in vitro* kinase assay to add phosphate group on tyrosine residues.

Dephosphorylation:	10X buffer	3 μ l
	Recombinant protein	5 μ g ~ 20 μ l
	PP2A/PTP1B	3 μ l
	Total volume	30 μ l
	H ₂ O	Add to 30 μ l

Elution buffer:	50 mM Tris-HCl (pH 7.5)
	300 mM NaCl
	250 mM imidazole

Dialysis buffer:	50 mM Tris-HCl (pH 7.5)
	300 mM NaCl
	20 mM imidazole
	10% Glycerol

7.4.3.2 Phosphorylation by c-Abl kinase

Exploring of cellular function of phosphor-p68 in the mammalian cells revealed that tyrosine phosphorylation of p68 plays a critical role in cell proliferation and tumor cells Epithelial-Mesenchymal Transition (EMT) (unpublished data). The tyrosine phosphorylation of p68 was added by tyrosine kinase c-Abl on residue Y593 (unpublished data). To generate Y593 tyrosine phosphorylated p68, dephosphorylated recombinant p68 was further incubated with recombinant active c-Abl protein kinase (Upstate) to gain phosphate group on tyrosine residue Y593. About 5 µg of recombinant p68 was incubated with c-Abl at 37°C for 30 min with 1 mM non-radioactive ATP. After the incubation, the reaction mixture underwent Ni-NTA beads spin column (Active Motif) to divide recombinant p68 with c-Abl. After extensive washes, the phosphorylated protein was eluted with Elution Buffer as described above. The protein was then microdialyzed against the Dialysis Buffer with 100 mM of imidazole (Pierce). After dialysis, phosphorylated protein was concentrated by VIVAspin 500 (VIVAScience) for either SDS-PAGE (2.4.6.1) to confirm tyrosine phosphorylation or further experiments.

Phosphorylation:	10X buffer	1 µl
	Recombinant protein	5 µg ~ 5 µl
	c-Abl	1 µl
	Total volume	10 µl
	H ₂ O	Add to 10 µl

7.4.4 Generation of anti-p68 antibody

Recombinant C-terminal domain (a.a.437-614) of human p68 RNA helicase (GenBank™/EBI Data Bank accession number [NM_004396](#)) purified from *E. coli* by

6xHis tag was used to immunize either rabbits (Invitrogen) or mouse (Auburn hypoderma facility).

7.4.5 Preparation of Lysates

7.4.5.1 Whole Cell Lysates

Cells were grown and transfected as described (2.6 & 2.7). For harvesting, cells were washed twice with ice-cold PBS. PBS was removed by a pipette tip attached to a vacuum line. Cells were scraped off from the culture dishes using a rubber policeman and PBS (1 ml/10 cm dish) supplemented with protease inhibitor cocktail (1:1000 dilutions, Sigma). Subsequently, cells were spun down at 4°C for 3000 rpm for 5 min. Cell pellets were resuspended by 1XRIPA buffer (Upstate, supplemented with 1mM NaF, 1mM PMSF, 1mM NaSOV₃ and 1:100 dilution of protease inhibitor cocktail) and rotated at 4°C for 60 min. To remove cellular debris, lysates were centrifuged (15,000 x g, 10 min at 4°C) and the supernatants were stored at -80°C until use. Protein concentrations were determined by Bio-Rad protein assay (2.4.2).

7.4.5.2 Tissue Lysates

Frozen patient tissue specimens were obtained from Southern Division, Cooperative Human Tissue Network (Birmingham, AL). Tissue specimens (200 ~ 300mg) were weighed and diced into very small pieces using a clean razor blade. Collected pieces in a pre-chilled 1.5 ml micro-centrifuge tube were disrupted and homogenized in 3 ml ice-cold 1XRIPA buffer (as described above) per gram of tissue

with a dounce homogenizer. After gently homogenize for 10 stroke, the mixture were further rotated at 4°C for 60 min. Temperature was maintained at 4°C throughout all procedures. To remove debris, probes were centrifuged at 10,000 x g for 10 minutes at 4°C. Clear supernatants were transferred to new pre-chilled tubes and stored at -80°C till use.

7.4.4.3 Preparation of Nucleic Extraction

Nucleic Extraction Kit (Active Motif) was used to prepare nucleic extraction for all experiments according to manufacture's instruction. Cells were treated as described (2.6 & 2.7) in a 100 mm tissue culture dish. First, the cells were collected in ice-cold PBS in the presence of phosphatase inhibitors (Sigma) to limit further protein modifications (expression, proteolysis, dephosphorylation, etc.). Then, the cells were resuspended in hypotonic buffer to swell the cell membrane and make it fragile. Addition of the Detergent caused leakage of the cytoplasmic proteins into the supernatant. After collection of the cytoplasmic fraction by brief centrifuge (5000 rpm for 10 min at 4°C), the nuclei were lysed by Complete Lysis Buffer (supplemented with 1mM DTT and 1:100 dilution of protease inhibitor) and the nuclear proteins were stored at -80°C till use.

7.4.6 Western Blotting Analysis

7.4.6.1 SDS gel electrophoresis

Electrophoretic separation of proteins was carried out in the discontinuous buffer system for SDS polyacrylamide gels as originally described by Laemmli (1970). SDS-

PAGE stands for sodium dodecyl (lauryl) sulfate-polyacrylamide gel electrophoresis. SDS is an anionic detergent that binds quantitatively to proteins, giving them linearity and uniform charge, so that they can be separated solely on the basis of their size. The polyacrylamide gel electrophoresis works in a similar fashion to an agarose gel, separating protein molecules according to their size. 50 µg of total protein sample were denatured in 2x SDS loading buffer (MBI Fermentas). After heating for 5 min at 95°C, samples were loaded on the gel. Subsequently, the gel was run at a current of 30 mA for a period of 2-3 hours. To observe protein bands on the polyacrylamide gel, the gel was either transferred to nitrocellulose (2.4.5.2) or fixed and stained by coomassie brilliant blue Staining buffer for 5 min under gentle shaking, followed by washing with destain buffer overnight. The destained gels were analyzed by UVP BioImaging and Analysis System (Upland).

Coomassie Stain buffer: (500 ml)	0.5 g Coomassie Blue 225 ml Methanol 225 ml ddH ₂ O 50 ml Acetic Acid
Destain buffer: (1 Liter)	70 ml Acetic Acid 50 ml Methanol 880 ml ddH ₂ O

7.4.6.2 Transfer to Nitrocellulose

Transferring protein from SDS gel to nitrocellulose facilitates exposing probes to antibodies for detection. After electrophoresis, gel was removed from electrophoresis apparatus and rinsed in transfer buffer. Gel was placed on a sheet of Whatman 3MM

paper pre-wetted in transfer buffer. A layer of nitrocellulose membrane (Piece, first wetted in transfer buffer) was applied on the top of the gel. Air bubbles were squeezed out by a roller apparatus. Membrane was with another layer of pre-wetted Whatman 3MM paper and placed in a blotting sandwich assembly (Owl). The assembly was immersed in a blot cell filled with transfer buffer, making certain that the membrane side faces the positive electrode and the gel faces the negative electrode. Transfer of proteins was carried out at 120 mA current at room temperature and terminated after 120 min. After blotting, the membrane was checked by Ponceau S staining for correct electrophoretic transfer and equal loading.

Transfer Buffer:	0.192 M Glycine
	25 mM Tris
	20% Methanol

7.4.6.3 Immunoblotting

The transferred nitrocellulose membrane was rinsed in 1x TBST (1x TBS + 0.1% Tween-20) buffer briefly. Non-specific binding sites were blocked by shaking the membrane in a 1x TBST-buffered 5% BSA for 1 h at room temperature or overnight at 4°C. The membrane was subsequently exposed to primary antibodies (diluted 1:500–1:2000 in 1x TBST buffer) specific for the protein of interest for incubation at 4°C for overnight. The blot was washed three times for 5 min in 1x TBST. The primary antibody was detected by incubation of the membrane with a specific secondary antibody coupled to horseradish peroxidase (diluted 1:5000 in 1x TBST) for 90 min at room temperature. For detection of the corresponding bands, SuperSignal[®]

West Dura Extended Duration Substrate (Piece) was used according to the instructions of the manufacturer. The membrane was exposed and analyzed using the UVP BioImaging and analysis System (Upland).

7.4.7 Immunoprecipitation

Immunoprecipitation (IP) followed by SDS-PAGE and immunoblotting, is routinely used in a variety of applications: to determine the molecular weights of protein antigens, to study protein-protein interactions, to determine specific enzymatic activity, to monitor protein post-translational modifications and to determine the presence and quantity of proteins. In the IP method, the protein from the cell or tissue homogenate is precipitated in an appropriate lysis buffer by means of an immune complex which includes the antigen (protein), primary antibody and Protein A-, G-, or L-agarose conjugate or a secondary antibody-agarose conjugate. The choice of agarose conjugate depends on the species origin and isotypes of the primary antibody.

500 ng to 1 mg whole cell lysates, tissue lysates or nucleic extracts were diluted by 1x RIPA buffer supplemented as described above (2.4.5) to 500 μ l. 1-3 μ g of primary antibody were used to capture interesting protein. After gentle rotation at 4°C for overnight, 40 μ l of 50 % protein G agarose conjugate slurry was added to the mixture for further incubation of 1.5hr. After extensive wash, proteins captured by agarose were eluted and denatured by SDS loading dye (MBI Fermentas) followed by SDS-PAGE and western blotting (2.4.6) to detect precipitated and co-immunoprecipitated proteins.

7.4.8 Kinase Assay

7.4.8.1 Peptide Kinase Assay

To examine phosphorylation site of interesting protein by specific kinase, peptide including potential phosphorylation site(s) were generated and peptide kinase assay were used to study the possibility of phosphorylation by identified kinase. To examine phosphorylation of IRAK peptides (synthesized by the Macromolecular Structure Facility, University of Kentucky) by aPKC, a peptide kinase assay was employed. Each reaction contained 1 μg of synthesized IRAK peptide control or mutant in 50 μl peptide kinase buffer (list below) with or without 100 ng purified aPKC (CalbioChem) and 1 μCi of [γ - ^{32}P] ATP for 10 min at 30°C. The reaction was stopped by adding 280 mM H_3PO_4 and spotted onto P81 paper followed by washing in 75 mM H_3PO_4 three times. Radioactivity was counted using Cerenkov.

Peptide Kinase Buffer:	15 mM PIPES pH 7.5
	1 mM EDTA
	20 mM MgCl_2
	0.04 mg/ml phosphatidylserine

7.4.8.2 *In Vitro* Kinase Assay

To further confirm the phosphorylation site(s) of IRAK phosphorylated by aPKC, an *in vitro* kinase assay were performed. Purified IRAK protein (50 ng) and purified aPKC (CalbioChem) (1, 100, 200, 300 ng) were incubated in 20 μl of kinase buffer with 5 μCi of [γ - ^{32}P] ATP for 20 min at 30°C. Reactions were stopped by adding of 20 μl of

SDS loading dye and boiling for 2 min followed by 10% SDS-PAGE and autoradiography. The program QuantiScan was used to scan and analyze the blots.

Kinase Buffer:	20 mM Tris, pH 7.6
	1 mM DTT
	20 mM MgCl ₂
	20 mM <i>p</i> - nitrophenyl phosphate
	1 mM EDTA
	1 mM NaVO ₃
	1 mM PMSF

7.4.8.3 Endogenous Kinase Assay

To examine IRAK auto-phosphorylation and trans-phosphorylation ability by co-expressed aPKC, an endogenous kinase assay was employed. Transfected HEK cells were lysed in PD buffer (list below) and IRAK was captured by immunoprecipitation of 750 µg cell lysates with anti-Myc polyclonal antibody. The beads were washed three times in PD buffer followed by the addition of 30 µl of kinase buffer (as described above) and 5 µCi of [γ -³²P] ATP for 20 min at 30°C. 20 µl of SDS loading buffer was added to the samples to stop the reaction and the reaction was separated by 10% SDS-PAGE and exposed to x-ray film. Aliquots of the whole cell lysates were blotted with anti-GST and anti-Myc to validate expression of iota PKC and IRAK.

PD Buffer:	40 mM Tris, pH 7.6
	500 mM NaCl
	0.1% Nonidet P-40
	6 mM EDTA
	6 mM EGTA
	10 mM β -glycerophosphate

10 mM NaF
10 mM *p*- nitrophenyl phosphate
300 μ M NaOV₃
1 mM DTT
2 μ M PMSF
10 μ g/ml aprotinin
1 μ g/ml leupeptin

7.4.8.4 Immune Complex Kinase Assay

To detect the activity of IRAK enzyme, anti-Myc immunoprecipitates (capturing expressed His/Myc-tagged IRAK) was incubated with 20 μ l of kinase buffer (as described above) with 5 μ Ci of [γ -³²P] ATP and 5 mg of MBP for 10 min at 37°C. 20 μ l of SDS loading buffer was added to the samples to stop the reaction. Phosphorylated MBP was analyzed by 10% SDS-PAGE and autoradiography. Changes in IRAK activity were monitored as a function of the enzyme's ability to phosphorylate MBP as determined by phosphorimaging analysis.

7.4.9 Chromatin Immunoprecipitation (ChIP)

Chromatin Immunoprecipitation (ChIP) is a powerful tool for the study of protein-DNA interactions (Solomon, Larsen et al. 1988). In this method, intact cells are fixed using formaldehyde, which cross-links and preserves protein-DNA interactions. The DNA is then sheared into small, uniform fragments using either sonication or enzymatic digestion and specific protein/DNA complexes are immunoprecipitated using an antibody directed against the DNA-binding protein of interest. Following immunoprecipitation, cross-linking is reversed, the proteins are removed by treatment

with proteinase K and the DNA is purified. The DNA is then analyzed to determine which DNA fragments were bound by the protein of interest.

HT-29 or SW620 cells were treated as indicated (2.7) in 6-well plates. Post 48 to 72 hr transfection, cell media were removed and cells were fixed with 3.7% formaldehyde in complete culture media at room temperature for 10 min. after washing briefly with ice-cold PBS, fixation was stopped by 1x glycine stop buffer at room temperature for 5 min. cells were collected in micro-centrifuge tube by scrapping followed by centrifuge at 4°C for 10 min. cell pellets were either frozen at -80°C or resuspended with 200 µl ice-cold 1x lysis buffer supplemented with 1 µl protease inhibitor cocktail and 1 µl PMSF. After incubate on ice for 30 min, the swollen cells were gently dounced 10 stroke by homogenizer to help release of nuclei. Nuclei were collected by spin at 4°C 5000 rpm for 10 min and resuspended with 350 µl shearing buffer. Chromatins were broken down to small pieced by sonication in ice at 25% output for 10 X 10 sec pulse and 20 sec off. After centrifuge at 4°C for 10 min to remove debris, 50 µl of chromatin were aliquoted for pre-clear to remove background. Other aliquots were stored at -80°C for future experiments. 50 µl chromatins were combined with ChIP buffer and protein G beads for incubate at 4C for 1.5hr to remove non-specific binding. After brief spin to remove beads, supernatants were incubated with primary antibody of interest at 4°C for overnight. 100 µl of protein G agarose were used to capture protein/DNA complex. After extensive wash, protein/DNA complexes were eluted from agarose by 1% SDS. The crosslinks were reversed by incubation with 200

mM NaCl at 65°C for overnight. Protein and RNA molecule were removed by RNase A and Protease K treatment. After clean-up and concentrate, chromatins were amplified by PCR using primers targeting interesting regions.

7.5 Ribonucleic Acid Techniques

7.5.1 *In Vitro* Transcription

Radio-labeled and non-isotopically labeled RNA probes, generated in small scale transcription reactions, can be used in blot hybridizations and nuclease protection assays. Small scale reactions may also be used for structure analysis (protein-RNA binding), function analysis (exon splicing) and mechanistic studies (spliceosome analyses). The common RNA polymerases used in *in vitro* transcription reactions are SP6, T7 and T3 polymerases, named for the bacteriophages from which they were cloned. RNA polymerases are DNA template-dependent with distinct and very specific promoter sequence requirements. Depending on the orientation of cDNA sequence relative to the promoter, the template may be designed to produce sense strand or anti-sense strand RNA.

RNAs were synthesized by run-off transcriptions of the linearized transcription vectors that carry appropriate DNA inserts in the transcription region using T7 or SP6 RNA polymerase. The recombinant plasmids (see table below) were linearized with restriction enzymes, phenol/chloroform extracted, precipitated and dissolved in RNase free H₂O to a final concentration of 1 µg/µl. The RNAs were uniformly labeled with [α -

^{32}P] UTP. For the reaction, $\sim 1 \mu\text{g}$ of DNA template were incubated with transcription buffer containing 20 mM Tris-HCl, pH 7.5, 200 mM NaCl, 1 mM MgCl_2 , 5 mM DTT, RNA polymerase, NTP and $[\alpha\text{-}^{32}\text{P}]\text{UTP}$ at 30°C for 90 min. Reaction products were passed through Sephadex[®] G-50 column to remove uncoupled UTP. Synthesized RNA concentration was determined by scintillation counting. The DNA vectors for transcribing each RNA substrate are listed in **Table 3**.

<i>In Vitro</i> Transcription:	5x transcription buffer	4 μl
	NTPs (ATP, CTP, GTP; each 3 mM)	2 μl
	100 mM DTT	1 μl
	Cap-analog	1.4 μl
	RNasein (40 U/ μl)	0.4 μl
	$[\alpha\text{-}^{32}\text{P}]\text{UTP}$ (800 Ci/mM)	2 μl
	Linerized template (1 $\mu\text{g}/\mu\text{l}$)	6 μl
	RNA polymerase	2.5 μl
	RNase Free H_2O	Add to 20 μl

7.5.2 Formation of Double-Strand RNA

The partial dsRNAs were prepared by annealing each pair of complementary transcripts at a 3-fold excess of unlabeled strand over labeled strand. The dsRNA substrate for both ATPase assays and RNA binding assays is the hybridization of equal molar amounts of two complementary strands. Annealing solution contained 30 mM Tris-HCl, pH 7.5, 100 mM NaCl and 80% formamide. The RNA annealing mixture was heated to 85°C for 10 min and was then slowly cooled down to room temperature. The RNA hybrids were used without further treatments.

7.5.3 ATPase Assay

ATPase activities were determined by measuring the released inorganic phosphate during ATP hydrolysis using a direct colorimetric assay (Chan, Delfert et al. 1986) (Pugh, Nicol et al. 1999). The method is based on the change in absorbance ($A_{623\text{ nm}}$) of malachite green-molybdenum complex in the presence and absence of inorganic phosphate. An improved procedure for phosphate determination based on a highly colored complex of phosphomolybdate and malachite green in the presence of 6 N acid. The time of color development at 25°C is about 3 min. A typical ATPase assay was carried out in 50- μ l reaction volumes, containing 20 mM Tris-HCl, pH 7.5, 200 mM NaCl, 1 mM MgCl_2 , 5 mM DTT, ~1-2 μ g of appropriate RNA, 40 units of RNasin (Fisher Scientific), 4 mM NTP and 10 μ l of recombinant helicase protein. The ATPase reactions were incubated at 37 °C for 30 min. After incubation, 1 ml of malachite green-molybdenum reagent was added to the reaction mixture and reactions were further incubated at room temperature for exactly 5 min. The absorption (A) at 630 nm was then measured. The concentrations of inorganic phosphate were determined by matching the $A_{630\text{ nm}}$ in a standard curve of $A_{630\text{ nm}}$ versus known phosphate concentrations.

ATPase assay:	2 M Tris, pH 7.6	0.5 μ l
	3 M NaCl	3.3 μ l
	25 mM DTT	2.5 μ l
	100 mM DTT	1 μ l
	RNasein (40 U/ μ l)	0.7 μ l
	100 mM ATP	1 μ l
	ssRNA	2.2 μ l
	Recombinant p68 (~1 μ g)	10 μ l
	RNase Free H_2O	Add to 50 μ l

7.5.4 RNA Binding Assay

RNA bindings were analyzed by gel-mobility shift assays and Methylene Blue (MB)-mediated dsRNA-protein cross-linking (Liu, Wilkie et al. 1996) (Liu, Laggerbauer et al. 1997). In a typical gel mobility shift assay, 100 ng of recombinant proteins were mixed with 5 fmol of appropriate RNA in buffer solution containing 30 mM Tris-HCl, pH 7.5, 100 mM NaCl, 2 mM MgCl₂, 1 mM DTT and 20 units of RNasin with or without ATP as indicated. After 15 min of incubation at room temperature, the reaction mixtures were loaded on to 6% native-PAGE (acrylamide:bis = 40:1). The methylene blue mediated cross-linkings were carried out as described previously (Liu, Wilkie et al. 1996) (Liu, Sargueil et al. 1998). The same protein:RNA reaction mixtures used in the gel mobility shift assays were used in the cross-linking experiments. After RNase mixture (RNase A, T1 and V1) digestion, the cross-linking mixture was separated by the appropriate percentage of SDS-PAGE and subjected to autoradiography.

RNA Binding Assay:	5x binding buffer	4 µl
	dsRNA (5 ng)	8 µl
	Recombinant p68 (~20 ng)	5 µl
	2 mM ATP	2 µl
	RNasein (40 U/µl)	0.2 µl
	RNase Free H ₂ O	Add to 20 µl

7.5.5 RNA Unwinding Assay

RNA unwinding activities were determined by the method similar to that described by Rozen and co-workers (Rozen, Edery et al. 1990). Briefly, the RNA unwinding reactions were carried out in a 20 µl reaction volume containing 70 mM Tris-

HCl, pH 7.5, 200 mM NaCl, 1 mM MgCl₂, 5 mM DTT, 2.5 fmol of partial dsRNA, 40 units of RNasin, 16 mM ATP and 2-4 µl of helicase. Reactions were incubated at 37 °C for 60 min. The reaction mixtures were directly loaded onto the appropriate percentage of SDS-PAGE and the gel was subjected to autoradiography.

<i>In Vitro</i> Transcription:	2 M Tris, pH 7.6	0.7 µl
	3 M NaCl	1.3 µl
	25 mM MgCl ₂	0.8 µl
	100 mM DTT	1 µl
	RNasein (40 U/µl)	1 µl
	100 mM ATP	3.2 µl
	dsRNA (~2.5 fmol)	6 µl
	Recombinant p68 (100 ng)	4 µl
	RNase Free H ₂ O	Add to 20 µl

7.5.6 The Pre-mRNA Splicing Assay

Extract from nuclei is required in studying the pre-mRNA splicing and spliceosome complex assembly *in vitro*. HeLa nuclear extract was prepared as described in previous reports (Dignam, Lebovitz et al. 1983; Krainer, Maniatis et al. 1984; Liu, Sargueil et al. 1998) with modification (Abmayr, Workman et al. 1988). The procedure for the nuclear protein extraction method is to allow cells to swell with hypotonic buffer. The cells are then disrupted, the cytoplasmic fraction is removed and the nuclear proteins are released from the nuclei by a high salt buffer. Briefly, 1 liter of HeLa cell suspension culture was collected by spin down and washed twice by PBS. Cell pellets were resuspended by hypotonic lysis buffer (10mM HEPES, pH 7.9, 15 mM MgCl₂ and 100 mM KCl₂) on ice for 15 min to allow cell swell. To the swollen cells in lysis buffer, 10%

IGEPAL CA-620 solution was added to a final concentration of 0.6%. The mixture was vortex vigorously for 10 sec and centrifuged immediately at 10,000g for 30 sec to collect nuclei. The supernatant was transferred to fresh tube as cytoplasmic fraction. Nuclei pellets were resuspended with extraction buffer (20mM HEPES, pH 7.9, 1.5mM MgCl₂, 0.42 M NaCl, 0.2 mM EDTA and 25% Glycerol) for incubation at 4°C for 60 min. After removing debris, the nucleic extract was aliquot and stored at -80°C.

The antibody, PAb204 or PAbN1, was used to remove endogenous p68 from HeLa nuclear extract. To gain better depletion results, the salt concentration of the HeLa nuclear extracts was raised to 600 mM NaCl before addition of antibody. After 3 h of incubation at 4°C, the mixtures were passed through a protein G or protein A agarose bead column. The column fractions were analyzed by SDS-PAGE. The fractions that contained the most proteins were collected together and dialyzed against buffer E (20 mM Tris-HCl pH 7.5, 50 mM NaCl, 0.3 mM EDTA pH 8.0 and 15% glycerol) twice for six hours. The recovered p68-depleted HeLa nuclear extracts were used in other *in vitro* assays.

Splicing reactions were carried out with pPIP10A in 40% HeLa nuclear extracts or p68 depleted-HeLa nuclear p68 RNA helicase was depleted from the nuclear extracts by the experimental procedure that was described in our previous report (Liu 2002). To reconstitute the splicing activity, the phosphorylated/dephosphorylated his-tag protein was added to the p68-depleted nuclear extracts to a final concentration of ~20 ng/μl. The mixture was incubated at 30°C for 15 min. About 25 fmol of pre-mRNA pPIP10A was

then added to the 10 μ l of pre-incubated extracts and the splicing reaction was incubated at 30°C for an additional 150 min or time points as indicated. The splicing products were analyzed by 12% urea-PAGE.

Pre-mRNA Splicing Assay:	100 mM ATP	0.8 μ l
	Creatine Phosphate	0.8 μ l
	100 mM DTT	1 μ l
	RNasin (40 U/ml)	0.2 μ l
	Pre-labeled RNA (~25 fmol)	1.2 μ l
	HeLa nucleic extract	8 μ l
	RNase Free H ₂ O	Add to 20 μ l

7.5.7 Trioxsalen Crosslinking Assay

For the trioxsalen cross-linking, splicing reactions were performed with pPIP10A in 30% HeLa nuclear extracts for the indicated times. The stock solution of trioxsalen (5 mg/ml dissolved in dimethyl sulfoxide) was added to the reactions to a final concentration of 15 μ g/ml. The reaction mixtures were placed on ice and photolyzed with a UV cross-linker containing four 15 W, 282-nm (maximum) UV bulbs for 12 min. The reaction mixtures were then treated with proteinase K and phenol-chloroform extraction. The RNAs were precipitated by ethanol. To identify the trioxsalen cross-linked RNA species, the precipitated RNAs were redissolved in 40 μ l of RNase H reaction buffer. Five micromoles of the DNA oligonucleotide α U1₆₄₋₇₅ or unspecific oligonucleotide Actin- β and RNase H were added to the solution. The mixture was incubated at 30°C for 30 min. The products were treated with phenol-chloroform extraction and subsequent ethanol

precipitation. The final RNAs were analyzed by denatured urea-6% PAGE and subjected to autoradiography.

7.5.8 Methylene Blue Crosslinking Assay

To study RNA-protein interactions, an alternative RNA-protein photo-crosslinking method was developed to efficiently induces RNA-protein crosslinks in double-stranded regions of RNA (Liu, Wilkie et al. 1996). Recombinant human p68 RNA helicase and dsRNA binding substrate were crosslinked by methylene blue (MB).

Methylene blue crosslinking experiments were carried out as described in the previous report (Liu, Sargueil et al. 1998). Appropriate amounts of RNAs (~5 ng) were mixed with 100-150 ng of proteins (or appropriate percentage of HeLa nuclear extract and protein mixture) in a total volume of 10 μ l. Methylene blue was added into the solution to 0.2-1 ng/ μ l. after a short incubation at room temperature, the mixture was placed in a micro-titer plate. The plates was then placed 4-5 cm below a 60 W fluorescent tube light. The crosslinking was conducted on ice for 20 min. The mixture was then digested with RNase A (1 mg/ml), RNase T1 (0.3 U/ml) and RNase V1 (0.035 U/ml), at 37C for 20 min. Crosslinking results were analyzed by electrophoresis on 10% SDS gel followed by autoradiography and coomassie blue staining.

7.5.9 The Spliceosome Complex Assembly

For assembly of the spliceosome complexes, splicing reactions were performed with pPIP10A in 20 – 25% intact HeLa nuclear extracts or the reconstituted nuclear extracts (described in the above 2.5.6). After incubation for 30 minutes, heparin was added to the reaction mixture to a final concentration of 0.5 mg/ml. The reactions were incubated at 30°C for an additional 5 minutes. The reaction products were analyzed by 4% (80:1 acrylamide:bis-acrylamide) native PAGE. The gel was subjected to autoradiography.

7.5.10 RNA Isolation

Total RNA from mammalian cell culture was isolated by using RNeasy[®] Mini kit (Qiagen) according to manufacture's instruction. To isolate RNA, mammalian cells were grown to 80-90% confluence in 100 mm cell-culture dish. Cells were directly lysed and homogenized in the presence of a highly denaturing guanidine isothiocyanate (GITC)-containing buffer, which immediately inactivates RNases to ensure isolation of intact RNA. Cell lysates were applied to mini column for binding. RNAs were bound to a selective binding silica-gel-based membrane. Contaminants were efficiently washed away by high-salt buffer. After remove extra ethanol, high-quality RNA is then eluted in 30 µl of DEPC-treated water.

7.5.11 Reverse Transcriptase PCR (RT-PCR)

RT-PCR is the most sensitive technique to determine the mere presence or relative quantity of specific RNA templates, e.g. in gene expression studies. In two-step RT-PCR, reverse transcription of RNA into cDNA is performed prior to amplification of cDNA by PCR in a separate reaction. RT-PCR reactions were performed with 1 µg of total RNA using One Step RT-PCR kit (Roche, Titan kit) by following the manufacturer's instruction. RT-PCR results were analyzed on a 2% agarose gel. Quantization of RT-PCR products were carried out by scanning the image of the agarose gel using LabWork Image Acquisition and Analysis System. The primers for all RT-PCR or PCR reactions are listed in **Table 4**.

7.5.12 RNA Immunoprecipitation

RNA immunoprecipitation (RNA-IP) was performed using essentially the same procedure as described by Gilbert and colleagues (Gilbert, Kristjuhan et al. 2004). Briefly, 48 hours post transfection (indicated), HT-29 cells were fixed in 1% formaldehyde for 30 minutes at room temperature. The cells were lysed in ChIP lysis buffer (Active motif) containing RNase inhibitor (50 U/500 µl). The cell nuclei were released by homogenization. The collected nuclei were further lysed by FA buffer (50 mM HEPES-KOH [pH 7.5], 140 mM NaCl, 1 mM EDTA, 1% Triton X-100, 0.1% sodium deoxycholate, protease inhibitors) containing RNase inhibitor. The resultant samples were treated by extensive sonication followed by treatment with RNase-free

DNase I at 37°C for 30 minutes. Immunoprecipitation using anti-HA antibody (Upstate) was carried out with the samples. The immunoprecipitates were adjusted to 200 mM NaCl and incubated at 65 °C overnight. The samples were further treated with 20 µg protease K and phenol: chloroform extraction followed by ethanol precipitation at -80°C. RT-PCR (as described above) was performed using 1/100 RNA of precipitates or 1/2000 RNA of input. RT-PCR results were analyzed on a 2% agarose gel.

7.6 Cell Culture

PC12, HEK, HeLa S3, HT-29, SW480 cells and SW620 cells were purchased from ATCC and were grown in Dulbecco's modified Eagle's medium, McCoy's 5A modified medium and Leibovitz's L-15 Medium respectively supplemented with 10% Fetal Bovine Serum, penicillin (100 U/ml) and streptomycin (100 µg/ml). IRAK⁻ deficient I1A cells were obtained as a gift from Dr. Xiaoxia Li, Lerner Research Institute and cultured in Dulbecco's modified Eagle's medium.

7.7 Transfection

7.7.1 Plasmid Transfection

Subconfluent IRAK-deficient I1A cells were transfected with His/Myc mPLK/IRAK and/or GST-aPKC active/inactive plasmids employing the Mammalian Cell Transfection kit (Cell & Molecular Technologies). All other plasmids and cells lines were transfected with LipofectamineTM 2000 (Invitrogen) according to manufacture's

instruction. A typical transfection was performed using the following procedure to transfect DNA into the mammalian cells in a 6-well format. For other formats, transfection mixture was prepared as scaled up or down. One day before transfection, cells were plated $2-5 \times 10^5$ cells in 2 ml of growth medium without antibiotics so that cells will be 90-95% confluent at the time of transfection. DNA was diluted in 250 μ l of pre-warmed Opti-MEM[®] I Reduced Serum Medium without serum (or other medium without serum) and mixed gently. Lipofectamine[™] 2000 was diluted in 250 μ l of Opti-MEM[®] I Medium for incubation for 5 minutes at room temperature. After the 5 minute incubation, diluted DNA was combined with diluted Lipofectamine[™] 2000 (total volume = 500 μ l) for gently mix and incubation for 20 minutes at room temperature. After incubation, the 500 μ l of complex was added to each well containing cells and complete medium. Fresh medium were changed after incubating cells at 37°C in a CO₂ incubator for 4-6 hours. Post transfection 48-72 hours, cells were treated or harvest for analysis.

7.7.2 siRNA Transfection

For all siRNA experiment, Lipofectamine[™] 2000 was used as transfection reagent employing similar procedure. Cells were grown to 50% confluence and transfected with siRNA (100 pM) mixed with 5 μ l of Lipofectamine[™] 2000. The duplex RNA oligonucleotides for targeting p68 RNA helicase were purchased from Dharmacon siGENOME[™] and SMARTpool[®]. For transient expression of p68 wild-type or mutants in p68 knock down cells, four nucleotides in the siRNA targeting sequence were mutated

to avoid RNAi targeting. The mutations did not change the amino acid sequence. The cells were transfected with the indicated plasmid DNA 24 hours after the cells were transfected with duplex siRNA and harvested after additional 48 hours incubation. The cell extracts were prepared immediately after harvest.

7.7.3 Protein Transfection

Chariot™ was used as transfection reagent to deliver proteins, peptides and antibodies into cultured mammalian cells. Chariot form a non-covalent complex with the protein, peptide or antibody of interest. The Chariot-macromolecule complex stabilizes the macromolecule and helps to protect it from degradation during the transfection process. Upon internalization, the complex dissociates and the macromolecule is free to proceed to its target organelle.

To transfect protein, 40-50% confluent cells were seeded into 6-well plates with complete medium before the day of transfection. 0.5-1 µg of protein or 1/1000 dilution of antibodies were mixed with PBS. 6 µl of Chariot™ was diluted by sterile water. The two dilutions were combined and incubated at room temperature for 30 min. After incubation, the mixture was applied to cells with 400 µl of serum-free media. 1 ml of complete media was added to cells after 1 hr. Post transfection 2 hrs, cells were harvested and analyzed.

7.8 Establish Stable Cell lines

Stable overexpression of HA-tag p68 wild-type or Y593F mutant was carried out using the ViralPower lentiviral expression system (Invitrogen) by following the manufacturer's instructions. The ORFs of p68 wild type or Y593F mutant with N-terminal HA-tag were cloned into pLenti6/TOPO (Invitrogen) plasmid. The infections of SW620/SW480 cells with the lentiviruses that carry pLenti6-p68 were carried out in the presence of 6 $\mu\text{g/mL}$ of polybrene and 10 mM HEPES. Following transduction, the SW620/SW480 cells were selected by 8 $\mu\text{g/ml}$ of Blasticidin (Invitrogen). Individual colonies were picked up and cultured separately. Cultured colonies were screened by western blotting using anti-HA antibody to detect exogenous p68 expression. The colony with highest expression level was amplified and used for experiments.

7.9 Reporter Gene Assay

7.9.1 Dual Reporter Gene Assay

Before cells were appropriately treated (indicated in figures), cells were transfected with 1 μg of the indicated reporter plasmid and 0.01 μg of pRL null, which expresses Renilla luciferase from Renilla reniformis as an internal control. The total amount of plasmid DNA was adjusted with pcDNA3- β -Galactosidase. Firefly and Renilla luciferase activities present in cellular lysates were assayed using the Dual-Luciferase Reporter System (Promega). Light emission was measured using a Sirius Luminometer (Berthold Technologies). Data were represented as Firefly luciferase activity normalized

by Renilla luciferase activity. The values plotted were the average \pm S.E. of triplicate samples from typical experiments.

7.9.2 Splicing Reporter Gene Assay

HT-29 cells were appropriately treated (indicated in figures). The cells were transfected with 0.5 μ g of reporter plasmid pTN23 (Nasim, Chowdhury et al. 2002) and 0.5 μ g of pHM6-p68 wt/mutant. The total amount of plasmid DNA was adjusted with pHM6-blank vector. Firefly luciferase and β -galactosidase activities present in cellular lysates were assayed using a Dual-light Reporter System (Biosystem). Light emission was measured using a Sirius Luminometer (Berthold Technologies). Data were represented as Firefly luciferase activity divided by β -galactosidase activity. The values plotted were the average \pm S.E. of triplicate samples from typical experiment.

7.10 HDAC Activity Assay

Inhibition of histone deacetylases (HDACs) has been implicated to modulate transcription and to induce apoptosis or differentiation in cancer cells. The First, the HDAC colorimetric substrate, which comprises an acetylated lysine side chain, is incubated with a sample containing HDAC activity. Deacetylation sensitizes the substrate and thus in the second step, treatment with the Lysine Developer produces a chromophore, which can be analyzed using a colorimetric plate reader.

SW620 cells were lysed in RIPA buffer (Upstate) 48 hr after transfection as described above. The lysate was then diluted in RIPA buffer and HA-tagged proteins immunoprecipitated with anti-HA polyclonal antibody (Upstate). HDAC activities were determined by HDAC Activity Colorimetric Assay Kit (BioVision) according to manufacturer's instructions. Antibody-bound beads were washed in HDAC assay buffer prior to being added to the 96-well plate, to remove immunoprecipitation buffer. Reactions were incubated for 30 min at 37°C with or without the addition of 1 μ M TSA. Samples were read in a VICTOR³™ plate reader (PerkinElmer) at 405 nm. Typically each assay was performed 3 times.

7.11 Immunostaining

The cells were seeded on chambered microslides (BD Biosciences) and treated as indicated. The cells were washed, fixed and permeabilized with 4% formaldehyde and 0.1% Triton X-100 in 1× PBS. The cells were then blocked with Image-iT™ FX signal enhancer (Molecular Probes) and subsequently incubated with appropriate antibodies for 1 hour. After extensive wash, the samples were incubated with Alexa Fluor 488 or 555 goat anti-mouse IgG (Molecular Probes) (1:1000) to stain primary antibodies. Microslides were washed and mounted in ProLong® Gold antifade reagent with DAPI (Molecular Probes) and viewed using a Zeiss LSM510 Confocal Microscop.

7.12 Invasive Assay

The cell invasion assays were performed with HT-29 cells expressing p68 wild-type or mutant using a BioCoat tumor invasion system by following the manufacturer's instructions (BD Biosciences). The invasion assays were carried out with cells with/without PDGF treatment (20 ng/ml). The invaded cells were stained with 4 μ g/ml Calcein, AM (Molecular Probes). The fluorescence of invaded cells was read in VICTOR³TM plate reader (PerkinElmer).

Table 3. Transcription Vectors Used in This Study.

RN A	Length nt	RNA polymeras e	Vector	Modifications	Digestio n
1	167	SP6	pGEM- 3Z	Delete the sequence between <i>EcoRI/HindIII</i>	<i>PvuII</i>
2	222	T7	pGEM- 3Z	Delete the sequence between <i>EcoRI/HindIII</i>	<i>PvuII</i>

Table 4: The RT-PCR Primers Used in this Study

Name	Sequence	Location
ActinF	CACGGCCGAGCGGGAAAT	Exon 4
Actin4R	CGGGAGACAGTCTCCAC	Intron 4
Actin5R	TGCATCCTGTCTGGCAATGC	Exon 5
GAPDHF	TGTTCCAATATGATTCCACCC	Exon 4
GAPDH4R	AAGGGAGCCACACCATCCT	Intron 4
GAPDH5R	CTTCTCCATGGTGGTGAAGA	Exon 5
CEBPF	AGCACACGACTTCCTCTC	
CEBPR	GGGTGCAGGGGCGCGAA	
HistoneF	CCAGTGTACCTGGCGGCA	
HistoneR	GTACTCCTGGGAGGCCTG	

REFERENCE

- Abmayr, S. M., J. L. Workman, et al. (1988). "The pseudorabies immediate early protein stimulates in vitro transcription by facilitating TFIID: promoter interactions." Genes Dev **2**(5): 542-53.
- Abovich, N. and M. Rosbash (1997). "Cross-intron bridging interactions in the yeast commitment complex are conserved in mammals." Cell **89**(3): 403-12.
- Akileswaran, L., J. W. Taraska, et al. (2001). "A-kinase-anchoring protein AKAP95 is targeted to the nuclear matrix and associates with p68 RNA helicase." J Biol Chem **276**(20): 17448-54.
- Alberga, A., J. L. Boulay, et al. (1991). "The snail gene required for mesoderm formation in Drosophila is expressed dynamically in derivatives of all three germ layers." Development **111**(4): 983-92.
- Alland, L., R. Muhle, et al. (1997). "Role for N-CoR and histone deacetylase in Sin3-mediated transcriptional repression." Nature **387**(6628): 49-55.
- An, Z., X. Wang, et al. (1998). "Surgical orthotopic implantation allows high lung and lymph node metastatic expression of human prostate carcinoma cell line PC-3 in nude mice." Prostate **34**(3): 169-74.
- Anzick, S. L., J. Kononen, et al. (1997). "AIB1, a steroid receptor coactivator amplified in breast and ovarian cancer." Science **277**(5328): 965-8.

- Arber, W. and D. Dussoix (1962). "Host specificity of DNA produced by Escherichia coli. I. Host controlled modification of bacteriophage lambda." J Mol Biol **5**: 18-36.
- Arias, A. M. (2001). "Epithelial mesenchymal interactions in cancer and development." Cell **105**(4): 425-31.
- Aslakson, C. J. and F. R. Miller (1992). "Selective events in the metastatic process defined by analysis of the sequential dissemination of subpopulations of a mouse mammary tumor." Cancer Res **52**(6): 1399-405.
- Auble, D. T., D. Wang, et al. (1997). "Molecular analysis of the SNF2/SWI2 protein family member MOT1, an ATP-driven enzyme that dissociates TATA-binding protein from DNA." Mol Cell Biol **17**(8): 4842-51.
- Bannister, A. J. and T. Kouzarides (2005). "Reversing histone methylation." Nature **436**(7054): 1103-6.
- Barcellos-Hoff, M. H. (2001). "It takes a tissue to make a tumor: epigenetics, cancer and the microenvironment." J Mammary Gland Biol Neoplasia **6**(2): 213-21.
- Bates, D. O. and R. O. Jones (2003). "The role of vascular endothelial growth factor in wound healing." Int J Low Extrem Wounds **2**(2): 107-20.
- Bates, G. J., S. M. Nicol, et al. (2005). "The DEAD box protein p68: a novel transcriptional coactivator of the p53 tumour suppressor." Embo J **24**(3): 543-53.
- Batlle, E., E. Sancho, et al. (2000). "The transcription factor snail is a repressor of E-cadherin gene expression in epithelial tumour cells." Nat Cell Biol **2**(2): 84-9.

- Benz, J., H. Trachsel, et al. (1999). "Crystal structure of the ATPase domain of translation initiation factor 4A from *Saccharomyces cerevisiae*--the prototype of the DEAD box protein family." Structure **7**(6): 671-9.
- Berx, G., A. M. Cleton-Jansen, et al. (1995). "E-cadherin is a tumour/invasion suppressor gene mutated in human lobular breast cancers." Embo J **14**(24): 6107-15.
- Birnboim, H. C. and J. Doly (1979). "A rapid alkaline extraction procedure for screening recombinant plasmid DNA." Nucleic Acids Res **7**(6): 1513-23.
- Bolos, V., H. Peinado, et al. (2003). "The transcription factor Slug represses E-cadherin expression and induces epithelial to mesenchymal transitions: a comparison with Snail and E47 repressors." J Cell Sci **116**(Pt 3): 499-511.
- Bouwmeester, T., A. Bauch, et al. (2004). "A physical and functional map of the human TNF-alpha/NF-kappa B signal transduction pathway." Nat Cell Biol **6**(2): 97-105.
- Bowen, N. J., N. Fujita, et al. (2004). "Mi-2/NuRD: multiple complexes for many purposes." Biochim Biophys Acta **1677**(1-3): 52-7.
- Brabant, G., C. Hoang-Vu, et al. (1993). "E-cadherin: a differentiation marker in thyroid malignancies." Cancer Res **53**(20): 4987-93.
- Bresalier, R. S., J. C. Byrd, et al. (1998). "Liver metastasis and adhesion to the sinusoidal endothelium by human colon cancer cells is related to mucin carbohydrate chain length." Int J Cancer **76**(4): 556-62.
- Bresalier, R. S., E. S. Hujanen, et al. (1987). "An animal model for colon cancer metastasis: establishment and characterization of murine cell lines with enhanced liver-metastasizing ability." Cancer Res **47**(5): 1398-406.

- Buelt, M. K., B. J. Glidden, et al. (1994). "Regulation of p68 RNA helicase by calmodulin and protein kinase C." J Biol Chem **269**(47): 29367-70.
- Burdsal, C. A., C. H. Damsky, et al. (1993). "The role of E-cadherin and integrins in mesoderm differentiation and migration at the mammalian primitive streak." Development **118**(3): 829-44.
- Buszczak, M. and A. C. Spradling (2006). "The Drosophila P68 RNA helicase regulates transcriptional deactivation by promoting RNA release from chromatin." Genes Dev **20**(8): 977-989.
- Cano, A., M. A. Perez-Moreno, et al. (2000). "The transcription factor snail controls epithelial-mesenchymal transitions by repressing E-cadherin expression." Nat Cell Biol **2**(2): 76-83.
- Carmel, A. B. and B. W. Matthews (2004). "Crystal structure of the BstDEAD N-terminal domain: a novel DEAD protein from Bacillus stearothermophilus." Rna **10**(1): 66-74.
- Caruthers, J. M., E. R. Johnson, et al. (2000). "Crystal structure of yeast initiation factor 4A, a DEAD-box RNA helicase." Proc Natl Acad Sci U S A **97**(24): 13080-5.
- Carver, E. A., R. Jiang, et al. (2001). "The mouse snail gene encodes a key regulator of the epithelial-mesenchymal transition." Mol Cell Biol **21**(23): 8184-8.
- Causevic, M., R. G. Hislop, et al. (2001). "Overexpression and poly-ubiquitylation of the DEAD-box RNA helicase p68 in colorectal tumours." Oncogene **20**(53): 7734-43.
- Chambers, A. F., A. C. Groom, et al. (2002). "Dissemination and growth of cancer cells in metastatic sites." Nat Rev Cancer **2**(8): 563-72.

- Chan, K. M., D. Delfert, et al. (1986). "A direct colorimetric assay for Ca^{2+} -stimulated ATPase activity." Anal Biochem **157**(2): 375-80.
- Chen, H., R. J. Lin, et al. (1997). "Nuclear receptor coactivator ACTR is a novel histone acetyltransferase and forms a multimeric activation complex with P/CAF and CBP/p300." Cell **90**(3): 569-80.
- Chen, J. Y., L. Stands, et al. (2001). "Specific alterations of U1-C protein or U1 small nuclear RNA can eliminate the requirement of Prp28p, an essential DEAD box splicing factor." Mol Cell **7**(1): 227-32.
- Chen, Y., Y. W. Ebright, et al. (1994). "Identification of the target of a transcription activator protein by protein-protein photocrosslinking." Science **265**(5168): 90-2.
- Christofori, G. and H. Semb (1999). "The role of the cell-adhesion molecule E-cadherin as a tumour-suppressor gene." Trends Biochem Sci **24**(2): 73-6.
- Chuang, R. Y., P. L. Weaver, et al. (1997). "Requirement of the DEAD-Box protein ded1p for messenger RNA translation." Science **275**(5305): 1468-71.
- Collins, C. A. and C. Guthrie (2000). "The question remains: is the spliceosome a ribozyme?" Nat Struct Biol **7**(10): 850-4.
- Comijn, J., G. Berx, et al. (2001). "The two-handed E box binding zinc finger protein SIP1 downregulates E-cadherin and induces invasion." Mol Cell **7**(6): 1267-78.
- Cote, J., J. Quinn, et al. (1994). "Stimulation of GAL4 derivative binding to nucleosomal DNA by the yeast SWI/SNF complex." Science **265**(5168): 53-60.
- Crawford, L., K. Leppard, et al. (1982). "Cellular proteins reactive with monoclonal antibodies directed against simian virus 40 T-antigen." J Virol **42**(2): 612-20.

- de la Cruz, J., D. Kressler, et al. (1999). "Unwinding RNA in *Saccharomyces cerevisiae*: DEAD-box proteins and related families." Trends Biochem Sci **24**(5): 192-8.
- Dignam, J. D., R. M. Lebovitz, et al. (1983). "Accurate transcription initiation by RNA polymerase II in a soluble extract from isolated mammalian nuclei." Nucleic Acids Res **11**(5): 1475-89.
- Dobosy, J. R. and E. U. Selker (2001). "Emerging connections between DNA methylation and histone acetylation." Cell Mol Life Sci **58**(5-6): 721-7.
- Dominguez, D., B. Montserrat-Sentis, et al. (2003). "Phosphorylation regulates the subcellular location and activity of the snail transcriptional repressor." Mol Cell Biol **23**(14): 5078-89.
- Drees, F., S. Pokutta, et al. (2005). "Alpha-catenin is a molecular switch that binds E-cadherin-beta-catenin and regulates actin-filament assembly." Cell **123**(5): 903-15.
- Duband, J. L., F. Monier, et al. (1995). "Epithelium-mesenchyme transition during neural crest development." Acta Anat (Basel) **154**(1): 63-78.
- Dubey, P., R. C. Hendrickson, et al. (1997). "The immunodominant antigen of an ultraviolet-induced regressor tumor is generated by a somatic point mutation in the DEAD box helicase p68." J Exp Med **185**(4): 695-705.
- Durrin, L. K., R. K. Mann, et al. (1991). "Yeast histone H4 N-terminal sequence is required for promoter activation in vivo." Cell **65**(6): 1023-31.

- Eisen, J. A., K. S. Sweder, et al. (1995). "Evolution of the SNF2 family of proteins: subfamilies with distinct sequences and functions." Nucleic Acids Res **23**(14): 2715-23.
- Endoh, H., K. Maruyama, et al. (1999). "Purification and identification of p68 RNA helicase acting as a transcriptional coactivator specific for the activation function 1 of human estrogen receptor alpha." Mol Cell Biol **19**(8): 5363-72.
- Englesberg, E., J. Irr, et al. (1965). "Positive control of enzyme synthesis by gene C in the L-arabinose system." J Bacteriol **90**(4): 946-57.
- Erives, A., J. C. Corbo, et al. (1998). "Lineage-specific regulation of the Ciona snail gene in the embryonic mesoderm and neuroectoderm." Dev Biol **194**(2): 213-25.
- Fairman, M. E., P. A. Maroney, et al. (2004). "Protein displacement by DExH/D "RNA helicases" without duplex unwinding." Science **304**(5671): 730-4.
- Fidler, I. J. (2003). "The pathogenesis of cancer metastasis: the 'seed and soil' hypothesis revisited." Nat Rev Cancer **3**(6): 453-8.
- Ford, M. J., I. A. Anton, et al. (1988). "Nuclear protein with sequence homology to translation initiation factor eIF-4A." Nature **332**(6166): 736-8.
- Forsberg, E. C. and E. H. Bresnick (2001). "Histone acetylation beyond promoters: long-range acetylation patterns in the chromatin world." Bioessays **23**(9): 820-30.
- Fredriksson, L., H. Li, et al. (2004). "The PDGF family: four gene products form five dimeric isoforms." Cytokine Growth Factor Rev **15**(4): 197-204.
- Fujita, N., D. L. Jaye, et al. (2004). "MTA3 and the Mi-2/NuRD complex regulate cell fate during B lymphocyte differentiation." Cell **119**(1): 75-86.

- Fujita, T., Y. Kobayashi, et al. (2003). "Full activation of estrogen receptor alpha activation function-1 induces proliferation of breast cancer cells." J Biol Chem **278**(29): 26704-14.
- Garcia-Castro, M. I., C. Marcelle, et al. (2002). "Ectodermal Wnt function as a neural crest inducer." Science **297**(5582): 848-51.
- Gilbert, C., A. Kristjuhan, et al. (2004). "Elongator interactions with nascent mRNA revealed by RNA immunoprecipitation." Mol Cell **14**(4): 457-64.
- Gingras, A. C., B. Raught, et al. (1999). "eIF4 initiation factors: effectors of mRNA recruitment to ribosomes and regulators of translation." Annu Rev Biochem **68**: 913-63.
- Giroldi, L. A., P. P. Bringuier, et al. (1997). "Role of E boxes in the repression of E-cadherin expression." Biochem Biophys Res Commun **241**(2): 453-8.
- Gray, S. G. and B. T. Teh (2001). "Histone acetylation/deacetylation and cancer: an "open" and "shut" case?" Curr Mol Med **1**(4): 401-29.
- Greenburg, G. and E. D. Hay (1982). "Epithelia suspended in collagen gels can lose polarity and express characteristics of migrating mesenchymal cells." J Cell Biol **95**(1): 333-9.
- Grooteclaes, M. L. and S. M. Frisch (2000). "Evidence for a function of CtBP in epithelial gene regulation and anoikis." Oncogene **19**(33): 3823-8.
- Guha, A., K. Dashner, et al. (1995). "Expression of PDGF and PDGF receptors in human astrocytoma operation specimens supports the existence of an autocrine loop." Int J Cancer **60**(2): 168-73.

- Guil, S., R. Gattoni, et al. (2003). "Roles of hnRNP A1, SR proteins, and p68 helicase in c-H-ras alternative splicing regulation." Mol Cell Biol **23**(8): 2927-41.
- Guilford, P., J. Hopkins, et al. (1998). "E-cadherin germline mutations in familial gastric cancer." Nature **392**(6674): 402-5.
- Guo, W. and F. G. Giancotti (2004). "Integrin signalling during tumour progression." Nat Rev Mol Cell Biol **5**(10): 816-26.
- Hajra, K. M., D. Y. Chen, et al. (2002). "The SLUG zinc-finger protein represses E-cadherin in breast cancer." Cancer Res **62**(6): 1613-8.
- Hajra, K. M., X. Ji, et al. (1999). "Extinction of E-cadherin expression in breast cancer via a dominant repression pathway acting on proximal promoter elements." Oncogene **18**(51): 7274-9.
- Hall, M. C. and S. W. Matson (1999). "Helicase motifs: the engine that powers DNA unwinding." Mol Microbiol **34**(5): 867-77.
- Hamm, J. and A. I. Lamond (1998). "Spliceosome assembly: the unwinding role of DEAD-box proteins." Curr Biol **8**(15): R532-4.
- Hartmuth, K., H. Urlaub, et al. (2002). "Protein composition of human prespliceosomes isolated by a tobramycin affinity-selection method." Proc Natl Acad Sci U S A **99**(26): 16719-24.
- Hassig, C. A., T. C. Fleischer, et al. (1997). "Histone deacetylase activity is required for full transcriptional repression by mSin3A." Cell **89**(3): 341-7.
- Hay, E. D. (1995). "An overview of epithelio-mesenchymal transformation." Acta Anat (Basel) **154**(1): 8-20.

- Hecht, A., T. Laroche, et al. (1995). "Histone H3 and H4 N-termini interact with SIR3 and SIR4 proteins: a molecular model for the formation of heterochromatin in yeast." Cell **80**(4): 583-92.
- Heinlein, U. A. (1998). "Dead box for the living." J Pathol **184**(4): 345-7.
- Heinzel, T., R. M. Lavinsky, et al. (1997). "A complex containing N-CoR, mSin3 and histone deacetylase mediates transcriptional repression." Nature **387**(6628): 43-8.
- Hennig, G., O. Lowrick, et al. (1996). "Mechanisms identified in the transcriptional control of epithelial gene expression." J Biol Chem **271**(1): 595-602.
- Hermanson, M., K. Funa, et al. (1992). "Platelet-derived growth factor and its receptors in human glioma tissue: expression of messenger RNA and protein suggests the presence of autocrine and paracrine loops." Cancer Res **52**(11): 3213-9.
- Hirling, H., M. Scheffner, et al. (1989). "RNA helicase activity associated with the human p68 protein." Nature **339**(6225): 562-4.
- Hodges, P. E. and J. D. Beggs (1994). "RNA splicing. U2 fulfils a commitment." Curr Biol **4**(3): 264-7.
- Holliday, R. and J. E. Pugh (1975). "DNA modification mechanisms and gene activity during development." Science **187**(4173): 226-32.
- Honig, A., D. Auboeuf, et al. (2002). "Regulation of alternative splicing by the ATP-dependent DEAD-box RNA helicase p72." Mol Cell Biol **22**(16): 5698-707.
- Huang, Y. and Z. R. Liu (2002). "The ATPase, RNA unwinding, and RNA binding activities of recombinant p68 RNA helicase." J Biol Chem **277**(15): 12810-5.

- Hynes, R. O. (2003). "Metastatic potential: generic predisposition of the primary tumor or rare, metastatic variants-or both?" Cell **113**(7): 821-3.
- Iggo, R. D. and D. P. Lane (1989). "Nuclear protein p68 is an RNA-dependent ATPase." Embo J **8**(6): 1827-31.
- Imhof, B. A., H. P. Vollmers, et al. (1983). "Cell-cell interaction and polarity of epithelial cells: specific perturbation using a monoclonal antibody." Cell **35**(3 Pt 2): 667-75.
- Ippen, K., J. H. Miller, et al. (1968). "New controlling element in the Lac operon of E. coli." Nature **217**(131): 825-7.
- Jacob, F. and J. Monod (1961). "Genetic regulatory mechanisms in the synthesis of proteins." J Mol Biol **3**: 318-56.
- Jamora, C., R. DasGupta, et al. (2003). "Links between signal transduction, transcription and adhesion in epithelial bud development." Nature **422**(6929): 317-22.
- Jamora, C., P. Lee, et al. (2005). "A signaling pathway involving TGF-beta2 and snail in hair follicle morphogenesis." PLoS Biol **3**(1): e11.
- Jan, Y. N. and L. Y. Jan (1993). "HLH proteins, fly neurogenesis, and vertebrate myogenesis." Cell **75**(5): 827-30.
- Jankowsky, E., C. H. Gross, et al. (2001). "Active disruption of an RNA-protein interaction by a DExH/D RNA helicase." Science **291**(5501): 121-5.
- Jensen, T. H., J. Boulay, et al. (2001). "The DECD box putative ATPase Sub2p is an early mRNA export factor." Curr Biol **11**(21): 1711-5.
- Jones, P. A. and S. M. Taylor (1980). "Cellular differentiation, cytidine analogs and DNA methylation." Cell **20**(1): 85-93.

- Jost, J. P., S. Schwarz, et al. (1999). "A chicken embryo protein related to the mammalian DEAD box protein p68 is tightly associated with the highly purified protein-RNA complex of 5-MeC-DNA glycosylase." Nucleic Acids Res **27**(16): 3245-52.
- Jurica, M. S., L. J. Licklider, et al. (2002). "Purification and characterization of native spliceosomes suitable for three-dimensional structural analysis." Rna **8**(4): 426-39.
- Jurica, M. S. and M. J. Moore (2003). "Pre-mRNA splicing: awash in a sea of proteins." Mol Cell **12**(1): 5-14.
- Kahlina, K., I. Goren, et al. (2004). "p68 DEAD box RNA helicase expression in keratinocytes. Regulation, nucleolar localization, and functional connection to proliferation and vascular endothelial growth factor gene expression." J Biol Chem **279**(43): 44872-82.
- Kato, S. (1999). "Function of estrogen receptor (ER) in gene expression." Jpn J Clin Oncol **29**(7): 321-2.
- Kehle, J., D. Beuchle, et al. (1998). "dMi-2, a hunchback-interacting protein that functions in polycomb repression." Science **282**(5395): 1897-900.
- Kimura, A., K. Matsubara, et al. (2005). "A decade of histone acetylation: marking eukaryotic chromosomes with specific codes." J Biochem (Tokyo) **138**(6): 647-62.
- Kipreos, E. T. and J. Y. Wang (1990). "Differential phosphorylation of c-Abl in cell cycle determined by cdc2 kinase and phosphatase activity." Science **248**(4952): 217-20.

- Kipreos, E. T. and J. Y. Wang (1992). "Cell cycle-regulated binding of c-Abl tyrosine kinase to DNA." Science **256**(5055): 382-5.
- Kistler, A. L. and C. Guthrie (2001). "Deletion of MUD2, the yeast homolog of U2AF65, can bypass the requirement for sub2, an essential spliceosomal ATPase." Genes Dev **15**(1): 42-9.
- Klein Gunnewiek, J. M., L. B. van de Putte, et al. (1997). "The U1 snRNP complex: an autoantigen in connective tissue diseases. An update." Clin Exp Rheumatol **15**(5): 549-60.
- Knoepfler, P. S. and R. N. Eisenman (1999). "Sin meets NuRD and other tails of repression." Cell **99**(5): 447-50.
- Kodym, R., C. Henockl, et al. (2005). "Identification of the human DEAD-box protein p68 as a substrate of Tlk1." Biochem Biophys Res Commun **333**(2): 411-7.
- Konopka, J. B., S. M. Watanabe, et al. (1984). "An alteration of the human c-abl protein in K562 leukemia cells unmask associated tyrosine kinase activity." Cell **37**(3): 1035-42.
- Krainer, A. R., T. Maniatis, et al. (1984). "Normal and mutant human beta-globin pre-mRNAs are faithfully and efficiently spliced in vitro." Cell **36**(4): 993-1005.
- Kuhn, A. N., Z. Li, et al. (1999). "Splicing factor Prp8 governs U4/U6 RNA unwinding during activation of the spliceosome." Mol Cell **3**(1): 65-75.
- Kumar, V., S. Green, et al. (1987). "Functional domains of the human estrogen receptor." Cell **51**(6): 941-51.

- Kurdistani, S. K. and M. Grunstein (2003). "Histone acetylation and deacetylation in yeast." Nat Rev Mol Cell Biol **4**(4): 276-84.
- Kwon, H., A. N. Imbalzano, et al. (1994). "Nucleosome disruption and enhancement of activator binding by a human SW1/SNF complex." Nature **370**(6489): 477-81.
- Laggerbauer, B., T. Achsel, et al. (1998). "The human U5-200kD DEXH-box protein unwinds U4/U6 RNA duplexes in vitro." Proc Natl Acad Sci U S A **95**(8): 4188-92.
- Le Douarin, B., C. Zechel, et al. (1995). "The N-terminal part of TIF1, a putative mediator of the ligand-dependent activation function (AF-2) of nuclear receptors, is fused to B-raf in the oncogenic protein T18." Embo J **14**(9): 2020-33.
- Lee, C. G. (2002). "RH70, a bidirectional RNA helicase, co-purifies with U1snRNP." J Biol Chem **277**(42): 39679-83.
- Leibovitz, A., J. C. Stinson, et al. (1976). "Classification of human colorectal adenocarcinoma cell lines." Cancer Res **36**(12): 4562-9.
- Lewis, J. M., R. Baskaran, et al. (1996). "Integrin regulation of c-Abl tyrosine kinase activity and cytoplasmic-nuclear transport." Proc Natl Acad Sci U S A **93**(26): 15174-9.
- Li, M., H. Moyle, et al. (1994). "Target of the transcriptional activation function of phage lambda cI protein." Science **263**(5143): 75-7.
- Libri, D., N. Graziani, et al. (2001). "Multiple roles for the yeast SUB2/yUAP56 gene in splicing." Genes Dev **15**(1): 36-41.

- Liem, K. F., Jr., G. Tremml, et al. (1995). "Dorsal differentiation of neural plate cells induced by BMP-mediated signals from epidermal ectoderm." Cell **82**(6): 969-79.
- Lin, C., L. Yang, et al. (2005). "ATPase/helicase activities of p68 RNA helicase are required for pre-mRNA splicing but not for assembly of the spliceosome." Mol Cell Biol **25**(17): 7484-93.
- Liu, Z. R. (2002). "p68 RNA helicase is an essential human splicing factor that acts at the U1 snRNA-5' splice site duplex." Mol Cell Biol **22**(15): 5443-50.
- Liu, Z. R., B. Lagerbauer, et al. (1997). "Crosslinking of the U5 snRNP-specific 116-kDa protein to RNA hairpins that block step 2 of splicing." Rna **3**(11): 1207-19.
- Liu, Z. R., B. Sargueil, et al. (1998). "Detection of a novel ATP-dependent cross-linked protein at the 5' splice site-U1 small nuclear RNA duplex by methylene blue-mediated photo-cross-linking." Mol Cell Biol **18**(12): 6910-20.
- Liu, Z. R., A. M. Wilkie, et al. (1996). "Detection of double-stranded RNA-protein interactions by methylene blue-mediated photo-crosslinking." Rna **2**(6): 611-21.
- Lochter, A., M. D. Sternlicht, et al. (1998). "The significance of matrix metalloproteinases during early stages of tumor progression." Ann N Y Acad Sci **857**: 180-93.
- Lock, L. S., M. M. Frigault, et al. (2003). "Grb2-independent recruitment of Gab1 requires the C-terminal lobe and structural integrity of the Met receptor kinase domain." J Biol Chem **278**(32): 30083-90.
- Lokker, N. A., C. M. Sullivan, et al. (2002). "Platelet-derived growth factor (PDGF) autocrine signaling regulates survival and mitogenic pathways in glioblastoma

- cells: evidence that the novel PDGF-C and PDGF-D ligands may play a role in the development of brain tumors." Cancer Res **62**(13): 3729-35.
- Luking, A., U. Stahl, et al. (1998). "The protein family of RNA helicases." Crit Rev Biochem Mol Biol **33**(4): 259-96.
- Madhani, H. D. and C. Guthrie (1994). "Dynamic RNA-RNA interactions in the spliceosome." Annu Rev Genet **28**: 1-26.
- Madhani, H. D. and C. Guthrie (1994). "Randomization-selection analysis of snRNAs in vivo: evidence for a tertiary interaction in the spliceosome." Genes Dev **8**(9): 1071-86.
- Mangelsdorf, D. J., C. Thummel, et al. (1995). "The nuclear receptor superfamily: the second decade." Cell **83**(6): 835-9.
- Martin, C. and Y. Zhang (2005). "The diverse functions of histone lysine methylation." Nat Rev Mol Cell Biol **6**(11): 838-49.
- Masood, S. (1992). "Estrogen and progesterone receptors in cytology: a comprehensive review." Diagn Cytopathol **8**(5): 475-91.
- McKnight, S. L. and R. Kingsbury (1982). "Transcriptional control signals of a eukaryotic protein-coding gene." Science **217**(4557): 316-24.
- Melo, J. V. (1996). "The diversity of BCR-ABL fusion proteins and their relationship to leukemia phenotype." Blood **88**(7): 2375-84.
- Minard, M. E., M. H. Herynk, et al. (2005). "The guanine nucleotide exchange factor Tiam1 increases colon carcinoma growth at metastatic sites in an orthotopic nude mouse model." Oncogene **24**(15): 2568-73.

- Moore, M. J. and P. A. Sharp (1993). "Evidence for two active sites in the spliceosome provided by stereochemistry of pre-mRNA splicing." Nature **365**(6444): 364-8.
- Morikawa, K., S. M. Walker, et al. (1988). "Influence of organ environment on the growth, selection, and metastasis of human colon carcinoma cells in nude mice." Cancer Res **48**(23): 6863-71.
- Mount, S. M., I. Pettersson, et al. (1983). "The U1 small nuclear RNA-protein complex selectively binds a 5' splice site in vitro." Cell **33**(2): 509-18.
- Mullis, K. B. and F. A. Faloona (1987). "Specific synthesis of DNA in vitro via a polymerase-catalyzed chain reaction." Methods Enzymol **155**: 335-50.
- Nagy, L., H. Y. Kao, et al. (1997). "Nuclear receptor repression mediated by a complex containing SMRT, mSin3A, and histone deacetylase." Cell **89**(3): 373-80.
- Nan, X., H. H. Ng, et al. (1998). "Transcriptional repression by the methyl-CpG-binding protein MeCP2 involves a histone deacetylase complex." Nature **393**(6683): 386-9.
- Narlikar, G. J., H. Y. Fan, et al. (2002). "Cooperation between complexes that regulate chromatin structure and transcription." Cell **108**(4): 475-87.
- Nasim, M. T., H. M. Chowdhury, et al. (2002). "A double reporter assay for detecting changes in the ratio of spliced and unspliced mRNA in mammalian cells." Nucleic Acids Res **30**(20): e109.
- Neely, K. E. and J. L. Workman (2002). "Histone acetylation and chromatin remodeling: which comes first?" Mol Genet Metab **76**(1): 1-5.

- Neubauer, G., A. King, et al. (1998). "Mass spectrometry and EST-database searching allows characterization of the multi-protein spliceosome complex." Nat Genet **20**(1): 46-50.
- Nieto, M. A. (2002). "The snail superfamily of zinc-finger transcription factors." Nat Rev Mol Cell Biol **3**(3): 155-66.
- Nieto, M. A., M. G. Sargent, et al. (1994). "Control of cell behavior during vertebrate development by Slug, a zinc finger gene." Science **264**(5160): 835-9.
- Nilsen, T. W. (2003). "The spliceosome: the most complex macromolecular machine in the cell?" Bioessays **25**(12): 1147-9.
- Noueiry, A. O., J. Chen, et al. (2000). "A mutant allele of essential, general translation initiation factor DED1 selectively inhibits translation of a viral mRNA." Proc Natl Acad Sci U S A **97**(24): 12985-90.
- Oft, M., K. H. Heider, et al. (1998). "TGFbeta signaling is necessary for carcinoma cell invasiveness and metastasis." Curr Biol **8**(23): 1243-52.
- Ogilvie, V. C., B. J. Wilson, et al. (2003). "The highly related DEAD box RNA helicases p68 and p72 exist as heterodimers in cells." Nucleic Acids Res **31**(5): 1470-80.
- Onate, S. A., S. Y. Tsai, et al. (1995). "Sequence and characterization of a coactivator for the steroid hormone receptor superfamily." Science **270**(5240): 1354-7.
- Peinado, H., E. Ballestar, et al. (2004). "Snail mediates E-cadherin repression by the recruitment of the Sin3A/histone deacetylase 1 (HDAC1)/HDAC2 complex." Mol Cell Biol **24**(1): 306-19.

- Peinado, H., M. Quintanilla, et al. (2003). "Transforming growth factor beta-1 induces snail transcription factor in epithelial cell lines: mechanisms for epithelial mesenchymal transitions." J Biol Chem **278**(23): 21113-23.
- Perez-Moreno, M. A., A. Locascio, et al. (2001). "A new role for E12/E47 in the repression of E-cadherin expression and epithelial-mesenchymal transitions." J Biol Chem **276**(29): 27424-31.
- Plattner, R., L. Kadlec, et al. (1999). "c-Abl is activated by growth factors and Src family kinases and has a role in the cellular response to PDGF." Genes Dev **13**(18): 2400-11.
- Poser, I., D. Dominguez, et al. (2001). "Loss of E-cadherin expression in melanoma cells involves up-regulation of the transcriptional repressor Snail." J Biol Chem **276**(27): 24661-6.
- Pugh, G. E., S. M. Nicol, et al. (1999). "Interaction of the Escherichia coli DEAD box protein DbpA with 23 S ribosomal RNA." J Mol Biol **292**(4): 771-8.
- Radisky, D. C., D. D. Levy, et al. (2005). "Rac1b and reactive oxygen species mediate MMP-3-induced EMT and genomic instability." Nature **436**(7047): 123.
- Radisky, D. C., D. D. Levy, et al. (2005). "Rac1b and reactive oxygen species mediate MMP-3-induced EMT and genomic instability." Nature **436**(7047): 123-7.
- Raghuathan, P. L. and C. Guthrie (1998). "RNA unwinding in U4/U6 snRNPs requires ATP hydrolysis and the DEIH-box splicing factor Brr2." Curr Biol **8**(15): 847-55.

- Rajendran, R. R., A. C. Nye, et al. (2003). "Regulation of nuclear receptor transcriptional activity by a novel DEAD box RNA helicase (DP97)." J Biol Chem **278**(7): 4628-38.
- Rappsilber, J., U. Ryder, et al. (2002). "Large-scale proteomic analysis of the human spliceosome." Genome Res **12**(8): 1231-45.
- Riethmacher, D., V. Brinkmann, et al. (1995). "A targeted mutation in the mouse E-cadherin gene results in defective preimplantation development." Proc Natl Acad Sci U S A **92**(3): 855-9.
- Rocak, S. and P. Linder (2004). "DEAD-box proteins: the driving forces behind RNA metabolism." Nat Rev Mol Cell Biol **5**(3): 232-41.
- Rogers, G. W., Jr., A. A. Komar, et al. (2002). "eIF4A: the godfather of the DEAD box helicases." Prog Nucleic Acid Res Mol Biol **72**: 307-31.
- Romano, L. A. and R. B. Runyan (2000). "Slug is an essential target of TGFbeta2 signaling in the developing chicken heart." Dev Biol **223**(1): 91-102.
- Rossow, K. L. and R. Janknecht (2003). "Synergism between p68 RNA helicase and the transcriptional coactivators CBP and p300." Oncogene **22**(1): 151-6.
- Rozen, F., I. Edery, et al. (1990). "Bidirectional RNA helicase activity of eucaryotic translation initiation factors 4A and 4F." Mol Cell Biol **10**(3): 1134-44.
- Saito, M. and F. Ishikawa (2002). "The mCpG-binding domain of human MBD3 does not bind to mCpG but interacts with NuRD/Mi2 components HDAC1 and MTA2." J Biol Chem **277**(38): 35434-9.

- Sambrook, J. and M. J. Gething (1989). "Protein structure. Chaperones, paperones." Nature **342**(6247): 224-5.
- Sato, N., M. E. Gleave, et al. (1997). "A metastatic and androgen-sensitive human prostate cancer model using intraprostatic inoculation of LNCaP cells in SCID mice." Cancer Res **57**(8): 1584-9.
- Schekman, R. (1994). "Translocation gets a push." Cell **78**(6): 911-3.
- Schwer, B. (2001). "A new twist on RNA helicases: DExH/D box proteins as RNPsases." Nat Struct Biol **8**(2): 113-6.
- Schwer, B. and C. H. Gross (1998). "Prp22, a DExH-box RNA helicase, plays two distinct roles in yeast pre-mRNA splicing." Embo J **17**(7): 2086-94.
- Schwer, B. and T. Meszaros (2000). "RNA helicase dynamics in pre-mRNA splicing." Embo J **19**(23): 6582-91.
- Seelig, H. P., I. Moosbrugger, et al. (1995). "The major dermatomyositis-specific Mi-2 autoantigen is a presumed helicase involved in transcriptional activation." Arthritis Rheum **38**(10): 1389-99.
- Sengoku, T., O. Nureki, et al. (2006). "Structural Basis for RNA Unwinding by the DEAD-Box Protein Drosophila Vasa." Cell **125**(2): 287-300.
- Seufert, D. W., R. Kos, et al. (2000). "p68, a DEAD-box RNA helicase, is expressed in chordate embryo neural and mesodermal tissues." J Exp Zool **288**(3): 193-204.
- Shafman, T., K. K. Khanna, et al. (1997). "Interaction between ATM protein and c-Abl in response to DNA damage." Nature **387**(6632): 520-3.
- Sharp, P. A. (1994). "Split genes and RNA splicing." Cell **77**(6): 805-15.

- Shook, D. and R. Keller (2003). "Mechanisms, mechanics and function of epithelial-mesenchymal transitions in early development." Mech Dev **120**(11): 1351-83.
- Singh, R. (2002). "RNA-protein interactions that regulate pre-mRNA splicing." Gene Expr **10**(1-2): 79-92.
- Smith, C. L. and C. L. Peterson (2005). "A conserved Swi2/Snf2 ATPase motif couples ATP hydrolysis to chromatin remodeling." Mol Cell Biol **25**(14): 5880-92.
- Smith, C. W. and J. Valcarcel (2000). "Alternative pre-mRNA splicing: the logic of combinatorial control." Trends Biochem Sci **25**(8): 381-8.
- Solari, F. and J. Ahringer (2000). "NURD-complex genes antagonise Ras-induced vulval development in *Caenorhabditis elegans*." Curr Biol **10**(4): 223-6.
- Solomon, M. J., P. L. Larsen, et al. (1988). "Mapping protein-DNA interactions in vivo with formaldehyde: evidence that histone H4 is retained on a highly transcribed gene." Cell **53**(6): 937-47.
- Staley, J. P. and C. Guthrie (1998). "Mechanical devices of the spliceosome: motors, clocks, springs, and things." Cell **92**(3): 315-26.
- Stevenson, R. J., S. J. Hamilton, et al. (1998). "Expression of the 'dead box' RNA helicase p68 is developmentally and growth regulated and correlates with organ differentiation/maturation in the fetus." J Pathol **184**(4): 351-9.
- Stoker, M. and M. Perryman (1985). "An epithelial scatter factor released by embryo fibroblasts." J Cell Sci **77**: 209-23.

- Story, R. M., H. Li, et al. (2001). "Crystal structure of a DEAD box protein from the hyperthermophile *Methanococcus jannaschii*." Proc Natl Acad Sci U S A **98**(4): 1465-70.
- Strasser, K. and E. Hurt (2001). "Splicing factor Sub2p is required for nuclear mRNA export through its interaction with Yra1p." Nature **413**(6856): 648-52.
- Sun, D., S. Baur, et al. (2000). "Epithelial-mesenchymal transformation is the mechanism for fusion of the craniofacial primordia involved in morphogenesis of the chicken lip." Dev Biol **228**(2): 337-49.
- Suzuki, H., D. N. Watkins, et al. (2004). "Epigenetic inactivation of SFRP genes allows constitutive WNT signaling in colorectal cancer." Nat Genet **36**(4): 417-22.
- Svitkin, Y. V., L. P. Ovchinnikov, et al. (1996). "General RNA binding proteins render translation cap dependent." Embo J **15**(24): 7147-55.
- Taagepera, S., D. McDonald, et al. (1998). "Nuclear-cytoplasmic shuttling of C-ABL tyrosine kinase." Proc Natl Acad Sci U S A **95**(13): 7457-62.
- Takeichi, M. (1995). "Morphogenetic roles of classic cadherins." Curr Opin Cell Biol **7**(5): 619-27.
- Tan, C., P. Costello, et al. (2001). "Inhibition of integrin linked kinase (ILK) suppresses beta-catenin-Lef/Tcf-dependent transcription and expression of the E-cadherin repressor, snail, in APC^{-/-} human colon carcinoma cells." Oncogene **20**(1): 133-40.
- Tanner, N. K. (2003). "The newly identified Q motif of DEAD box helicases is involved in adenine recognition." Cell Cycle **2**(1): 18-9.

- Tanner, N. K., O. Cordin, et al. (2003). "The Q motif: a newly identified motif in DEAD box helicases may regulate ATP binding and hydrolysis." Mol Cell **11**(1): 127-38.
- Tanner, N. K. and P. Linder (2001). "DExD/H box RNA helicases: from generic motors to specific dissociation functions." Mol Cell **8**(2): 251-62.
- Tasset, D., L. Tora, et al. (1990). "Distinct classes of transcriptional activating domains function by different mechanisms." Cell **62**(6): 1177-87.
- Taunton, J., C. A. Hassig, et al. (1996). "A mammalian histone deacetylase related to the yeast transcriptional regulator Rpd3p." Science **272**(5260): 408-11.
- Tepass, U., K. Truong, et al. (2000). "Cadherins in embryonic and neural morphogenesis." Nat Rev Mol Cell Biol **1**(2): 91-100.
- Thalmann, G. N., P. E. Anezinis, et al. (1994). "Androgen-independent cancer progression and bone metastasis in the LNCaP model of human prostate cancer." Cancer Res **54**(10): 2577-81.
- Thiery, J. P. (2002). "Epithelial-mesenchymal transitions in tumour progression." Nat Rev Cancer **2**(6): 442-54.
- Thiery, J. P. and J. P. Sleeman (2006). "Complex networks orchestrate epithelial-mesenchymal transitions." Nat Rev Mol Cell Biol **7**(2): 131-42.
- Tjian, R. (1978). "The binding site on SV40 DNA for a T antigen-related protein." Cell **13**(1): 165-79.
- Toh, Y., E. Oki, et al. (1997). "Overexpression of the MTA1 gene in gastrointestinal carcinomas: correlation with invasion and metastasis." Int J Cancer **74**(4): 459-63.

- Toh, Y., S. D. Pencil, et al. (1994). "A novel candidate metastasis-associated gene, mta1, differentially expressed in highly metastatic mammary adenocarcinoma cell lines. cDNA cloning, expression, and protein analyses." J Biol Chem **269**(37): 22958-63.
- Tora, L., J. White, et al. (1989). "The human estrogen receptor has two independent nonacidic transcriptional activation functions." Cell **59**(3): 477-87.
- Tsukiyama, T., P. B. Becker, et al. (1994). "ATP-dependent nucleosome disruption at a heat-shock promoter mediated by binding of GAGA transcription factor." Nature **367**(6463): 525-32.
- Tsukiyama, T., C. Daniel, et al. (1995). "ISWI, a member of the SWI2/SNF2 ATPase family, encodes the 140 kDa subunit of the nucleosome remodeling factor." Cell **83**(6): 1021-6.
- Tsukiyama, T. and C. Wu (1995). "Purification and properties of an ATP-dependent nucleosome remodeling factor." Cell **83**(6): 1011-20.
- Van Etten, R. A., P. K. Jackson, et al. (1994). "The COOH terminus of the c-Abl tyrosine kinase contains distinct F- and G-actin binding domains with bundling activity." J Cell Biol **124**(3): 325-40.
- Veltmaat, J. M., C. C. Orelia, et al. (2000). "Snail is an immediate early target gene of parathyroid hormone related peptide signaling in parietal endoderm formation." Int J Dev Biol **44**(3): 297-307.
- Verdone, L., M. Caserta, et al. (2005). "Role of histone acetylation in the control of gene expression." Biochem Cell Biol **83**(3): 344-53.

- Viebahn, C. (1995). "Epithelio-mesenchymal transformation during formation of the mesoderm in the mammalian embryo." Acta Anat (Basel) **154**(1): 79-97.
- Vincent-Salomon, A. and J. P. Thiery (2003). "Host microenvironment in breast cancer development: epithelial-mesenchymal transition in breast cancer development." Breast Cancer Res **5**(2): 101-6.
- Voegel, J. J., M. J. Heine, et al. (1996). "TIF2, a 160 kDa transcriptional mediator for the ligand-dependent activation function AF-2 of nuclear receptors." Embo J **15**(14): 3667-75.
- Voronova, A. F. and F. Lee (1994). "The E2A and tal-1 helix-loop-helix proteins associate in vivo and are modulated by Id proteins during interleukin 6-induced myeloid differentiation." Proc Natl Acad Sci U S A **91**(13): 5952-6.
- Wade, P. A., A. Geggion, et al. (1999). "Mi-2 complex couples DNA methylation to chromatin remodelling and histone deacetylation." Nat Genet **23**(1): 62-6.
- Wang, H. B. and Y. Zhang (2001). "Mi2, an auto-antigen for dermatomyositis, is an ATP-dependent nucleosome remodeling factor." Nucleic Acids Res **29**(12): 2517-21.
- Wang, W., J. Cote, et al. (1996). "Purification and biochemical heterogeneity of the mammalian SWI-SNF complex." Embo J **15**(19): 5370-82.
- Wang, W., Y. Xue, et al. (1996). "Diversity and specialization of mammalian SWI/SNF complexes." Genes Dev **10**(17): 2117-30.
- Wang, Y., J. D. Wagner, et al. (1998). "The DEAH-box splicing factor Prp16 unwinds RNA duplexes in vitro." Curr Biol **8**(8): 441-51.

- Warner, D. R., V. Bhattacharjee, et al. (2004). "Functional interaction between Smad, CREB binding protein, and p68 RNA helicase." Biochem Biophys Res Commun **324**(1): 70-6.
- Watanabe, M., J. Yanagisawa, et al. (2001). "A subfamily of RNA-binding DEAD-box proteins acts as an estrogen receptor alpha coactivator through the N-terminal activation domain (AF-1) with an RNA coactivator, SRA." Embo J **20**(6): 1341-52.
- Weintraub, H. (1993). "The MyoD family and myogenesis: redundancy, networks, and thresholds." Cell **75**(7): 1241-4.
- Weiss, L. (1992). "Comments on hematogenous metastatic patterns in humans as revealed by autopsy." Clin Exp Metastasis **10**(3): 191-9.
- Wen, S. T., P. K. Jackson, et al. (1996). "The cytostatic function of c-Abl is controlled by multiple nuclear localization signals and requires the p53 and Rb tumor suppressor gene products." Embo J **15**(7): 1583-95.
- Will, C. L. and R. Luhrmann (2001). "Molecular biology. RNP remodeling with DExH/D boxes." Science **291**(5510): 1916-7.
- Will, C. L., S. Rumpler, et al. (1996). "In vitro reconstitution of mammalian U1 snRNPs active in splicing: the U1-C protein enhances the formation of early (E) spliceosomal complexes." Nucleic Acids Res **24**(23): 4614-23.
- Wilson, B. J., G. J. Bates, et al. (2004). "The p68 and p72 DEAD box RNA helicases interact with HDAC1 and repress transcription in a promoter-specific manner." BMC Mol Biol **5**: 11.

- Witty, J. P., S. McDonnell, et al. (1994). "Modulation of matrilysin levels in colon carcinoma cell lines affects tumorigenicity in vivo." Cancer Res **54**(17): 4805-12.
- Wu, J. J., D. E. Afar, et al. (2002). "Recognition of multiple substrate motifs by the c-ABL protein tyrosine kinase." Comb Chem High Throughput Screen **5**(1): 83-91.
- Xu, J. and Q. Li (2003). "Review of the in vivo functions of the p160 steroid receptor coactivator family." Mol Endocrinol **17**(9): 1681-92.
- Xue, Y., J. Wong, et al. (1998). "NURD, a novel complex with both ATP-dependent chromatin-remodeling and histone deacetylase activities." Mol Cell **2**(6): 851-61.
- Yamada, S., S. Pokutta, et al. (2005). "Deconstructing the cadherin-catenin-actin complex." Cell **123**(5): 889-901.
- Yang, J., S. A. Mani, et al. (2004). "Twist, a master regulator of morphogenesis, plays an essential role in tumor metastasis." Cell **117**(7): 927-39.
- Yang, L., C. Lin, et al. (2005). "Phosphorylations of DEAD box p68 RNA helicase are associated with cancer development and cell proliferation." Mol Cancer Res **3**(6): 355-63.
- Yang, L., C. Lin, et al. (2005). "Signaling to the DEAD box--regulation of DEAD-box p68 RNA helicase by protein phosphorylations." Cell Signal **17**(12): 1495-504.
- Yang, L. and Z. R. Liu (2004). "Bacterially expressed recombinant p68 RNA helicase is phosphorylated on serine, threonine, and tyrosine residues." Protein Expr Purif **35**(2): 327-33.

- Yang, L., J. Yang, et al. (2004). "Phosphorylation of p68 RNA helicase regulates RNA binding by the C-terminal domain of the protein." Biochem Biophys Res Commun **314**(2): 622-30.
- Yang, M., P. Jiang, et al. (1999). "A Fluorescent Orthotopic Bone Metastasis Model of Human Prostate Cancer." Cancer Res **59**(4): 781-786.
- Yao, Y. L. and W. M. Yang (2003). "The metastasis-associated proteins 1 and 2 form distinct protein complexes with histone deacetylase activity." J Biol Chem **278**(43): 42560-8.
- Yeh, S. and C. Chang (1996). "Cloning and characterization of a specific coactivator, ARA70, for the androgen receptor in human prostate cells." Proc Natl Acad Sci U S A **93**(11): 5517-21.
- Yook, J. I., X. Y. Li, et al. (2005). "Wnt-dependent regulation of the E-cadherin repressor snail." J Biol Chem **280**(12): 11740-8.
- Yoshiura, K., Y. Kanai, et al. (1995). "Silencing of the E-cadherin invasion-suppressor gene by CpG methylation in human carcinomas." Proc Natl Acad Sci U S A **92**(16): 7416-9.
- Yuan, Z. M., Y. Huang, et al. (1997). "Regulation of DNA damage-induced apoptosis by the c-Abl tyrosine kinase." Proc Natl Acad Sci U S A **94**(4): 1437-40.
- Yuan, Z. M., Y. Huang, et al. (1996). "Role for c-Abl tyrosine kinase in growth arrest response to DNA damage." Nature **382**(6588): 272-4.

- Zenklusen, D., P. Vinciguerra, et al. (2002). "Stable mRNP formation and export require cotranscriptional recruitment of the mRNA export factors Yra1p and Sub2p by Hpr1p." Mol Cell Biol **22**(23): 8241-53.
- Zhang, M. and M. R. Green (2001). "Identification and characterization of yUAP/Sub2p, a yeast homolog of the essential human pre-mRNA splicing factor hUAP56." Genes Dev **15**(1): 30-5.
- Zhang, Y., G. LeRoy, et al. (1998). "The dermatomyositis-specific autoantigen Mi2 is a component of a complex containing histone deacetylase and nucleosome remodeling activities." Cell **95**(2): 279-89.
- Zhang, Y., H. H. Ng, et al. (1999). "Analysis of the NuRD subunits reveals a histone deacetylase core complex and a connection with DNA methylation." Genes Dev **13**(15): 1924-35.
- Zhang, Z., G. Izaguirre, et al. (2004). "The phosphorylation of vinculin on tyrosine residues 100 and 1065, mediated by SRC kinases, affects cell spreading." Mol Biol Cell **15**(9): 4234-47.
- Zhou, B. P., J. Deng, et al. (2004). "Dual regulation of Snail by GSK-3beta-mediated phosphorylation in control of epithelial-mesenchymal transition." Nat Cell Biol **6**(10): 931-40.
- Zhou, Z., L. J. Licklider, et al. (2002). "Comprehensive proteomic analysis of the human spliceosome." Nature **419**(6903): 182-5.
- Zhu, J. and J. Y. Wang (2004). "Death by Abl: a matter of location." Curr Top Dev Biol **59**: 165-92.

APPENDIX

GENOME-WIDE GENE EXPRESSION PROFILES AFFECTED BY TYROSINE PHOSPHORYLATED DEAD-BOX p68 RNA HELICASE

9.1.1 Abstract

DEAD-box protein p68 RNA helicase has been suggested to act as an essential splicing factor and plays central roles in tumor cell EMT. We have analyzed genome-wide gene expression profiles affected by DEAD-box protein p68 in the mammalian cell lines, HEK and SW620 by means of large scale of DNA microarray technique. Overexpression of exogenous p68s, wild type, Y593F, Y595F and HLIGR showed a dramatic change of global gene expression pattern. Gene cluster analysis has grouped these genes into distinct clusters that appear to correlate with major cellular processes. These processes include cell proliferation, anti-programmed cell apoptosis, cell adhesion, cell cycle and cell migration. These data should provide valuable molecular and genetic understanding of the cellular function of DEAD-box protein p68.

9.1.2 Introduction

The proto-type DEAD-box protein p68 is documented as a putative RNA helicase. Studies from our laboratory have established p68 RNA helicase as an essential factor in the general pre-mRNA splicing process {Lin, 2005 #43; Liu, 2002 #48; Liu, 1998 #56}. Depletion or non-functional mutations of p68 abolished the splicing reaction *in vitro* and *in vivo*. The protein is also suggested to act as a transcription coactivator or corepressor in particular signaling pathways {Bates, 2005 #174; Endoh, 1999 #65;

Kahlina, 2004 #172; Rossow, 2003 #90}. It has been suggested that p68 RNA helicase regulates gene expression in sequence-specific manner {Wilson, 2004 #173}. However, the genes targeted by p68 and the cellular function of p68 are not known

The breakthrough of DNA microarray technology has become a powerful method to globally identify gene expression profiles. Instead of studying single genes in biological experiments, microarray technology allows identification of thousands of genes simultaneously. With the completion of human genome project, DNA microarray can be applied for identifying disease-related genes, examining drug effects and classifying gene regulation by certain proteins.

There are two types of microarrays: cDNA array and oligonucleotide array. We used the oligonucleotide microarray (Affymetrix) in our experiments. DNA microarray assay has been performed by inspecting the gene expression profile change among the total RNA extraction of HEK cells transfected with blank vector as control, or HA-tagged p68 wild type, or transiently expression of wild type or ATPase mutant in the p68-knockdown SW620 cells. HGU133 2.0plus chips were utilized to be hybridized and scanned in Morehouse Medical School. Subfamilies of genes related to cellular processes were identified. Further confirmation will be performed by RT-PCR and western targeting to three to six examples.

9.1.3 Material and method

9.1.3.1 Total RNA isolation

HEK cells were transfected with control siRNA or siRNA targeting p68. SW620 cells were expressed HA-tagged p68s, (wt, Y593F or Y595F) in p68-knockdown cells. Total RNA were isolated using Qiagen RNeasy Mini Kit spin columns. The concentration of total RNA was determined by spectrometer at OD 280 nm. The isolated RNA samples were stored at -80°C.

9.3.2 Target labeling

Double stranded cDNA were synthesized from total RNA for each sample with SuperScript™ II Reverse Transcriptase (Invitrogen). Briefly, 10 µg of total RNA was used for reverse transcription to synthesiz the (–) strand cDNA using a primer containing poly T and T7 RNA polymerase promoter sequence. The second strand of cDNA was synthesized with incubation of T4 DNA polymerase I. The double stranded cDNA were cleaned up by phenol-chloroform extraction and ethanol-precipitation. The cDNA was resuspended in 10 µl of RNase-free water. 5 µl of resuspended cDNA were used as template for *in vitro* transcription in the presence of biotinylated CTP to generate labeled RNA. The *in vitro* transcription reaction was performed by using the GeneChip® IVT Labeling Kit (Affymetrix). Purification of the labeled RNA was carried out with the Qiagen RNeasy Mini Kit spin columns.

9.1.3.3 Array Hybridization and Scanning.

The labeled cRNA was fragmented in fragmentation buffer (200 mM Tris pH 8.1, 50 mM KOAc, 150 mM MgOAc) and hybridized to the microarrays (U133 or U133 2.0 plus GeneChip®) (Affymetrix) in 200 µl of hybridization solution containing 20 µg labeled target in 13Mes buffer [0.1MMesy1.0 M NaCl, 0.01% Triton X-100 (pH 6.7)] and 0.1 mg/ml herring sperm DNA. Arrays were placed on a rotisserie and rotated at 60 rpm for 16 h at 45°C. Following hybridization, the arrays were washed with 63 SSPE-T (0.9 M NaCl, 60 mM NaH₂PO₄, 6 mM EDTA, 0.005% Triton X-100) at 22°C on a fluidics station (Affymetrix) for 10 3 2 cycles, and subsequently with 0.1 Mes at 45°C for 30 min. The arrays were then stained with a streptavidin-phycoerythrin conjugate (Molecular Probes), followed by 10 3 2 wash cycles. After 10 3 2 additional wash cycles, the arrays were scanned at a resolution of 3 mm, using the High Resolution GCS3000 scanner (Affymetrix).

9.1.3.4 Data Analysis

The image data were analyzed by Affymetrix GeneChip Operating Software (GCOS) Version 1.0.

Figure IX-1. The schematic illustration of targeting labeling and array hybridization.

The total RNA isolated from treated mammalian cells was used for reversely transcription in the presence of poly T oligonucleotide T7 primer. The synthesized cDNA were further used as temple for *in vitro* transcription in the presence of biotinylated CTP for RNA labeling. The labeled cRNA was hybridized to Genechip® oligonucleotide assays. After incubation with streptavidin-phycoerythrin conjugate and extensive wash, the arrays were scanned by GCS3000 scanner.

Figure IX-1

One-Cycle Target Labeling

(for 1-15 µg total RNA or 0.2-2 µg mRNA)

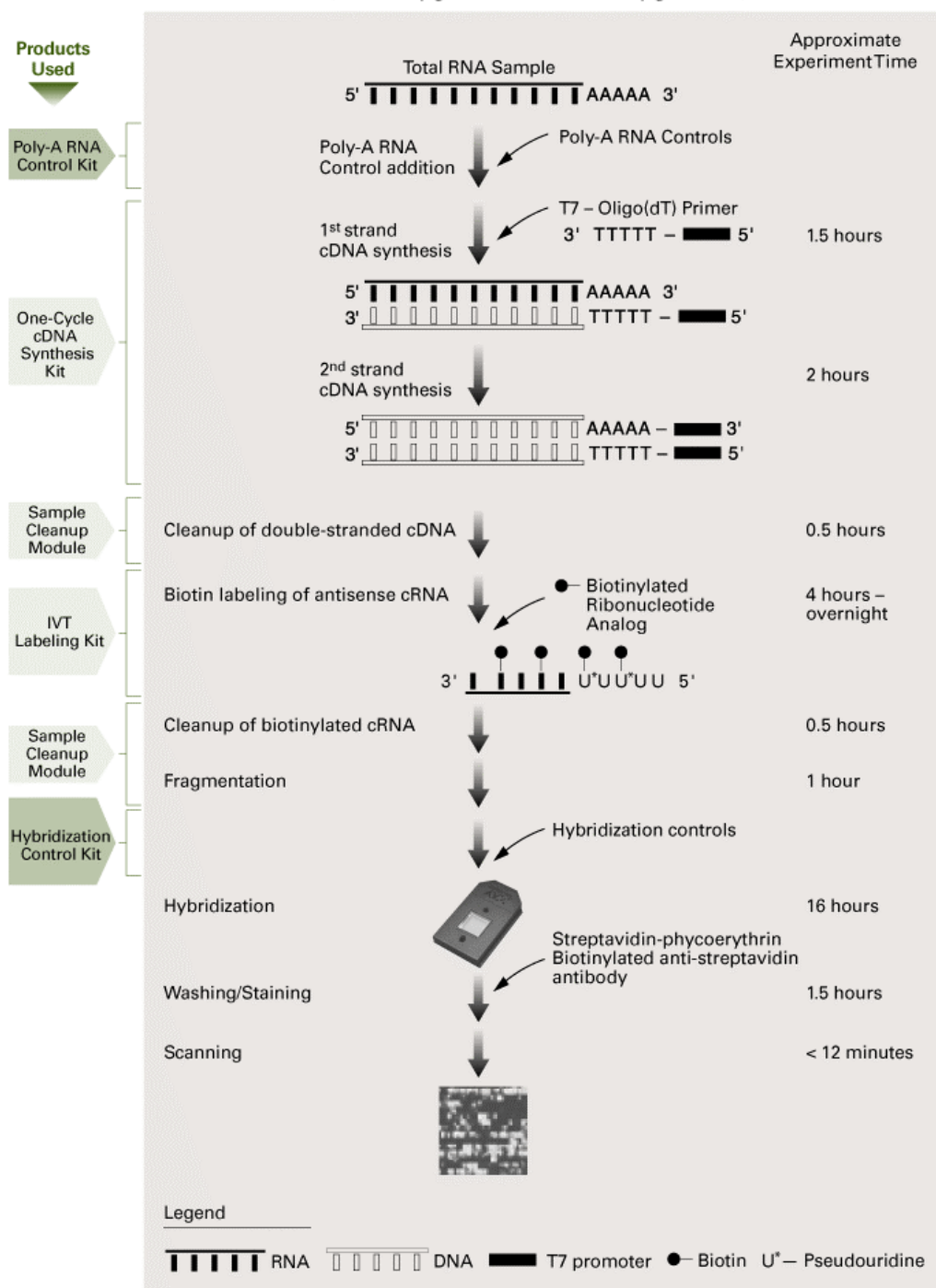


Figure IX-2. The expression of HA-tagged p68s in HEK 293 and SW620 cells.

(A) HEK cells were transfected with blank vector (pHM6) or HA-tagged p68s (wt, or HLIGR). The cell lysates were immunoblotted using antibody against HA epitope.

(B) HA-tagged p68s (wt or HLIGR) were expressed in p68-knockdown SW620 cells. The expression of endogenous p68 and exogenously expressed HA-tagged p68s were examined by immunoblotting using antibodies against p68-rgg and HA epitope.

(C) HA-tagged p68s (wt, Y593F and Y593/595F) were expressed in p68-knockdown SW620 cells. The expression of endogenous p68 and exogenously expressed HA-tagged p68s were examined by immunoblotting using antibodies against p68-rgg and HA epitope.

Figure IX-2

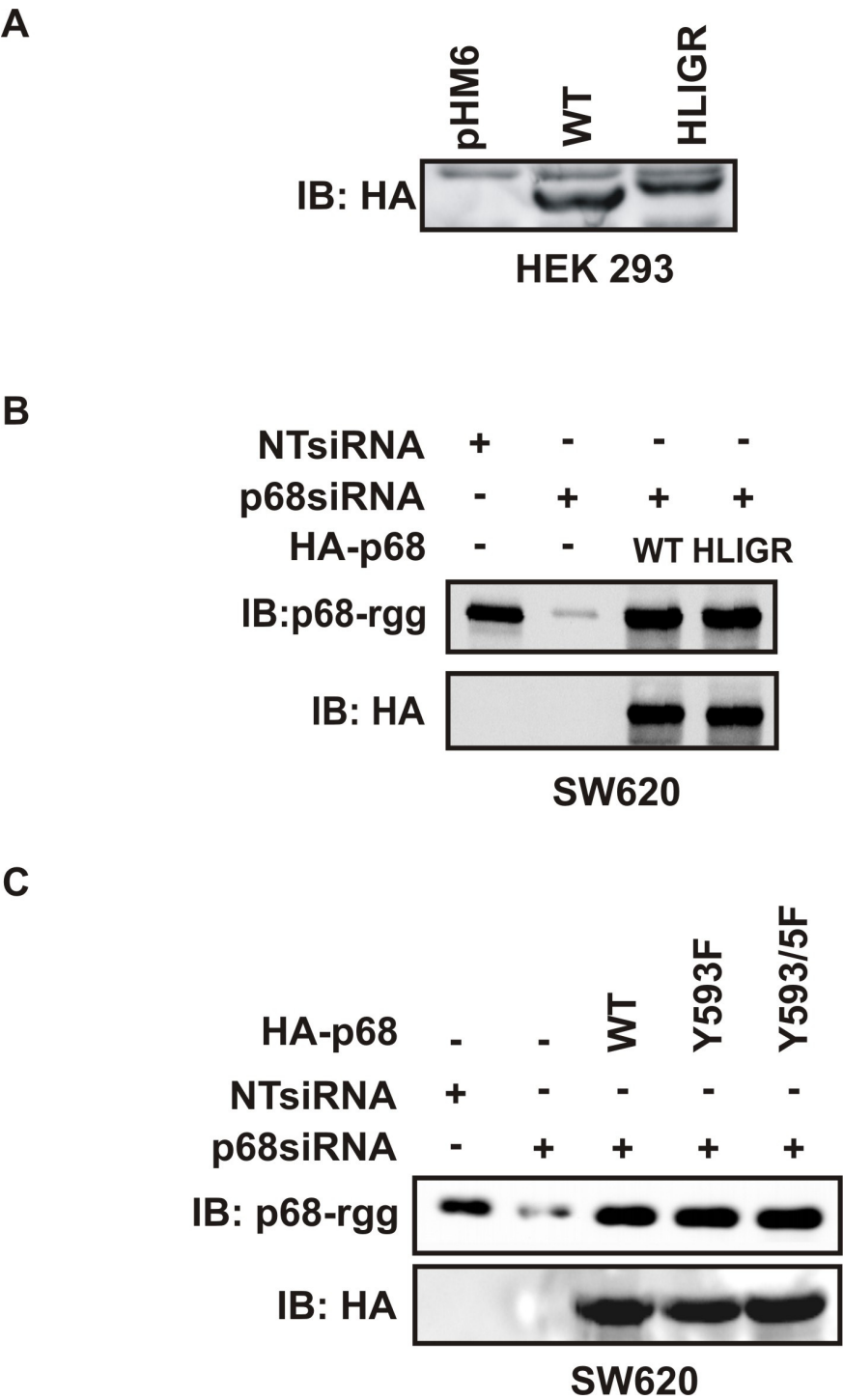


Figure IX-3. Reproducibility of the genes identified by the microarray technology.

The red dots represent the genes detected in both P1 samples, an estimated 34% of the genes on a single chip. The yellow or blue dots represent the genes detected only in one of the samples, and thus these signals only constitute about 0.25–0.3% of the genes on the chip. An intensity of 400 to 500 corresponds to approximately one copy per cell. The axes represent gene expression intensity. Five percent of probe sets showed more than 3-fold changes.

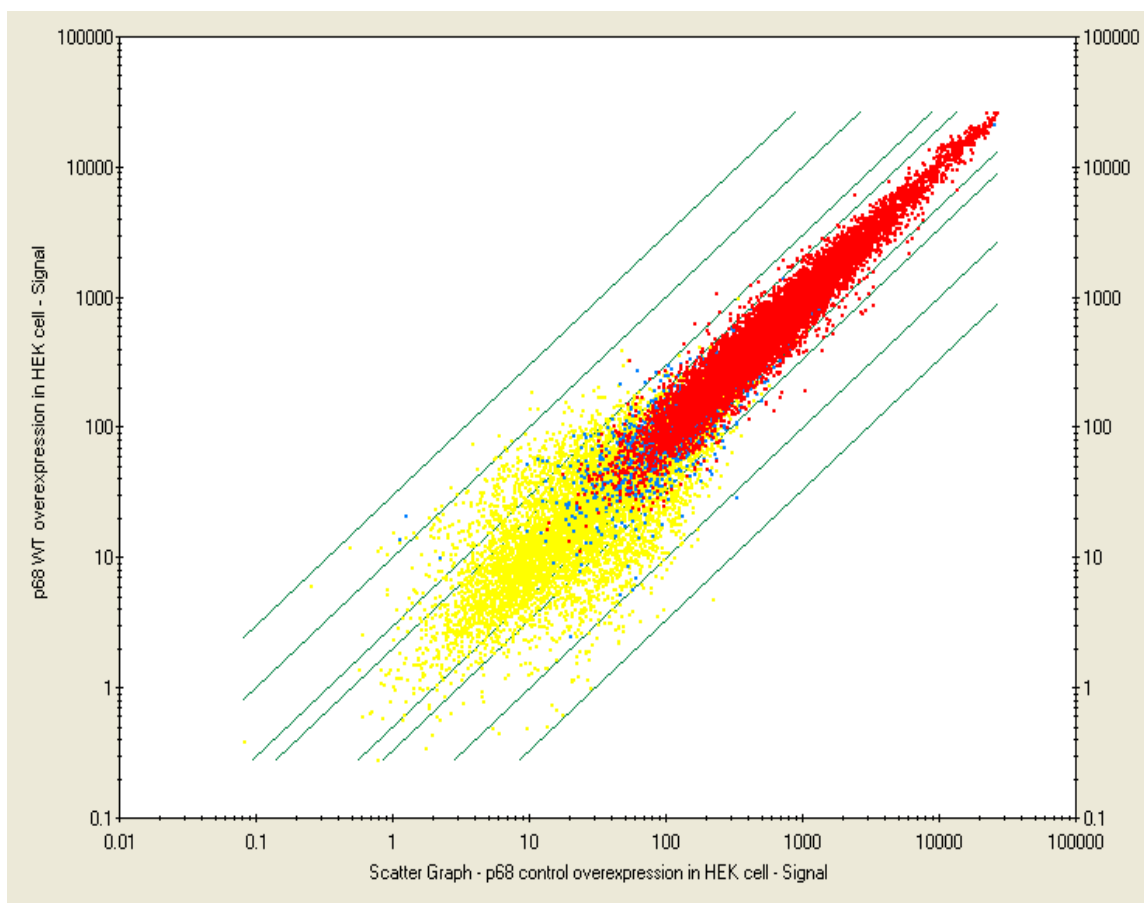
Figure IX-3

Table 5. Identification of genes affected by p68 RNA helicase.

Gene Bank No.	Description	NTsiRNA	P68siRNA	wild type	HLIGR
NM_004893	Histone 2a	292	261	265	269
NM_001101	Actin beta	634	638	899	877
M55643	NF-kB	18.1	30.9	33.5	52.8
X60188	ERK1	10.6	10.8	1.4	19.7
NM_006270	R-RAS	28.4	50	26.7	54.6
NM_007315	STAT1	114	174	256.6	180.1
AL039831	JAK1	17.5	16.8	47.4	88
AL121758	Snail	48.6	33.8	97	54.4
NM_001904	CTNND1	36.5	35	100	24.9
NM_004360	E-cadherin	113	98	140	53
NM_003376	VEGF	30	37	41.6	98.6
NM_005902	SMAD3	16.8	26.8	90	60.6
U19599	BAX delta	29.8	10.5	26.8	26.1
NM_000546	P53	18.9	18.1	34.8	56
NM_006186	Nuclear receptor	7.3	5	80.7	8.9

Table 6. Identification of genes affected by phosphorylation of p68.

Gene Bank No.	Gene description	WT	Y593F	Y593-5F
NM_016527	HAO2	10.9	130.5	39.2
NM_012267	hsp70-interacting protein	72.5	226.2	214
NM_002875	RAD51	85.1	207.1	125
NM_014623	male-enhanced antigen	448.2	221.7	295.9
NM_005224	dead ringer-like 1	239.5	114.4	393.7
NM_001610	acid phosphatase 2	252.1	115.4	167
NM_017450	BAI1-associated protein 2	243.9	110.4	276.2
NM_004223	ubiquitin-conjugating E2L 6	303.5	128.5	175
NM_006763	BTG family, member 2	240.2	101.4	189
NM_002502	NFKB2	211.8	87.8	192.4
NM_001616	activin A receptor, type II	310.1	124.7	308.7
NM_00140	EDG2	339.2	136.2	309.6
NM_002623	prefoldin 4 (PFDN4),	224.4	82.5	224
NM_024501	homeo box D1 (HOXD1)	11.7	92.3	133.4
NM_000014	alpha-2-macroglobulin	11.3	110.5	123.2
NM_003377	VEGFB	15.9	93.7	144.3
NM_001738	carbonic anhydrase I	67.8	129.1	286.5
NM_006180	NTKR	115.1	88.1	330.2
NM_016195	M-phase phosphoprotein 1	84.8	119.5	203.9
NM_021077	neuromedin B	131.8	133.4	307.8
NM_005228	EGFR	96.6	109.9	212.4
NM_012125	cholinergic receptor, muscarinic 5	123.4	149.5	269.4
NM_003243	TGFBR3	200.4	159.6	98.3
NM_003177	SYK	264.3	240.4	129.3
NM_003825	synaptosomal-associated protein	226.5	219	110.2
NM_000610	CD44	245.7	154.7	117.9
NM_012177	F-box only protein 5 (FBXO5)	475.8	349.3	226.7
NM_001432	epiregulin (EREG),	746.4	633.7	355.2
NM_003095	small nuclear ribonucleoprotein polypeptide F	1144.8	1041.4	498.8
NM_012225	nucleotide binding protein 2 (NUBP2),	381.8	193	164.7